The Stability of Cement Superplasticiser and its Effect on Radionuclide Behaviour

By

Amy Jean Young

Doctoral Thesis

Submitted in partial fulfillment of the requirements for the award of

Doctor of Philosophy of Loughborough University

9th August 2012

Acknowledgements

It would not have been possible to successfully complete this thesis without the help, support and love of the wonderful and kind people around me.

I would like to thank my supervisors, firstly Prof. Peter Warwick for giving me the opportunity to do the research and for his constant support and extensive knowledge of radionuclide behaviour. For pushing me to be the best that I could be and encouraging my tenacity! Thank you also to Prof. David Read who 'took me on' in the final year of my research, supported me continuously and provided exciting ideas and unsurpassed knowledge that have enhanced the project no end.

Thank you to the EPSRC DIAMOND Consortium and the Nuclear Decommissioning Authority for the funding for this research, particularly Dr Steve Williams and Dr Tara Beattie for their interest and input into the project.

Completing a large amount of the analysis for this research would not have been possible without the expertise and patience of a number of very helpful people. Thank you to Paul Allen at Enviras for his help with cement digestion and analysis, Alistair Daley for his advice on GC-MS and Dr Jim Reynolds for his incredible knowledge of ESI-MS. Thank you to Dr Keith Yendell for his help with SEM imaging and Dr Antoni Milowdowski at the British Geological Survey for his expertise and enthusiasm for autoradiography.

Very special thanks go to the Radiochemistry Group at Loughborough University especially Mr John Hinchliff, Dr Nick Evans, Dr Monica Felipe-Sotelo and Dr Sneh Jain who not only gave me advice and technical guidance in the lab, but also provided the most wonderful cakes! I would also like to thank the late Mr David Wilson, who was an instrumentation genius, helped me fiddle and get otherwise redundant instruments working and who I miss very much.

Thank you to my Mum and Dad, for viewing me as a 'good investment', for supporting and encouraging me, for never letting me give up, for instilling the mantra of 'You can do it!' and for all the fillet steaks, Bolly, Ciel shoes and pony related treats that always kept my spirits up! Thank you also to my family, especially my Grannies and Granddads who, although not all are here today,

will be very proud and enjoy telling absolutely anyone who will listen about my thesis!

To all my fabulous friends Ricky, Jo, Sneh, Jenna, Steve, Marijana, Nat and all of Loughborough Polo Club past and present, thank you for so much fun, food, cocktails, pool and polo! Special thanks to Stuart Pinkney for fixing everything I have broken, being a computer genius and making me laugh daily.

To Edward Shelton, thank you for simply being you. For putting up and coping with me, for making every weekend one to look forward to and for supporting me through both the exciting and difficult stages of completing this PhD. I love you very much. Thank you also to all of the Shelton clan, especially Graham and Julia for making Church Farm such a wonderful place to escape to.

And finally, thanks must go to the tool that every thesis writer should have at their disposal, for generally being tolerant of all the fuss I make, the most wonderful pony one could ever wish for, Mr Farol Young!

Abstract

Superplasticisers are used to improve the flow properties of fresh cement and offer undoubted benefits to the construction sector. There is concern in the nuclear industry, however, that organic additives may increase the solubility of radionuclides when in contact with cementitious grouts or backfill.

The research presented in this thesis describes the effect of a commercial polycarboxylated poly ether comb type superplasticiser on the behaviour of U (VI), Th (IV), Eu (III) and Ni (II) in blended cements. Both Blast Furnace Slag (BFS) and Pulverised Fly Ash (PFA) blends with Ordinary Portland Cement (OPC) were investigated. Solubility experiments approached from oversaturation were conducted in a range of high pH aqueous solutions that are representative of the respective cement pore waters. Results show that the 'as received' superplasticiser is responsible for an increase in solubility of all the metals investigated, however, the extent of solubility enhancement is dependent on the metal investigated and the nature of the high pH solution. U (VI) and Eu (III) display solubility enhancement over several orders of magnitude while Ni (II) and Th (IV) solubility is enhanced to a lesser extent.

Batch experiments of Ni (II) and Eu (III) uptake onto BFS:OPC and PFA:OPC cement were investigated from two view points

i. By regarding the superplasticiser as a 'ligand' where batch experiments of metal uptake on crushed cement are carried out with increasing concentrations of free superplasticiser in solution.

ii. By investigating metal uptake in cements prepared with superplasticiser already present.

Results of the batch experiments show that the presence of free superplasticiser in solution reduces uptake of Ni (II) and Eu (III) by both BFS:OPC and PFA:OPC. Further, metal bound in the presence of free superplasticiser is readily remobilised on exposure to fresh cement solution. Conversely, metal uptake is quantitative and irreversible when exposed to crushed cement prepared with superplasticiser in the original mix.

Leaching of U (VI), Th (IV) and Ni (II) from hardened cement with and without the addition of superplasticiser was investigated by the preparation of monolithic BFS:OPC and PFA:OPC cement samples. BFS:OPC samples prepared with superplasticiser suffered from bleed and a significant proportion of the original metal inventory was found in the BFS:OPC bleed water after 48 hours, varying from 19% in the case of nickel to 32% for uranium. Autoradiography of the monoliths showed accumulation of uranium and thorium in the region adjacent to, and in contact with, the bleed water. Therefore, the bulk of the metal inventory had not been incorporated into the cement.

The stability of the superplasticiser under conditions likely to be present in a Geological Disposal Facility (GDF) was investigated by exposing the superplasticiser to chemical, thermal and radiolytic attack. Several analytical techniques were assessed for their ability to characterise the products of these experiments. Whereas Infra-Red (IR) spectrometry provided comparative information regarding the functionality of the superplasticiser before and after exposure, Gel Permeation Chromatography with Refractive Index Detection (GPC-RID) was found to be the best technique available to observe changes to the superplasticiser. Under chemical (alkali) attack by exposure to 0.1 mol dm^{-3} NaOH and 95% saturated $Ca(OH)_2$, the superplasticiser samples were found to decrease in molecular weight, a result consistent with alkaline hydrolysis of the polymer chains. Little change to the superplasticiser were observed on heating to 80ºC, however, on exposure to gamma radiation (^{60}Co), further polymerisation and cross-linking of the polymer chains was initiated, with a significant increase of the polymer's molecular weight.

Solubility experiments on U (VI), Th (IV), Eu (III) and Ni (II) were repeated to investigate the effect of irradiated superplasticiser. As with the 'as received' material, the results show that the presence of irradiated superplasticiser causes an increase in solubility of all the metals investigated. In this case however, Th (IV) and U (VI) display a much greater enhancement in solubility, whereas Eu (III) and Ni (II) show solubility enhancement similar to that observed in the non-irradiated samples.

The results presented in this thesis give a representation of the behaviour of metals in the presence of polycarboxylated poly ether comb superplasticiser and highlight the importance of considering the consequences of the use of cement additives in the concept of the GDF. The metals studied encompass a range of oxidation states from Ni (II), through Eu (III) and Th (IV) to U (VI). The behaviour of these metals here is of potentially great significance as it may indicate similar behaviour by other actinide species, most notably the behaviour and apparent mobility of Th (IV) may suggest analogous behaviour of tetravalent Pu (IV) and Np (IV).

Contents

Table of Figures

Table of Tables

1 Introduction

The United Kingdom has accumulated a substantial legacy of radioactive waste, initially through the activities of the defence sector in the development of a nuclear deterrent, and more recently through the generation of energy by nuclear reactors. If the Government takes the decision to include nuclear power as an option for future UK energy generation, waste created by new facilities plus the pre-existing legacy waste must be managed and disposed of safely to ensure that significant quantities of radioactivity do not reach the surface environment.

In 2001, the UK Government initiated the Managing Radioactive Waste Safely (MRWS) programme to produce a solution for the disposal of radioactive wastes and to achieve long term protection of people and the environment (1). In 2006, it was recommended by the Committee on Radioactive Waste Management (CoRWM) that a geological disposal facility (GDF) preceded by secure interim storage, was the best available long-term solution for the disposal of higher activity radioactive waste (2).

1.1 Geological Disposal

Geological disposal is a multi-barrier, multi-phased approach based on placing the waste deep underground, beyond any disruption from man-made, or natural events. Interim surface storage provides a safe and secure store for packaged waste throughout the period while the geological disposal facility is planned and developed.

1.1.1 *UK Waste Inventory*

A report outlining an estimate of the current radioactive waste inventory was prepared for the Nuclear Decommissioning Authority (NDA) and recently published (3). An overview of these data is given in Table 1 while a list of the classifications of waste types are shown below –

- High Level Waste (HLW) – wastes in which the temperature may rise significantly as a result of their radioactivity, this factor must be taken into account in the design and development of a disposal route.
- Intermediate Level Waste (ILW) – wastes exceeding the upper boundaries for Low Level Waste but do not generate heat as a result of their radioactivity.
- Low Level Waste (LLW) – wastes having a radioactive content not exceeding 4 GBq per tonne of alpha or 12 GBq per tonne of beta/gamma activity.

Table 1 Estimate of current (2010) UK Radioactive Waste Inventory

Waste	**Packaged Volume**		**Radioactivity**	
	meters^3	**%**	**Terabequerels**	**%**
HLW	1,020	<0.1	80,000,000	95.4
ILW	287,000	6.1	3,900,000	4.65
LLW	4,430,000	93.9	40	0.00004
Total	**4,720,000**	**100**	**83,900,040**	**100**

Most Intermediate Level Waste (ILW) and Low Level Waste (LLW) in the UK will be immobilised in standardised stainless steel or concrete lined stainless steel containers and mixed with a cement based grout material. The waste packages will then be stored in engineered vaults within the host geological environment. These packages can remain underground in the vault until the vault is full (which could take many decades) and the decision made to either; leave the vault open with the option of retrieving the waste in the future, or, to backfill the vault and the shafts and tunnels with cement grout in order to permanently immobilise the waste. The cement backfill is designed to provide an important chemical barrier to radionuclide migration. Firstly via a high surface area available for the retention of radionuclides and secondly in the conditioning of the chemistry of the cement pore water.

1.2 Cement Materials

There are a number of applications for concrete and cement grouts in the design and implementation of the GDF. Standard techniques used for underground construction would be employed and therefore cements and concretes would be used for the walls, floors and ceilings of the vaults, shafts and tunnels. Cement grouts are also used for the encapsulation of ILW and LLW into standardised packages and will be a key component of the barrier system (4).

1.2.1 *Cement Production*

1.2.1.1 Ordinary Portland Cement

Ordinary Portland Cement (OPC) is the main cement used in the construction industry and is produced by roasting limestone and clay at high temperatures (1500˚C) to produce what is known as clinker (5,6). OPC is the most energy consuming and expensive component of cement and concrete therefore the addition of other less expensive materials is commonplace. Modern cements and concretes also utilise additives that can control cement flow, set time and strength. It is important to note that the composition of OPC is dependent on the origin of the limestone and clay used in manufacture although all cement sold must conform to certain standard specifications as to its composition, fineness, and strength (7). Since 2004, however, the implementation of European Standard EN197-1 permits cement manufacturers to add up to 5% 'minor constituents' to the clinker to try to reduce overall energy consumption.

1.2.1.2 Blast Furnace Slag

Blast Furnace Slag (BFS) is a by-product of the iron production industry. During iron making, acidic impurities from the iron ore are removed by the addition of limestone. In the high temperatures of the blast furnace, calcium carbonate in the limestone breaks down forming carbon dioxide and calcium oxide. The calcium oxide reacts with acidic impurities to form molten blast furnace slag which is removed from the blast furnace (8). UK production of BFS originates today from three integrated steel making facilities at Teesside, Scunthorpe and Port Talbot. Typically 3 million tonnes of BFS are produced annually.

1.2.1.3 Pulverised Fly Ash

Pulverised Fly Ash (PFA) is a fine particle residue transported by flue gas after the combustion of coal in a coal fired power station. The fly ash is obtained by electrostatic or mechanical precipitation of dust from the flue gas. The fine particle size, mineralogical nature and amorphous character make fly ashes pozzolanic and in some cases, self cementitious. The chemical composition of PFA is inherently variable because of a number of factors including the type and mineralogical composition of the coal, type of furnace, oxidising conditions including air to fuel ratio and the manner in which the fly ash is collected and stored before use (6,9,10).

Literature data regarding the general chemical composition of OPC, BFS and PFA are given in Table 2.

Table 2 Composition of cement materials (%) - Literature values

	LOI	**CaO**	**SiO_2**	**Al_2O_3**	**Fe_2O_3**	**MgO**	**SO_3**	**Na_2O**	**K_2O**	**REF**
OPC	n.d	61.3	20.1	4.15	2.5	3.13	4.04	0.24	0.39	(11)
BFS	n.d	45.3	33.9	13.1	1.7	2	Trace	n.d	n.d	(7)
PFA	3.86	3.06	46.16	26.99	10.44	1.99	1.59	0.9	3.26	(10)

* LOI = Loss on Ignition

1.2.2 *Cement Chemistry*

The chemistry of cement hydration is a complex, non-stoichiometric process which has been subject to scientist attentions for many years. As such, there is a large knowledge base about the processes involved in cement hydration and many books and journal papers are available for review. The intricate nature of the individual compounds present in hydrating cement has resulted in the formation of a notation convention which was developed to simplify equations. The key to this notation is given in Table 3 (7).

Table 3 Cement notation convention

Notation	Oxide Form
C	CaO
A	Al_2O_3
S	SiO_2
F	Fe_2O_3
$\bar{S}$	SO_3
F″	FeO
M	MgO
N	Na_2O
K	K_2O
L	Li_2O
T	TiO_2
P	P_2O_5
H	H_2O

The hydration reactions of the major mineral phases of Portland cement have been characterised well. The main pure phase hydration reactions are given in Figure 1. However it is acknowledged that further hydration reactions involve coupling of equations (1-8) shown below and lead to a highly complex final product (12).

$$2C_3S + 6H \longrightarrow C_3S_2H_3 + 3CH \quad (1)$$

$$2C_2S + 4H \longrightarrow C_3S_2H_3 + CH \quad (2)$$

$$2C_3A + 21H \longrightarrow C_4AH_{13} + C_2AH_8 \quad (3)$$

$$C_4AH_{13} + C_2AH_8 \longrightarrow 2C_3AH_6 + 9H \quad (4)$$

$$C_3A + 3C\bar{S}H_2 + 26H \longrightarrow C_6A\bar{S}_3H_{32} \quad (5)$$

$$2C_3A + C_6A\bar{S}_3H_{32} + 4H \longrightarrow 3C_4A\bar{S}H_{12} \quad (6)$$

$$C_4AF + 3C\bar{S}H_2 + 29H \longrightarrow C_6(A,F)\bar{S}_3H_{32} + (A,F)H_3 \quad (7)$$

$$C_4AF + C_6(A,F)\bar{S}_3H_{32} + 7H \longrightarrow 3C_4(A,F)\bar{S}H_{12} + (A,F)H_3 \quad (8)$$

Figure 1 Pure phase cement hydration reactions

For example, using the cement notation convention, C_3S represents a phase with a chemical formula of $3CaO{\cdot}SiO_2$ which is known as tricalcium silicate (or alite). Similarly, C_4AF represents tetracalcium aluminoferrite which has a chemical formula of $4CaO{\cdot}Al_2O_3{\cdot}Fe_2O_3$.

There are 5 stages in the evolution of Portland cement hydration reactions with time,

1. The initial hydration process (0-15 min)

2. Induction period or lag phase (15 min – 4 h)

3. Acceleration and set (4-8 h)

4. Deceleration and hardening (8-24 h)

5. Curing (1- 28 days)

Hydration of aluminate phases, particularly C_3A govern early hydration (0- 1 h) while set and early strength behaviour is controlled by the hydration of silicates, namely C_3S (13).

Chemical compounds known as admixtures are frequently added to cement formulations to improve the properties of the product for a specific application. Such improvements may include water reduction, fluidification, corrosion inhibition, shrinkage control and freeze-thaw resistance. The chemical admixtures work by interfering with the cement hydration process and disrupt particle-particle interactions. The research reported in this thesis is concerned with one type of admixture in particular, superplasticisers.

1.2.3 *Mechanisms for Uptake by Cement Phases*

The cement backfill is designed to provide an important chemical barrier to radionuclide migration. Firstly via a high surface area available for the retention of radionuclides (CSH has a surface area in the region of 10 to 50 $m^2\ g^{-1}$ (14)) and secondly in the chemistry of the cement pore water. The chemistry of the cement pore water is dominated by the presence of $Ca(OH)_2$ (portlandite). With a solubility of ca. 1g dm^{-3} at 25ºC, the presence of portlandite buffers the pH of the pore solution to ca. pH 12.5.

Subject to these high pH conditions many metals, including the actinides, have low solubility and may precipitate as salts. There are several other processes which can determine concentration of a radionuclide within cement porewater

including adsorption onto the cement surface itself, co-precipitation with other phases present and lattice incorporation into cement hydration products(15).

The process by which radionuclides are removed from solution is generally called ‘sorption’ but this tells us little of the mechanism. Sorption can incorporate the contributions of absorption, physical adsorption and chemical adsorption to the removal of radionuclides (16).

While absorption refers to the incorporation of a species within the physical and molecular structure of a sorbent, adsorption may divided into 3 types:

1. Surface Complexation
2. Ion Exchange
3. Other mechanisms – e.g. co-precipitation

The strongest ‘sorption’ between a metal species and a sorbent is that which leads to a chemical reaction rather than the action of electrostatic or ionic forces (17).

Due to the wide use of cement in the GDF concept and the uncertainties surrounding the complex chemical interactions of cement within a repository environment, it is important to gain a broad knowledge of the implications of using cement based materials in the concept of the GDF. There are many combinations of cement matrices with the inclusion of powders such as BFS (Blast Furnace Slag) and PFA (Pulverised Fly Ash) plus additives which provide cement with specific characteristics that are desirable to the user. These characteristics include the production of high strength concrete, cement with low water content and cement with greater flow properties. Moreover, an important principle in any generic cement based system is to use the least amount of OPC (Ordinary Portland Cement) possible in the concrete or cement mix. OPC powder is the most expensive and energy consuming ingredient of cement and concrete, therefore reducing the ratio of OPC in the cement matrix will preserve natural resources and be more economical. Another consideration is the long term durability of the concrete. An excessive amount of OPC in the cement matrix will result in a high heat of hydration leading to a high risk of the

cement or concrete cracking (18). One group of additives which present benefits that are attractive to the nuclear industry is superplasticisers.

1.3 Superplasticisers

Superplasticisers belong to a group of cement additives known as high range water reducers. They are polymeric molecules and are widely used in the construction industry to increase the flow characteristics of cement based systems whilst still being capable of reducing the water content of a cement formulation by around 30% (19). Superplasticisers are synthetic chemicals consisting of high molecular weight, water soluble polymers. Solubility is ensured by the presence of adequate hydroxyl, sulfonate or carboxylate groups attached to the main organic repeat unit which is usually anionic in nature (20).

1.3.1 *Superplasticiser Classification*

A number of different types of superplasticiser are available commercially. Classification of superplasticiser type is made according to chemical structure. The 4 main groups are outlined below:

1.3.1.1 Sulphonated Melamine Formaldehyde Condensates (SMF)

Developed in Germany and available since 1964, SMF is a synthetic polymer with the structure shown in Figure 2. The condensation number, *n*, (number of repeating unit in the polymer chain) is generally between 50 and 60 giving a molecular weight between 12,000 and 15,000 (20).

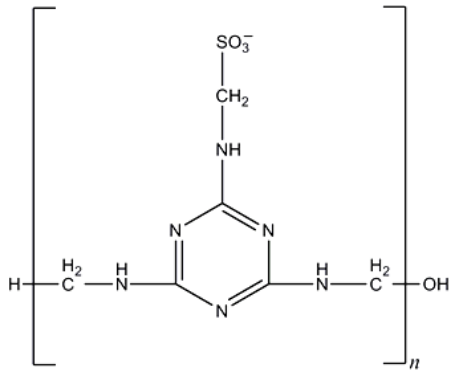

Figure 2 Sulphonated melamine formaldehyde condensate

1.3.1.2 Sulphonated Naphthalene Formaldehyde Condensates (SNF)

SNF was developed in Japan and has been available commercially since 1963. The structure of the polymer repeat unit is given in Figure 3. In this case *n* is 5-10 giving a typical molecular weight range of between 1,000 and 2,000.

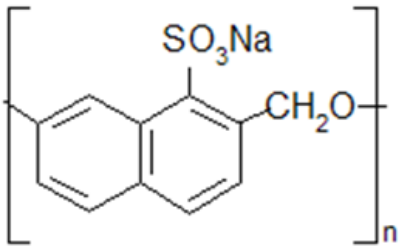

Figure 3 Sulphonated naphthalene formaldehyde condensate

1.3.1.3 Modified Lignosulphonates

Lignosulphonates are produced from the naturally occurring polymer lignin via a sulphonation process that ensures the solubility of the polymer. The chemical structure of the repeat unit is shown in Figure 4.

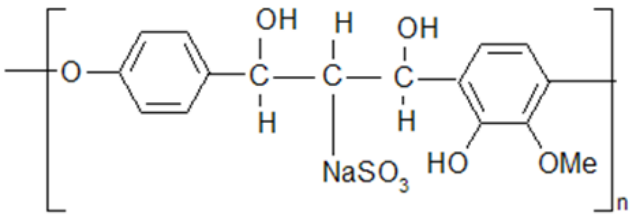

Figure 4 Sodium lignosulphonate

1.3.1.4 Comb Type Polycarboxylates

Comb type polymers are part of a more novel group of superplasticiser which are thought to work via a different mechanism to the original superplasticisers. The comb type structure consists of a main linear chain with lateral carboxylate and ether groups. The research reported in this thesis is concerned with one comb type superplasticiser, ADVA Cast 551. The structure of this polymer is shown in Figure 5.

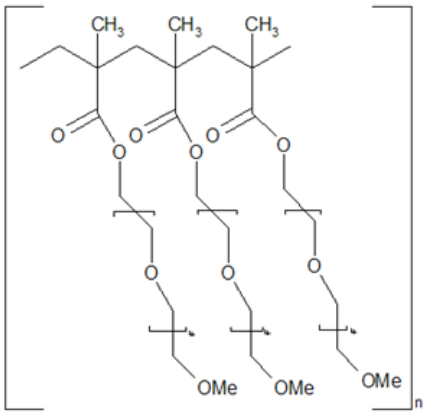

Figure 5 Comb type polycarboxylate superplasticiser, ADVA Cast 551

1.3.2 *Mode of Action*

Superplasticisers strongly adsorb onto cement particles via interaction between charged groups on the polymer (SO_3^-, COO^-) and the cement surface. Polar function groups such as –OH can also interact strongly with polar hydrating phases via electrostatic forces and hydrogen bonding phenomena.

Once adsorbed on the cement particles, SNF, SMF and lignosulphonates work by conveying a net negative charge (zeta potential) which leads to particle-particle electrostatic repulsion, and in turn, cement dispersion (13).

In the case of polycarboxylated comb polymers, dispersion is thought to occur in part by electrostatic forces, but primarily via steric repulsion between the grafted chains on the polymer backbone (21-23).

Superplasticiser adsorption does not exclude water molecules from the cement particle surface entirely; therefore hydration reactions may still proceed. In fact, better particle dispersion leads to more efficient hydration and a higher early strength. The effect of superplasticisers on cement hydration involves several factors (24);

1. The polymer hinders water and Ca^{2+} ion diffusion across the solution-cement interface.
2. Ca^{2+} ions complex with the superplasticiser which inhibits the growth of calcium rich species.

3. The action of superplasticisers alters reaction product kinetics and cement morphology.

An example of a morphological change associated with the presence of superplasticiser is a refinement in cement pore size and in turn, a reduction in cement porosity. Despite changes in morphology, mineralogical analysis has shown that the same hydration products are formed with or without the presence of superplasticiser (25,26).

1.4 Metals of Interest

A range of metals were investigated in this research not only to include elements of particular relevance to the UK radioactive waste inventory, but also to reflect a series of different oxidation states. Information regarding each element used during this research including its oxidation state is given below. The oxidation state of an atom in a molecule refers to the number of valence electrons that have been gained or lost. For a monoatomic ion, the oxidation state is equal to the net charge on the ion. The higher the oxidation state, the greater the degree of oxidation while the lower the oxidation state, the greater the degree of reduction.

1.4.1 *Uranium*

Uranium is a major constituent of nuclear industry waste. ^{238}U and ^{235}U are of greatest significance due to their substantially long half-lives.

^{238}U is the most common isotope of uranium found in nature being 99.3% of natural uranium by mass. Decay is by alpha emission with a half-life of 4.47 x 10^9 years. ^{238}U is not directly usable as nuclear fuel; however, it may be used to breed the fissile ^{239}Pu.

^{235}U makes up 0.7% of natural uranium by mass. ^{235}U also decays by alpha emission and has a half-life of 7 x 10^8 years (27).

In this research, only hexavalent uranium is considered.

1.4.2 *Thorium*

Thorium is a naturally occurring primordial radioelement but is also a daughter product of uranium decay, (e.g. ^{234}Th, ^{230}Th). Natural ^{232}Th has a half-life of 1.4 x 10^{10} years and decays by alpha emission. Thorium compounds are most stable in the +4 oxidation state (27).

1.4.3 *Europium*

Europium is used as a component of nuclear reactor control rods, since ^{151}Eu is a very useful neutron absorber (generating ^{152}Eu). ^{152}Eu, ^{154}Eu and ^{155}Eu are produced as fission products. ^{152}Eu decays with a half-life of 13.5 years by two modes – electron capture (to ^{152}Sm) and beta emission (to ^{152}Gd) which yields characteristic gamma emissions of 0.344, 1.112 and 1.408 MeV. ^{152}Eu is therefore easily analysed by gamma spectrometry. The oxidation state of europium in this research was +3, and may be used as an analogue for trivalent actinides such as ^{241}Am (27).

1.4.4 *Nickel*

Reactor components are generally constructed from various metal alloys containing nickel. Two radioactive isotopes of concern are produced by neutron activation of these metal components. ^{63}Ni and ^{69}Ni have half-lives of 100 years and 75,000 years respectively while all other nickel isotopes have half-lives of less than six days. ^{63}Ni is a low energy beta emitter which is easily analysed by Liquid Scintillation Counting (LSC). Natural ^{59}Ni is also used in this research and is analysed by ICP-OES and ICP-MS. In this research the oxidation state of Ni was +2 (28).

1.4.5 *Previously Reported U (VI), Th (IV), Eu (III) and Ni (II) Solubility Data*

There are few references available for the solubility of the metals of interest in high pH solution; however, a review of published literature values is recorded below.

Table 4 U (VI) Literature Solubility Data

Uranium salt	Experimental Conditions	U (VI) Solubility	Ref
$UO_2(NO_3)_2$	Uranium in $Ca(OH)_2$ with 7 day equilibration time at pH 12. Filtered through 0.2µm filters and U (VI) measured by LSC	2.5 x 10^{-6} mol dm^{-3}	(29)
$UO_2(NO_3)_2$	Uranium in NaOH with 7 day equilibrium time at pH 12. Filtered through 0.2µm filters and U (VI) measured by LSC	2.5 x 10^{-6} mol dm^{-3}	(29)
$UO_2(ClO_4)_2$	Uranium in 0.1 mol dm^{-3} NaClO4 with 30 day equilibration time at pH 5.4	1.7 x 10^{-5} mol dm^{-3}	(30)
$UO_2(ClO_4)_2$	Uranium in BFS:OPC (9:1) equilibrated water at pH 13	1 x 10^{-5} mol dm^{-3}	(31)
$UO_2(ClO_4)_2$	Uranium in BFS:OPC (9:1) equilibrated water at pH 10.5	1 x 10^{-7} mol dm^{-3}	(31)

Table 5 Th (IV) Literature Solubility Data

Thorium salt	Experimental Conditions	Th (IV) Solubility	Ref
$ThCl_4$	Thorium in OPC/BFS/L (1:3 ordinary Portland cement: blast furnace slag plus limestone aggregate) equilibrated water at pH 12	4 x 10^{-9} mol dm^{-3}	(31)
$ThCl_4$	Thorium in OPC/L (Ordinary Portland cement and limestone aggregate) equilibrated water at pH 12	4 x 10^{-9} mol dm^{-3}	(31)
ThO_2 (microcrystalline)	Thorium in cement equilibrated water (CEMI42.5 HS). 25 days equilibration. pH 12.5	2.5 x 10^{-10} mol dm^{-3}	(32)
ThO_2 (cr)	Thorium in NaCl-NaOH at pH 11-13.5	5 x 10^{-10} mol dm^{-3}	(33)

Table 6 Eu (III) Literature Solubility Data

Europium salt	Experimental Conditions	Eu (III) Solubility	Ref
$Eu(OH)_3$	Europium in simulated cement pore water. Solubility approached from Undersaturation, N_2 atmosphere	2 x 10^{-9} mol dm^{-3}	(34)
Eu (III)	N_2 atmosphere, pH 13.3, 8 weeks equilibrated	5.9 x 10^{-7} mol dm^{-3}	(35)
$Eu(NO_3)_3$	Europium in $NaClO_4/HClO_4$	5.9 x 10^{-7} mol dm^{-3}	(36)
$Eu(OH)_3$	Europium in 4 mol dm^{-3} $NaClO_4$ with the addition of NaOH	5.2 x 10^{-7} mol dm^{-3}	(37)

Table 7 Ni (II) Literature Solubility Data

Nickel salt	Experimental Conditions	Ni (II) Solubility	Ref
$Ni(OH)_2$ (cr)	Undersaturation in N_2 atmosphere. 0.01 mol dm^{-3} $NaClO_4$. pH 12.6, 90 days equilibrium time	8.5 x 10^{-8} mol dm^{-3}	(38)
$Ni(OH)_2$ (cr)	Nickel in saturated $Ca(OH)_2$ solution, N_2 atmosphere with 28 days equilibrium time	6.3 x 10^{-8} mol dm^{-3}	(39)
$Ni(OH)_2$ (cr)	Low temperature flow cell experiment in $B(OH)_3$. pH 8	2.8 x 10^{-5} mol dm^{-3}	(40)

1.5 Previously Reported Solubility Experiments

1.5.1 *Organic Contaminants*

Intermediate level radioactive waste contains significant concentrations of organic contaminants such as EDTA, citrate and oxalate. These are present since they are used in decontamination projects or are the products of degrading waste constituents e.g. oxalate is produced by radiolytic degradation of bitumen (41). These contaminants have been shown to complex with metals and increase their solubility and mobility within the environment. A review of metal solubility data in the presence of organic contaminants is given in Table 8.

Table 8 Metal solubility data in the presence of organic contaminants

Metal	Experimental Conditions	Solubility	Ref
Nickel $Ni(OH)_2$ (cr)	NaOH (0.01 – 11.6 mol dm^{-3}) with EDTA (0.01 mol dm^{-3})	>1 x 10^{-4} mol dm^{-3}	(39)
Nickel $Ni(NO_3)_2$	Saturated $Ca(OH)_2$ with EDTA 0.01 mol dm^{-3})	2.9 x 10^{-4} mol dm^{-3}	(42)
Nickel $Ni(NO_3)_2$	Saturated $Ca(OH)_2$ with Citrate 0.01 mol dm^{-3})	3.6 x 10^{-4} mol dm^{-3}	(42)
Thorium ThO_2	$NaNO_3$ (0.1 mol dm^{-3}) adjusted with NaOH, Citrate (0.01 mol dm^{-3}). 7 days equilibrium	2 x 10^{-9} mol dm^{-3}	(43)
Thorium ThO_2	$NaNO_3$ (0.1 mol dm^{-3}) adjusted with NaOH, Oxalate (0.01 mol dm^{-3}). 7 days equilibrium	1.6 x 10^{-9} mol dm^{-3}	(43)
Thorium ThO_2	Oversaturation in $NaNO_3$ (0.1 mol dm^{-3}) adjusted with NaOH, EDTA (0.01 mol dm^{-3}). 7 days equilibrium	2.3 x 10^{-9} mol dm^{-3}	(43)
$Th(NO_3)_4$	Saturated $Ca(OH)_2$ with EDTA 0.01 mol dm^{-3})	9 x 10^{-9} mol dm^{-3}	(42)
$Th(NO_3)_4$	Saturated $Ca(OH)_2$ with Citrate 0.01 mol dm^{-3})	1.3 x 10^{-6} mol dm^{-3}	(42)
$UO_2(NO_3)_2$	$Ca(OH)_2$ with Citrate (0.01 mol dm^{-3}) 7 days equilibrium	1 x 10^{-5} mol dm^{-3}	(29)
$UO_2(NO_3)_2$	Saturated $Ca(OH)_2$ with Oxalate (0.01 mol dm^{-3})	3.3 x 10^{-7} mol dm^{-3}	(42)

1.5.2 *Superplasticisers*

A number of advantages of the use of cement superplasticisers with regard to the Geological Disposal Facility and within the concepts for waste packaging have been identified. However, because of the enhancement of metal solubility in the presence of organic contaminants, as is shown in the tables above, it is unfavourable to add an organic into a matrix which is used for radioactive waste disposal. Superplasticisers (and their degradation products) are potential complexants which could increase the solubility of radionuclides and therefore increase the mobility of radionuclides within the environment. It is important to assess the impact of the addition of superplasticiser to cements on the solubility of radionuclides to allow accurate predictions of radionuclide behaviour within the near and far field of a radioactive waste repository. Few authors have reported on the effects of superplasticiser on metal solubilities. In the present section, previously reported solubility experiments are discussed.

1.5.2.1 Sikament 10

The effect of Sikament 10 (a formaldehyde free, low alkali and water soluble polymer) on the solubility of plutonium in cement equilibrated water was investigated by McCrohon and Williams (1997) (44). Plutonium solubility was studied in the presence of 0.5% and 1% (w/v) Sikament 10, ((w/v) refers to the weight (of solute) per volume (of solvent)).

The baseline solubility of plutonium in cement equilibrated water without the presence of superplasticiser at pH 12 was 1 x 10^{-10} mol dm^{-3}. Baseline solubility refers to the solubility of a metal in a given solvent without the presence of any ligand. After addition of 0.5% Sikament 10, the average plutonium solubility was found to be 5 x 10^{-5} mol dm^{-3}. At 1% addition of Sikament 10, the average plutonium solubility was found to be 9 x 10^{-5} mol dm^{-3}. An increase in Pu (IV) solubility over several orders of magnitude was observed in the presence of Sikament 10.

The solubility enhancement factor (SEF) in the presence of the superplasticiser may be calculated and allows a comparison between different superplasticisers. To calculate the enhancement factor, Equation 1 is used:

$$SEF = \frac{\text{Solubility in presence of superplasticiser (mol dm}^{-3})}{\text{Baseline Solubility (mol dm}^{-3})}$$

Equation 1 Solubility Enhancement Factor

The enhancement factors for the addition of 0.5% and 1% respectively are 5 x 10^5 and 9 x 10^5. This is a very significant solubility enhancement and Sikament 10 therefore was not recommended for use in cement formulations for use in the GDF concept.

1.5.2.2 Sikament N

Boult et al. (1998) (45) investigated the effect of Sikament N (an additive based on naphthalene formaldehyde) on the solubility of plutonium in cement equilibrated water. Sikament N was present at 0.5% and 1% (w/v). The baseline solubility of plutonium in cement equilibrated water is 1 x 10^{-10} mol dm^{-}

^{3} at pH 12. With the addition of 0.5% and 1% Sikament N, the average plutonium solubility was found to be 2 x 10^{-6} mol dm^{-3} and 5 x 10^{-6} mol dm^{-3} respectively.

The results for Sikament N showed a significant increase above the baseline solubility for plutonium in cement equilibrated water. The SEF values for 0.5% and 1% respectively are 20,000 and 50,000.

1.5.2.3 HS-100

The effect of HS-100 (a naphthalene sulphonic acid condensation and lignin sulphonic acid derivative polymer) on the solubility of uranium (VI), plutonium (IV), americium (III) and technetium (IV) were studied in cement equilibrated water at pH 12 by Greenfield et al. (1998) (46). The experiment was conducted at an additive: water ratio of 30g: 1kg. The solubility data recorded, plus the enhancement factors are shown in Table 9.

Table 9 Solubility of Tc (IV), U (IV), Am (III), Pu (IV) Solubility in the presence of HS-100

Element	**Solubility in cement equilibrated water (Baseline Solubility)**	**Solubility in the presence of HS-100**	**SEF**
Technetium (IV)	$7x10^{-9}$ mol dm^{-3}	$5x10^{-6}$ mol dm^{-3}	714
Uranium (IV)	$2x10^{-7}$ mol dm^{-3}	$5x10^{-5}$ mol dm^{-3}	250
Americium (III)	$5x10^{-11}$ mol dm^{-3}	$5x10^{-6}$ mol dm^{-3}	$1x10^{5}$
Plutonium (IV)	$2x10^{-10}$ mol dm^{-3}	$4x10^{-6}$ mol dm^{-3}.	$2x10^{4}$

All of the metals investigated experienced a solubility enhancement in the presence of HS-100. The element with the highest solubility enhancement factor observed was americium (III).

1.5.2.4 HS-700

The effect of HS-700 (a polycarboxylic acid polymer) on the solubility of uranium (IV), plutonium, americium and technetium (IV) was investigated in cement equilibrated water at pH 12 by Greenfield et al. (1998) (46). The experiment was conducted at an additive: water ratio of 50g: 1kg. The solubility

data recorded in the presence and absence of the HS-700 superplasticiser are shown in Table 10.

Table 10 Solubility of Tc (IV), U (IV), Am (III), Pu (IV) Solubility in the presence of HS-700

Element	Solubility in Cement Equilibrated water (Baseline Solubility)	Solubility in the presence of HS-100	SEF
Technetium (IV)	$7x10^{-9}$ mol dm^{-3}	$9x10^{-8}$ mol dm^{-3}	12.85
Uranium (IV)	$2x10^{-7}$ mol dm^{-3}	$7x10^{-5}$ mol dm^{-3}	350
Americium (III)	$5x10^{-11}$ mol dm^{-3}	$8x10^{-6}$ mol dm^{-3}	$1.6x10^{5}$
Plutonium (IV)	$2x10^{-10}$ mol dm^{-3}	$6x10^{-6}$ mol dm^{-3}	$3x10^{4}$

Similarly to HS-100, all of the metals investigated experienced a solubility enhancement in the presence of HS-700. The metal that was most significantly affected was americium. The authors concluded that the formation of mixed complexes of the radionuclide and additive was responsible for the increase in solubility observed.

1.6 Previously Reported Superplasticiser Degradation Studies

The conditions present in the GDF (high pH, elevated temperatures, presence of ionizing radiation) may have an effect on the physical and chemical characteristics of a superplasticiser. It is important to consider the potential mechanisms for polymer degradation under such circumstances. Palardy et al. (1998) suggest that the degradation of superplasticiser is not attributed to a single cause but arises due to a combination of factors plus the result of several degradation pathways (47). There are few studies reported in the literature regarding the degradation of superplasticisers, nevertheless, a review of the results from these studies is given below:

1.6.1 *Biodegradation*

Chemical, thermal and radiolytic degradation would be expected to act upon superplasticisers to a greater extent than the process of biodegradation. However, Ruckstuhl et al. (2002) report on the breakdown of sulphonated

melamine formaldehyde in this manner (48). The investigation was carried out after the discovery of SMF in ground water samples 5 meters away from a construction site which used the superplasticiser. A laboratory simulation of biodegradation was conducted in which pH and sulphate/oxygen levels were used which were similar to that at the field sampling site. The degradation pathway of SMF was found to be de-sulphonation, followed by a ring cleavage. Monosulphonated analogues were readily depleted. However, disulphonated analogues were found to be less biodegradable and so more persistent in the environment. The kinetics of this primary degradation was found to be of zero order.

1.6.2 *Chemical Degradation*

Yilmaz et al. (1993) (49) investigated the degradation of SMF and SNF superplasticisers in highly alkaline conditions. The superplasticiser (2 g) was dissolved in 1 dm^3 KOH (1 mol dm^{-3}) and kept in air-tight bottles for 20 days. At pre-determined intervals, samples of the solutions were removed from the stock, filtered and then neutralised. The quantitative determination of SMF and SNF was then conducted using UV spectroscopy. The wavelengths used for SMF and SNF were 215 and 226 nm respectively. In both cases, the concentration of superplasticiser in solution decreased with time, however, the SMF and SNF behaved very differently. SMF content decreased over time and a white solid precipitate was observed. UV measurement showed that more than 65% of the original SMF had precipitated. SNF did not show the same behaviour and only a small decrease in concentration was recorded a day after preparation but no precipitation was observed.

Çolak (2005) (50) reported the effect of sodium chloride attack on the strength of cement, with and without the addition of superplasticiser. Plain Portland Cement paste and a Portland Cement paste with the addition of SMF superplasticiser were immersed in a 2.5% (w/v) NaCl solution for a period of 62 days. The effect of the NaCl attack was reported as not instantaneous but a decrease the compressive strength of the pastes over time was observed. At 28 days, the plain paste and the superplasticised paste display similar compressive strengths of 56.23 MPa and 55.41 MPa respectively. After

exposure to the NaCl solution, the compressive strength of the plain paste and the superplasticised paste were 55.46 MPa and 25.12 MPa respectively. This large decrease (a 2/3 reduction in strength) was attributed to the effect of NaCl solution being absorbed by the polymer.

1.6.3 *Irradiation Degradation*

Chandler et al. (2008) (51) have prepared a report on the gamma irradiation testing of grout and aqueous samples containing ADVA Cast 550 (the commercial predecessor to ADVA Cast 551 with a similar structure). Irradiation was carried out at a Co-60 irradiation facility on two types of sample-cementitious and aqueous.

The cementitious formulations consisted of 3:1 PFA:OPC grout containing 0.8% (w/v) ADVA Cast 550 and 9:1 BFS:OPC grout containing 0.8% (w/v) ADVA Cast 550. The grout was poured into moulds, vibrated to remove trapped air and cured for twenty four hours at 18-22ºC at a relative humidity of greater that 90%. The samples were then placed in two positions within the irradiation chamber. The first was at the high dose rate position receiving a dose rate of 4 kGy h^{-1} to a total dose of 9 MGy. The second was placed at a low dose rate position and received a dose rate of 1 kGy h^{-1} to a total dose of 2 MGy. Pore fluid from these grout samples was then extracted by pore squeeze, after irradiation, for analysis.

The aqueous samples were prepared in saturated $Ca(OH)_2$ solution. One sample contained 1% (w/v) ADVA Cast 550 and a second contained 10%. These samples were irradiated at 3 different dose rates. Firstly 4 kGy h^{-1} to a total dose of 9 MGy, secondly 300 Gy h^{-1} to a total dose of 675 kGy and lastly, 30 Gy h^{-1} to a total dose of 67.5 kGy. Analysis of the samples was then conducted using TOC (Total Organic Carbon), organic screening by GCMS (Gas Chromatography Mass Spectrometry) and Ion Chromatography.

Irradiation was shown to decrease TOC of the samples and the effect was greater at higher dose rates. TOC measured from the pore squeeze solutions was observed to be dependent on the grout formulation. TOC from the BFS:OPC samples were higher than the PFA:OPC which suggests that not only

the pH but also the ions present in the pore water may have an effect on the degradation pathway.

When a polymer is exposed to ionising radiation there are generally two possible outcomes;

i. Chain Scission- where the backbone of the molecule is broken and lower molecular weight fragments are generated.
ii. Cross Linking- where individual molecules become attached to each other and form a network.

Organic screening by GCMS indicated that for the aqueous ADVA Cast 550 samples at low radiation doses, a wide range of degradation products was observed. These products were consistent with chain scission degradation since the products systematically decrease in molecular size. For the pore squeeze samples, the compounds identified were alcohols, ketones, carboxylic acid and hydrocarbons. These species were different from those generated in the aqueous samples.

Ion chromatography identified low values of organic ions in the 1% aqueous solutions which was consistent with the TOC and GCMS analysis. At 10% ADVA Cast 550, a significant amount of organic anions in particular acetate and lactates were identified. Again, this was consistent with TOC and GCMS analysis.

Conclusions of the work by the authors were that, in the investigation, there was no evidence for the formation or generation of undesirable potential complexing agents.

1.7 Project Objectives

The aim of this research is to consider the suitability of adding the polycarboxylated polyether superplasticiser ‘ADVA Cast 551’ to cementitious materials for use in the Geological Disposal Facility and, in the packaging of radioactive waste. ADVA Cast 551 was chosen to be studied as a representative polycarboxylated comb type superplasticiser in agreement with the Nuclear Decommissioning Authority. The results of preliminary stability

studies on a similar polymer ADVA Cast 550, described in section 1.6.3, indicated no evidence of the formation of undesirable complexing agents. Due to the similarities in the two polymers, it was suggested that ADVA Cast 551 also may not pose significant complexation potential but must be assessed before use. To meet this objective a range of experiments were conducted to ascertain the behaviour of both the superplasticiser itself and a range of key radionuclides, in conditions representative of the GDF. Experimental objectives are outlined below:

1. Assessment of the effect of ADVA Cast 551 on the solubility of U (VI), Th (IV), Eu (III) and Ni (II) in high pH aqueous solutions that are representative of conditions within the GDF. ADVA Cast 551 will be present at a range of concentrations that correspond to the manufacturers recommended dosage.
2. Evaluate the effect of the presence of ADVA Cast 551 on uptake of metals to cement surfaces, and the reversibility of metal adsorption in the presence of superplasticiser.
3. Investigate the leaching behaviour of superplasticiser and metals from hardened cement.
4. Carry out experiments to demonstrate the stability of ADVA Cast 551 to thermal, chemical and radiolytic degradation.
5. Assess the effect of irradiated ADVA Cast 551 on the solubility of U (VI), Th (IV), Eu (III) and Ni (II) in high pH aqueous solution.
6. Characterise the products associated with the degradation of ADVA Cast 551 under thermal, chemical and radiolytic attack.

2 Experimental

2.1 Chemicals and Reagents

2.1.1 *NaOH and $Ca(OH)_2$*

Analytical grade calcium hydroxide ($Ca(OH)_2$, Fisher, UK) and 2 mol dm^{-3} Sodium hydroxide (NaOH free from carbonate, Fisher, UK) were used for the preparation of solutions for solubility experiments. Deionised water (E-Pure, Barnstead) which had been boiled for 3 hours and sparged with N_2 for 3 hours was used to prepare all solutions.

95% Saturated $Ca(OH)_2$ solution was prepared by adding an excess of $Ca(OH)_2$ solid (5 g) to 1 dm^3 of boiled and sparged DI water. This was left to equilibrate for 48 hours on an orbital shaker. The solution was then transferred into a N_2 atmosphere glove box and pre-filtered by gravity filtration. The saturated solution was then filtered using 30 kDalton membrane filters (Millipore). The filters were preconditioned by soaking overnight in a solution of 0.1 mol dm^{-3} NaOH to remove the protective coating. Finally, the saturated solution was diluted with boiled and sparged DI water to give a final solution of 95% saturation. The final pH was 12.4 ± 0.4.

2.1.2 *Cement Materials*

Ordinary Portland Cement – BNFL specification 7th revision. Manufactured to comply with the requirements of BS EN 197-1:2000 type CEM I, Portland Cement Strength Class 42,5N (Ketton OP Ordinary Portland Cement, Castle Cement).

Blast Furnace Slag – BNFL specification 7th revision (Civil and Marine).

Pulverised Fly Ash – Class S, Category B Manufactured to comply with the requirements of BS EN:2005 to BNFL specification 6th revision (from Drax Power Station, CEMEX).

2.1.3 *Metal Salts*

Uranyl Nitrate $UO_2(NO_3)_2$ (BDH Laboratory Reagents)

Nickel Nitrate $Ni(NO_3)_2$ (Sigma Aldrich), ^{63}Ni Spike (Stock Specific Activity = 37 MBq ml^{-1}, Eckert & Ziegler).

Europium Chloride $EuCl_3$ (Acros Organics), ^{152}Eu Spike (Stock Specific Activity = 74 MBq ml^{-1}, Eckert & Ziegler).

Thorium Nitrate $Th(NO_3)_4$ (Fluka)

2.1.4 *ADVA Cast 551*

ADVA Cast 551 (Grace Construction Products) is a polycarboxylated poly ether comb type superplasticiser. It is an accelerating superplasticiser designed to yield high range water reduction, short setting times and high early compressive strength. The repeating unit for the polymer is shown in Figure 6.

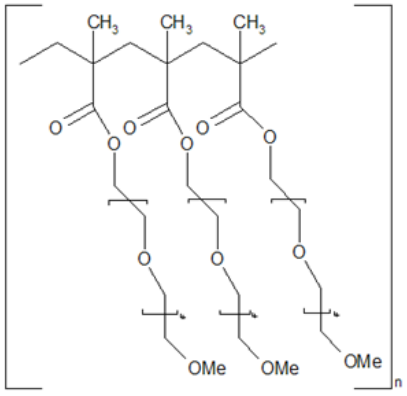

Figure 6 ADVA Cast 551

2.2 Instrumentation

2.2.1 *Glove Box*

A UNILab MBRAUN nitrogen atmosphere glove box was used for all experiments that were required to be conducted in anoxic conditions.

2.2.2 *pH Meter*

An Orion 720A pH meter and probe was calibrated daily using standards of pH 4, 7, 10 and 13 (Fisher) and was used only when the calibration slope (measure of reliability) was ≥95%.

2.2.3 *Liquid Scintillation Counter*

A Tri- Carb 2750 TR/LL (Packard) liquid scintillation counter and Gold Star Liquid Scintillation Cocktail (Meridian) were used for the measurement of ^{63}Ni. ^{63}Ni is a beta-emitter with emission energy of 65 keV. A counting channel between 0 and 100 keV was therefore selected for analysis. The count time for each sample was adjusted to ensure that the error associated with each count was 2σ (σ corresponds to the standard deviation of an infinite population of measurements, following a Gaussian distribution). This value represents the perecentage of uncertainty in a gross count value (with 95% confidence) and is calculated according to Equation 2.

$$2\sigma = \frac{200}{\sqrt{\text{accumulated counts}}}$$

Equation 2 Mathematical Determination of 2 Sigma

The liquid scintillation counting method was checked for quenching by the sample channels ratio method (52). No quenching was observed in these checks and therefore quench correction of the measurements was not necessary.

2.2.4 *Gamma Spectrometer*

A Cobra II Auto Gamma Spectrometer (Packard) was used for the radiometric measurement of ^{152}Eu. ^{152}Eu is a gamma-emitter which emits gamma photons with a range of energies (122, 344, 779, 1086, 1112 and 1408 keV). A counting channel with a range between 100 and 1500 keV was therefore selected for analysis. The count time for each sample was adjusted to ensure that the error associated with each count was 2σ.

2.2.5 *ICP-OES*

An iCAP 6000 Series ICP-OES Spectrometer (Thermo Scientific) was used for the analysis of uranium and nickel concentrations greater than 3×10^{-6} mol dm^{-3} and 2×10^{-7} mol dm^{-3} (The ICP-OES limit of quantification values for uranium and nickel respectively). Instrumental conditions are shown in Table 11.

Table 11 ICP-OES Instrumental Conditions

Instrumental Condition	**Uranium**	**Nickel**
λ (nm)	367.007	221.647
RF Power (W)	1150	1150
Auxiliary Gas Flow (dm^{-3} min^{-1})	0.5	0.5
Nebuliser Gas Flow (dm^{-3} min^{-1})	0.5	0.5
Coolant Gas Flow (dm^{-3} min^{-1})	12	12

2.2.6 *ICP-MS*

A 7700x Series quadrupole ICP-MS (Agilent Technologies) was used for the analysis of uranium and nickel for concentrations below 3 x 10^{-6} mol dm^{-3} and for all thorium measurements.

The ICP-MS instrument (plasma, flow and lenses) was tuned on a daily basis with a standard tuning solution of 1µg dm^{-3} Li, Mg, Y, Ce, Ti, Co (Agilent). This process was conducted to ensure the optimum signal and sensitivity for analysis.

2.2.7 *HPLC – Gel Permeation Chromatography*

A 1200 series HPLC (Agilent Technologies) with a Zorbax BIMODAL size exclusion chromatography column (Agilent Technologies) and refractive index detection was used for the analysis of superplasticiser. Polystyrene standards ranging from 2450 to 475,000 molecular weight (Polymer Laboratories) were used for calibration. Instrumental conditions are shown in Table 12

Table 12 Gel Permeation Chromatography Conditions

Eluent (Polystyrene)	THF
Eluent (Sample)	Methanol
Flow Rate (ml/min)	0.4
Temperature (Detector) ºC	35
Injection Volume (µl)	10

2.2.8 *Dionex Ion Chromatograph*

A Dionex DX-100 ion chromatograph, with supressed conductivity detection, in isocratic mode with an IonPac AS4A-SC column was used for the analysis of anions. Instrumental conditions are shown in Table 13.

Table 13 Dionex Instrumental Conditions

Eluent	2.2mM Sodium Carbonate: 2.8mM Sodium Bicarbonate. (AS3/AS4 Eluent Concentrate –Dionex)
Flow Rate (ml/min)	2.0
Temperature	Ambient temperature (25ºC)
Applied Current (mA)	27
Injection Volume (µl)	25

2.2.9 *Infrared Spectrophotometer*

Infrared spectra were obtained using a Perkin Elmer Spectrum 65 FT-IR spectrometer.

2.2.10 *Ultraviolet Spectrophotometer*

Ultraviolet spectroscopy was measured using a Varian 50Bio UV spectrometer.

2.2.11 *Electro-Spray Ionisation Mass Spectrometer*

Mass spectra were obtained using a Waters Micromass LCT Electro-Spray Ionisation Mass Spectrometer.

2.2.12 *GC-MS*

Gas chromatography- Mass spectrometry was performed using a GC 8000 series, GC 8060 Mass Spectrometer.

2.2.13 *Zetamaster*

Zeta Potential was measured using a Zetamaster (Malvern Instruments).

2.3 Characterisation of Materials

2.3.1 *Cement Materials*

BFS:OPC and PFA:OPC cement plus the individual components BFS, PFA and OPC were characterised by Inductively coupled plasma- optical emission spectrometry, Ion chromatography and BET.

2.3.1.1 Cement Preparation

BFS:OPC and PFA:OPC cement samples were prepared omitting superplasticiser to characterise the cations and anions present.

BFS:OPC cement was prepared at a ratio of 9:1 (w/w – weight for weight) whilst PFA:OPC cement was prepared at a ratio of 3:1 (w/w). The cement powder components were weighed according to the composition shown in Table 14 and mixed thoroughly. The water portion was weighed into a plastic beaker and the powder added slowly over two minutes with stirring. The mix was stirred for a further four minutes before being poured into a plastic mould. This method for cement preparation was obtained from Morgan and Constable (2008) (53). The moulds were covered with parafilm and left for twenty four hours before de-moulding. The specimens were then cured submerged in water for twenty eight days. After curing, the samples were allowed to dry for twenty four hours and broken up first using a geological hammer and then a mortar and pestle.

Table 14 Cement Mix Formulations

Sample	Water (g)	BFS (g)	PFA (g)	OPC (g)	w/s
BFS:OPC	52.92	132.3	0	14.7	0.36
PFA:OPC	52.92	0	110.25	36.75	0.36

2.3.1.2 Cement Analysis

Acid digestion uses oxidising acids and an external heat source/microwave to decompose a sample matrix (54). The sample can then be analysed by ICP-OES. BFS:OPC cement, PFA:OPC cement plus the individual components of BFS, PFA and OPC were decomposed by two types of acid digestion, Aqua Regia and HF, by Enviras Ltd.

Aqua Regia is a 1:3 (v/v) mixture of concentrated HNO_3:HCl and forms the reactive intermediate NOCl on mixing. HF is also used as it is the only acid able to digest the silica (SiO_2) in the samples.

For digestion by Aqua Regia, 100 mg of each cement sample were digested in Aqua Regia (8 cm^3) in a CEM microwave. The samples were filtered by gravity and diluted with deionised water to 100 cm^3. 1 cm^3 of this stock was further diluted to 100 cm^3 before analysis.

For digestion by HF, 100 mg of each cement sample were digested in HF (3 cm^3) in a CEM microwave. The samples were filtered by gravity and diluted with deionised water to 250 cm^3. 1 cm^3 of this stock was further diluted to 100 cm^3 before analysis.

Cation analysis was performed using ICP-OES. A multi- element standard (Thermo Scientific) was used to calibrate the instrument. Metals investigated were: Al, As, Ba, Ca, Co, Cr, Cu, Fe, K, Mg, Mn, Na, Nb, Ni, P, Pb, S, Si, Sr, Ti, V, Zn, Zr (Calibration data shown in APPENDIX 1 – Instrument Calibration Data).

2.3.1.1 BET

BET measurements of each of the samples were made at the British Geological Survey according to the method by Kemp et al. (2009) (55).

BET is named after Brunauer, Emmet and Teller who first published a paper on BET theory in 1938. BET measures the specific surface area of a material based on the adsorption of gas on the surface. The amount of gas adsorbed at a given pressure allows for the determination of the surface area. The standard BET equation may be written as shown in Equation 3 (56)

$$\frac{P_{rel}}{V\,(1-P_{rel})} = \frac{1}{V_m\,C_{BET}} + \frac{P_{rel}\,(C_{BET}-1)}{V_m\,C_{BET}}$$

Equation 3 BET equation

Where P_{rel} is the pressure of the gas in equilibrium with the specimen P, relative to the saturation vapour pressure P_0. V is the amount of gas adsorbed at

pressure P. C_{BET} is a constant and V_m is the amount of gas required for a monolayer of coverage. The specific surface area, S (m^2 g^{-1}), may then be calculated using Equation 4.

$$S = \frac{N_m \sigma}{m}$$

Equation 4 Specific surface area

Where N_m is the number of gas molecules in one monolayer and may be substituted for (V_m/v) where v is one molecular volume. σ is the cross sectional area of a gas molecule and m is the mass of the specimen.

2.3.2 *Characterisation of ADVA Cast 551*

2.3.2.1 Infrared Spectroscopy

Due to the aqueous nature of the superplasticiser samples, a Micro Quik Cell Kit with AgCl window was used to obtain IR spectra. Care was taken to avoid over exposure of the AgCl plates to light as discolouration may occur.

A blank was taken of the AgCl plate prior to the analysis of the samples. The samples were pipetted onto the AgCl plate and the sample cell placed in the sample holder.

2.3.2.2 Ultraviolet Spectroscopy

A UV spectrum was recorded by preparing an aqueous solution of the superplasticiser (1% w/v) and measuring the UV/Vis absorption using a 1 cm^2 quartz cell. The superplasticiser (a carboxylate polymer) has an absorption maximum below the lower wavelength limit of the equipment (190 nm) and therefore only an increase in signal is observed towards 190 nm.

2.3.2.3 Gas Chromatography – Mass Spectrometry

2 cm^3 samples of superplasticiser were prepared for GC-MS by extraction into 5 cm^3 of dichloromethane (DCM). The superplasticiser were first acidified with 0.5 mol dm^{-3} HNO_3 to ensure the organics were in acidic form, and then shaken with DCM. The aqueous phase was separated from the organic phase and the organic portion analysed.

2.3.2.4 Electrospray Ionisation – Mass Spectrometry

An electrospray is the aerosol formed when a high voltage is applied to a liquid stream (the analyte and solvent). The electrospray contains positively and negatively charged droplets and is sampled into a vacuum via a capillary where solvent evaporation occurs. Solvent evaporation continues until the droplet becomes unstable, reaching its Rayleigh Limit and deforms to release ions into the gas phase. The ions are separated according to their mass to charge ratio (m/z) in a mass analyser by the application of electromagnetic fields.

Before analysis by ESI-MS the samples were prepared by performing a solid phase extraction (SPE) to remove any salts present in the samples. Salts prevent the formation of an electro-spray and can damage the capillary.

The samples were centrifuged for thirty minutes at 6000 rpm and then acidified with 1 mol dm^{-3} HCl. SPE cartridges (Supelco Discovery DSC-18) were fitted to a vacuum pump then conditioned firstly with methanol, and then acidified with HCl. 1cm^3 of sample was then injected into the column. The column was washed with water (acidified with HCl) to remove the soluble salts and finally washed with methanol to remove the analytes of interest.

2.3.2.5 Gel Permeation Chromatography

Gel permeation chromatography (also known as size exclusion chromatography) separates analytes on the basis of size. There is no chemical or physical interaction of the analyte with the column. Separation is possible via porous silica beads packed into the column. Small analytes are able to enter the pores and are therefore retained longer on the column. Larger molecules are unable to fit into the pores and are eluted more quickly (see Figure 7 Schematic to show pore vs analyte size).

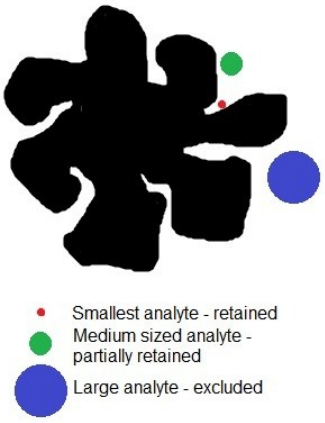

Figure 7 Schematic to show pore vs analyte size

GPC with refractive index (RI) detection was used for the analysis of superplasticiser. Refractive index detection is used commonly in polymer analysis and although less sensitive than UV detection, it is useful in the detection of analytes which do not have a chromophore.

The refractive index detector works by measuring the refractive index of a medium in a sample cell relative to that of a reference cell. As light passes from one transparent medium to another, there is a change in velocity and the light bends. The extent of this bending depends on the refractive index of the media, and the angle between the light ray and the line perpendicular to the surface separating the media (normal). Each medium has a different refractive index. The angle between the light ray and the normal as it leaves a medium is the angle of incidence and the angle between the light ray and the normal as it enters a new medium is the angle of refraction (see Figure 8).

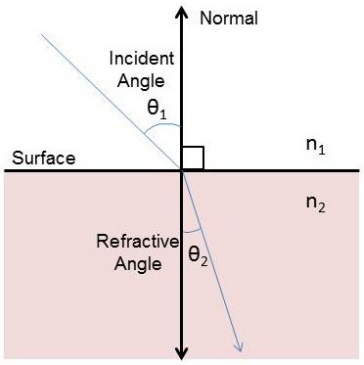

Figure 8 Refraction of light at the interface of two media

The refractive index may be defined mathematically as the ratio of the sines of the angle of incidence and angle of refraction as light passes through the two mediums. This definition is based on Snell's Law (Equation 5)

$$\frac{n_1}{n_2} = \frac{\sin\theta_1}{\sin\theta_2}$$

Equation 5 Snell's Law

Where n_1 and n_2 are the refractive indexes of medium 1 and 2 and θ_1 and θ_2 are the angles of incidence and refraction respectively.

To optimise the RI detector and check for sensitivity to the superplasticiser polymer, a number of solutions were pumped through the detector with the column detached and the response recorded. The changes in detector response were quoted in nRIU which are arbitrary units. After each change of solution, the signal was allowed to stabilise for 10 minutes. The reference cell was kept constant as methanol. The solutions pumped and their RI responses are shown in Table 15.

Table 15 Refractive Index Detector Optimisation

Solution	Response (nRIU)
Methanol	30,000
Deionised Water	140,000
THF	60,000
0.1% ADVA Cast (w/v) in methanol	90,000
1% ADVA Cast (w/v) in methanol	700,000

Table 15 shows that the RI detector is sensitive enough to detect the superplasticiser in solution.

To determine the molecular weight of the superplasticiser and the products of the stability experiments, the GPC was calibrated using polystyrene standards. The standards were dissolved in THF and run for 25 minutes at a flow rate of

0.4 ml/min. This flow rate was chosen as the optimum for a fast sample time but with optimum peak separation and sharpness. The molecular weights and retention times for these standards are shown in Table 16.

Table 16 GPC Calibration - M_w vs Retention time

Standard M_w	Retention Time (min)
2450	10.375
5000	9.843
7000	9.689
11,600	9.410
22,000	9.121
106,000	8.452
198,000	8.069
336,000	7.962
475,000	7.793

A calibration curve of log[M_w] vs retention time was plotted (Figure 9) and used to determine M_w of the superplasticiser samples.

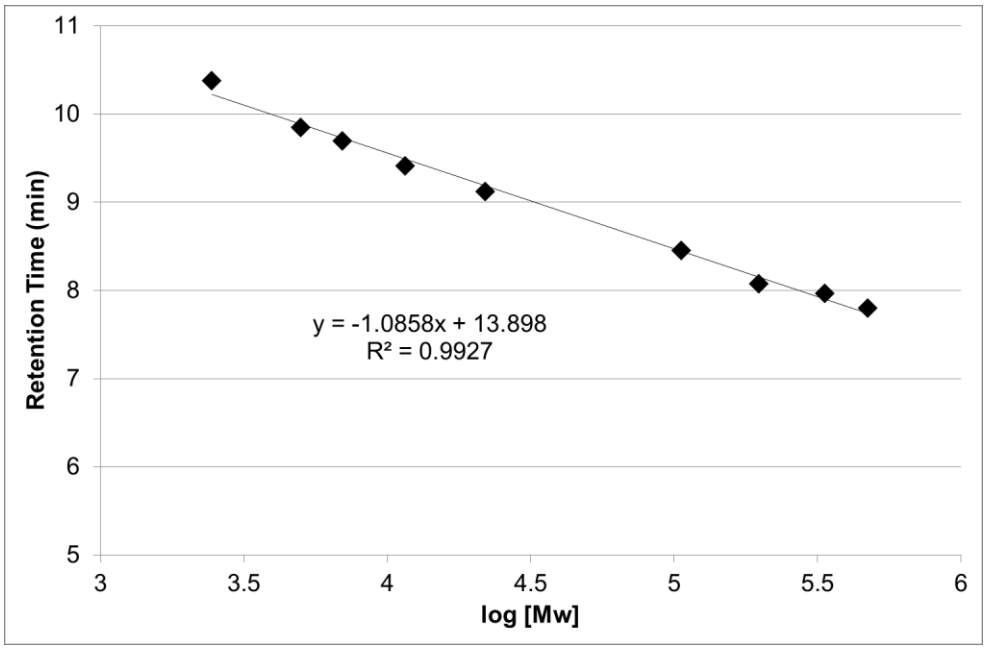

Figure 9 GPC Calibration log[Mw] vs Retention time

2.4 Characterisation of Cement Equilibrated Water

2.4.1 *Preparation of Cement Equilibrated Water*

Cement equilibrated water was prepared by contacting boiled and N_2 sparged DI water with cement powders with agitation for twenty eight days. The ratio of DI water to cement solid was 50:1 (volume of water to weight of cement solid) (ratio previously reported by Greenfield et al. (1998) (46)).

1 dm^3 of cement equilibrated water was therefore prepared by adding the following cement powders to 1 dm^3 of boiled and sparged DI water:

1. BFS:OPC (Ratio of 9:1 (w/w) 18 g BFS powder and 2 g OPC powder)
2. PFA:OPC (Ratio of 3:1 (w/w) 15 g PFA powder and 5 g OPC powder)
3. BFS only (20 g)
4. PFA only (20 g)
5. OPC only (20 g)

After equilibration, the solutions were transferred to a N_2 atmosphere glove box and filtered first by gravity to remove the solid cement and then with 30 kDalton membrane filters (Millipore). The final pH of all the cement equilibrated water solutions was 12.4 ± 0.3 except for PFA equilibrated water which had a final pH of 10 ± 0.5.

2.4.2 *Cation Analysis of Cement Equilibrated Waters*

Cation analysis was performed using ICP-OES. A multi-element standard (Thermo Scientific) was used to calibrate the instrument. Metals investigated were: Al, Ca, Cd, Co, Cr, Cu, Fe, K, Li, Mg, Mn, Na, Ni, Pb and Zn (Calibration data shown in APPENDIX 1 – Instrument Calibration Data). 5 cm^3 of each cement equilibrated solution was acidified with 0.5% analytical grade HNO_3 before analysis. Ca was analysed separately due to the expected high concentration of Ca in the samples. These samples were diluted 100 times before analysis. Si was measured using ICP-MS due to the low solubility of silica in high pH solution. The instrument was calibrated using a separate Si

standard (Thermo Scientific). (Calibration data is shown in APPENDIX 1 – Instrument Calibration Data).

2.4.3 *Anion Analysis of Cement Equilibrated Waters*

Anion analysis was performed using a Dionex DX-100 ion chromatograph (instrumental conditions given in 2.2.8). Instrument calibration was performed daily with a multi-anion standard (Dionex) plus sodium thiosuphate and sodium sulphite individually. Anions investigated were F^-, Cl^-, NO_3^-, SO_4^{2-}, SO_3^{2-} and $S_2O_3^{2-}$ (calibration data shown in APPENDIX 1 – Instrument Calibration Data). The cement equilibrated water samples were injected without dilution.

2.4.4 *Speciation Calculations*

Aqueous speciation of U (VI), Th (IV), Eu (III) and Ni (II) was predicted using the speciation tool JCHESS (71). The complex nature of cement systems means that simple hand calculations are not sufficient to describe the range of possible reactions and species formed in solution. Geochemical modelling software is widely used as a predictive tool which allows the user to ascertain how materials could behave in a certain environment. JCHESS is capable of predicting possible reactions and is especially useful in this research in predicting aqueous metal speciation in a given solution, along with an estimation of the concentration of each species. The total concentration of all aqueous metal species then gives an indication as to the solubility of that metal in the solution.

2.5 Effect of Superplasticiser on Metal Solubilities

2.5.1 *Oversaturation*

An oversaturated solution becomes a saturated solution by forming a solid (precipitate) and reducing the dissolved material. The equilibrium constant for a saturated solution and precipitate formation is the solubility product $K_{sp.}$ In high pH solution, metal solubility is generally low. To approach a metal solubility measurement from oversaturation, an excess of the metal (a concentration which exceeds the solubility limit) is added to solution so that a precipitate is

formed. The solubility of a metal in a given solution may then be measured by removing an aliquot of supernatant, and analysing for the metal of interest. The effect of a ligand on metal solubility may be observed by adding a known concentration of the ligand to the solution and comparing the difference in the metal concentration in the supernatant.

All sample preparation and sampling was conducted inside a N_2 atmosphere glove box at 22ºC unless stated otherwise. Solutions of ADVA Cast 551 were prepared at a range of concentrations (%w/v) using 95% saturated $Ca(OH)_2$, 0.1 mol dm^{-3} NaOH and cement equilibrated solutions (BFS:OPC, PFA:OPC plus BFS, PFA and OPC individually). NaOH and $Ca(OH)_2$ were prepared as in (2.1.1) and cement equilibrated solution as in (2.4.1). The manufacturer's guidelines suggest that ADVA Cast should be added to cement at between 0.3% and 1% (v/w) (57) therefore the following solutions of ADVA Cast 551 were prepared: 0%, 0.1%, 1% and 10% (w/v) for investigation. 10% samples were prepared in order to assess the effect of the superplasticiser at exceptionally high concentrations.

25 cm^3 of sample were placed into a 50 cm^3 screw-top centrifuge tube and the metal nitrate/chloride added at a concentration greater than the solubility limit. The total inventory of metal added to each sample is shown in Table 17. Samples were produced in quadruplicate along with blank samples containing no metal.

The steady state pH of the cement equilibrated solutions was >pH 12 in all cases except PFA equilibrated water which was pH 10. Adjustments were made to PFA equilibrated samples using 2 mol dm^{-3} carbonate free NaOH so that each sample had a pH of between pH 12 – 13. If the PFA samples were allowed to equilibrate at their natural pH, it is expected that the solubility of metal would be higher since a decrease in pH correlates with an increase in metal solubility. For completeness and to confirm this theory, an experiment was conducted using non-adjusted PFA equilibrated water on U (VI) solubility with the presence of 0% and 1% ADVA Cast 551 at day 7 and day 28.

Table 17 Total Inventory of Metal Salt per Sample

Metal Salt	**Inventory per sample (mol dm^{-3})**
$Ni(NO_3)_2$	5×10^{-3}
$EuCl_3$	5×10^{-4}
$Th(NO_3)_4$	5×10^{-4}
$UO_2(NO_3)_2$	5×10^{-3}

The Ni (II), Eu (III) and U (VI) samples were equilibrated on a flat-bed shaker. Th (IV) samples were prepared, sealed and then transferred to a fridge between sampling days. This modification to the method was necessary due to the colloidal nature of the ThO_2 precipitate which was very easily re-dispersed giving a falsely high solubility value.

The experiment was conducted over 28 days. 2 cm^3 samples were removed every 7 days as part of a kinetic study. The samples were filtered through 0.45 µm syringe filters before analysis. 0.45 µm filters were used rather than 0.22 µm filters due to the polymeric nature of the ADVA Cast 551 which blocked the filter membrane, not allowing any solution through. The solubility values obtained were within the ranges of published data (see Table 4, Table 5, Table 6, and Table 7 for U (VI), Th (IV), Eu (III) and Ni (II) respectively) and so observed increases in solubility due to colloidal matter rather than the superplasticiser can be discounted.

2.5.2 *Metal Analysis*

2.5.2.1 Nickel

Nickel was measured using ICP-OES and ICP-MS. The filtered samples were acidified with 0.5% analytical grade HNO_3 before analysis. The instruments were calibrated using nickel standard solutions (Thermo Scientific) on a daily basis. (Instrumental conditions shown in 2.2.5 and calibration data shown in APPENDIX 1 – Instrument Calibration Data)

2.5.2.2 Europium

The filtered europium samples were measured using Gamma Spectrometry. (Instrumental conditions shown in 2.2.4)

2.5.2.3 Thorium

Thorium was analysed using ICP-MS. Filtered samples were acidified with 0.5% analytical grade HNO_3 before analysis. The ICP-MS was calibrated using a thorium standard (Thermo Scientific) on a daily basis (Instrumental conditions shown in 2.2.6 and calibration data shown in APPENDIX 1 – Instrument Calibration Data).

2.5.2.4 Uranium

Uranium was measured using ICP-OES and ICP-MS (Instrumental conditions shown in 2.2.5 and 2.2.6 respectively). The filtered samples were acidified with 0.5% analytical grade HNO_3 before analysis. Calibration of the instruments was conducted using uranium standard solutions (Thermo Scientific) on a daily basis (Calibration data shown in APPENDIX 1 – Instrument Calibration Data)

2.6 Uptake of Superplasticiser onto Cement Surfaces

Uptake of ADVA Cast 551 onto crushed BFS:OPC grout, crushed PFA:OPC grout and the individual cement components (BFS, PFA and OPC) were evaluated by TOC (Total Organic Carbon) analysis. This method was adapted from the methods reported in (21,58,59). BFS:OPC grout and PFA:OPC grout were prepared without superplasticiser (according to 2.3.1.1), crushed, sieved and the <180 μm fraction used for the experiments. BFS, PFA and OPC powders were used without modification. (BET data shown in Table 20)

Solutions of ADVA Cast 551 were prepared using the appropriate cement equilibrated water at 0%, 0.2%, 0.5% and 1% (w/v). 0.5 g of solid were weighed into a plastic vial and 10 cm^3 of solution added. The liquid to solid ratio for the samples was 20:1. The samples were allowed to equilibrate on a flat-bed shaker for twenty eight days at 22ºC. After this time, all the supernatant was removed from the solid, filtered through 0.45 μm syringe fingers and placed into

TOC analysis vials. The samples were weighed and diluted to 40 cm^3 before analysis.

The TOC analyser was calibrated daily using a 1000 ppm sucrose standard (Sievers). Quantification of ADVA Cast 551 was possible by analysing samples of known concentrations of ADVA Cast 551 (1000, 500, 250, 100, 50, 10 and 1ppm) and producing a calibration graph (shown in APPENDIX 1 – Instrument Calibration Data)

2.6.1 *Reversibility of Superplasticiser Removal from Cement Materials*

To measure the reversibility of superplasticiser uptake onto cement materials, all remaining supernatant were removed from the solid samples. 10 cm^3 of the relevant fresh cement equilibrated water, which contained no superplasticiser, were then added to the solid. The samples were allowed to equilibrate on a flatbed shaker for twenty eight days.

Aliquots of each sample supernatant were then removed and analysed as described in 2.6.

2.6.2 *Zeta Potential Measurements*

The zeta potentials of cements were measured by preparing a 1% (w/v) active slurry of each cement component – BFS, PFA and OPC and also a 1% (w/v) active slurry of BFS:OPC and PFA:OPC crushed cements (25). The samples were shaken intermittently for one week. The supernatant (cement particle suspensions) were then subjected to microelectrophoresis using a Zetamaster (60).

2.7 Uptake of Metals onto Cement Surfaces in the Presence and Absence of Superplasticiser.

All experiments were conducted at a temperature of 22ºC.

2.7.1 *Uptake of Metals onto Cement Prepared Without Superplasticiser*

Uptake of Ni (II), Eu (III) and U (VI) onto crushed BFS:OPC grout and crushed PFA:OPC grout was investigated by a batch experiment. BFS:OPC or

PFA:OPC grout (prepared as in 2.3.1.1) were crushed, sieved and the <180 μm fraction used for the experiments. 0.5 g of solid were weighed into plastic vials.

Solutions of $Ni(NO_3)_2$, $EuCl_3$ and $UO_2(NO_3)_2$ were prepared at a concentration of 1 x 10^{-9} mol dm^{-3} using the appropriate cement equilibrated water. This concentration was lower than the reported solubility limit for each metal (reported in Table 4, Table 6 and Table 7 for U (VI), Eu (III) and Ni (II) respectively) though it is noted that the conditions here are not exactly the same. Such a concentration was taken to be indicative of the level necessary to ensure that changes in the concentration of metal in solution were unlikely to be due to a solubility effect caused by metal precipitation. 10 cm^3 of solution were added to the solid and a spike of ^{63}Ni or ^{152}Eu was added to the nickel and europium samples to bring the activity of each sample to 3 kBq. No radioactive spike was added to the uranium samples. The samples were allowed to equilibrate on a flat-bed shaker for twenty eight days at.

Nickel samples were analysed by LSC (Liquid Scintillation Counting). 1 cm^3 of supernatant were filtered through 0.45 μm filters and weighed into a LSC vial. 10 cm^3 of Gold Star LSC cocktail added. The samples were shaken on a whirl-mixer and allowed to settle for one hour before counting.

Europium samples were analysed by Gamma Spectrometry. 2 cm^3 of supernatant were filtered through 0.45 μm filters and weighed into a plastic gamma vial then counted.

Uranium samples were measured by ICP-MS. 2 cm^3 of supernatant were removed, filtered through 0.45 μm filters and acidified with 0.5% analytical grade HNO_3 before analysis.

(For Instrumental Conditions see 2.2)

A blank experiment was also conducted to check for metal loss to the walls of the sample vials. A set of sample vials that had contained no solid, but had contained the metal solutions and the radioactive spike, were washed three times with 1 cm^3 aliquots of 0.5% HNO_3 and the washings were measured for the metals of interest. No loss to the vials was observed and so correction calculations were not required.

2.7.2 *Uptake of Metals onto Cement Prepared with 0.5% (w/s) ADVA Cast 551*

Hardened cement containing superplasticiser were prepared as follows; the cement powder components were weighed according to the composition shown in Table 18 and mixed thoroughly. The water portion were weighed into a plastic beaker and the superplasticiser added. The powder was then added slowly over two minutes with stirring. The mix was stirred for a further 4 min before being poured into a plastic mould. This method for cement preparation was obtained from Morgan and Constable (2008) (53). The moulds were covered with parafilm and left for twenty four hours before de-moulding. The specimen were then cured in >90% humidity (submerged in water) for twenty eight days. After curing, the samples were allowed to dry for twenty four hours and broken up first using a geological hammer and then a mortar and pestle. The samples were sieved and the ≤180µm fraction was used for the experiment.

Table 18 Cement Mix Formulations (with Superplasticiser)

Sample	**Water (g)**	**% SP**	**ADVA Cast 551 (g)**	**BFS (g)**	**PFA (g)**	**OPC (g)**	**w/s**
BFS:OPC	51.92	0.5	1	132.3	0	14.7	0.36
PFA:OPC	51.92	0.5	1	0	110.25	36.75	0.36

It was found that uranium uptake by cement that did not contain superplasticiser could not be measured by ICP-MS as the concentration of U (VI) in solution was lower than the detection limits for the instrument. Metal uptake to cement containing superplasticiser was therefore investigated with Ni (II) and Eu (III) only.

0.5g of solid were weighed into plastic vials. Solutions of $Ni(NO_3)_2$ and $EuCl_3$ were prepared as in 2.7.1 and a spike of ^{63}Ni or ^{152}Eu were added to each sample respectively to bring the activity of each sample to 3 kBq.

The samples were allowed to equilibrate on a flat-bed shaker for twenty eight days.

Nickel samples were analysed by LSC (Liquid Scintillation Counting). 1 cm^3 of supernatant were filtered through 0.45 μm filters and weighed into a LSC vial. 10 cm^3 of Gold Star LSC cocktail added. The samples were shaken on a whirl-mixer and allowed to settle for one hour before counting.

Europium samples were analysed by Gamma Spectrometry. 2 cm^3 of supernatant were filtered through 0.45 μm filters and weighed into a plastic gamma vial then counted.

2.7.3 *Reversibility of Metal Uptake by Cement Prepared Without Superplasticiser*

All remaining supernatant was removed from the solid samples. 10 cm^3 of the relevant fresh cement equilibrated water, which contained no metal, were added to the solid. The samples were allowed to equilibrate on a flatbed shaker for twenty eight days.

Aliquots of each sample supernatant were then removed and analysed as described in 2.7.1.

2.7.4 *Reversibility of Metal Uptake by Cement Prepared with 0.5% (w/s) ADVA Cast 551*

Measurement of the reversibility of metal uptake by cement containing superplasticiser was conducted as described in 2.7.3.

2.8 Leaching of Superplasticiser and Metals from Hardened Cement

All experimental preparation and sampling was conducted at a temperature of 22ºC.

2.8.1 *Cement Preparation*

2.8.1.1 Superplasticiser Leaching Experiment

BFS:OPC and PFA:OPC cement containing ADVA Cast 551 at 0.5% (w/v) were prepared as in 2.7.2. BFS:OPC and PFA:OPC were also prepared without the addition of superplasticiser as blanks. These blanks will enable any extra

organic present in the cement (such as grinding aid) to be taken into account in the leaching calculations.

2.8.1.2 Metal Leaching Experiment

The leaching behaviour of U (VI), Th (IV) and Ni (II) from BFS:OPC and PFA:OPC cement prepared with and without the addition of superplasticiser was investigated.

BFS:OPC and PFA:OPC cement were prepared containing the following concentrations of U (VI), Th (IV) and Ni (II):

- U (VI) – 8.4×10^{-7} mol g^{-1} (moles per gram of cement)
- Th (IV) – 8.6×10^{-7} mol g^{-1}
- Ni (II) – 3.4×10^{-6} mol g^{-1}

These concentrations correspond to a metal loading of 200ppm (w/w). $UO_2(NO_3)_2$, $Th(NO_3)_4$ and $Ni(NO_3)_2$ crystals were weighed and added to the water portion of each cement mix. Since these metal nitrates are soluble in water at near neutral pH, by adding them at this stage, before mixing with the powders, the resultant cement blocks were assumed to be homogeneous after mixing. The formulation of each cement block is shown in Table 19.

Table 19 Cement Formulations – U (VI), Th (VI) and Ni (II) leaching experiment

Sample	OPC (g)	BFS (g)	PFA (g)	ADVA Cast 551 (g)	Water (g)	w/s ratio	$UO_2(NO_3)_2$ (g)	$Th(NO_3)_4$ (g)	$Ni(NO_3)_2$ (g)
BFS:OPC No SP	14.7	132.3	-	0	52.92	0.36	-	-	-
BFS:OPC No SP – U(VI)	14.7	132.3	-	0	52.92	0.36	0.7*	-	-
BFS:OPC No SP – Th(IV)	14.7	132.3	-	0	52.92	0.36	-	0.08	-
BFS:OPC No SP – Ni(II)	14.7	132.3	-	0	52.92	0.36	-	-	0.14
BFS:OPC 0.5% SP	14.7	132.3	-	1	51.92	0.36	-	-	-
BFS:OPC 0.5% SP – U(VI)	14.7	132.3	-	1	51.92	0.36	0.7*	-	-
BFS:OPC 0.5% SP – Th(IV)	14.7	132.3	-	1	51.92	0.36	-	0.08	-
BFS:OPC 0.5% SP – Ni(II)	14.7	132.3	-	1	51.92	0.36	-	-	0.14
PFA:OPC No SP	36.75	-	110.25	0	52.92	0.36	-	-	-
PFA:OPC No SP – U(VI)	36.75	-	110.25	0	52.92	0.36	0.7*	-	-
PFA:OPC No SP – Th(IV)	36.75	-	110.25	0	52.92	0.36	-	0.08	-
PFA:OPC No SP – Ni(II)	36.75	-	110.25	0	52.92	0.36	-	-	0.14
PFA:OPC 0.5% SP	36.75	-	110.25	1	51.92	0.36	-	-	-
PFA:OPC 0.5% SP – U(VI)	36.75	-	110.25	1	51.92	0.36	0.7*	-	-
PFA:OPC 0.5% SP – Th(IV)	36.75	-	110.25	1	51.92	0.36	-	0.08	-
PFA:OPC 0.5% SP – Ni(II)	36.75	-	110.25	1	51.92	0.36	-	-	0.14

* Uranium blocks were prepared at 2000ppm (w/w) (8.4×10^{-6} mol g^{-1}) in error however the experiment was continued and the difference in concentration taken into account in the calculations.

2.8.2 *Leaching Experiments*

The design of the leaching experiment was based on the 'Tank Leach Test' as described by Takahashi et al. (2007) and Conner (1990) (61)(62). The amount of leaching is dependent on; the fixation of the elements by the CSH produced during the hydration of the cement, the formation of metal hydroxides at high pH and the decrease of metal diffusion due to the decrease of pore volume. Cement prepared with superplasticiser has a lower porosity than cement prepared without superplasticiser, therefore it may be expected that leaching of metal or superplasticiser through diffusion alone may be reduced in those samples.

After mixing, the cement was poured into plastic moulds, covered with parafilm, and allowed to set for forty eight hours. After this time, the samples were de-moulded and both ends of each block sealed with paraffin wax. The blocks were then submerged in the appropriate cement equilibrated water (either BFS:OPC or PFA:OPC equilibrated water depending on the formulation of the block) and sealed in screw top Pyrex jars. The samples were left for four months before sampling.

It was noted that in the case of the BFS:OPC samples, a significant amount of bleed water was present after the forty eight hours set time. The amount of bleed was greater in the samples that contained superplasticiser. In the case of the samples containing uranium, it was observed that the bleed was yellow indicating the presence of the metal within the bleed water. The bleed water was collected and analysed for the metal of interest by ICP-MS and the amount of metal leached in the bleed water was taken into account in all future calculations.

2.8.3 *Analysis of Leached Superplasticiser*

10 cm^3 of leachate were removed from the jar, filtered through 0.45 μm syringe filters and diluted to 40 cm^3 before analysis for TOC.

The TOC analyser was calibrated daily using a 1000 ppm sucrose standard (Sievers). Quantification of leached ADVA Cast 551 was possible by analysing

samples of known concentrations of ADVA Cast 551 (1000, 500, 250, 100, 50, 10 and 1ppm) and producing a calibration graph (shown in APPENDIX 1 – Instrument Calibration Data).

2.8.4 *Analysis of Leached Metals*

U (VI), Th (IV) and Ni (II) were measured by ICP-MS. 5 cm^3 of leachate were filtered through 0.45 µm syringe filters and then acidified with 0.5% analytical grade HNO_3 before analysis. Calibration of the instrument was conducted using uranium, thorium and nickel standard solutions (Thermo Scientific) (Calibration data shown in APPENDIX 1 – Instrument Calibration Data).

2.8.5 *Imaging of Cement Monoliths*

To investigate the distribution of U (VI), Th (IV) and Ni (II) in the cement blocks after the leaching period, two imaging techniques were employed, Scanning Electron Microscopy (SEM) and Digital Autoradiography. The cement blocks were removed from the leachate solution and allowed to dry in air. A diamond circular blade saw was used to cut the blocks in half lengthways. Wet/dry sand paper was used to smooth the cut surface of the blocks before imaging.

2.8.5.1 SEM

Nickel was observed by Scanning Electron Microscopy (Field Emission Gun – SEM). The cut surface of each block was sputter coated with gold. Sputter coating is the process of covering a specimen with a thin layer of a conducting material, typically gold or palladium. This conductive coating is required to prevent the charging of the specimen with the electron beam. Due to the size of the sample, it was not possible to create a map of each block in its entirety. Set sampling points at the top edge, middle and bottom edge of the specimen were therefore chosen as representative samples.

2.8.5.2 Digital Autoradiography

Eu^{2+} doped BaClF storage phosphor autoradiography plates were used as a two dimensional radiation detection and recording medium.

The active component of the autoradiography plates is a thin layer of photostimulatable phosphor powder deposited on a polyester support and coated with an inert protective layer. When the plate is exposed to radiation, the energy is deposited in the phosphor crystals and transferred to a number of Eu^{2+} sites. The Eu^{2+} is oxidised to Eu^{3+} and an electron is excited into the conduction band of the crystal.

The electron is trapped in a lattice defect produced by the absence of a halogen counter ion known as 'F centres'. These centres are created during the manufacture of the plates. The electrons trapped in the F centres are metastable and collectively make up the digital image.

The image is read by an image reader that scans the plate with a focal-spot red laser. The photostimulated light is collected by a photomultiplier tube and converted to a digital image.

Although the image intensity is measured as a dimensionless quantity-photostimulated luminescence (PSL) it has been shown that PSL is linearly proportional to the radiation dose (63).

The storage phosphor plates were 'wiped' before use by exposure to a light box for thirty minutes. After exposure, the cement blocks were placed onto the plate and the plate sealed in a light tight box. The ^{238}U containing blocks were exposed for seven days while the ^{232}Th containing blocks were exposed for fourteen days due to the lower activity of ^{232}Th compared to ^{238}U.

After exposure, the images were read by a STORM 860 Laser Photostimulated Fluorescence Scanner (Amersham Biosciences) at the British Geological Survey.

2.9 Stability of ADVA Cast 551

2.9.1 *ADVA Cast 551 Stability*

There are a number of potential degradation pathways for superplasticisers under the conditions present within the near field of the geological disposal facility. The fate of superplasticisers under these conditions is unknown.

Temperatures within the repository can reach 80ºC due to the occurrence of exothermic chemical reactions such as the heat generating nature of cement hydration (64). The conditions of the repository porewater are also highly alkaline at between pH 12 and 13 and therefore there is the potential for the ADVA Cast 551 to undergo alkaline hydrolysis. The nature of the radioactive waste matrix also means there will be a presence of ionising radiation. This can cause degradation of the polymer by radiolysis induced chain scission or in contrast, further polymerisation may occur by cross linking of chains.

To assess the stability of superplasticisers to these conditions, and to analyse any changes in the superplasticiser itself, a number of stability experiments were conducted.

2.9.1.1 Chemical Stability

Resistance of the superplasticiser to alkaline hydrolysis was investigated by preparing 10% solutions of ADVA Cast 551 in 95% saturated $Ca(OH)_2$ and 0.1 mol dm^{-3} NaOH. These high pH solutions represent the pore solution of cement. 100 cm^3 of each solution were prepared in pyrex crew top bottles (Fisher Scientific) and after preparation, the solutions were stored in O_2 free conditions at ambient temperature for six months before analysis.

2.9.1.2 Thermal Stability

Without modification, a 50 cm^3 sample of 'as received' superplasticiser were placed in a pyrex screw top bottle in a temperature controlled oven at 80ºC. The sample was stored in this way for six months before analysis.

2.9.1.3 Radiolytic Stability

Four 20 cm^3 samples of 'as received' ADVA Cast 551 were prepared and sealed in glass vials and sent to the ^{60}Co facility at the University of Notre Dame, Illinois, USA:

2 dose rates were investigated:

- 3.23 Gy min^{-1} to a total of 65 kGy
- 10.9 Gy min^{-1} to a total of 220 kGy

2.9.2 *Degradation Product Analysis*

2.9.2.1 Infrared Spectroscopy

IR spectra were obtained via the method described in 2.3.2.1

2.9.2.2 Scanning Electron Microscopy

SEM images of ADVA Cast 551 that had been subject to radiolysis by a ^{60}Co sources were taken at the British Geological Survey.

2.9.2.3 Electrospray Ionisation – Mass Spectrometry

ESI-MS method is described in 2.3.2.4

2.9.2.4 Gel Permeation Chromatography

GPC method and calibration is described in 2.3.2.5

2.10 Effect of Degraded Superplasticiser on Metal Solubilities

The solubility experiments were conducted as described in 2.5.1 with the following modifications:

ADVA Cast 551 that had been irradiated to a dose of 65 kGy was used in the experiments. All sample preparation and sampling was conducted inside a N_2 atmosphere glove box. Solutions of irradiated ADVA Cast 551 were prepared at a range of concentrations (% w/v) using 95% saturated $Ca(OH)_2$, 0.1 mol dm^{-3} NaOH and cement equilibrated solutions (BFS:OPC, PFA:OPC plus BFS, PFA and OPC individually). NaOH and $Ca(OH)_2$ plus the cement equilibrated solutions were prepared as described in sections 2.1.1 and 2.4.1 respectively.

Irradiated ADVA Cast 551 was present at 0%, 0.1%, 0.5% and 1%. Due to space constraints within the irradiation chamber at the University of Notre Dame, there was not enough irradiated ADVA Cast 551 available to produce samples containing 10% ADVA Cast 551. 1% ADVA Cast 551 however, is higher than the largest superplasticiser dose recommended by the manufacturer and should provide a suitable range of concentrations to assess the effect of the presence of the irradiated superplasticiser on U (VI), Th (IV), Eu (III) and Ni (II) solubilities.

3 Results

3.1 Characterisation of Materials

3.1.1 *Cement Materials*

3.1.1.1 BET

The specific surface area of BFS:OPC and PFA:OPC crushed grout (<180μm particle size) plus the raw materials BFS, PFA and OPC were measured at the British Geological Survey. Results are shown in Table 20.

Table 20 Specific surface area of cement

Sample	BET (m^2 g^{-1})
BFS:OPC crushed grout	7.09 ± 0.06
PFA:OPC crushed grout	4.08 ± 0.03
BFS powder	0.48 ± 0.01
PFA powder	1.87 ± 0.04
OPC powder	0.98 ± 0.01

BFS:OPC cement has a larger surface area than PFA:OPC. BFS powder has the lowest surface area of the raw materials.

3.1.1.2 Elemental Analysis

Acid digestion of BFS:OPC and PFA:OPC crushed grout plus BFS, PFA and OPC powder was conducted in aqua regia and HF. Composition of the cement materials is shown in Table 21 and Table 23 for aqua regia and HF digestion respectively. Trace elements also present in the samples are recorded in Table 22 and Table 24 for aqua regia and HF digestion respectively. The differences in elemental analysis between the two digestion techniques demonstrates that the HF method is a better digestion method for these types of samples and a more complete digestion of the cement is possible than with aqua regia.

Table 21 Composition of Cement Materials - Digestion by Aqua Regia

%	BFS:OPC	PFA:OPC	BFS	PFA	OPC
CaO	67.4	56	67.3	13.5	75
SiO_2	1.3	0.06	0.36	2	12
Al_2O_3	9	18	8.2	33.5	4.6
Fe_2O_3	0.48	6	0.5	13.5	1
MgO	16	4	17.3	10	2
K_2O	0.4	1.4	0.4	3.3	0.3
Na_2O	0.3	0.8	0.3	2.3	0.2
SO_3	3.4	5.8	3	3.3	0.3

Table 22 Composition of Cementitious Materials: Trace Elements - Digestion in Aqua Regia

µg / g cement	BFS:OPC	PFA:OPC	BFS	PFA	OPC
As	2.4	72.7	1.4	105.6	11.6
Ba	704.4	549.5	880.5	823.4	187.6
Co	5.6	32.2	5.7	48.8	12.2
Cr	23.5	193	29.8	290.2	85.4
Cu	55.7	168.9	<LOD	114.7	82.6
Mn	1638.6	285.9	2061.6	339.2	305.2
Nb	<LOD	23.9	<LOD	36.4	0.6
Ni	<LOD	28.1	<LOD	25.8	<LOD
P	131.9	1177	32.8	1418	1175
Pb	1.2	163.4	<LOD	268.1	26.4
Sr	601.3	377.7	714.9	425.4	536.3
Ti	1268.9	1065.9	1493.9	1399.9	1265.9
V	11.9	181.8	12	268.7	49.6
Zn	7.3	311.7	<LOD	460.1	106.9
Zr	194.8	56.3	236.6	68	154.5

Table 23 Composition of Cement Materials - Digestion by HF

%	BFS:OPC	PFA:OPC	BFS	PFA	OPC
CaO	76	79	80.4	81	58.8
SiO_2	8.7	9.2	8.5	8.9	16.25
Al_2O_3	6.9	7.7	6.7	6.2	11.25
Fe_2O_3	0.08	0.4	0.07	0.5	0.75
MgO	3	0.4	3.2	0.5	1.25
K_2O	0.1	0.3	0.07	0.3	0.25
Na_2O	0.04	0.25	0.04	0.13	0.125
SO_3	0.5	0.3	0.3	0.08	2.5

Table 24 Composition of Cementitious Materials: Trace Elements - Digestion in HF

µg / g cement	BFS:OPC	PFA:OPC	BFS	PFA	OPC
As	1.5	79.5	5.8	106.5	9.8
Ba	704	861	868	12223.8	187
Co	<LOD	14.6	<LOD	22.5	<LOD
Cr	16.9	97.6	12.7	123.8	38.5
Cu	21.5	78.7	<LOD	57.6	30.8
Mn	664	156.1	821.6	186.3	127.6
Nb	9.4	21.9	13.1	25	14.9
P	46.6	556.2	10.1	647.8	474.3
Pb	59.4	178.5	65.1	247.7	48.1
Sr	240	213	283.1	248.9	220.8
Ti	515.1	990.1	592	1305	528.5
V	1.2	95.6	3.4	140.3	16
Zn	1.5	183.8	<LOD	259.1	36.8
Zr	67.2	62.1	78.1	70.2	51.5

3.1.2 *ADVA Cast 551 Analysis.*

A number of analytical methods were used for the characterisation of ‘as received’ ADVA Cast 551. Since the superplasticiser is a commercial product, the exact structure and production method are a trade secret. As received ADVA Cast 551 is a viscous amber coloured liquid of the polymer in a solvent (ethanol). The uncertainty surrounding the superplasticisers structure plus the aqueous nature of the sample made the product difficult to analyse.

3.1.2.1 Infrared Spectroscopy.

The IR spectra of ‘as received’ ADVA Cast 551 is shown in Figure 10.

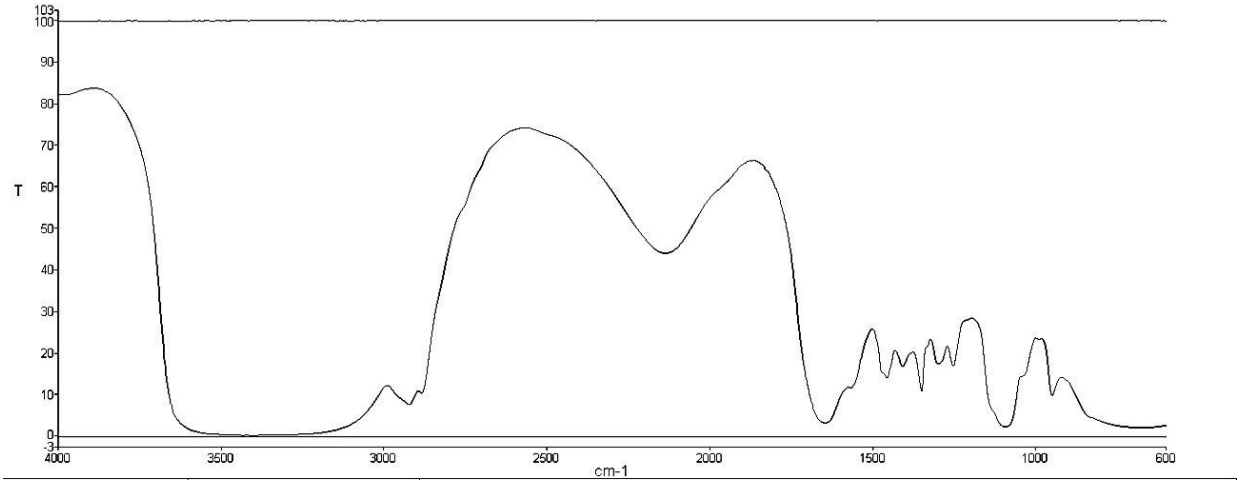

Figure 10 IR Spectra of ADVA Cast 551

From this spectrum, the following peaks may be identified from the structure of ADVA Cast 551 (Figure 10): 3700cm^{-1} to 2700cm^{-1} broad peak associated with water in the sample and possible contribution from the ethanol solvent: 1710cm^{-1} C=O stretch of the carboxylic acid groups on the polymer side chains: 1094cm^{-1} C-O stretch of the ether group on the polymer side chains. 1350cm^{-1} CH_3 methyl group 'umbrella' on the backbone of the polymer chain. There is also an unidentified broad peak at 2140cm^{-1}.

3.1.2.2 UV Spectroscopy

The UV – absorption spectrum of a 1% solution of ADVA Cast 551 in water is shown in Figure 11.

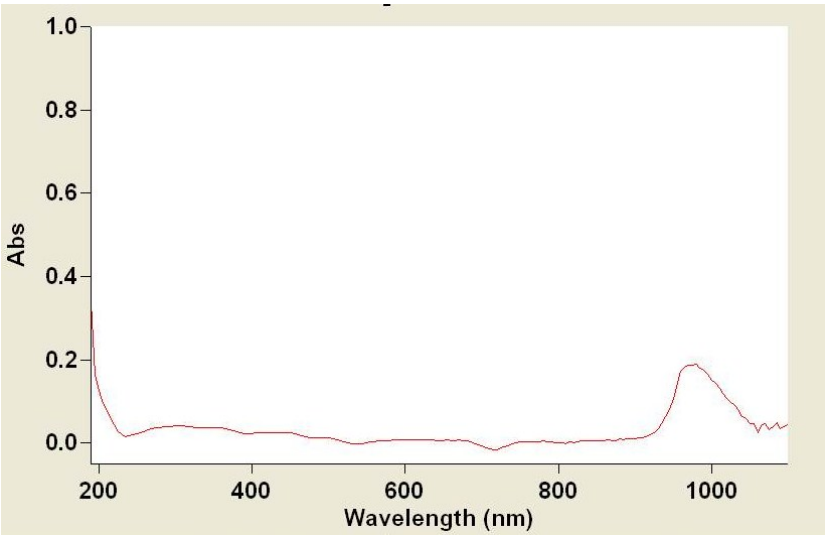

Figure 11 UV- absorption of a 1% solution of ADVA Cast 551 in water

The instrument was set to zero using a blank air scan. A water (solvent) blank was also taken where an absorbance was observed at 950 nm. This absorbance was also present in the polymer sample and can therefore be attributed to absorbance associated with water, not the polymer. The normal working range for the UV spectrophotometer is 200- 800 nm: no absorbance was observed within this range therefore UV was discounted as a detection method for superplasticiser analysis.

3.1.2.3 GC-MS

The recorded chromatogram for ‘as received’ ADVA Cast 551 prepared as described in 2.3.2.3 is shown in Figure 12.

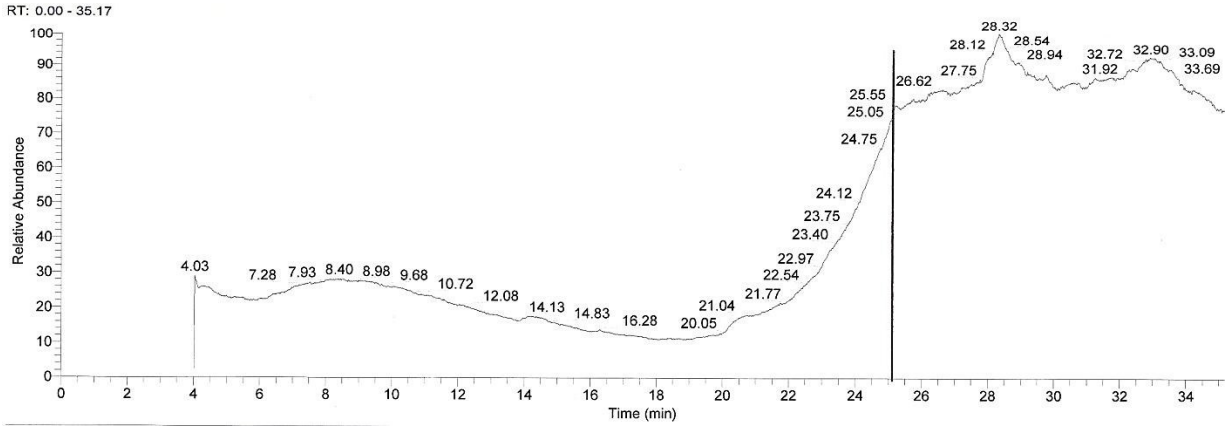

Figure 12 Gas chromatogram of 'as received' ADVA Cast 551

It was not possible to obtain a clear chromatogram from the ADVA Cast 551 sample. The likely reason for this is that the polymer is not volatile enough to be injected and separated satisfactorily in a gas chromatography column. The broad unresolved peaks shown in Figure 12 and the drifted increase in signal towards the end of the sample run time are likely to be due to a mix of very low volatility analyte. The heavier non-volatile fractions were retained in the head of the capillary column. GC-MS was discounted for use in further characterisation experiments.

3.1.2.4 ESI- MS

The electro-spray mass spectrum of a sample of ‘as received’ ADVA Cast prepared as described in 2.3.2.4 is shown in Figure 13.

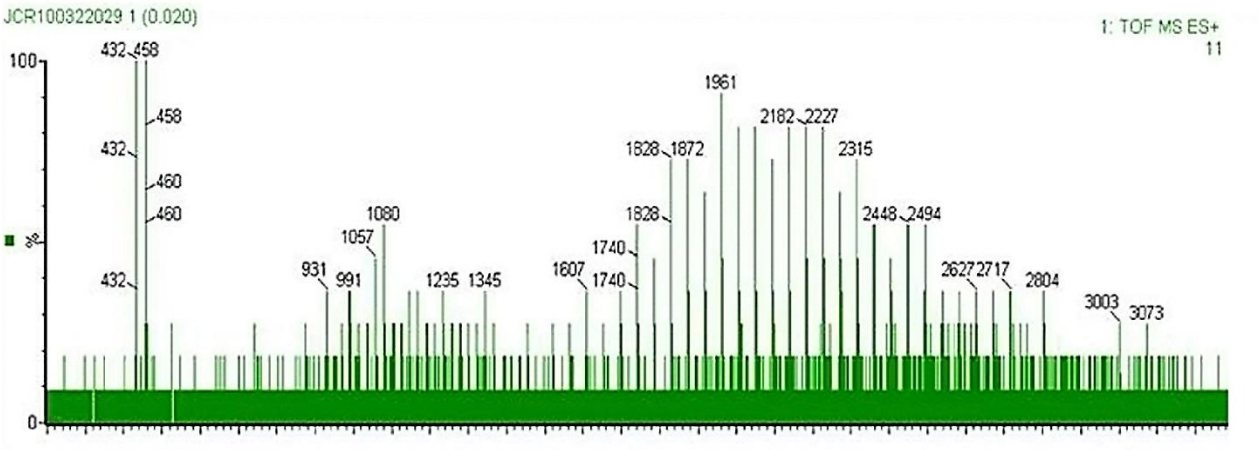

Figure 13 Mass Spectrum of an 'as received' sample of ADVA Cast 551

There are numerous polymer distribution patterns observed in the spectrum indicating the variation in the length of the polymer chains within the sample. Although ESI-MS is a promising technique for analysing the superplasticiser, it has a limit of detection of Mw 3000 and is not able to detect masses reliably above this point. The expected mass of the superplasticiser is expected to range between 60,000 to 100,000 therefore the signals recorded in the spectrum are likely to be unreacted monomer and polymers with short chain length.

3.1.2.5 Gel Permeation Chromatography

The separation of ADVA Cast 551 has proven to be a challenge. Method development for the determination of the molecular weight of the constituents of ‘as received’ superplasticiser are shown below.

3.1.2.5.1 THF eluent

Tetrahydrofuran (THF) solvent was used initially as the eluent. Instrument calibration was carried out as described in 2.3.2.5 with THF soluble polystyrene standards. A calibration graph was produced which was then used to determine the molecular weights of eluted polymer fractions.

A method blank was taken by injecting THF (the eluent) through the column to distinguish any peaks or anomalies which are artefacts and not associated with the polymer sample. The reproducibility of the technique was confirmed by repeating a sample injection at least 4 times: if the same chromatogram was

obtained for the sample after four replicates, then the data were used confidently for molecular weight determination. The ‘blank’ chromatogram is shown in Figure 14.

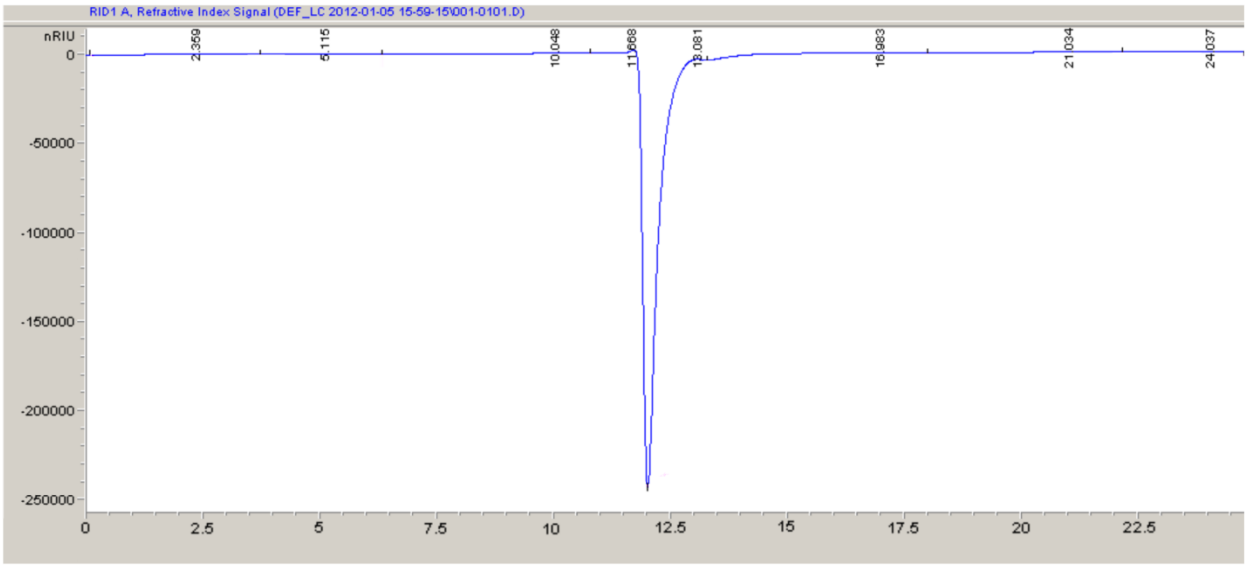

Figure 14 THF Blank Chromatogram

ADVA Cast 551 is not soluble in THF. An immiscible suspension forms on mixing and a precipitate/film is formed on the bottom of the vial after 24 hours. A ‘saturated’ solution of ADVA Cast 551 in THF was prepared (1% ADVA Cast (w/v) in THF), allowed to settle overnight and the supernatant removed and injected into the column. The resultant chromatogram is shown in Figure 15.

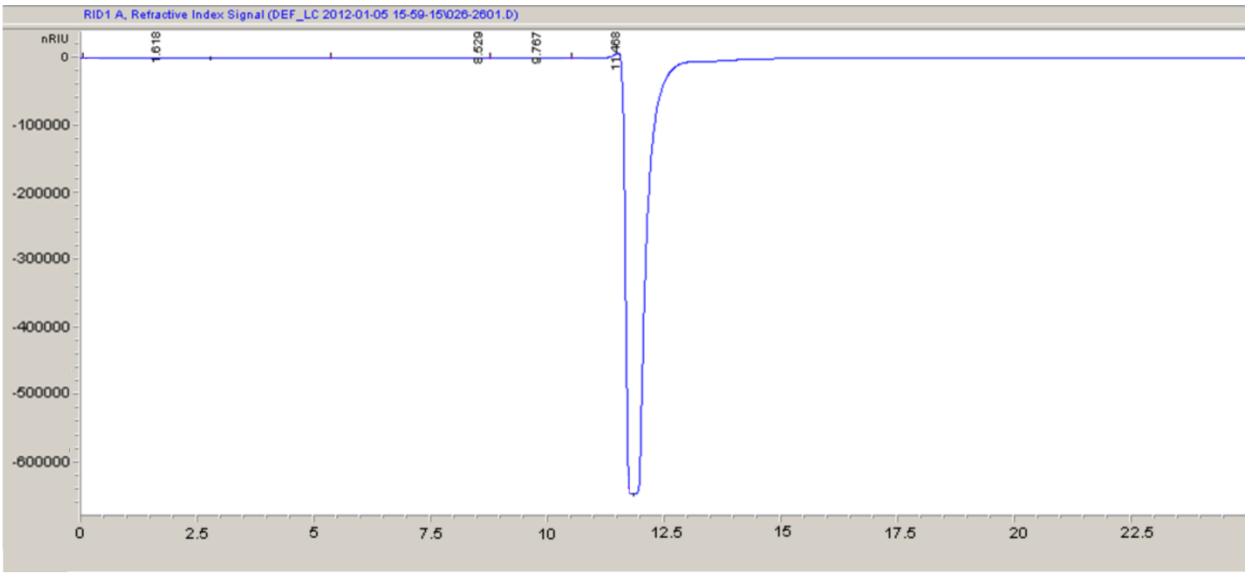

Figure 15 Chromatogram of a saturated solution of ADVA Cast 551 in THF

A similar chromatogram is obtained to that of the blank sample, indicating the absence of polymer. This is likely to be due to the low solubility of ADVA Cast 551 in THF, and the amount of polymer present in the sample is below the limit of detection of the instrument.

To try and increase the solubility of ADVA Cast 551 in the THF solution, a mixture of 20:80 of methanol: THF was used to prepare a 1% solution of ADVA Cast 551. ADVA Cast 551 was first mixed with the methanol portion before making up with THF. Although ADVA Cast 551 is completely soluble in methanol, the addition of the solvent did not have a marked effect on solubility of ADVA Cast 551 in THF and a precipitate had formed again when the samples settled overnight. The chromatogram for a 1% ADVA Cast 551 sample in MeOH: THF is shown in Figure 16. The peak noted in the chromatogram (11.5 minutes) is associated with the addition of methanol to the sample and is also present in a blank chromatogram of MeOH: THF containing no ADVA Cast 551. This means therefore than no ADVA Cast 551 polymer is detected in the sample.

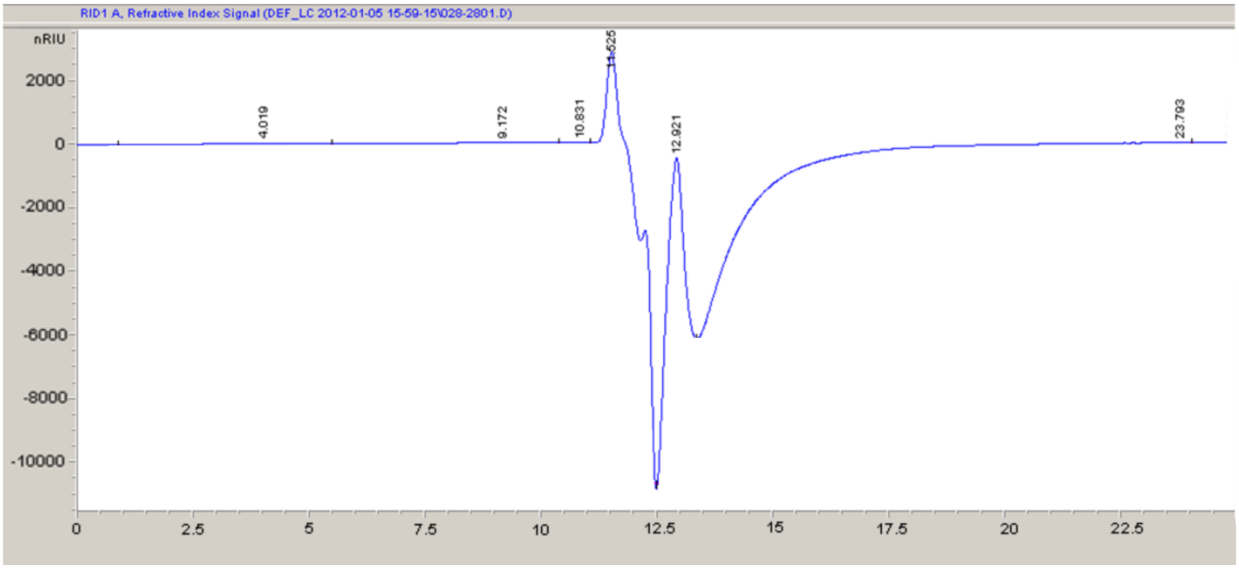

Figure 16 Chromatogram of 1% ADVA Cast 551 in 20:80 Methanol: THF

The lack of signal was associated with the low solubility of ADVA Cast 551 in THF. THF was discounted for further analysis as an unsuitable solvent for the analyte. The eluent was therefore changed to methanol, in which ADVA Cast 551 is completely soluble.

3.1.2.5.2 Methanol eluent

After changing the eluent, the instrument was flushed overnight and the refractive index detector reference cell purged before use.

A blank chromatogram of an injection of methanol through the column is shown in Figure 17 . A peak at 15.3 minutes is present in the blank sample. This peak was taken into account on all the sample runs and discounted as not being attributed to the polymer.

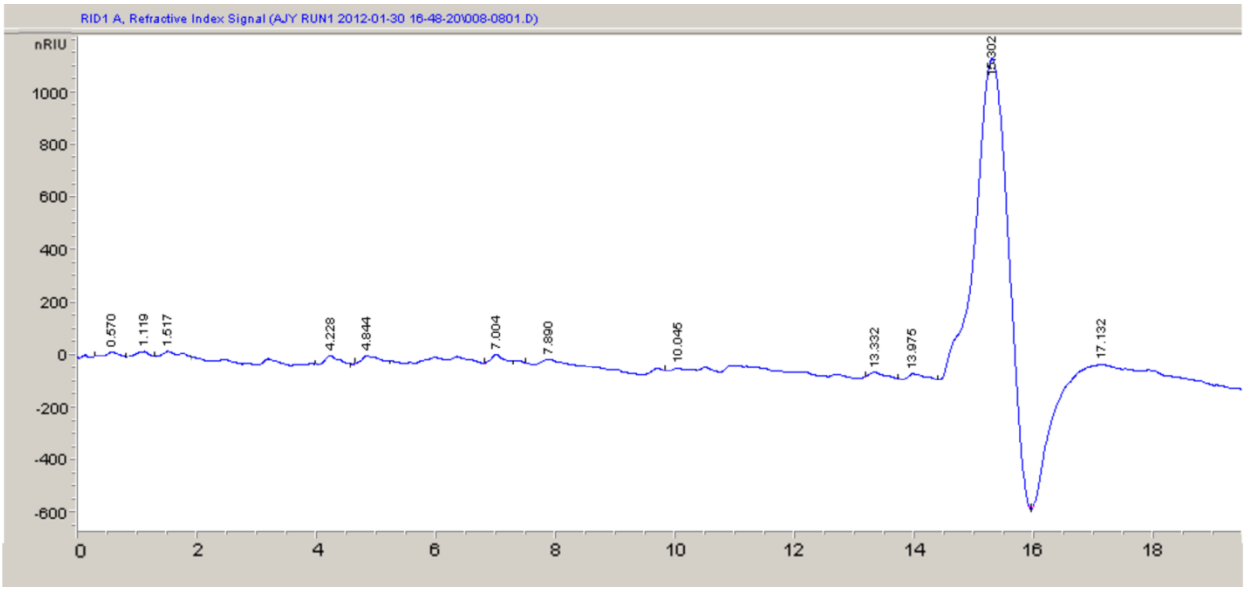

Figure 17 Methanol Blank Chromatogram

A 1% ADVA Cast 551 solution in methanol was eluted through the column and the chromtagoram is shown in Figure 18. Unfortunately, no peaks that could be attributed to the superplasticiser were identified.

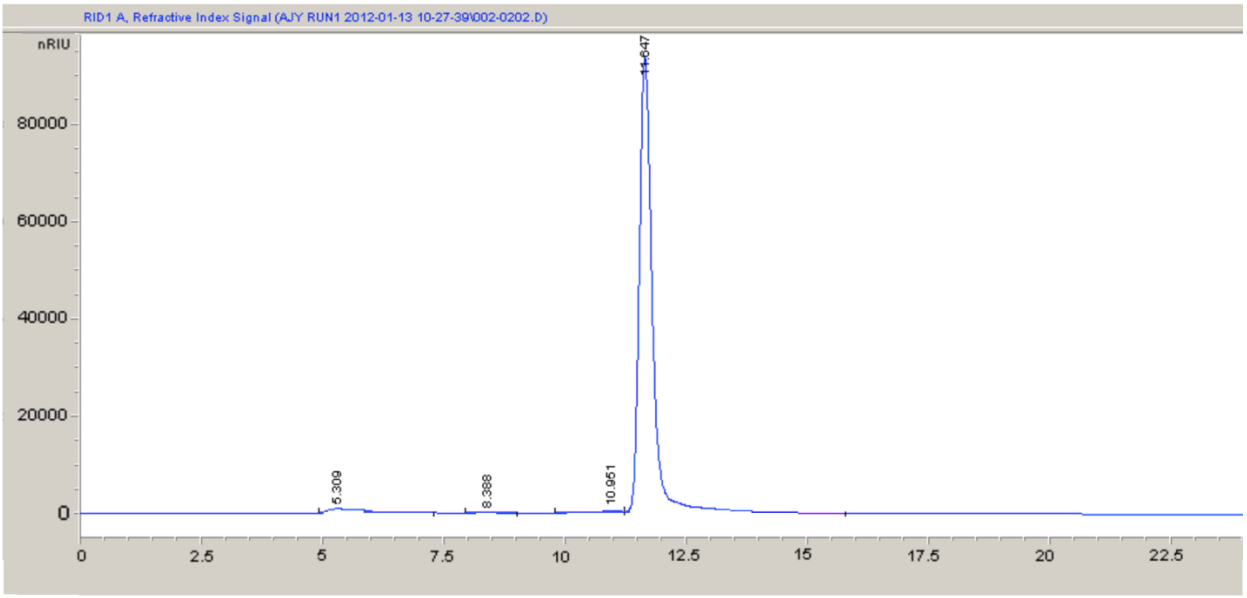

Figure 18 1% ADVA Cast 551 in methanol

A sample of ‘as received’ superplasticiser was dried using a vacuum pump to remove all solvent. No heating was applied during evaporation so that there would be no change to the polymer as a result of elevated temperature. The solid superplasticiser was an off white waxy solid which remained after solvent evaporation. This solid was re-suspended in methanol to 1% by weight of solid.

This 1% solid ADVA Cast 551 re-suspension was completely soluble and was eluted though the GPC giving the chromatogram shown in Figure 19.

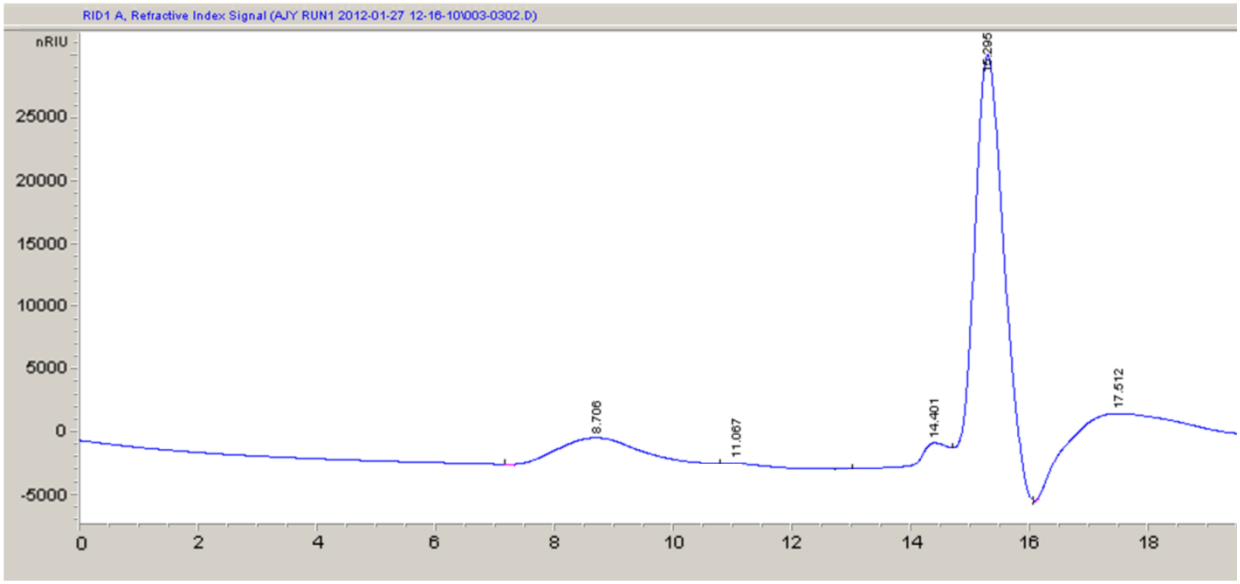

Figure 19 1% ADVA Cast 551 solid re-suspension in methanol

The peaks in the chromatogram are shown in more detail in Figure 20 while Table 25 gives the molecular weight distributions associated with the eluted peaks. A large range of molecular weights are eluted in a short time. The M_w range associated with the start and end of each peak is quoted along with the average M_w for each peak.

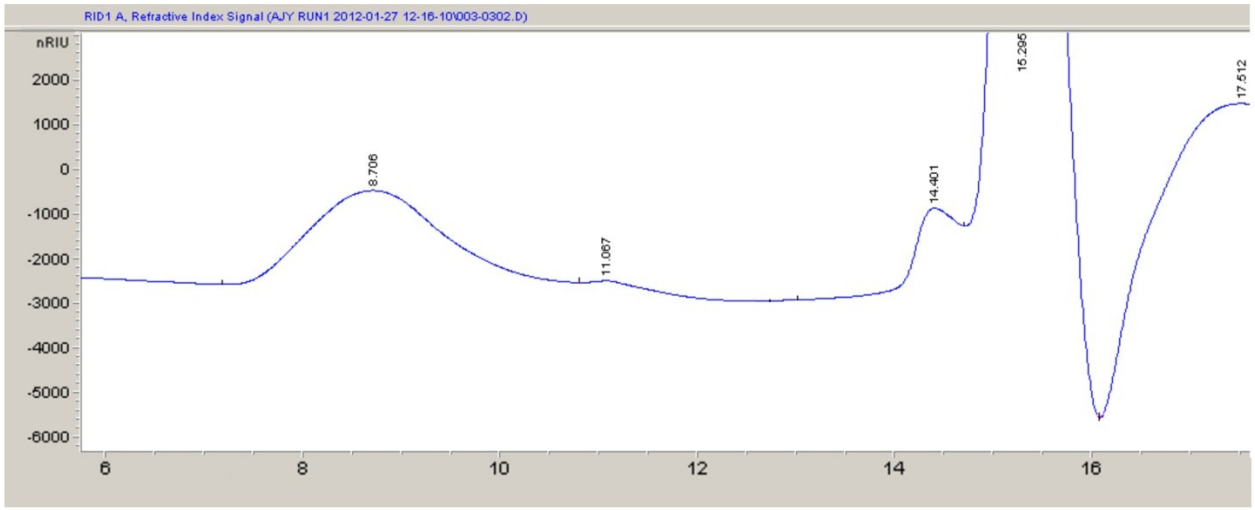

Figure 20 1% ADVA Cast 551 solid re-suspension in methanol (2)

Table 25 ADVA Cast 551 GPC Peak Table

Peak Label	Start Time (min)	End Time (min)	Size Range (Mw)	Average (Mw)
8.706	7.5	10.5	780,601 to 1346	390,974
11.067	10.5	12.0	1346 to 56	701
14.401	14.25	15.01	Out of calibration range	-

The large range of molecular weights associated with each peak demonstrates the variability of chain length of the polymer. One repeating unit of ADVA Cast 551 has the formula $C_{47}H_{88}O_{21}$ and therefore the theoretical M_w for one unit would be 989 Da. The peaks eluted cover this range however it was not possible to resolve individual fractions of specific molecular weight

The molecular weight of the species eluted at 14.401 minutes was out of the calibration range. This peak is therefore attributed to unreacted monomer and low molecular weight impurities within the sample.

3.1.2.6 Summary of ADVA Cast 551 Characterisation

Several techniques were used to analyse and characterise 'as received' ADVA Cast 551 with varied success. UV spectroscopy and Gas Chromatography-Mass Spectrometry were discounted from further experiments as no information regarding the polymer was gained using these techniques. Structural information regarding the functionality present on the polymer was obtained from IR data while information on the molecular weight distribution of the polymer was gained using both Electrospray Ionisation –Mass Spectrometry and Gel Permeation Chromatography with Refractive Index detection. These techniques will therefore be utilised further in the analysis of the products of ADVA Cast 551 stability experiments.

3.2 Characterisation of Cement Equilibrated Water

3.2.1 *Cation Analysis*

Cation analysis of cement equilibrated water was performed using ICP-OES for all elements except Si, which was analysed by ICP-MS. Calibration data are presented in APPENDIX 1 – Instrument Calibration Data. Cation analysis of each cement equilibrated water is shown in Table 26, Table 27, Table 28, Table 29 and Table 30 for BFS:OPC, PFA:OPC, BFS, PFA and OPC respectively. Values quoted represent the average of 4 sample replicates. Details of the method of preparation and ratios of cement solids to water are given in section 2.4.1. Calcium was the most abundant element analysed followed by potassium, sodium aluminium and zinc. The solution with the highest concentration of calcium was OPC equilibrated water. There is a larger proportion of calcium in PFA:OPC equilibrated water compared to BFS:OPC equilibrated water. This is due to the different ratios used to prepare the cement formulations. There is a larger amount of OPC in the PFA:OPC formulation (3:1) proportionally compared to the BFS:OPC ratio (9:1).

3.2.2 *Anion Analysis*

Anion analysis was performed using Dionex ion chromatography, results are shown in Table 26, Table 27, Table 28, Table 29 and Table 30 for BFS:OPC, PFA:OPC, BFS, PFA and OPC respectively. Values quoted represent the average of 4 sample replicates. Dionex Chromatograms and calibration data are shown in APPENDIX 1 – Instrument Calibration Data. Details of the method of preparation and ratios of cement solids to water are given in section 2.4.1. Significant amounts of sulphur species were observed, in particular, in the cement equilibrated solutions containing BFS. The origins of sulphur species within the BFS are from sulphur impurities present in the iron ore. The sulphur impurities are removed from the iron by reaction with magnesium (Equation 6).

$$Mg + S \longrightarrow MgS$$

Equation 6 Sulphur removal from iron by magnesium

The resultant MgS is incorporated into the BFS and removed. The presence of both sulphite and sulphate in solution is explained since sulphite readily oxidises to sulphate on exposure to air via the reaction shown in Equation 7 taken from Sivaji and Murty (1982) (65).

$$2SO_3^{2-}(aq) + O_2(g) \longrightarrow 2SO_4^{2-}(aq)$$

Equation 7 Oxidation of sulphite

Another sulphur containing species, thiosulphate, was observed in the BFS:OPC and BFS samples. In high pH solution, sulphur reacts with alkali hydroxide to produce thiosulphate via the reaction shown in Equation 8 taken from Satake et al. (1981) (66).

$$(4+2x)S + 6OH^- \longrightarrow 2S^{2-}_{x+1} + S_2O_3^{2-} + 3H_2O$$

Equation 8 Thiosulphate production at high pH

Table 26 BFS:OPC Equilibrated Water Analysis

Cations	ppm (μg ml^{-1})
Ca^{2+}	524.93
K^+	16.91
Al^{3+}	9.86
Na^+	6.96
Li^+	0.22
Si^{4+}	<LOD
Anions	
SO_4^{2-}	10.34
$S_2O_3^{2-}$	8.5
SO_3^{2-}	2.02
Cl^-	1.65
NO_3^-	0.46
Trace Elements	
Mg^{2+}	0.0307
Cu^{2+}	0.0116
Cr^{3+}	0.0049
Zn^{2+}	0.0049
Pb^{2+}	0.0045
Co^{2+}	0.0009

Table 27 PFA:OPC Equilibrated Water Analysis

Cations	ppm (μg ml^{-1})
Ca^{2+}	1480.93
K^{+}	28.65
Al^{3+}	5.72
Na^{+}	5.17
Li^{+}	0.5
Si^{4+}	<LOD
Anions	
SO_4^{2-}	5.34
Cl^{-}	1.5
NO_3^{-}	0.24
Trace Elements	
Mg^{2+}	0.0238
Cr^{3+}	0.0224
Pb^{2+}	0.0133
Cu^{2+}	0.0042
Co^{2+}	0.0012

Table 28 BFS Equilibrated Water Analysis

Cations	ppm (μg ml^{-1})
Ca^{2+}	371.27
Al^{3+}	5.27
K^{+}	3.74
Na^{+}	2.31
Li^{+}	0.086
Si^{4+}	0.009
Anions	
$S_2O_3^{2-}$	12.48
SO_4^{2-}	10.66
SO_3^{2-}	4.49
Cl^{-}	0.75
NO_3^{-}	0.122
Trace Elements	
Zn^{2+}	3.44
Mg^{2+}	0.084
Pb^{2+}	0.033
Cu^{2+}	0.005
Cr^{3+}	0.002
Mn^{2+}	0.002
Co^{2+}	0.001

Table 29 PFA Equilibrated Water Analysis

Cations	ppm (μg ml^{-1})
Ca^{2+}	262.67
Al^{3+}	9.87
Na^{+}	7.7
K^{+}	6.08
Li^{+}	0.42
Si^{4+}	<LOD
Anions	
SO_4^{2-}	6.23
Cl^{-}	0.74
NO_3^{-}	0.14
Trace Elements	
Zn^{2+}	5.05
Mg^{2+}	0.48
Cr^{3+}	0.115
Cu^{2+}	0.016
Pb^{2+}	0.004
Co^{2+}	0.0005
Mn^{2+}	0.0004
Cd^{2+}	0.0003

Table 30 OPC Equilibrated Water Analysis

Cations	ppm (μg ml^{-1})
Ca^{2+}	2371.3
K^{+}	64.05
Na^{+}	15.56
Al^{3+}	0.63
Li^{+}	0.51
Si^{4+}	<LOD
Anions	
SO_4^{2-}	6.81
NO_3^{-}	3.6
Cl^{-}	3.34
Trace Elements	
Mg^{2+}	0.022
Cr^{3+}	0.02
Pb^{2+}	0.013
Cu^{2+}	0.006
Co^{2+}	0.002
Cd^{2+}	0.002
Mn^{2+}	0.0012

3.3 Effect of Superplasticiser on Metal Solubilities

3.3.1 *Uranium (VI) Solubility*

Experimental methods and analytical techniques are described in 2.5.1. All errors quoted represent ± the standard deviation of 4 sample replicates.

3.3.1.1 95% Saturated $Ca(OH)_2$

The solubility of U (VI) was monitored over 28 days. The kinetics of precipitation is shown in Figure 21.

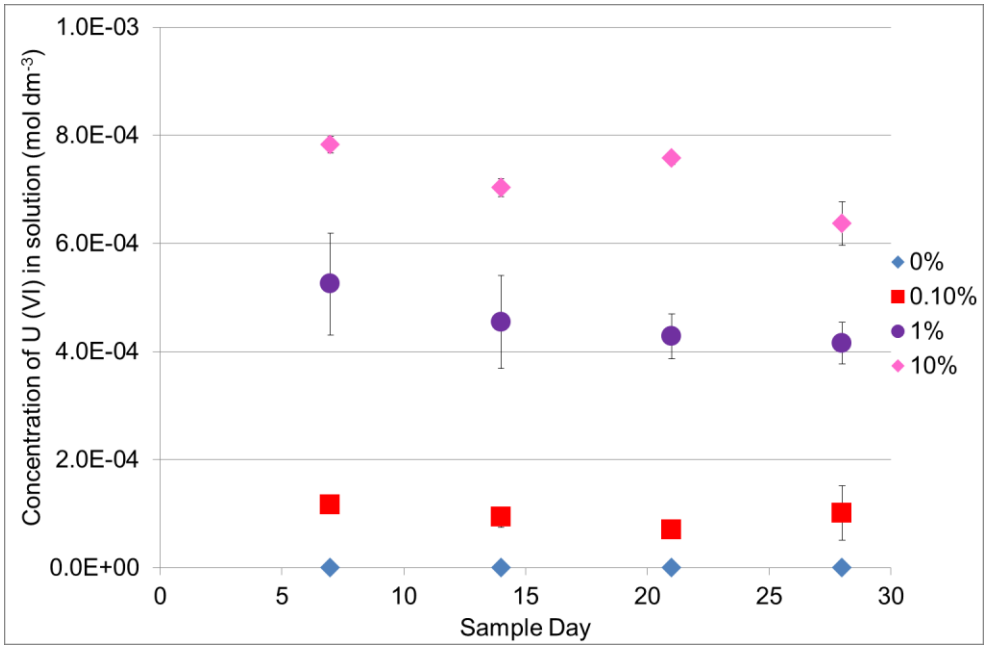

Figure 21 Kinetics of precipitation of U (VI) in the presence of ADVA Cast 551 in 95% saturated $Ca(OH)_2$

The blue sample points represent the baseline solubility of U (VI) in 95% saturated $Ca(OH)_2$ in the absence of the superplasticiser. The U (VI) concentration remains constant throughout the experiment indicating that the samples had reached steady state. The addition of the superplasticiser results in an increase in U (VI) solubility of several orders of magnitude. This increase is further demonstrated in Figure 22 which shows the final concentration of U (VI) in solution at each concentration of ADVA Cast 551. At 10% ADVA Cast 551 the concentration of U (VI) in solution was close to the inventory limit.

To make comparisons of U (VI) solubility in the different aqueous solutions investigated, the solubility enhancement factor (SEF) is calculated (SEF calculation is shown in Equation 1). SEF values for U (VI) in $Ca(OH)_2$ are

shown in Table 31. The presence of 0.1%, 1% and 10% ADVA Cast has a significant effect on the U (VI) concentration in solution with SEF values of 769, 3152 and 4830 respectively.

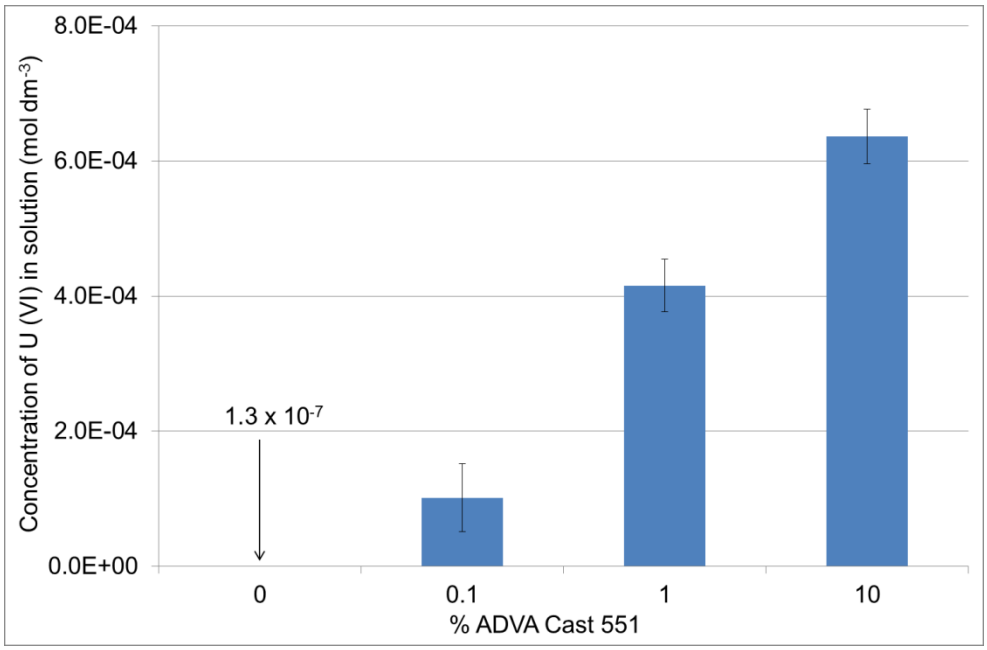

Figure 22 Final concentration of U (VI) in 95% saturated $Ca(OH)_2$ in the presence of ADVA Cast 551

Table 31 U (VI) solubility in 95% saturated $Ca(OH)_2$ in the presence of ADVA Cast 551

Solution	% ADVA Cast	Solubility (mol dm^{-3})	SEF
$Ca(OH)_2$	0	1.32E-07	1
	0.1	1.01E-04	769
	1	4.15E-04	3152
	10	6.37E-04	4830

An example of an estimation of error in SEF calculations is shown in Table 32. The errors reported represent ± the standard deviation of SEF calculations made on 4 sample replicates.

Table 32 Estimation of error in SEF calculations made for U (VI) in $Ca(OH)_2$ in the presence of ADVA Cast 551

Solution	% ADVA Cast	SEF	Error (±)
$Ca(OH)_2$	0	1	1
	0.1	769	118
	1	3152	293
	10	4830	304

3.3.1.2 0.1 mol dm^{-3} NaOH

Kinetics of precipitation of U (VI) in 0.1 mol dm^{-3} NaOH is shown in Figure 23. Steady state for all samples except 1% samples was reached by day 7. The value for the concentration of U (VI) in solution at day 7 with 1% ADVA Cast 551 has a much larger error associated with it than for the other samples therefore it may be assumed that this value is anomalous. Figure 24 shows the final concentration of U (VI) measured in solution while Table 33 reports the SEF values associated with the increase in solubility with increasing concentrations of superplasticiser. In this case the solubility enhancement is not as high as was observed in $Ca(OH)_2$ with an increase in the range of an order of magnitude. However the baseline solubility in this case was, itself, higher than for $Ca(OH)_2$. The concentration of U (IV) in solution at 0.1% and 10% ADVA Cast is close to the U(VI) inventory added to solution. No visible precipitate was present in these samples indicating that nearly all the U (VI) had been solubilised. The SEF values at 1% and 10% ADVA Cast are very similar at 24 and 22 respectively.

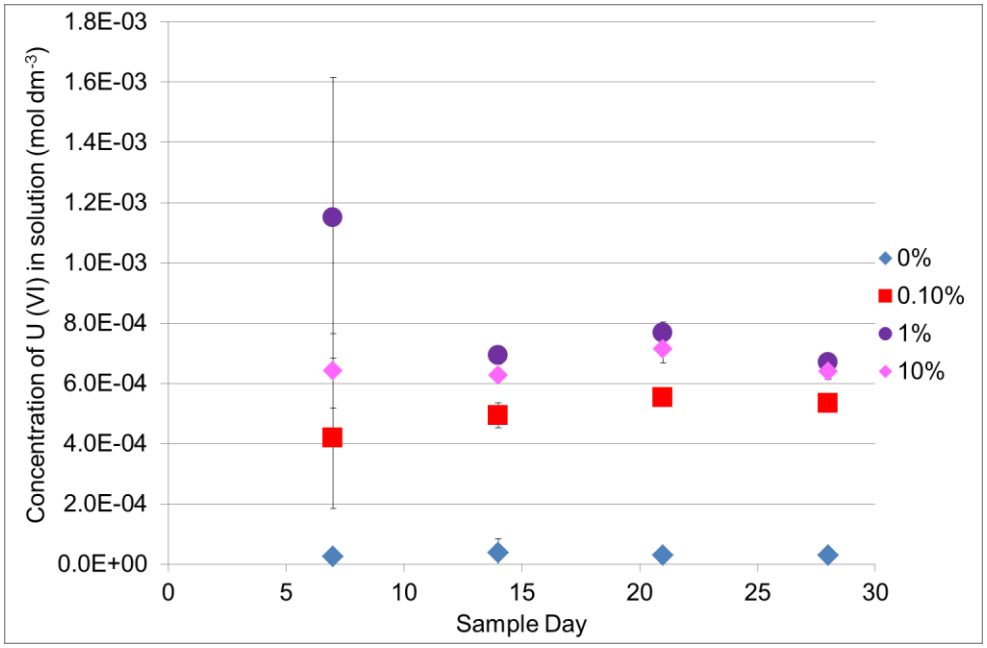

Figure 23 Kinetics of precipitation of U (VI) in the presence of ADVA Cast 551 in 0.1 mol dm^{-3} NaOH

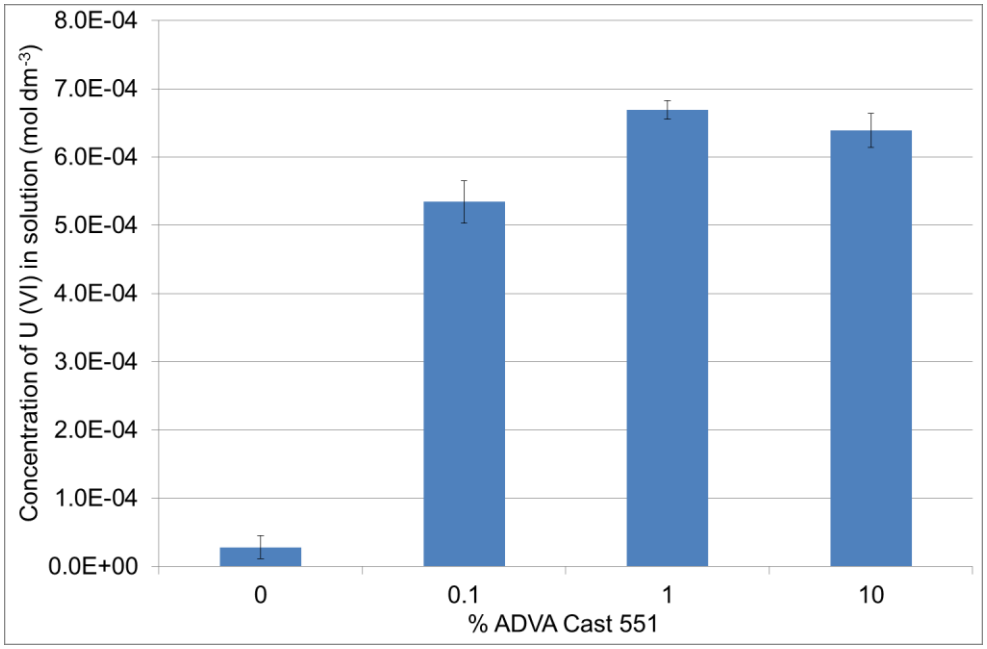

Figure 24 Final concentration of U (VI) in 0.1 mol dm^{-3} NaOH in the presence of ADVA Cast 551

Table 33 U (VI) solubility in 0.1 mol dm^{-3} NaOH in the presence of ADVA Cast 551

Solution	% ADVA Cast	Solubility (mol dm^{-3})	SEF
NaOH	0	2.84E-05	1
	0.1	5.34E-04	19
	1	6.69E-04	24
	10	6.39E-04	22

A second example of an estimation of error in SEF calculations is shown in Table 34. The errors reported represent ± the standard deviation of SEF calculations made on 4 sample replicates. A lower error is associated with lower SEF values compared to those for higher SEF values reported in Table 32.

Table 34 Estimation of error in SEF calculations made for U (VI) in NaOH in the presence of ADVA Cast 551

Solution	% ADVA Cast	SEF	Error (±)
NaOH	0	1	1
	0.1	19	1
	1	24	1
	10	22	1

3.3.1.3 BFS:OPC equilibrated water

The concentrations of U (VI) in BFS:OPC equilibrated water as a function of contact time are shown in Figure 25. The concentration of U (VI) measured in solution is consistent over 28 days indicating that all samples have reached steady state. An increase in U (VI) solubility is observed over several orders of magnitude with increasing concentrations of ADVA Cast 551. The final concentration of U (VI) in solution is shown in Figure 26.

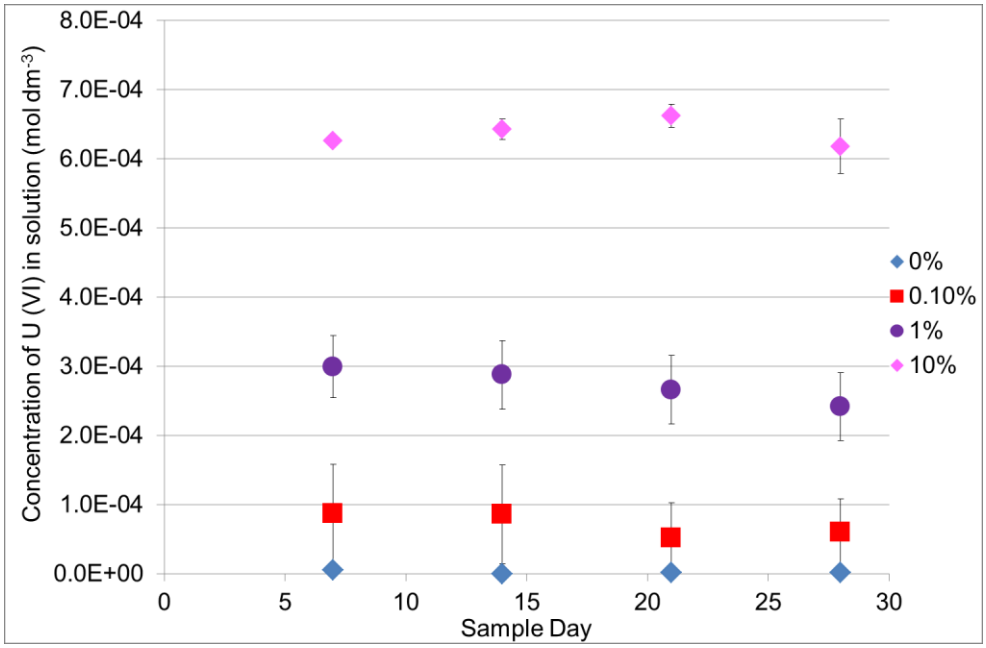

Figure 25 Kinetics of precipitation of U (VI) in the presence of ADVA Cast 551 in BFS:OPC equilibrated water

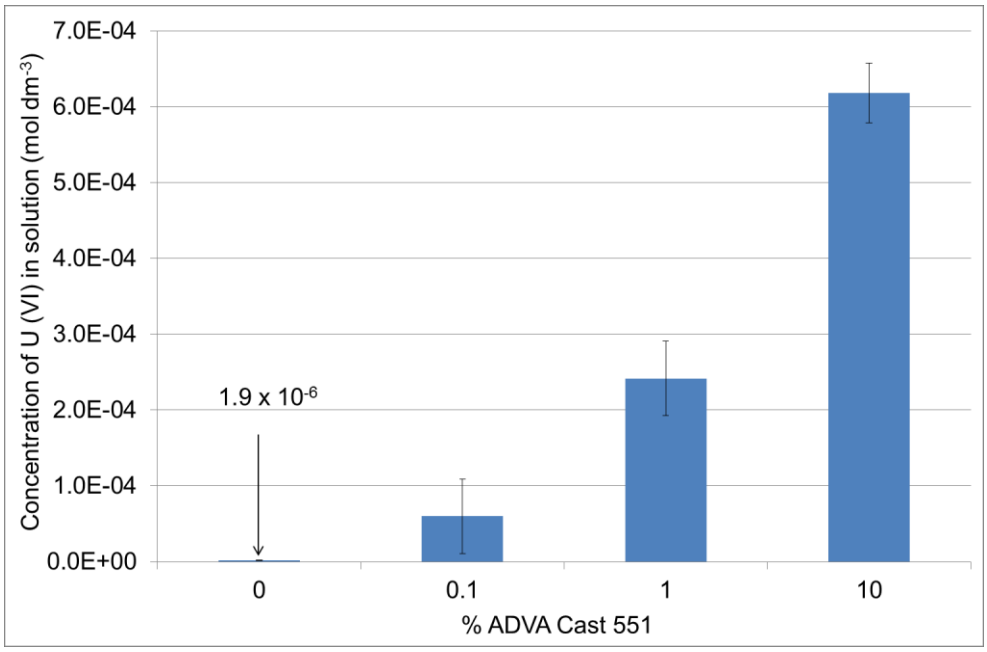

Figure 26 Final concentration of U (VI) in BFS:OPC equilibrated water in the presence of ADVA Cast 551

The SEF values are reported in Table 35 and show a more significant increase from the baseline solubility than in NaOH but a less significant increase than in the case of $Ca(OH)_2$. SEF values for 1% and 10% ADVA Cast were 125 and 320 respectively. At 10% ADVA Cast, the concentration of U (VI) in solution is

close to the U (IV) inventory and no precipitate was visible in the samples. This means therefore that all U (VI) in the sample has been solubilised.

Table 35 U (VI) solubility in BFS:OPC equilibrated water in the presence of ADVA Cast 551

Solution	% ADVA Cast	Solubility (mol dm^{-3})	SEF
BFS:OPC	0	1.93E-06	1
	0.1	5.98E-05	31
	1	2.42E-04	125
	10	6.18E-04	320

3.3.1.4 PFA:OPC equilibrated water

Figure 27 shows kinetics of precipitation of U (VI) in PFA:OPC equilibrated water. All samples except 1% reached steady state by day 7. The 1% samples reached steady state by day 14. At day 7 the error associated with the 1% is larger than for the other samples, it may be assumed therefore that this is an anomaly, likely to be cause by inadvertent re-suspension of the uranyl precipitate.

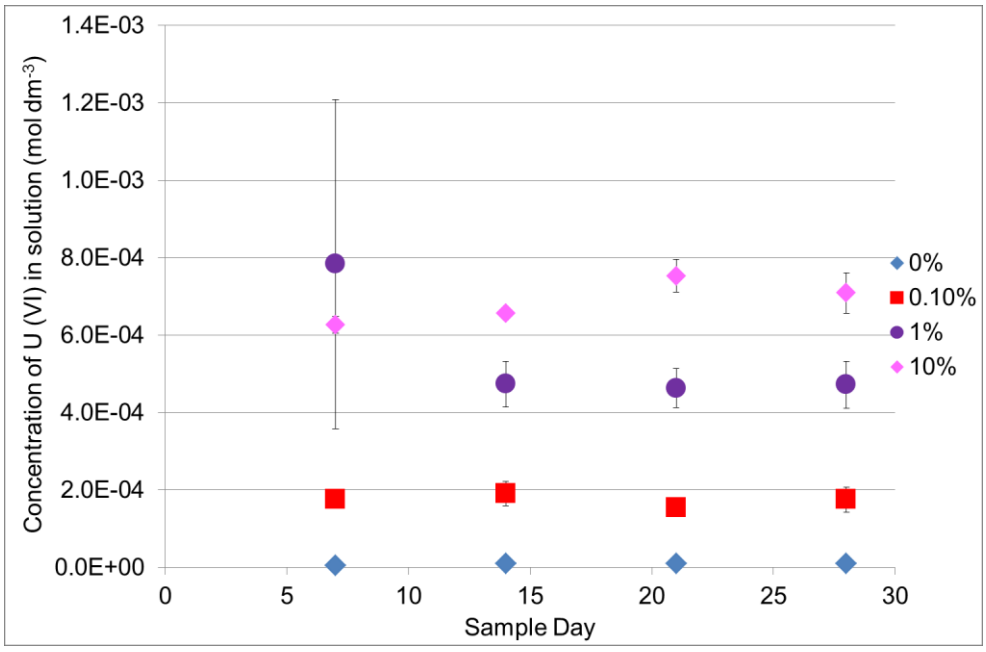

Figure 27 Kinetics of precipitation of U (VI) in the presence of ADVA Cast 551 in PFA:OPC equilibrated water

The final concentration of U (VI) in solution is shown in Figure 28. There is an increase in U (VI) solubility with increasing amounts of ADVA Cast 551 and at

10% ADVA Cast, the concentration of U (VI) in solution is close to the total inventory added. The SEF values recorded for 1% and 10% ADVA Cast 551 were 45 and 67 respectively and are shown in Table 36.

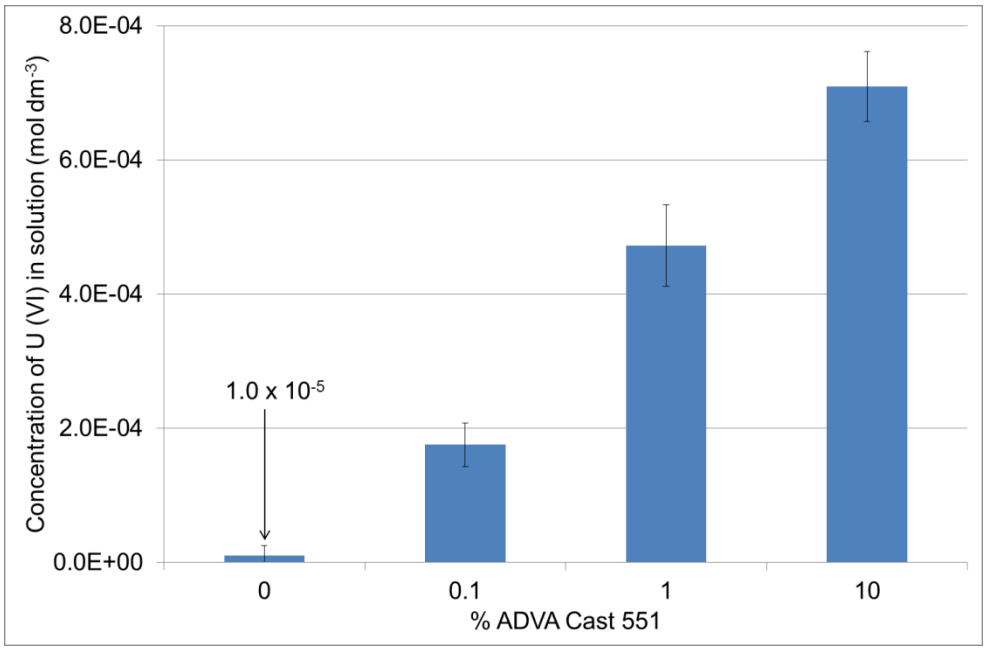

Figure 28 Final concentration of U (VI) in PFA:OPC equilibrated water in the presence of ADVA Cast 551

Table 36 U (VI) solubility in PFA:OPC equilibrated water in the presence of ADVA Cast 551

Solution	% ADVA Cast	Solubility (mol dm^{-3})	SEF
PFA:OPC	0	1.05E-05	1
	0.1	1.75E-04	17
	1	4.72E-04	45
	10	7.09E-04	67

3.3.1.5 BFS equilibrated water

U (VI) concentration in BFS equilibrated water as a function of time is shown in Figure 29. Steady state is reached by day 7 in all cases. There is an increase in solubility associated with the presence of 1% and 10% ADVA Cast 551. As was observed in the other solutions, at 10% ADVA Cast, the amount of U (VI) measured in solution has reached the total U (VI) inventory added. However, within errors, there is no increase in solubility with the presence of 0.1% ADVA Cast. The final concentration of U (VI) in solution is recorded in Figure 30. SEF

values for 1% and 10% ADVA Cast 551 were 17 and 36 respectively and are shown in Table 37.

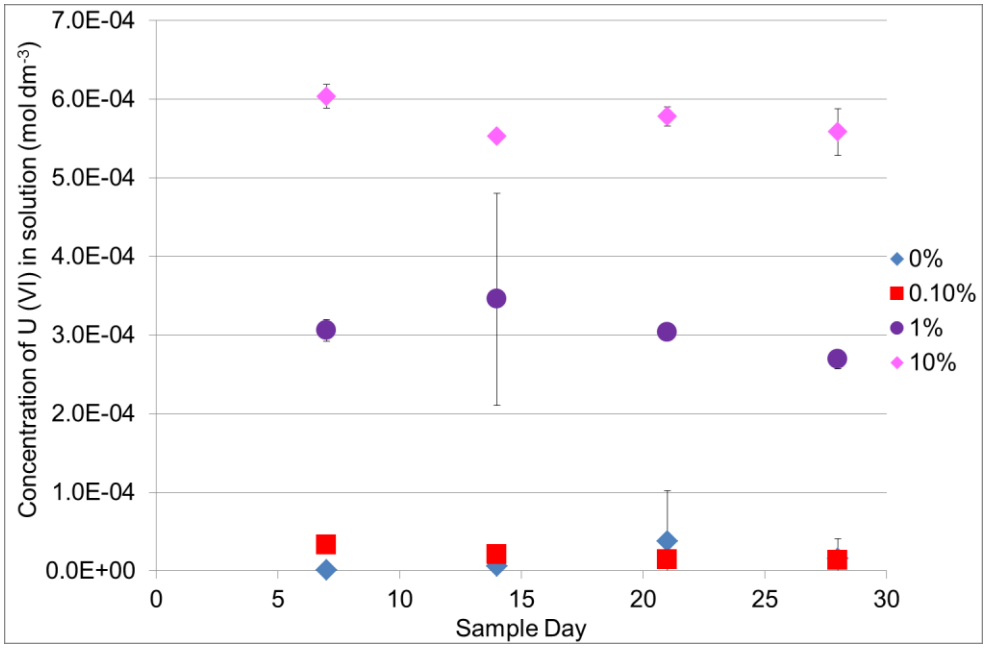

Figure 29 Kinetics of precipitation of U (VI) in the presence of ADVA Cast 551 in BFS equilibrated water

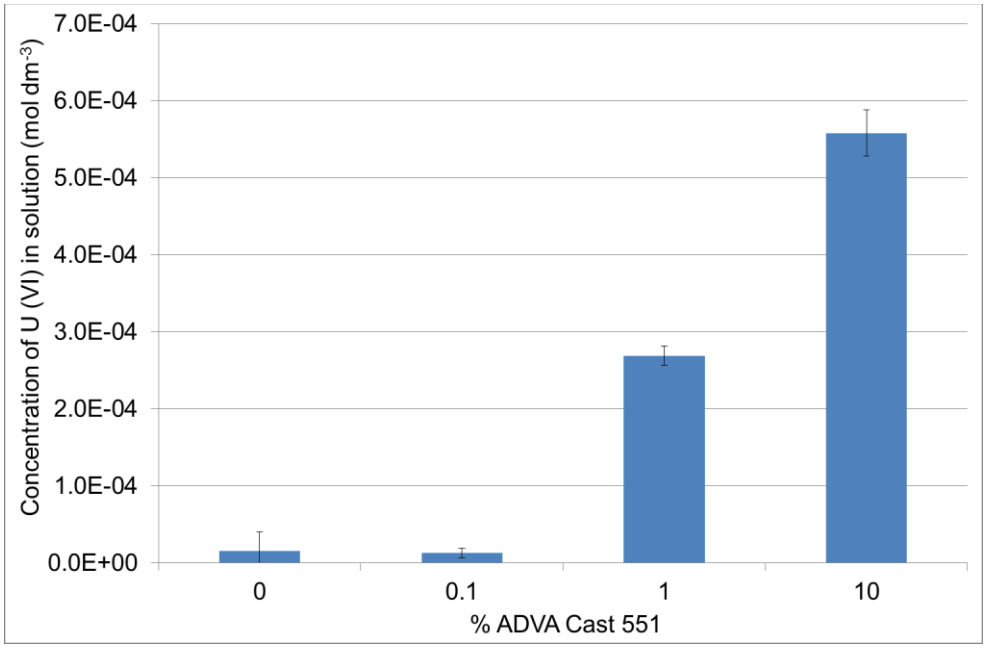

Figure 30 Final concentration of U (VI) in BFS equilibrated water in the presence of ADVA Cast 551

Table 37 U (VI) solubility in BFS equilibrated water in the presence of ADVA Cast 551

Solution	% ADVA Cast	Solubility (mol dm^{-3})	SEF
BFS	0	1.54E-05	1
	0.1	1.33E-05	1
	1	2.69E-04	17
	10	5.58E-04	36

3.3.1.6 PFA equilibrated water

It should be noted, that the pH of PFA equilibrated water samples was adjusted from pH 10 to pH 12.5 ± 0.5 using carbonate free 2 mol dm^{-3} NaOH solution. U (VI) concentration in PFA equilibrated water as a function of contact time is shown in Figure 31. In these experiments, all samples had reached steady state by day 7. In the 0.1% sample set, there are no data for day 21 as the sample was accidentally destroyed. Since all the other data points have reached steady state, it may be assumed that the data point for day 21 would also be within this range.

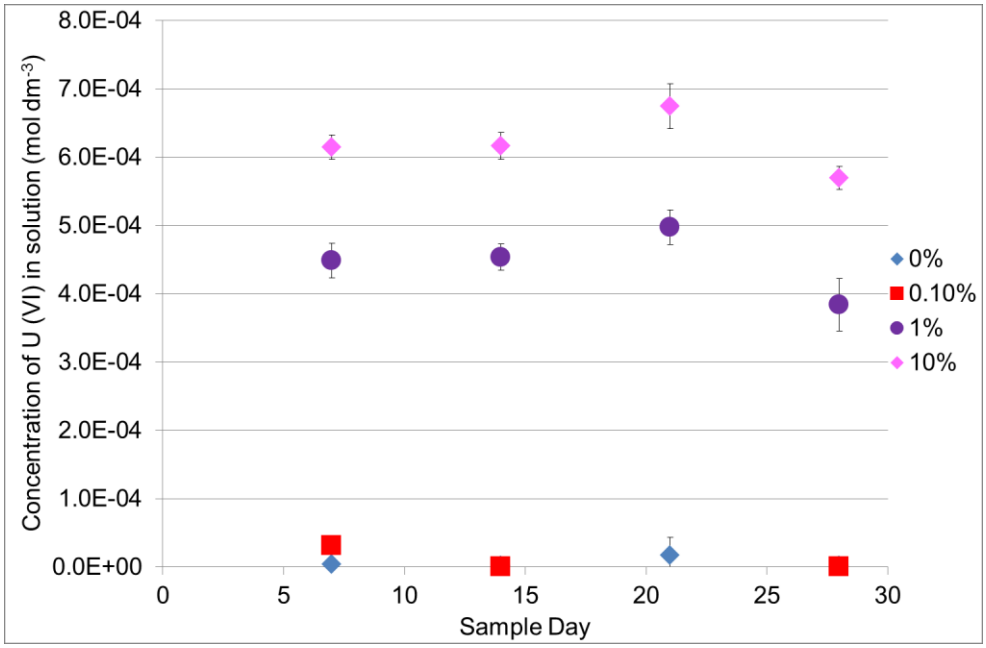

Figure 31 Kinetics of precipitation of U (VI) in the presence of ADVA Cast 551 in PFA equilibrated water

The final concentration of U (VI) in solution is shown in Figure 32. There is a much more significant increase in solubility associated with the PFA equilibrated water than with the BFS. Table 38 shows SEF values of 214 and

318 for 1% and 10% ADVA Cast 551 respectively. There is little difference between U (VI) concentration measured in 0% and 0.1%, within errors these values are the same. At 10% ADVA Cast, the concentration of U (VI) in solution is close to the total inventory.

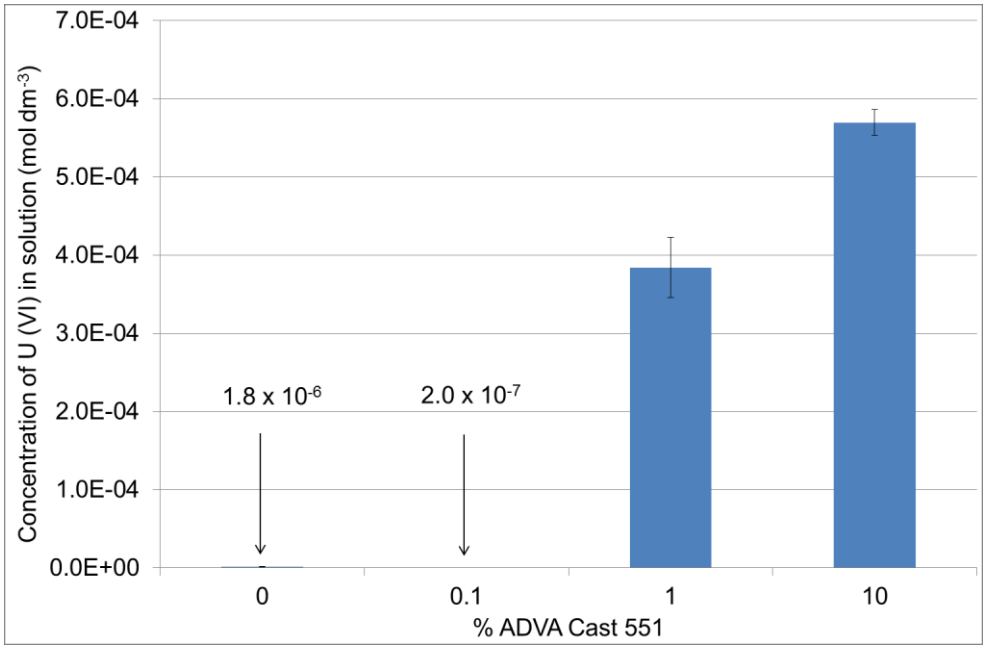

Figure 32 Final concentration of U (VI) in PFA equilibrated water in the presence of ADVA Cast 551

Table 38 U (VI) solubility in PFA equilibrated water in the presence of ADVA Cast 551

Solution	% ADVA Cast	Solubility (mol dm^{-3})	SEF
PFA	0	1.79E-06	1
	0.1	2.00E-07	0
	1	3.84E-04	214
	10	5.69E-04	318

3.3.1.7 OPC equilibrated water

Kinetics of precipitation of U (VI) in OPC equilibrated water is shown in Figure 33. Steady state is reached by day 7 in all cases. There is an increase in U (VI) concentration in solution of almost 2 orders of magnitude with the addition of 1% and 10% ADVA Cast 551. At 10% ADVA Cast the U (VI) in solution is close to the total inventory added. The increase in U (VI) with 0.1% ADVA Cast is not so high but is greater than observed with BFS and PFA equilibrated water. The final concentration of U (VI) in solution is demonstrated in Figure 34 while SEF

values are reported in Table 39. The presence of 1% and 10% ADVA Cast produces a solubility enhancement of 186 and 306 respectively.

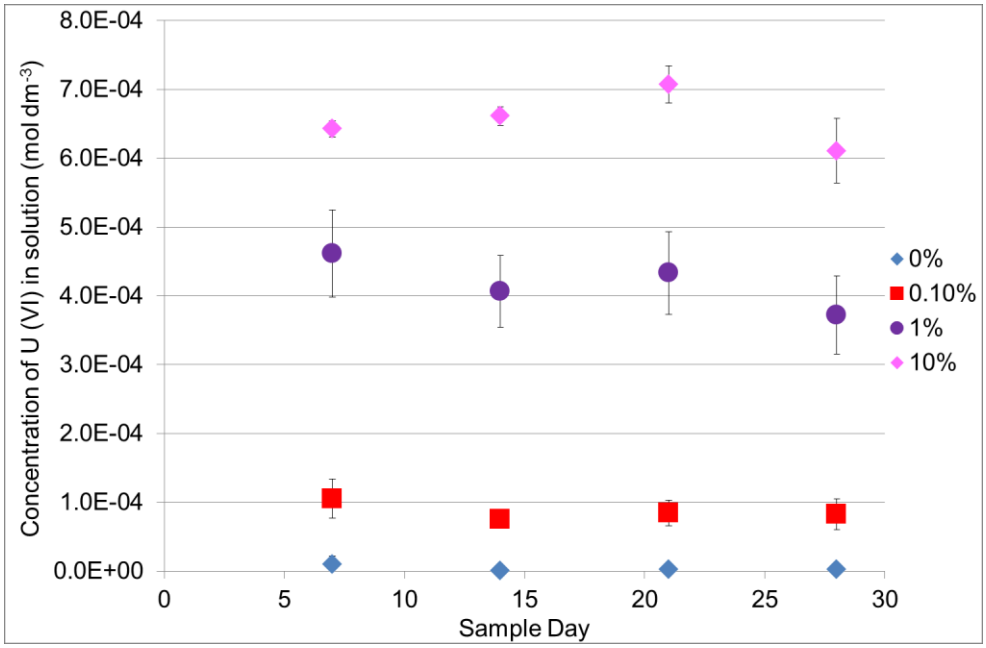

Figure 33 Kinetics of precipitation of U (VI) in the presence of ADVA Cast 551 in OPC equilibrated water

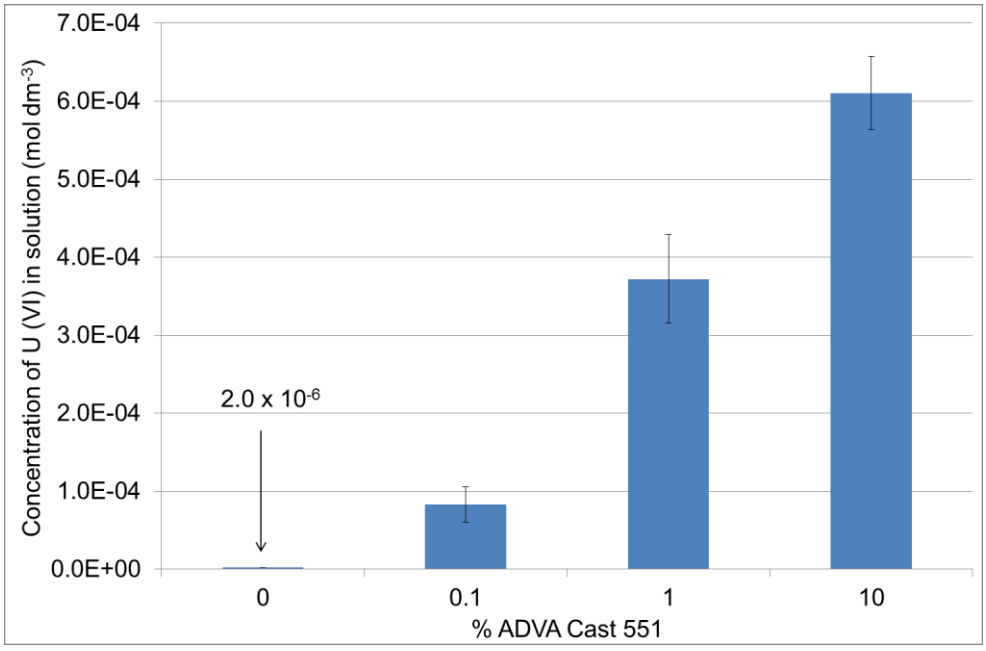

Figure 34 Final concentration of U (VI) in OPC equilibrated water in the presence of ADVA Cast 551

Table 39 U (VI) solubility in OPC equilibrated water in the presence of ADVA Cast 551

Solution	% ADVA Cast	Solubility (mol dm^{-3})	SEF
OPC	0	2.00E-06	1
	0.1	8.28E-05	41
	1	3.72E-04	186
	10	6.11E-04	306

3.3.1.8 U (VI) solubility in PFA equilibrated water – not pH adjusted

U (VI) solubility was measured in PFA equilibrated water that was not adjusted for pH in the presence of 0% and 1% ADVA Cast 551. The concentration of U (VI) in solution was measured at 7 and 28 days. The pH of the aqueous samples was pH 10±0.5. The final concentration of U (VI) measured in solution is shown in Figure 35. The baseline solubility of U (VI) without ADVA Cast 551 was 3.9 x 10^{-4} mol dm^{-3} which is a significantly higher baseline solubility than was observed in the adjusted PFA equilibrated water. This result is as expected since a decrease in solution pH correlates to an increase in metal solubility. This result highlights the importance of high pH conditions in helping to control the solubility and in turn, the migration of metals through cement media.

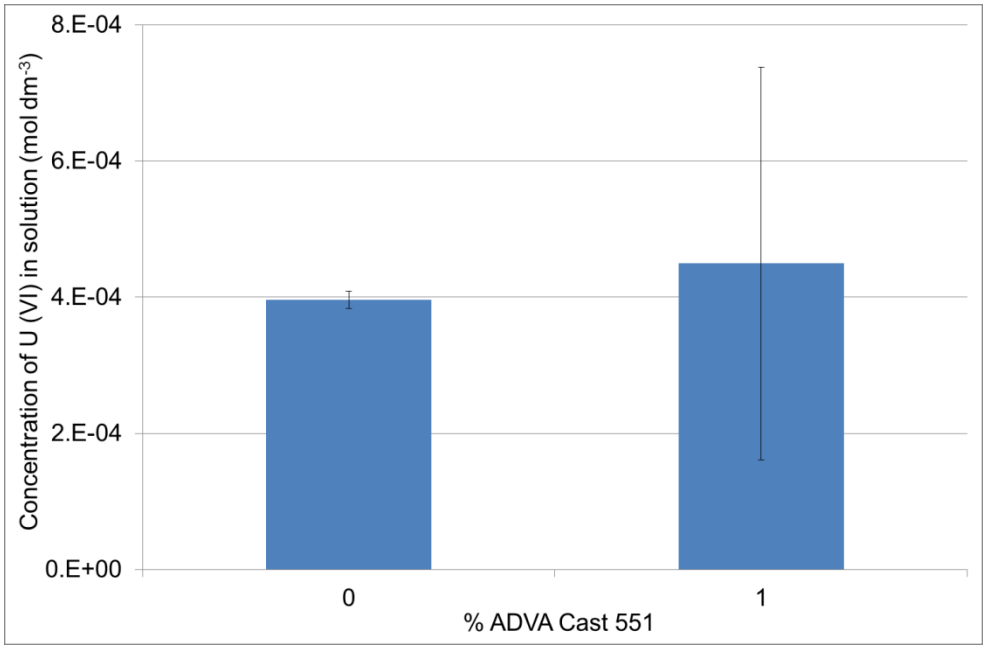

Figure 35 Final concentration of U (VI) PFA equilibrated water that was not adjusted for pH in the presence of ADVA Cast 551

3.3.2 *Thorium (IV) Solubility*

Experimental methods for the determination of Th (IV) solubility are described in 2.5.1. The baseline solubility of Th (IV) in each aqueous solutions investigated was below the limit of detection of the ICP-MS. To calculate SEF values for Th (IV) a representative baseline solubility value of $1x10^{-9}$ mol dm^{-3} was used. This value was determined experimentally by Wierczinski et al. (1998), Neck et al. (2003) and Altmaier et al. (2008) (32,33,67). All the errors reported represent ± the standard deviation of 4 sample replicates.

3.3.2.1 95% Saturated $Ca(OH)_2$

Th (IV) concentration in 95% saturated $Ca(OH)_2$ as a function of contact time is shown in Figure 36. In all cases, steady state was reached by day 7.

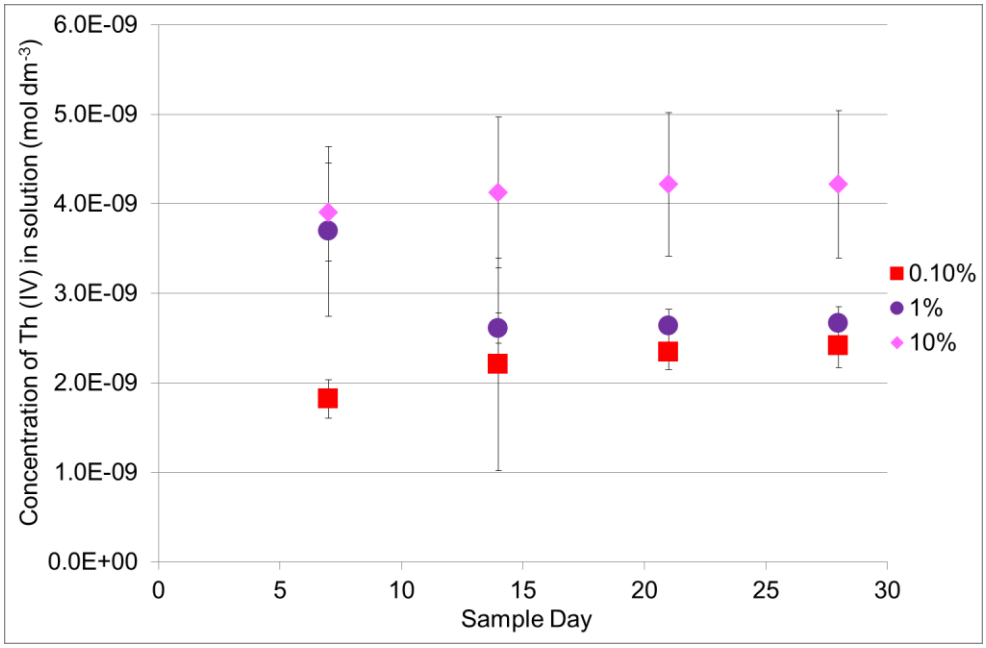

Figure 36 Kinetics of precipitation of Th (IV) in the presence of ADVA Cast 551 in 95% saturated $Ca(OH)_2$

There is a slight increase in the solubility of Th (IV) with increasing amounts of ADVA Cast 551, however the calculated SEF values (shown in Table 40) are significantly lower than those calculated for U (VI) in 95% saturated $Ca(OH)_2$.

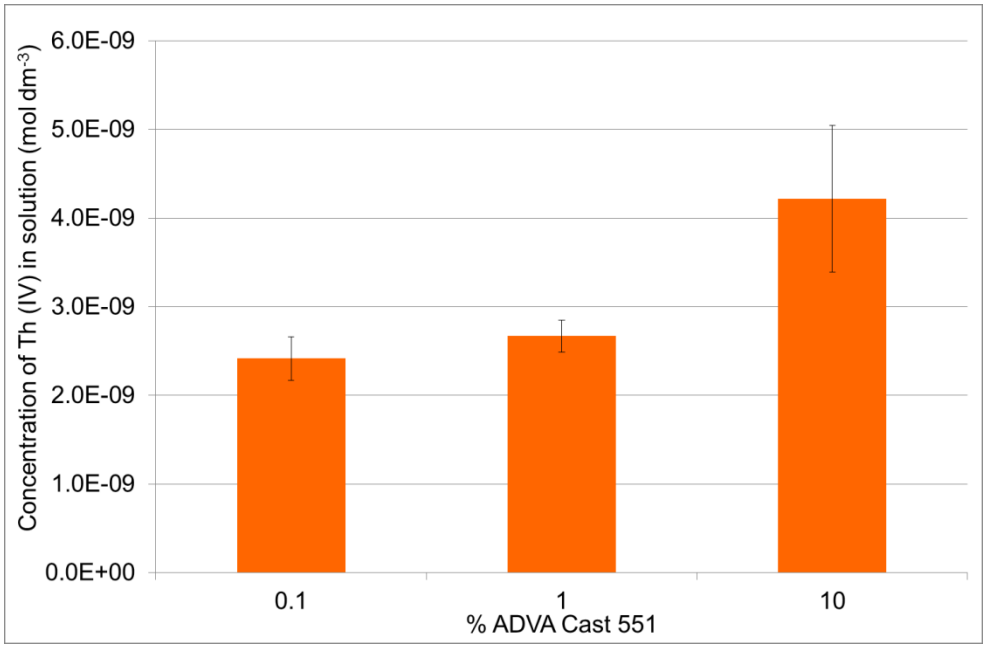

Figure 37 Final concentration of Th (IV) in 95% saturated $Ca(OH)_2$ in the presence of ADVA Cast 551

Table 40 Th (IV) solubility in 95% saturated $Ca(OH)_2$ in the presence of ADVA Cast 551

Solution	% ADVA Cast	Solubility (mol dm^{-3})	SEF
$Ca(OH)_2$	0	1.00E-09	1
	0.1	2.42E-09	2
	1	2.67E-09	3
	10	4.22E-09	4

3.3.2.2 0.1 mol dm^{-3} NaOH

Th (IV) kinetics of precipitation in 0.1 mol dm^{-3} NaOH is shown in Figure 38.

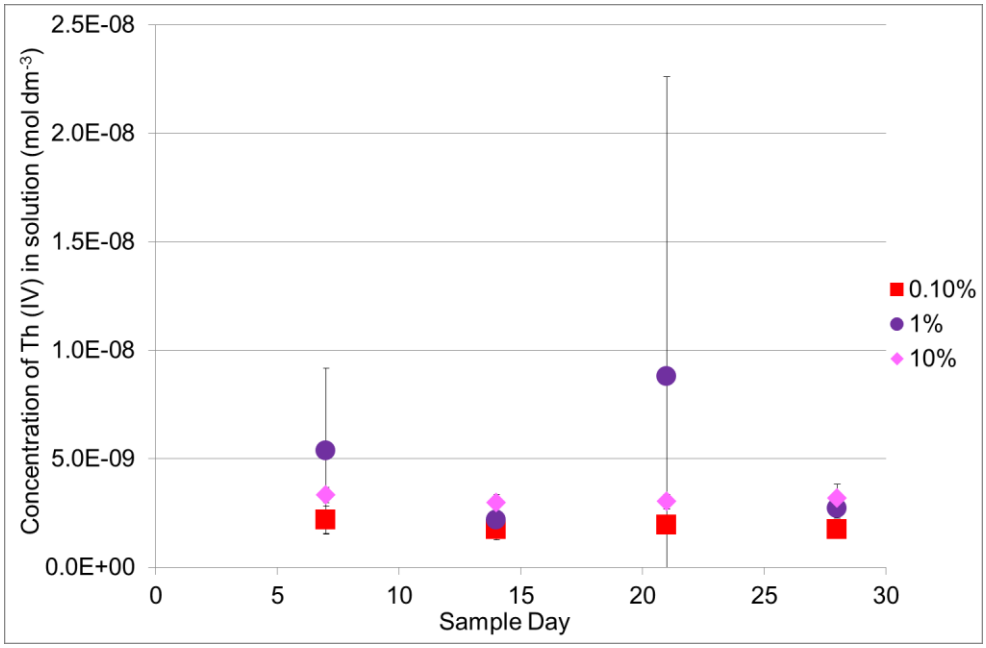

Figure 38 Kinetics of precipitation of Th (IV) in the presence of ADVA Cast 551 in 0.1 mol dm^{-3} NaOH

Steady state was reached by Day 7. There is little change in the Th (IV) concentration in solution with increasing amounts of ADVA Cast 551 (Figure 39). SEF values for 1% and 10% ADVA Cast were calculated to be the same at a value of 3 (SEF values are reported in Table 41).

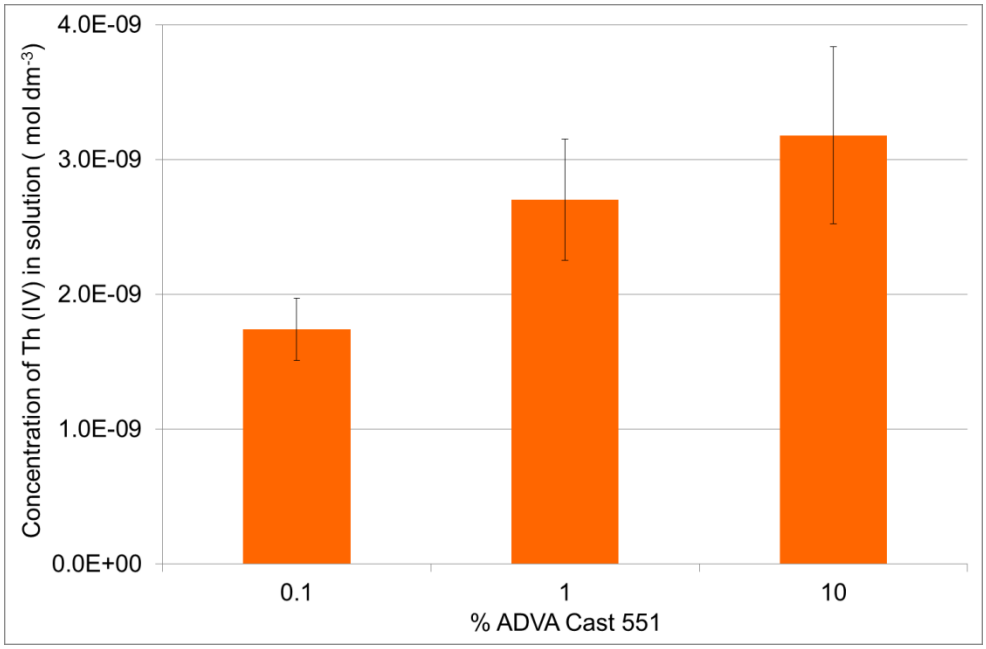

Figure 39 Final concentration of Th (IV) in 0.1 mol dm^{-3} NaOH in the presence of ADVA Cast 551

Table 41 Th (IV) solubility in 0.1 mol dm^{-3} NaOH in the presence of ADVA Cast 551

Solution	% ADVA Cast	Solubility (mol dm^{-3})	SEF
NaOH	0	1.00E-09	1
	0.1	1.74E-09	2
	1	2.70E-09	3
	10	3.18E-09	3

3.3.2.3 BFS:OPC equilibrated water

As demonstrated in Figure 40, in BFS:OPC equilibrated water, Th (IV) solubility reached steady state by day 21. This was 14 days longer than in the case of $Ca(OH)_2$ and NaOH. One reason for the samples taking longer to reach steady state is experimental error. As described in section 2.5.1, Th (IV) samples were prepared in a glove box, sealed and then transferred to a fridge for their equilibration time. The vials were transferred back to the glove box once per week to take samples for the solubility kinetics study. The precipitates were delicate and easily disturbed and although great care was taken, some samples may have been knocked in transfer.

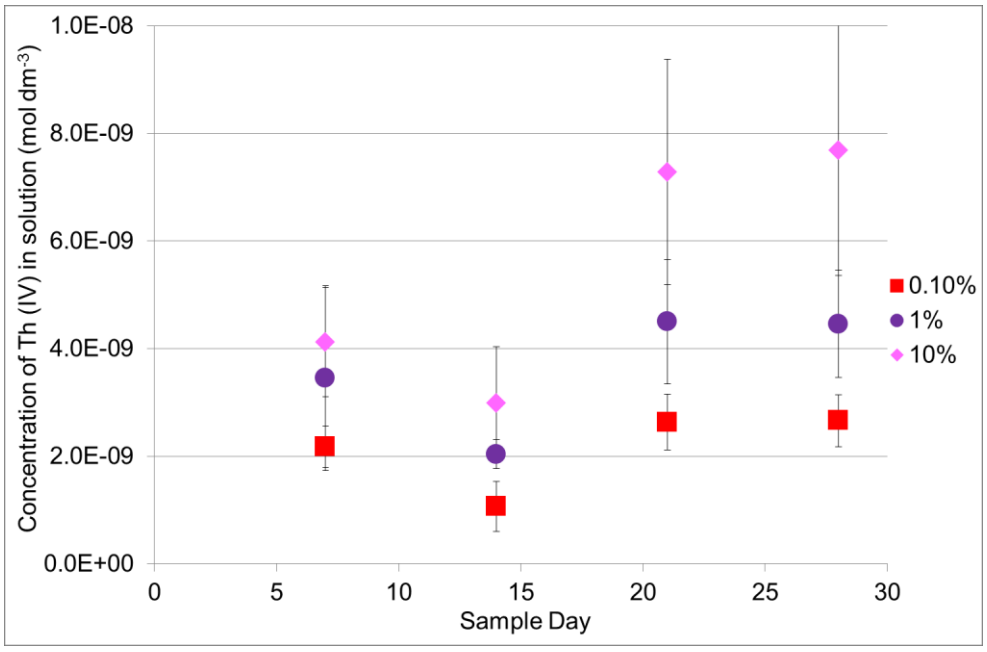

Figure 40 Kinetics of precipitation of Th (IV) in the presence of ADVA Cast 551 in BFS:OPC equilibrated water

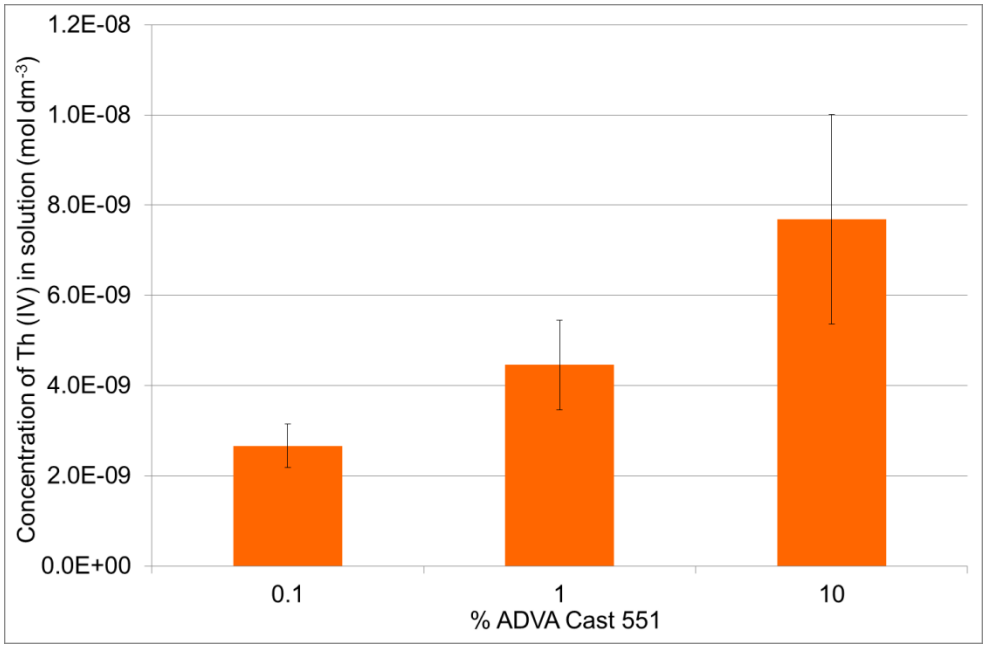

Figure 41 Final concentration of Th (IV) in BFS:OPC equilibrated water in the presence of ADVA Cast 551

Similarly to $Ca(OH)_2$ and NaOH, there is a small increase in solubility with increasing amounts of ADVA Cast 551 (Figure 41). The SEF value in the presence of 10% ADVA Cast 551 is 8, as shown in Table 42. This value is smaller than the SEF value of 320 for U (VI) in the same BFS:OPC solution in the presence of 10% ADVA Cast.

Table 42 Th (IV) solubility in BFS:OPC equilibrated water in the presence of ADVA Cast 551

Solution	% ADVA Cast	Solubility (mol dm^{-3})	SEF
BFS:OPC	0	1.00E-09	1
	0.1	2.66E-09	3
	1	4.46E-09	4
	10	7.69E-09	8

3.3.2.4 PFA:OPC equilibrated water

Kinetics of precipitation of Th (IV) in PFA:OPC equilibrated water are shown in Figure 42.

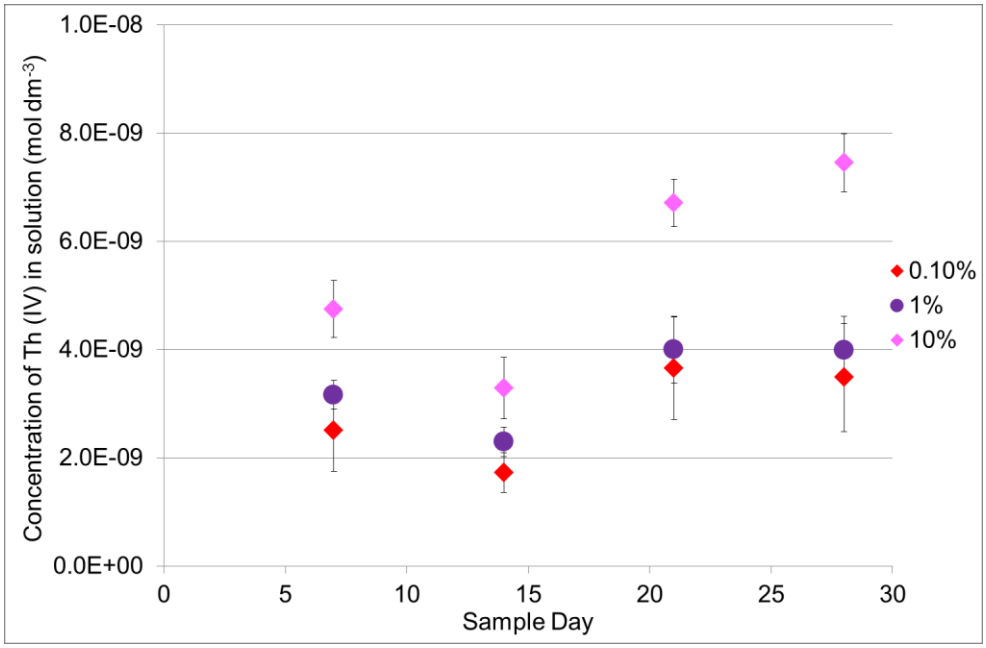

Figure 42 Kinetics of precipitation of Th (IV) in the presence of ADVA Cast 551 in PFA:OPC equilibrated water

Similarly to the BFS:OPC samples, steady state was reached by day 21 indicating experimental error associated with the transfer of samples from the fridge to the glove box. The final concentration of Th (IV) in solution is shown in Figure 43. A slight increase in solubility is observed at 10% ADVA Cast 551 with an SEF value of 7 (Table 43).

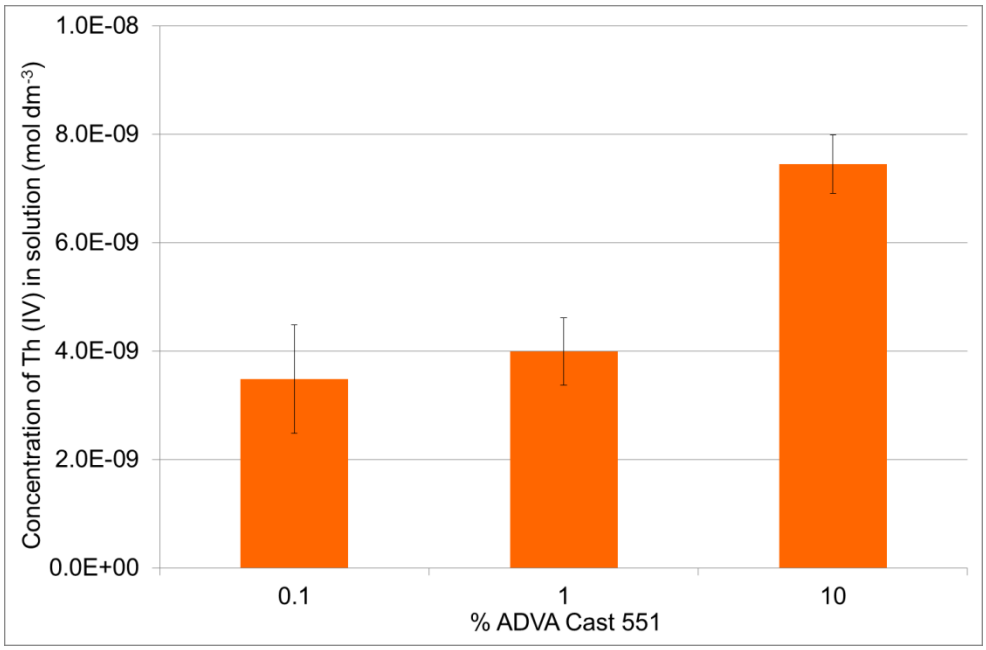

Figure 43 Final concentration of Th (IV) in PFA:OPC equilibrated water in the presenc of ADVA Cast 551

Table 43 Th (IV) solubility in PFA:OPC equilibrated water in the presence of ADVA Cast 551

Solution	% ADVA Cast	Solubility (mol dm^{-3})	SEF
PFA:OPC	0	1.00E-09	1
	0.1	3.48E-09	3
	1	3.99E-09	4
	10	7.45E-09	7

3.3.2.5 BFS equilibrated water

Figure 44 shows the concentration of Th (IV) in BFS equilibrated water as a function of time.

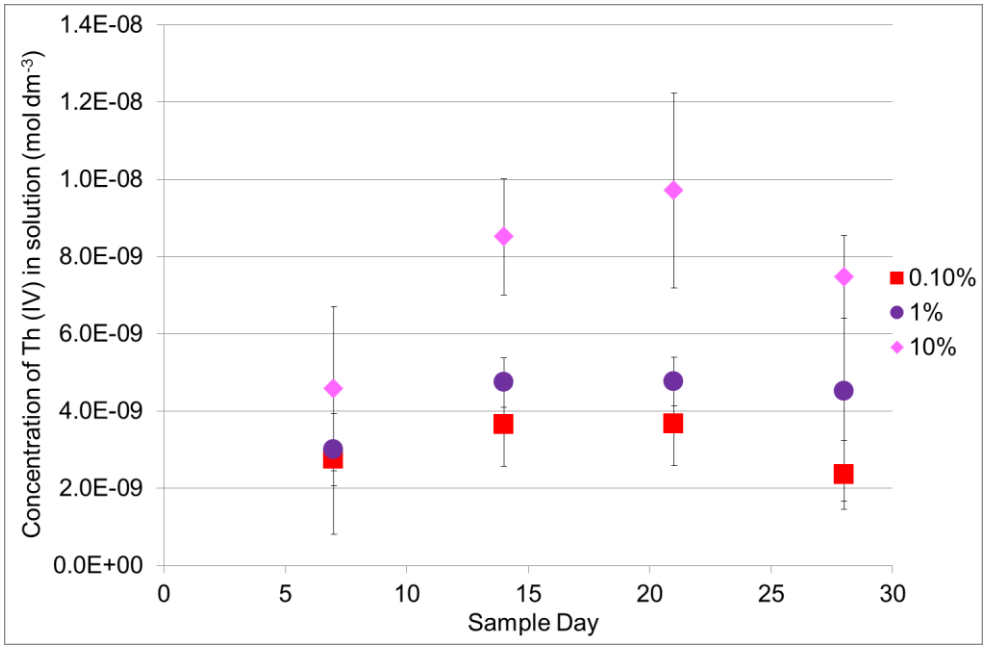

Figure 44 Kinetics of precipitation of Th (IV) in the presence of ADVA Cast 551 in BFS equilibrated water

Steady state was reached by day 14 and a similar increase in solubility was observed compared to BFS:OPC and PFA:OPC equilibrated water with an SEF value of 8 in the presence of 10% ADVA Cast 551 (SEF values are reported in Table 44). Figure 45 demonstrates the final concentration of Th (IV) measured in solution.

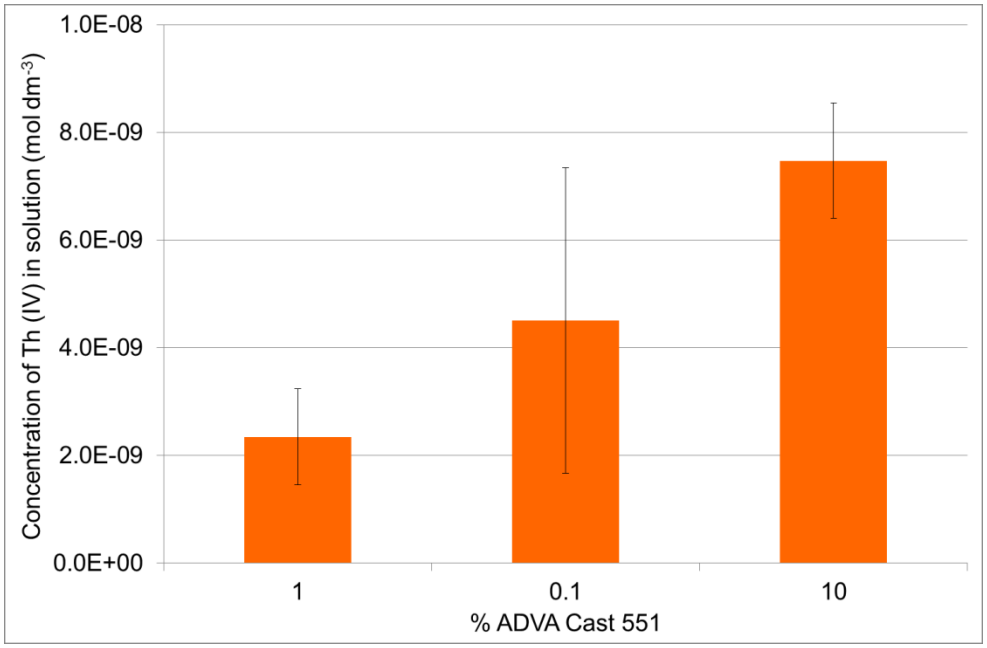

Figure 45 Final concentration of Th (IV) in BFS equilibrated water in the presence of ADVA Cast 551

Table 44 Th (IV) solubility in BFS equilibrated water in the presence of ADVA Cast 551

Solution	% ADVA Cast	Solubility (mol dm^{-3})	SEF
BFS	0	1.00E-09	1
	0.1	2.35E-09	2
	1	4.51E-09	5
	10	7.47E-09	7

3.3.2.6 PFA equilibrated water

Th (IV) solubility reached steady state by day 14 in PFA equilibrated water. Kinetics of precipitation is shown in Figure 46.

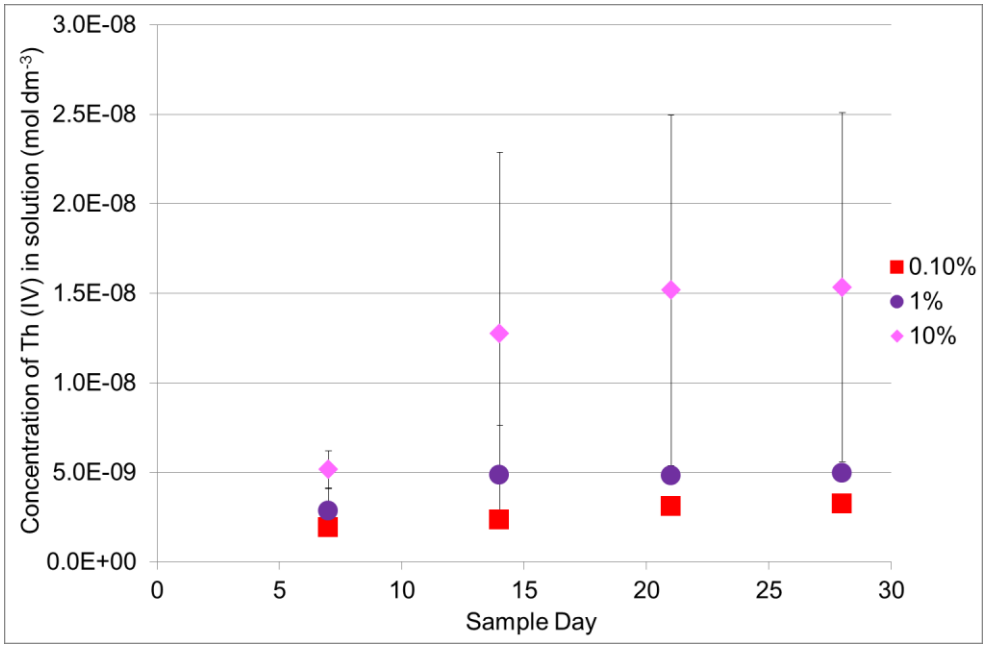

Figure 46 Kinetics of precipitation of Th (IV) in the presence of ADVA Cast 551 in PFA equilibrated water

As demonstrated in Figure 47 the increase in Th (IV) solubility with the presence of 10% ADVA Cast is slightly higher than observed in the other aqueous solutions. Table 45 reports SEF values of 5 and 15 for 1% and 10% ADVA Cast 551 respectively. This is the highest SEF observed for a Th (IV) solubility measurement.

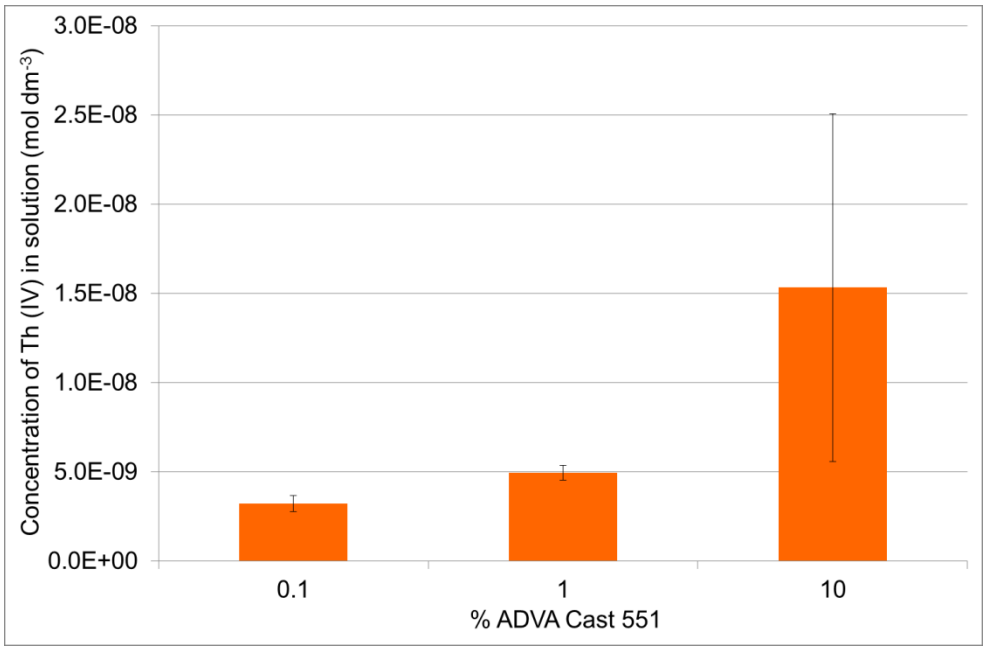

Figure 47 Final concentration of Th (IV) in PFA equilibrated water in the presence of ADVA Cast 551

Table 45 Th (IV) solubility in PFA equilibrated water in the presence of ADVA Cast 551

Solution	% ADVA Cast	Solubility (mol dm^{-3})	SEF
PFA	0	1.00E-09	1
	0.1	3.23E-09	3
	1	4.95E-09	5
	10	1.53E-08	15

3.3.2.7 OPC equilibrated water

Kinetics of precipitation for Th (IV) in OPC equilibrated water is shown in Figure 48. Steady state was reached by day 21. Figure 49 shows the final concentration of Th (IV) in solution and is similar to that recorded in BFS, BFS:OPC and PFA:OPC. SEF values shown in Table 46 are also similar with 10% ADVA Cast having an SEF value of 8.

Overall, across all high pH aqueous solutions investigated, the presence of ADVA Cast 551 does not have a significant effect on the solubility of Th (IV) in comparison to U (VI). At low concentrations of superplasticiser in particular, Th (IV) solubility is not greatly increased.

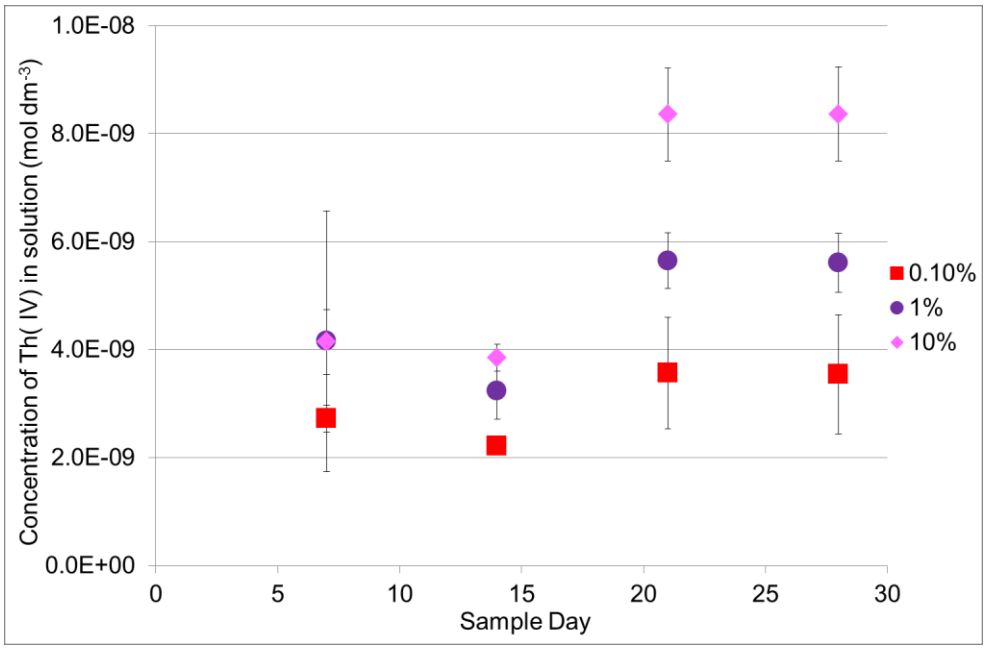

Figure 48 Kinetics of precipitation of Th (IV) in the presence of ADVA Cast 551 in OPC equilibrated water

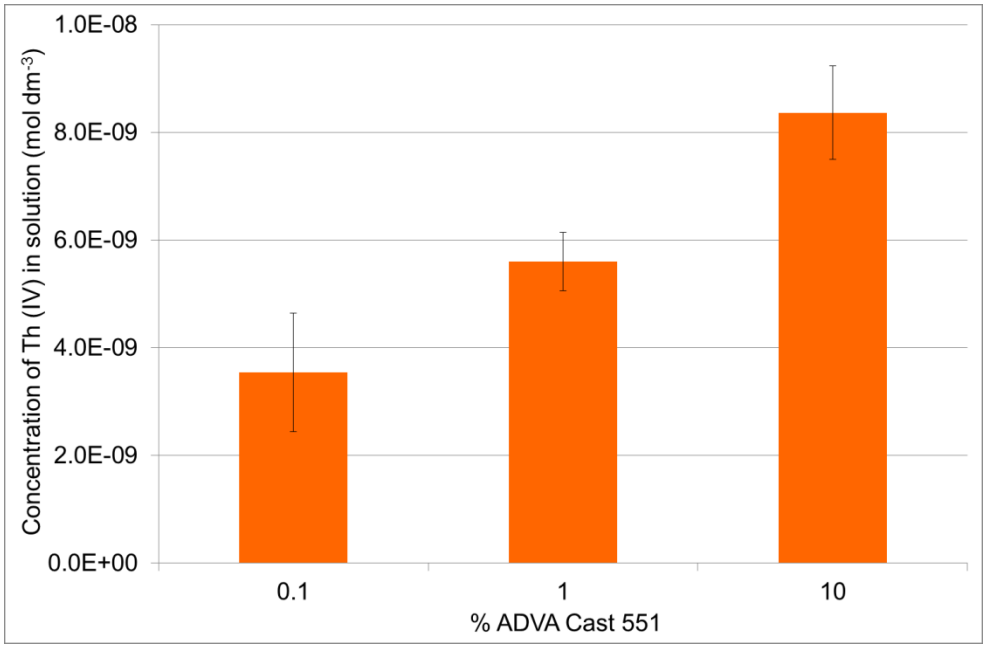

Figure 49 Final concentration of Th (IV) in OPC equilibrated water in the presence of ADVA Cast 551

Table 46 Th (IV) solubility in OPC equilibrated water in the presence of ADVA Cast 551

Solution	% ADVA Cast	Solubility (mol dm^{-3})	SEF
OPC	0	1.00E-09	1
	0.1	3.55E-09	4
	1	5.60E-09	6
	10	8.37E-09	8

3.3.3 *Europium (III) Solubility*

In contrast to the Th (IV) experiment, the solubility of Eu (III) is much more significantly affected by the presence of ADVA Cast 551.

3.3.3.1 95% Saturated $Ca(OH)_2$

Kinetics of precipitation of Eu (III) in 95% saturated $Ca(OH)_2$ is shown in Figure 50. Steady state was reached by day 14. The final concentration of Eu (III) measured in solution is shown in Figure 51; where it is clear there is a substantial increase in Eu (III) solubility between 0% and 10% AVDA Cast 551.

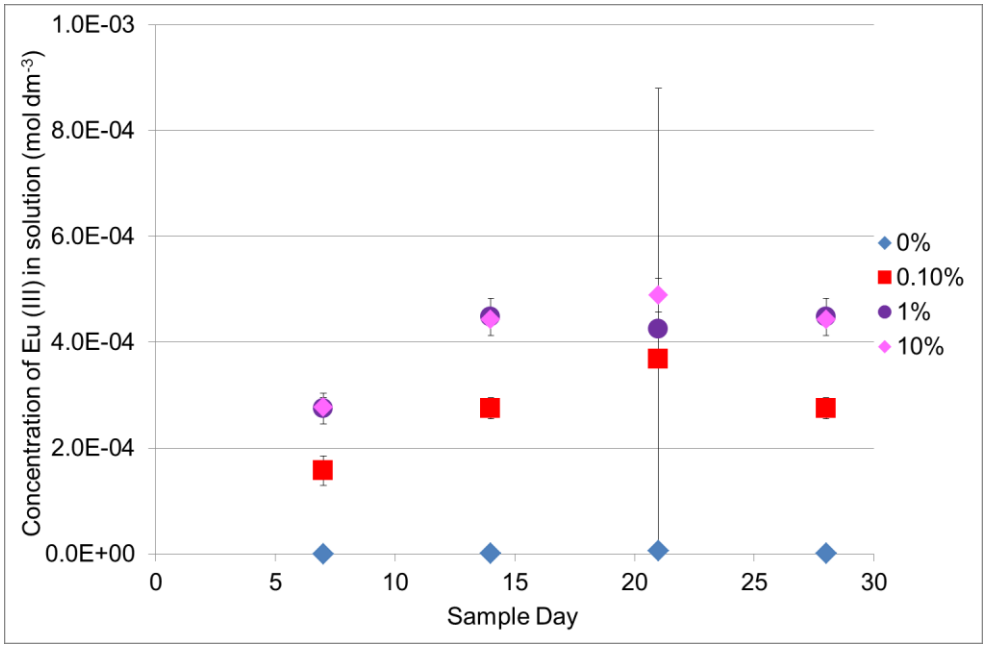

Figure 50 Kinetics of precipitation of Eu (III) in the presence of ADVA Cast 551 in 95% saturated $Ca(OH)_2$

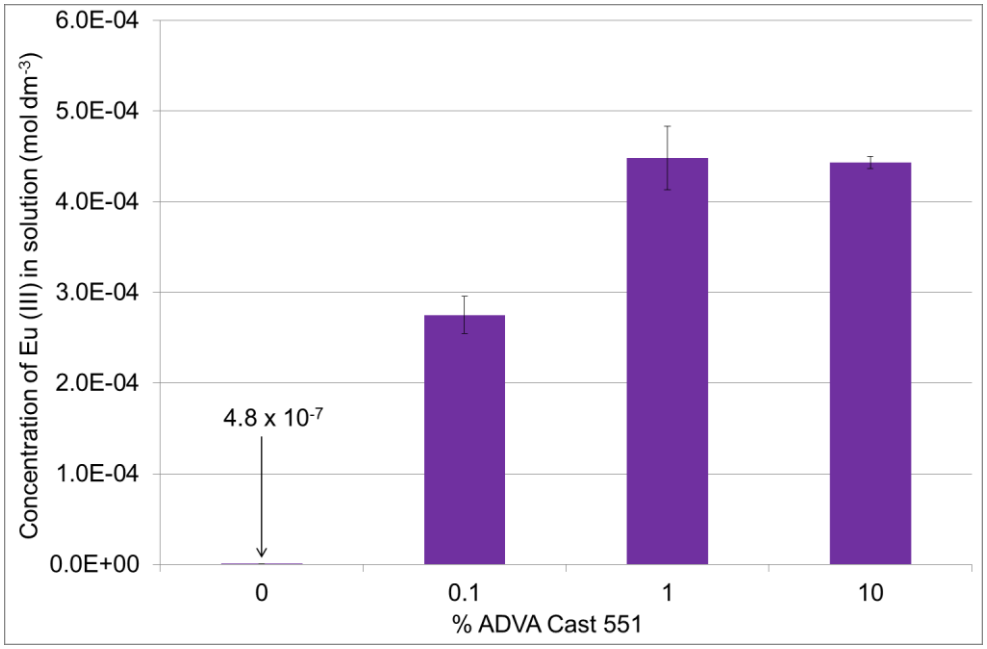

Figure 51 Final concentration of Eu (III) in 95% saturated $Ca(OH)_2$ in the presence of ADVA Cast 551

In this case, an increase in solubility of Eu (III) is observed at all concentrations of ADVA Cast 551. SEF values of 547, 936 and 926 were calculated for 0.1%, 1% and 10% superplasticiser respectively which demonstrates, an increase in solubility over several orders of magnitude (SEF values are reported in Table

47). The Eu (III) concentration in solution in the presence of 0.1%, 1% and 10% are close to the total inventory added. This means that if more Eu (III) had been present in solution, the concentration of Eu (III) measured could have been higher.

Table 47 Eu (III) solubility in 95% saturated $Ca(OH)_2$ in the presence of ADVA Cast 551

Solution	% ADVA Cast	Solubility (mol dm^{-3})	SEF
$Ca(OH)_2$	0	4.79E-07	1
	0.1	2.75E-04	574
	1	4.48E-04	936
	10	4.43E-04	926

3.3.3.2 0.1 mol dm^{-3} NaOH

A similar trend for Eu (III) solubility is observed in NaOH. A substantial increase in solubility is measured over all concentrations of AVDA Cast 551. Kinetics of precipitation is shown in Figure 52. Steady state was reached by day 7 in all cases.

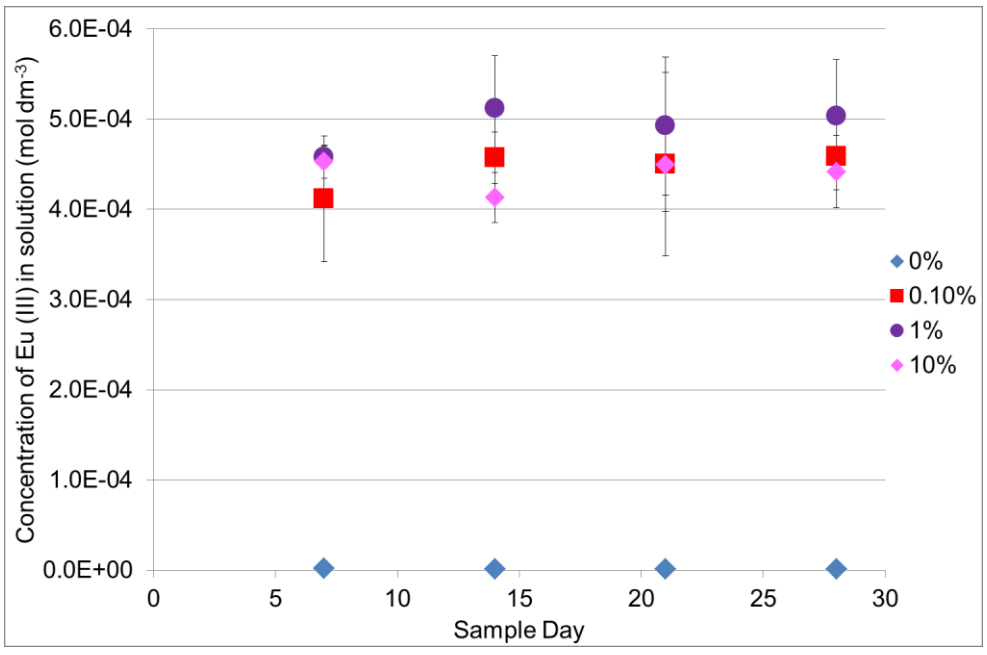

Figure 52 Kinetics of precipitation of Eu (III) in the presence of ADVA Cast 551 in 0.1 mol dm^{-3} NaOH

Figure 53 reports the final concentration of Eu (III) in solution while Table 48 shows the calculated SEF values. The concentration of Eu (III) in solution

measured in the presence of 0.1%, 1% and 10% ADVA Cast 551 are close to the total inventory added. This means that in the presence of ADVA Cast 551, all of the Eu (III) added to the samples has been solubilised.

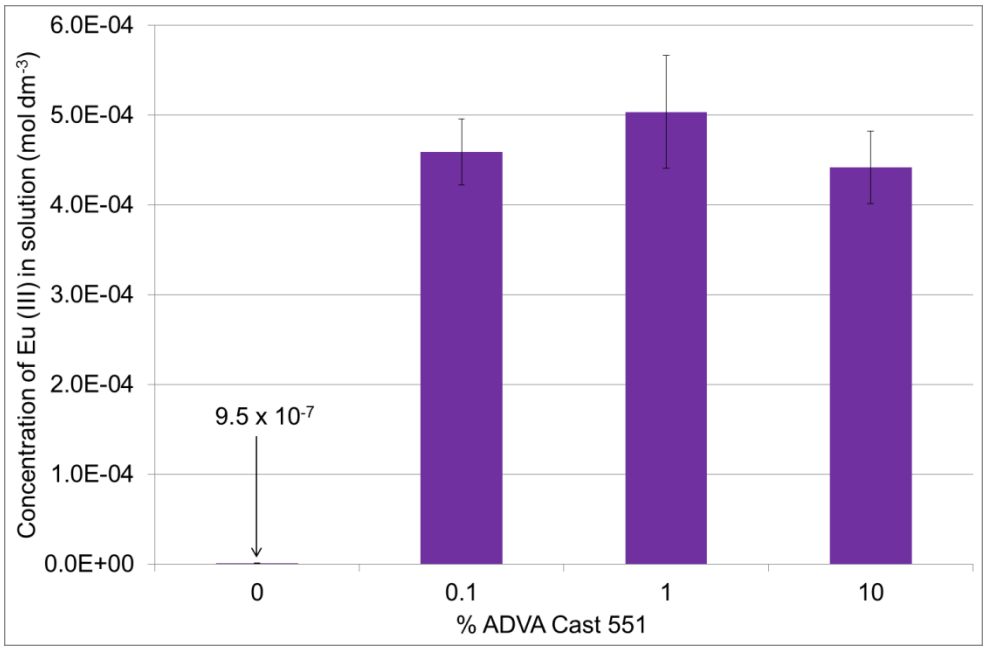

Figure 53 Final concentration of Eu (III) in 0.1 mol dm^{-3} NaOH in the presence of ADVA Cast 551

Table 48 Eu (III) solubility in 0.1 mol dm^{-3} NaOH in the presence of ADVA Cast 551

Solution	% ADVA Cast	Solubility (mol dm^{-3})	SEF
NaOH	0	9.48E-07	1
	0.1	4.59E-04	484
	1	5.03E-04	531
	10	4.42E-04	466

3.3.3.3 BFS:OPC equilibrated water

Eu (III) concentration in BFS:OPC equilibrated water as a function of time is shown in Figure 54. Steady state was reached by day 7 for all samples except the 0.1% samples which reached steady state by day 21. As was the case for NaOH and $Ca(OH)_2$, the concentration of Eu (III) measured in the 0.1%, 1% and 10% samples was close to the Eu (III) inventory limit (as shown in Figure 55).

Table 49 demonstrates similar SEF values for each concentration of ADVA Cast with 0.1%, 1% and 10% having SEF values of 314, 338 and 306 respectively.

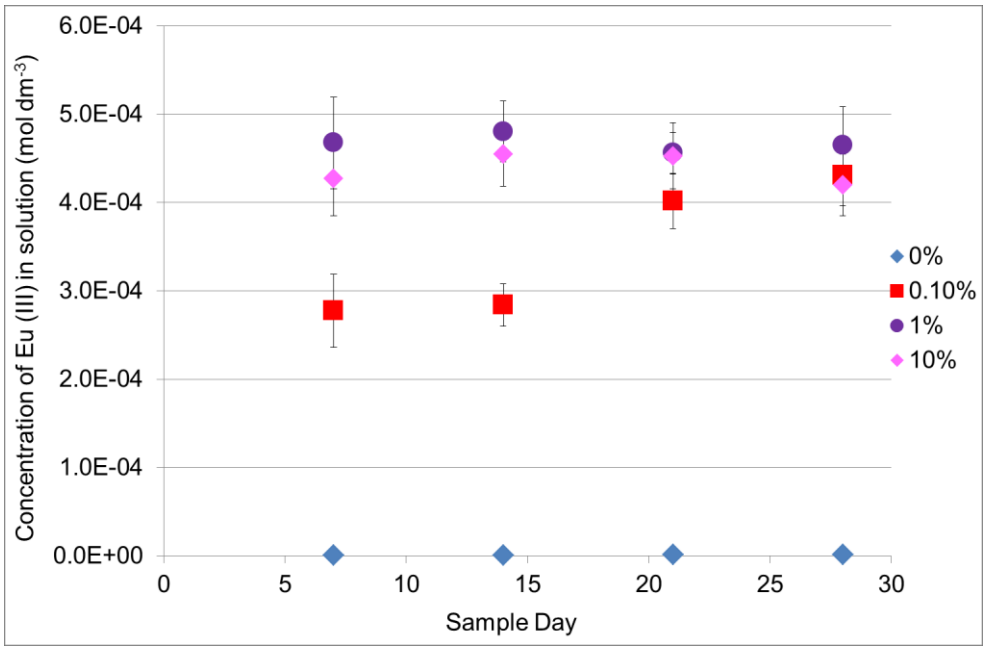

Figure 54 Kinetics of precipitation of Eu (III) in the presence of ADVA Cast 551 in BFS:OPC equilibrated water

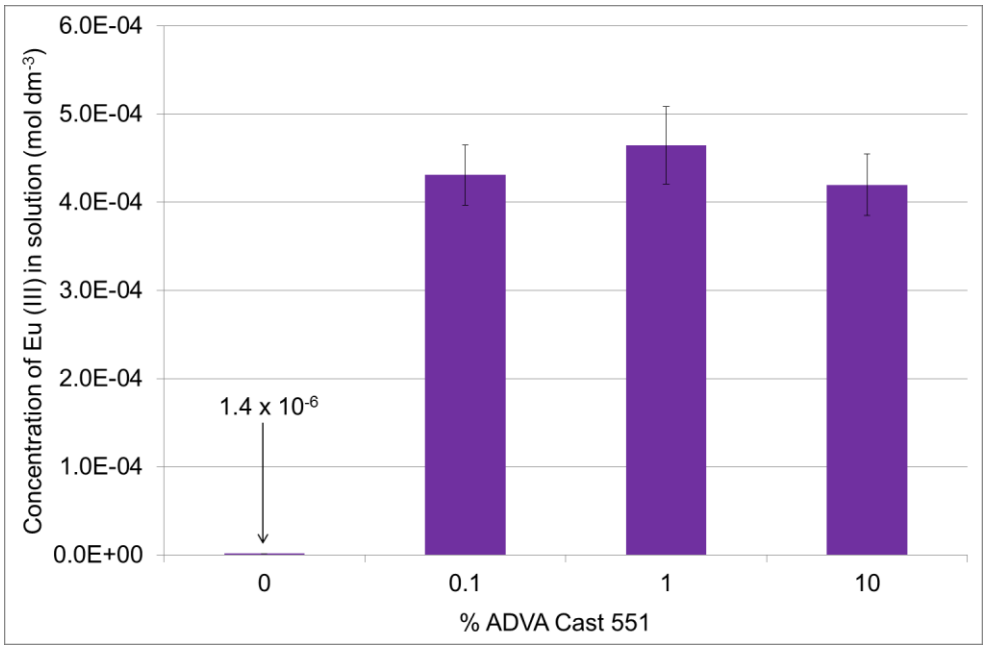

Figure 55 Final concentration of Eu (III) in BFS:OPC equilibrated water in the presence of ADVA Cast 551

Table 49 Eu (III) solubility in BFS:OPC equilibrated water in the presence of ADVA Cast 551

Solution	% ADVA Cast	Solubility (mol dm^{-3})	SEF
BFS:OPC	0	1.37E-06	1
	0.1	4.31E-04	314
	1	4.65E-04	338
	10	4.20E-04	306

3.3.3.4 PFA:OPC equilibrated water

Kinetics of precipitation of Eu (III) in PFA:OPC equilibrated water is shown in Figure 56.

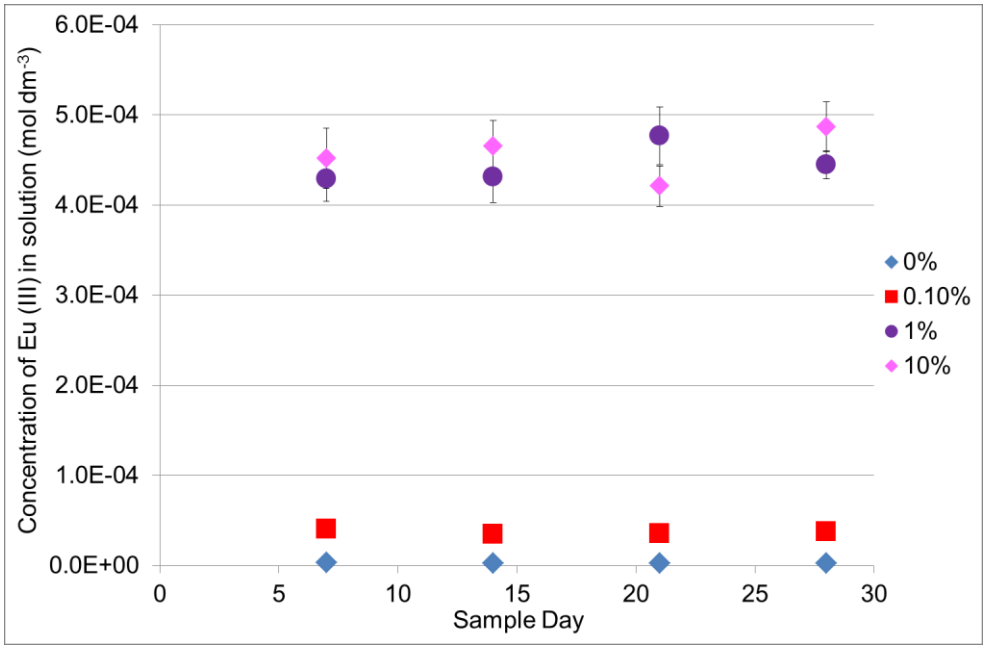

Figure 56 Kinetics of precipitation of Eu (III) in the presence of ADVA Cast 551 in PFA:OPC equilibrated water

In this case, the increase in Eu (III) solubility with the presence of 0.1% ADVA Cast is not as significant as was observed in BFS:OPC equilibrated water, however, the enhancement is in the region of an order or magnitude. Figure 57 shows that in the presence of 1% and 10% ADVA Cast 551, the Eu (III) concentration in solution is close to the total inventory added. SEF values reported in Table 50 indicate similar solubility enhancement at 1% and 10% ADVA Cast with values of 165 and 170 for 1% and 10% ADVA Cast respectively.

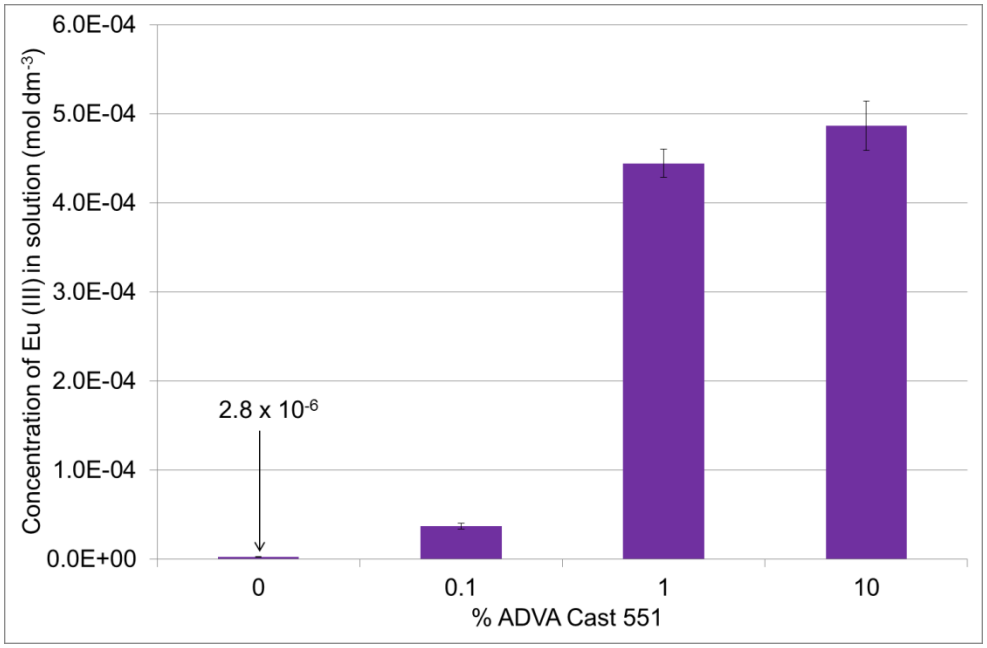

Figure 57 Final concentration of Eu (III) in PFA:OPC equilibrated water in the presence of ADVA Cast 551

Table 50 Eu (III) solubility in PFA:OPC equilibrated water in the presence of ADVA Cast 551

Solution	% ADVA Cast	Solubility (mol dm^{-3})	SEF
PFA:OPC	0	2.78E-06	1
	0.1	3.73E-05	13
	1	4.44E-04	160
	10	4.87E-04	175

3.3.3.5 BFS equilibrated water

A similar trend in solubility enhancement to the other aqueous solutions investigated was observed for Eu (III) in BFS equilibrated water. The concentration of Eu (III) measured in the presence of 1% and 10% ADVA Cast 551 is close to the total inventory added. Kinetics of precipitation is demonstrated in Figure 58 where steady state is reached by day 7 in all cases.

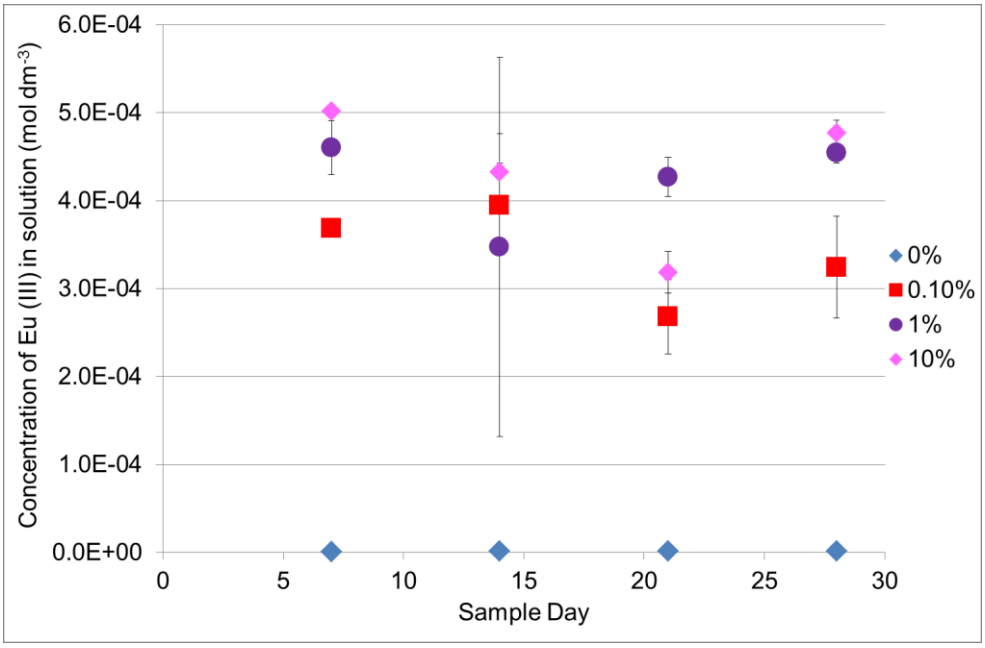

Figure 58 Kinetics of precipitation of Eu (III) in the presence of ADVA Cast 551 in BFS equilibrated water

The final concentration of Eu (III) measured in solution is shown in Figure 59. Eu (III) solubility enhancement is in the region of 2 orders of magnitude. SEF values of 243, 340 and 357 are reported for 0.1%, 1% and 10% ADVA Cast 551 respectively in Table 51.

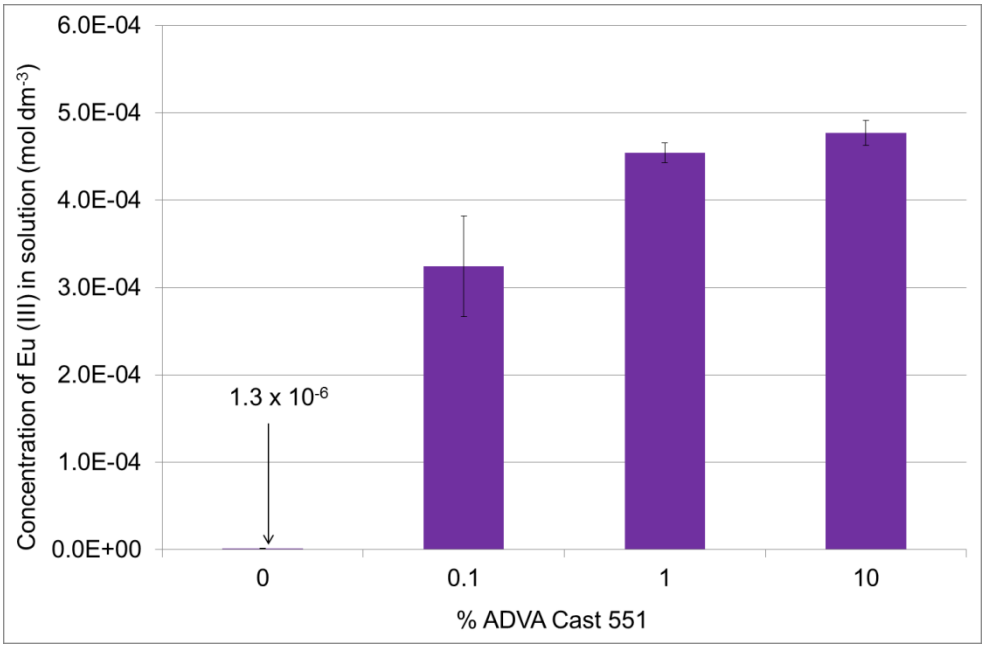

Figure 59 Final concentration of Eu (III) in BFS equilibrated water in the presence of ADVA Cast 551

Table 51 Eu (III) solubility in BFS equilibrated water in the presence of ADVA Cast 551

Solution	% ADVA Cast	Solubility (mol dm^{-3})	SEF
BFS	0	1.34E-06	1
	0.1	3.24E-04	243
	1	4.54E-04	340
	10	4.77E-04	357

3.3.3.6 PFA equilibrated water

Kinetics of precipitation of Eu (III) in PFA equilibrated water is shown in Figure 60. Steady state was reached by day 7 in all cases. In the presence of 10% ADVA Cast, the concentration of Eu (III) has reached the inventory limit therefore all Eu (III) in the sample has been solubilised. The solubility of Eu (III) in the presence of 0.1% and 1% ADVA Cast 551 are similar and have SEF values of 420 and 343 respectively as reported in Table 52.

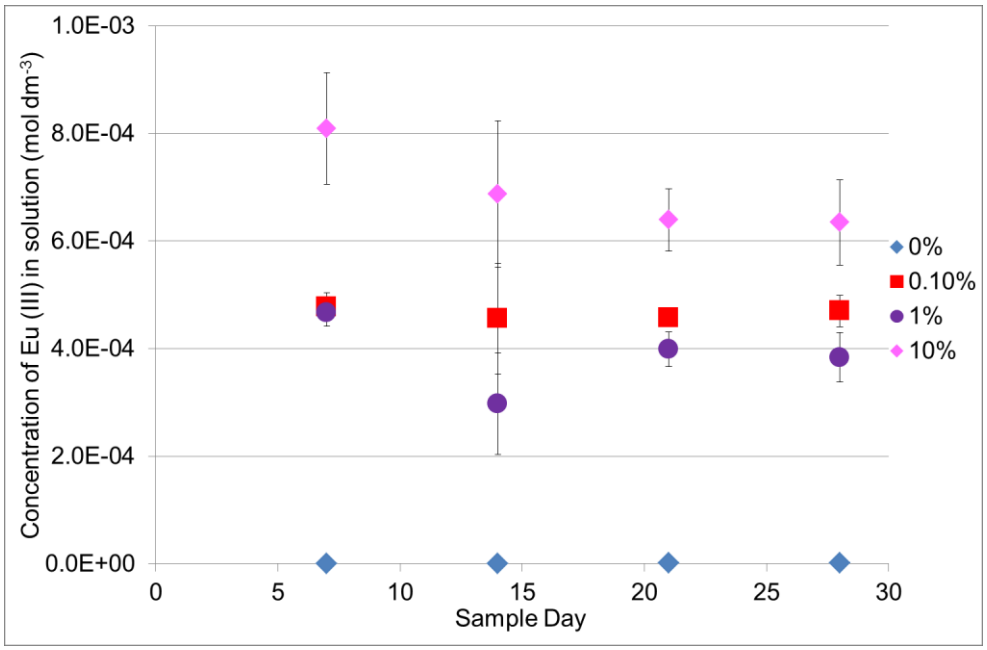

Figure 60 Kinetics of precipitation of Eu (III) in the presence of ADVA Cast 551 in PFA equilibrated water

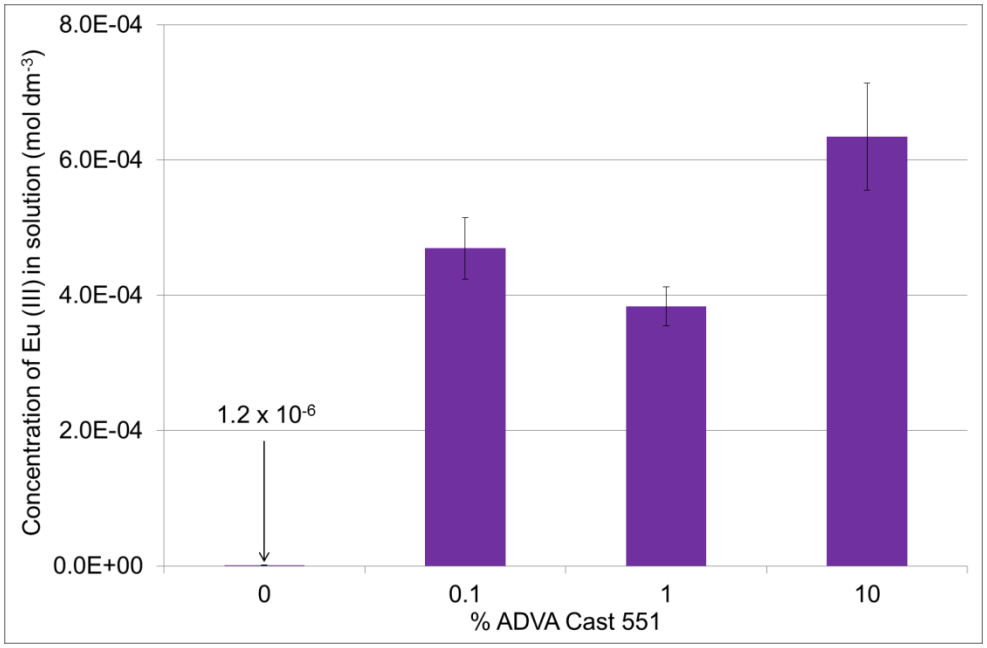

Figure 61 Final concentration of Eu (III) in PFA equilibrated water in the presence of ADVA Cast 551

Table 52 Eu (III) solubility in PFA equilibrated water in the presence of ADVA Cast 551

Solution	% ADVA Cast	Solubility (mol dm^{-3})	SEF
PFA	0	1.12E-06	1
	0.1	4.70E-04	420
	1	3.84E-04	343
	10	6.35E-04	568

3.3.4 *OPC equilibrated water*

Kinetics of precipitation of Eu (III) in OPC equilibrated water is shown in Figure 62. Steady state was reached by day 7 in all samples except the 10% ADVA Cast 551 samples which reached steady state by day 14. The final concentration of Eu (III) that was measured in solution is shown in Figure 63.

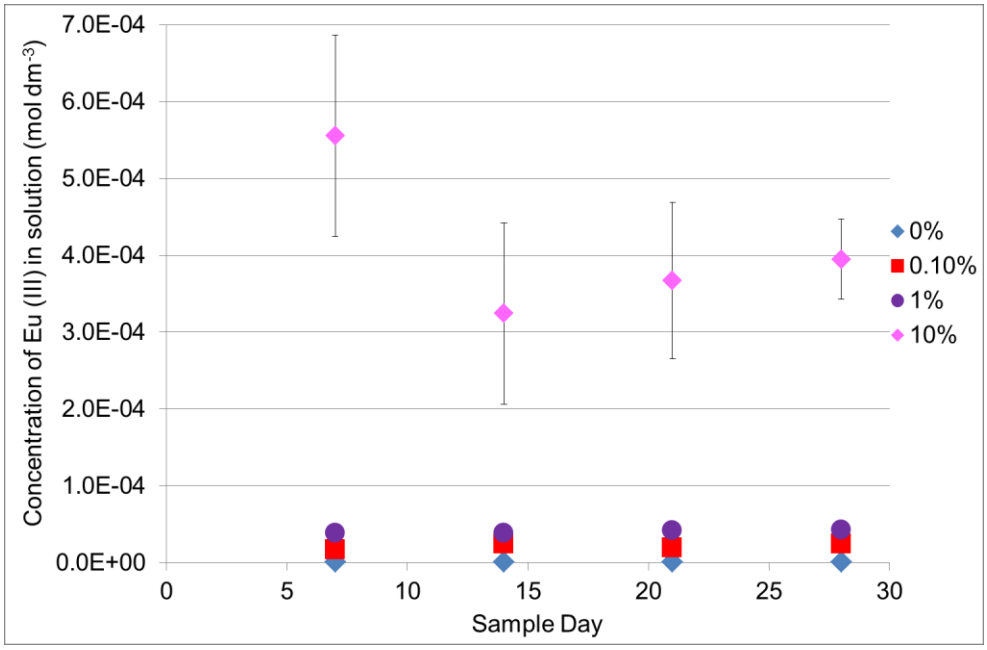

Figure 62 Kinetics of precipitation of Eu (III) in the presence of ADVA Cast 551 in OPC equilibrated water

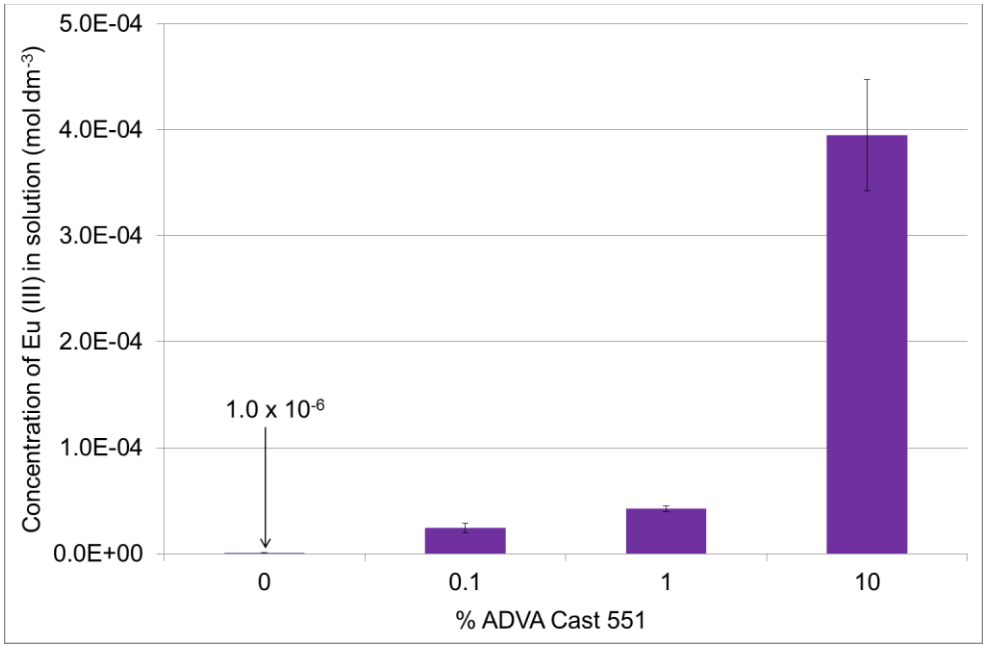

Figure 63 Final concentration of Eu (III) in OPC equilibrated water in the presence of ADVA Cast 551

In these experiments, there is much less solubility enhancement at 0.1 and 1% ADVA Cast 551. The measured value for Eu (III) solubility in the presence of 10% ADVA Cast 551 however is close to the inventory added and has a similar

SEF value (385) to that recorded in PFA and BFS equilibrated water. All SEF values for Eu (III) in OPC equilibrated water are reported in Table 53.

Table 53 Eu (III) solubility in OPC equilibrated water in the presence of ADVA Cast 551

Solution	% ADVA Cast	Solubility (mol dm^{-3})	SEF
OPC	0	1.02E-06	1
	0.1	2.45E-05	24
	1	4.26E-05	42
	10	3.95E-04	385

3.3.5 *Nickel (II) Solubility*

3.3.5.1 95% Saturated $Ca(OH)_2$

Ni (II) concentration in 95% saturated $Ca(OH)_2$ as a function of time is shown in Figure 64. It is unclear whether the samples have reached steady state or not as there is some variation in the concentration of Ni (II) measured in solution over time. If the Ni (II) distribution has not reached steady state between the solid phase and aqueous solution, the values reported for Ni (II) concentration in 95% saturated $Ca(OH)_2$ cannot be quoted as a true solubility value. Nevertheless, the final concentration of Ni (II) measured in solution is given in Figure 65 and SEF values are recorded in Table 54.

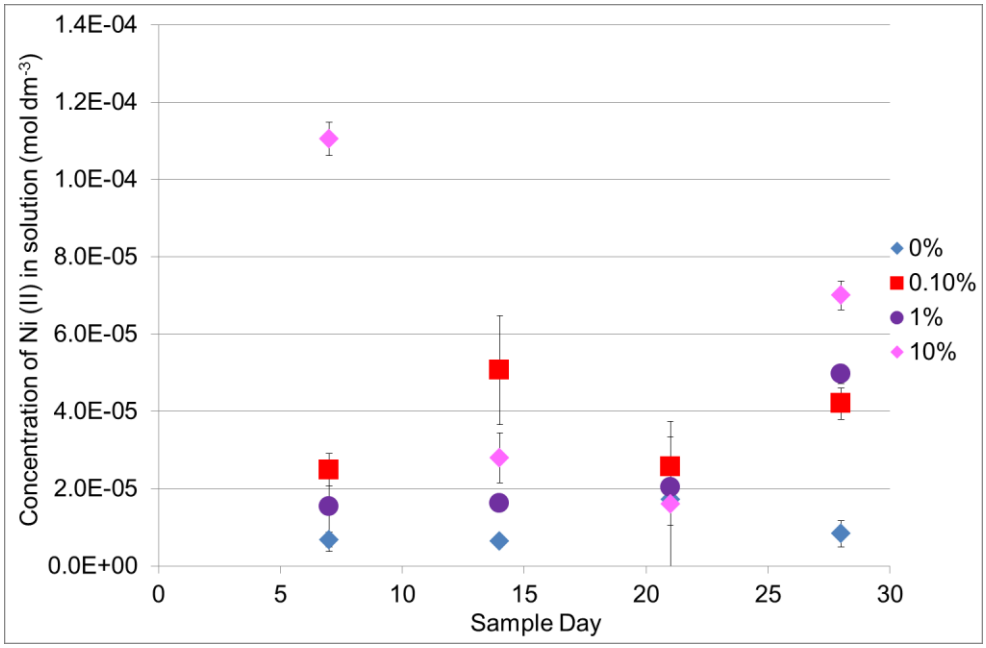

Figure 64 Kinetics of precipitation of Ni (II) in the presence of ADVA Cast 551 in 95% saturated $Ca(OH)_2$

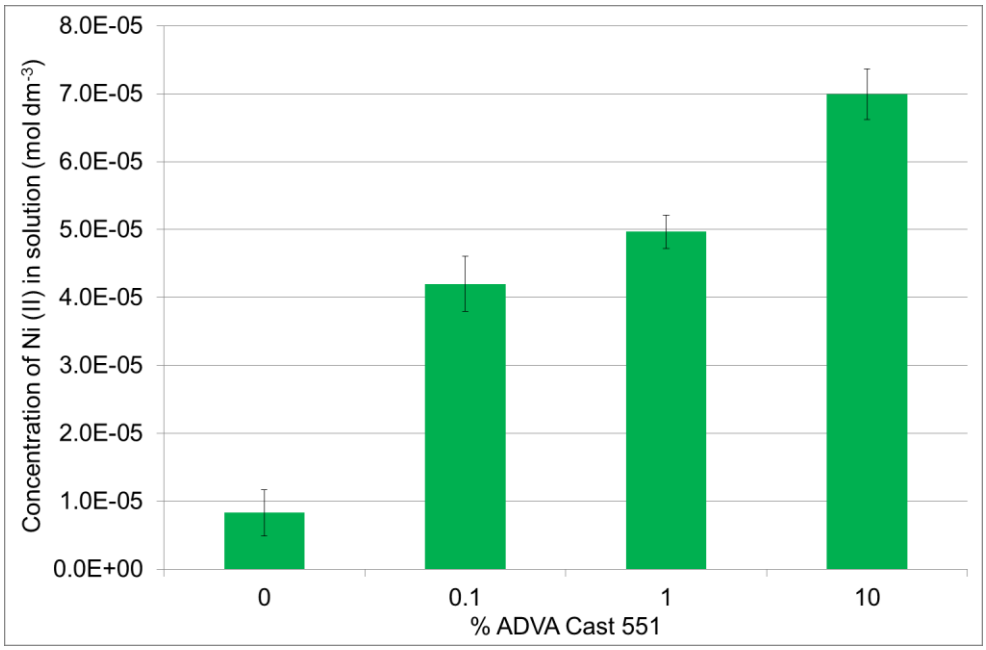

Figure 65 Final concentration of Ni (II) in 95% saturated $Ca(OH)_2$ in the presence of AVDA Cast 551

Table 54 Ni (II) solubility in 95% saturated $Ca(OH)_2$ in the presence of ADVA Cast 551

Solution	% ADVA Cast	Solubility (mol dm^{-3})	SEF
$Ca(OH)_2$	0	8.31E-06	1
	0.1	4.20E-05	5
	1	4.97E-05	6
	10	7.00E-05	8

The difference in Ni (II) solubility between the baseline (0%) and in the presence of 10% ADVA Cast is in the range of an order of magnitude. SEF values are lower than in comparison to Eu (III) with values of 6 and 8 for 1% and 10% respectively.

3.3.5.2 0.1 mol dm^{-3} NaOH

Similarly to the $Ca(OH)_2$ samples, the NaOH samples did not reach steady state over the 28 day sampling period therefore a true Ni (II) solubility value cannot be given. Kinetics of precipitation of Ni (II) in 0.1 mol dm^{-3} NaOH is reported in Figure 66. As shown in Figure 67, there is little change in the final concentration of Ni (II) in solution with increasing amounts of ADVA Cast 551. Within errors the solubility is the same in each case with only 0.1% and 1% ADVA Cast having slightly elevated SEF values of 2. These values should be considered with caution however, since the samples had not reached steady state.

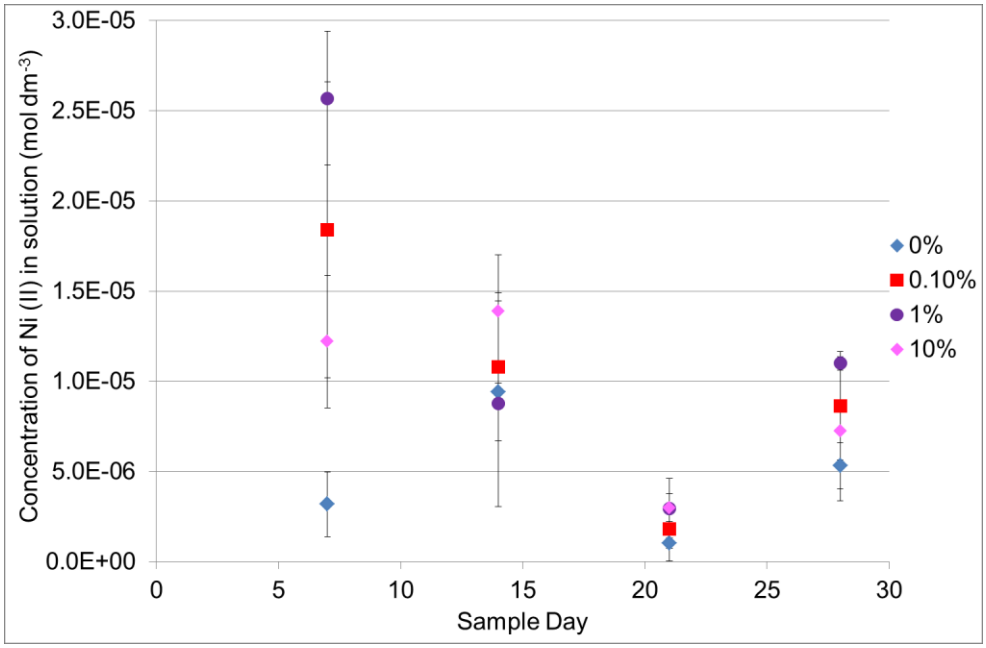

Figure 66 Kinetics of precipitation of Ni (II) in the presence of ADVA Cast 551 in 0.1 mol dm^{-3} NaOH

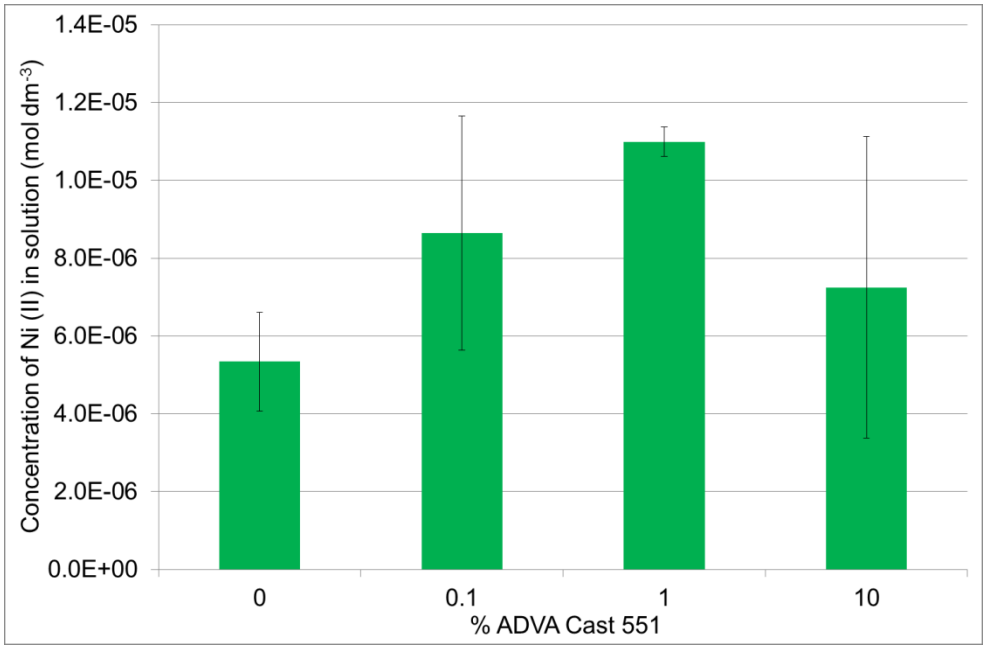

Figure 67 Final concentration of Ni (II) in 0.1 mol dm^{-3} NaOH in the presence of ADVA Cast 551

Table 55 Ni (II) solubility in 0.1 mol dm^{-3} NaOH in the presence of ADVA Cast 551

Solution	% ADVA Cast	Solubility (mol dm^{-3})	SEF
NaOH	0	5.34E-06	1
	0.1	8.65E-06	2
	1	1.10E-05	2
	10	7.25E-06	1

3.3.5.3 BFS:OPC equilibrated water

In contrast to $Ca(OH)_2$ and NaOH, Ni (II) concentration in BFS:OPC equilibrated water, reached steady state by day 14 for all samples. Kinetics of precipitation is reported in Figure 68.

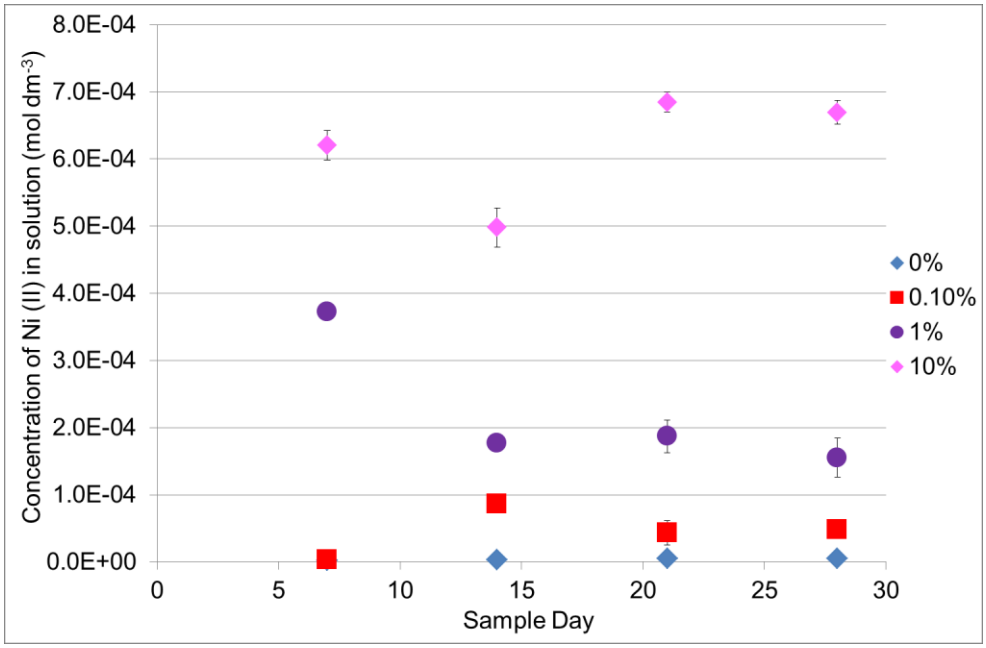

Figure 68 Kinetics of precipitation of Ni (II) in the presence of ADVA Cast 551 in BFS:OPC equilibrated water

The concentration of Ni (II) in solution increases with increasing concentrations of ADVA Cast 551. The final concentration of Ni (II) in solution is shown in Figure 69 and demonstrates that in the presence of 10% ADVA Cast 551, the Ni (II) concentration measured in solution is close to the inventory limit.

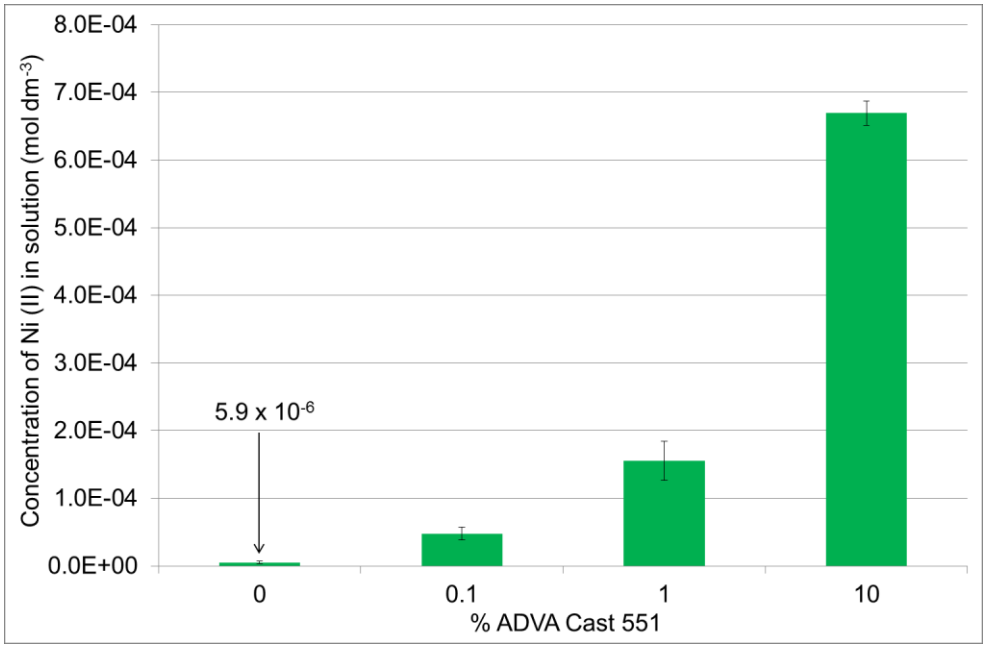

Figure 69 Final concentration of Ni (II) in BFS:OPC equilibrated water in the presence of ADVA Cast 551

There is a substantial difference between the solubility of Ni (II) in the presence of 1% and 10% ADVA Cast 551. These samples have SEF values of 30 and 129 respectively as reported in Table 56. The addition of 10% ADVA Cast results in an increase in Ni (II) solubility over 2 orders of magnitude.

Table 56 Ni (II) solubility in BFS:OPC equilibrated water in the presence of ADVA Cast 551

Solution	% ADVA Cast	Solubility (mol dm^{-3})	SEF
BFS:OPC	0	5.18E-06	1
	0.1	4.76E-05	9
	1	1.55E-04	30
	10	6.69E-04	129

3.3.5.4 PFA:OPC equilibrated water

Kinetics of precipitation of Ni (II) in PFA:OPC equilibrated water is shown in Figure 70. Steady state is reached by day 7 in all samples. There is little change in the solubility of Ni (II) in the presence of 0.1% and 1% ADVA Cast. SEF values are negligible at 2 as reported in Table 57. However, with 10% ADVA Cast the Ni (II) concentration measured is close the inventory limit and has an associated SEF value of 237.The final concentration on Ni (II) measured in solution is reported in Figure 71.

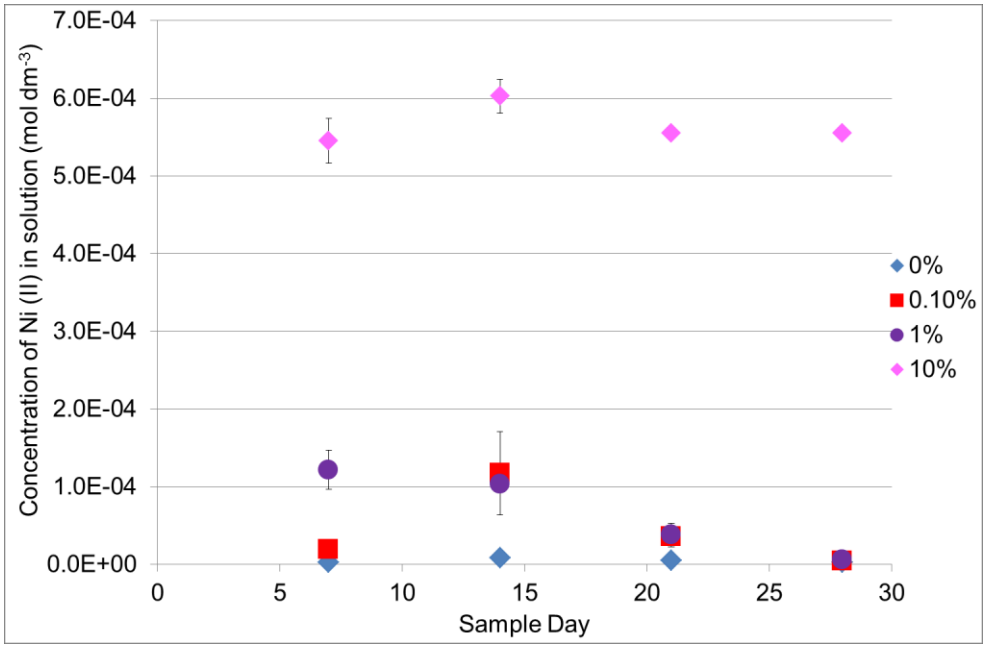

Figure 70 Kinetics of precipitation of Ni (II) in the presence of ADVA Cast 551 in PFA:OPC equilibrated water

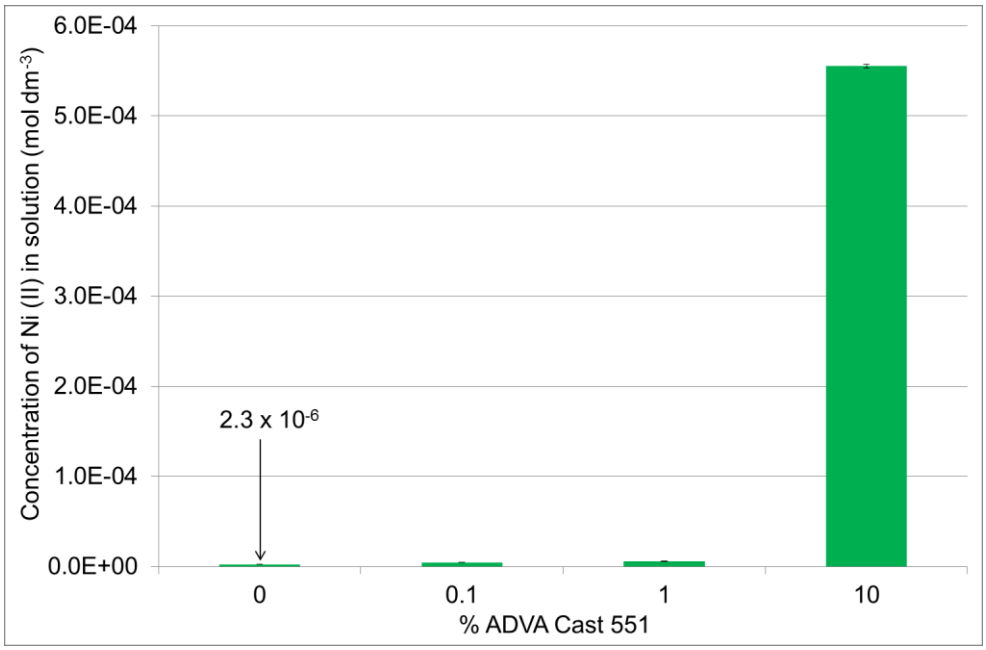

Figure 71 Final concentration of Ni (II) in PFA:OPC equilibrated water in the presence of ADVA Cast 551

Table 57 Ni (II) solubility in PFA:OPC equilibrated water in the presence of ADVA Cast 551

Solution	% ADVA Cast	Solubility (mol dm^{-3})	SEF
PFA:OPC	0	2.34E-06	1
	0.1	4.62E-06	2
	1	5.49E-06	2
	10	5.55E-04	237

3.3.5.5 BFS equilibrated water

Kinetics of precipitation of Ni (II) in BFS equilibrated water is shown in Figure 72. Steady state was reached by day 7 for the baseline solubility samples (0%) while 0.1%, 1% and 10% ADVA Cast 551 samples reached steady state by day 21. Figure 73 demonstrates an increase in solubility in the region of 2 orders of magnitude with the addition of 1% and 10% ADVA Cast 551. The increases in Ni (II) solubility at 1% and 10% ADVA Cast 551 are equivalent (within errors) and have SEF values of 68 and 73 for 1% and 10% respectively as reported in Table 58.

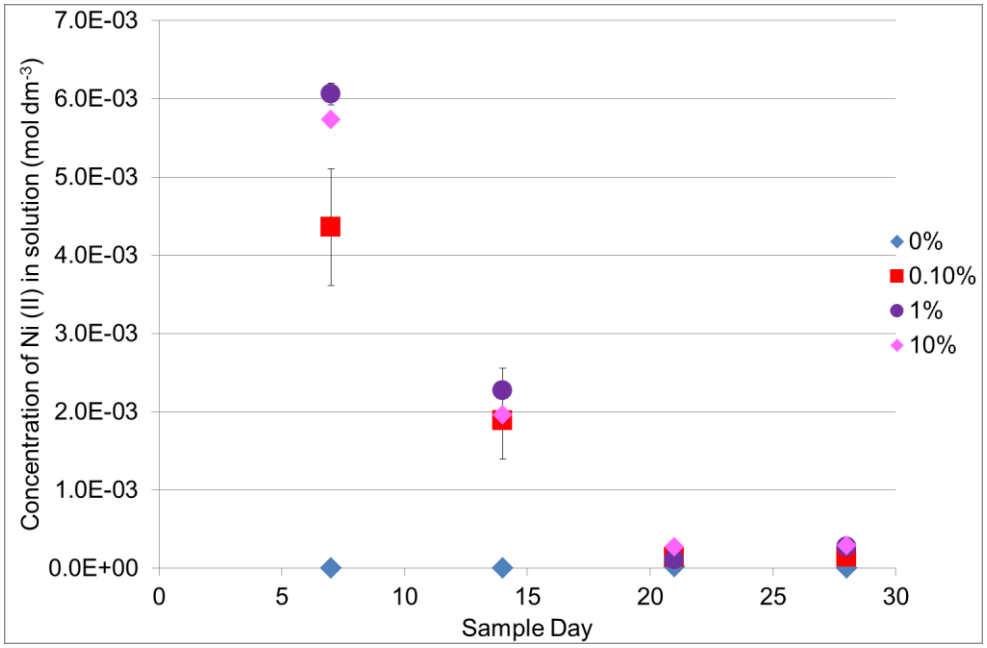

Figure 72 Kinetics of precipitation of Ni (II) in the presence of ADVA Cast 551 in BFS equilibrated water

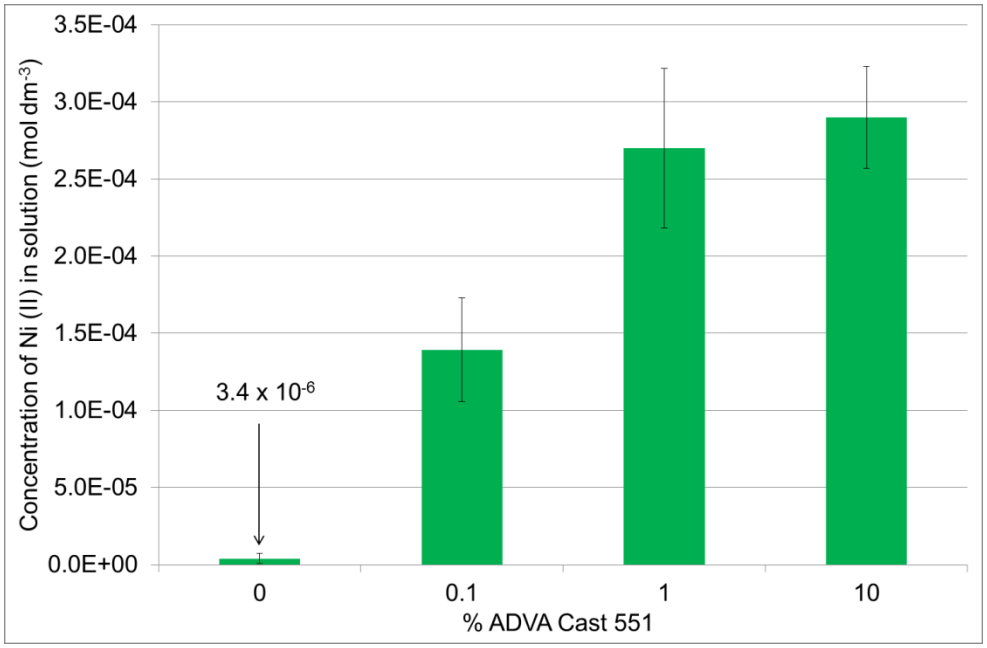

Figure 73 Final concentration of Ni (II) in BFS equilibrated water in the presence of ADVA Cast 551

Table 58 Ni (II) solubility in BFS equilibrated water in the presence of ADVA Cast 551

Solution	% ADVA Cast	Solubility (mol dm^{-3})	SEF
BFS	0	3.95E-06	1
	0.1	1.39E-04	35
	1	2.70E-04	68
	10	2.90E-04	73

3.3.5.6 PFA equilibrated water

Similarly to BFS equilibrated water, Ni (II) baseline solubility (0%) samples reached steady state by day 7 while all samples containing superplasticiser reached steady state by day 21. Figure 74 shows the kinetics of precipitation of Ni (II) in PFA equilibrated water.

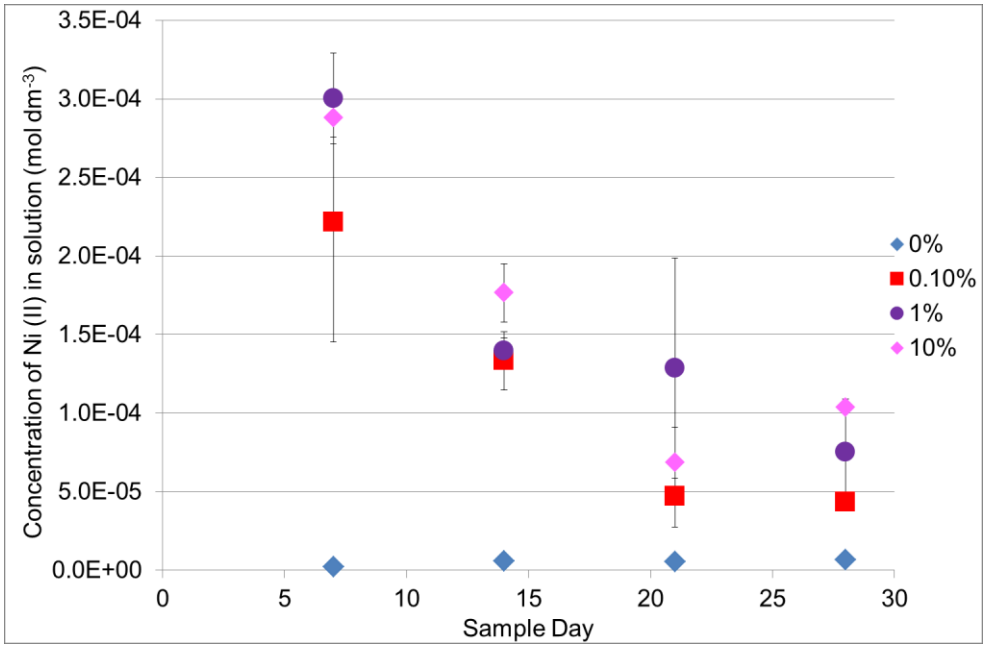

Figure 74 Kinetics of precipitation of Ni (II) in the presence of ADVA Cast 551 in PFA equilibrated water

There is an increase in Ni (II) solubility with increasing concentrations of ADVA Cast 551 as demonstrated in Figure 75. The largest increase in solubility is observed in the 10% ADVA Cast 551 samples with an increase in solubility in the range of 1 order of magnitude and an SEF value of 15. All SEF values are reported in Table 59.

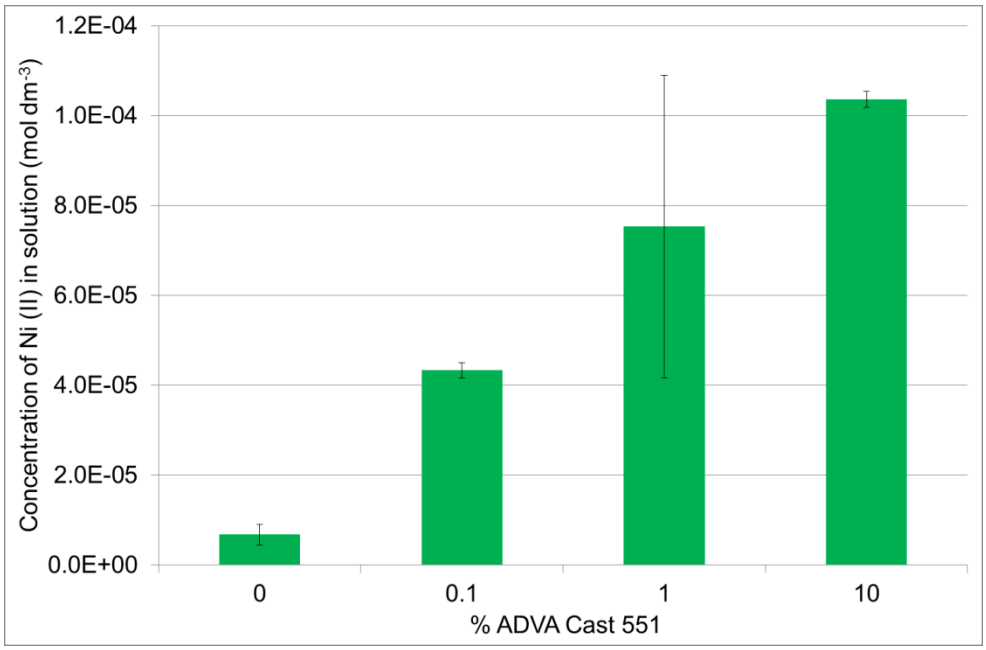

Figure 75 Final concentration of Ni (II) in PFA equilibrated water in the presence of ADVA Cast 551

Table 59 Ni (II) solubility in PFA equilibrated water in the presence of ADVA Cast 551

Solution	% ADVA Cast	Solubility (mol dm^{-3})	SEF
PFA	0	6.78E-06	1
	0.1	4.34E-05	6
	1	7.53E-05	11
	10	1.04E-04	15

3.3.5.7 OPC equilibrated water

Kinetics of precipitation of Ni (II) in OPC equilibrated water is shown in Figure 76. Steady state was reached by day 7 in all samples.

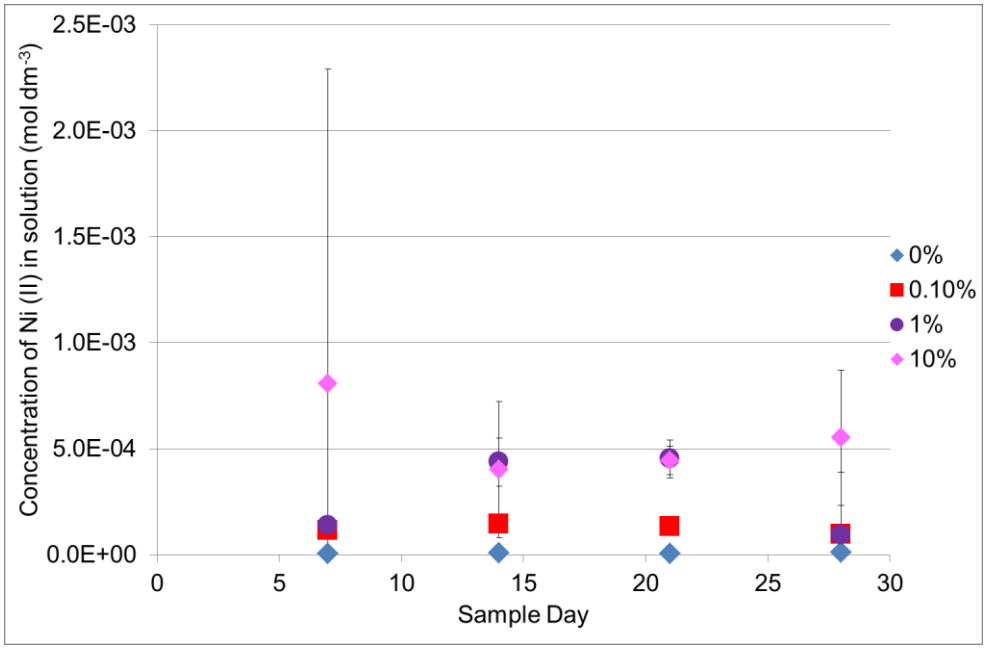

Figure 76 Kinetics of precipitation of Ni (II) in the presence of ADVA Cast 551 in OPC equilibrated water

Figure 77 reports the final Ni (II) concentration measured in solution and demonstrates that there was little increase in Ni (II) solubility in the presence of 0.1% and 1% ADVA Cast 551. In the presence of 10% ADVA Cast 551 however, an SEF value of 42 was calculated and is reported in Table 60. Despite this slightly higher SEF value, the increase in solubility was less than an order of magnitude.

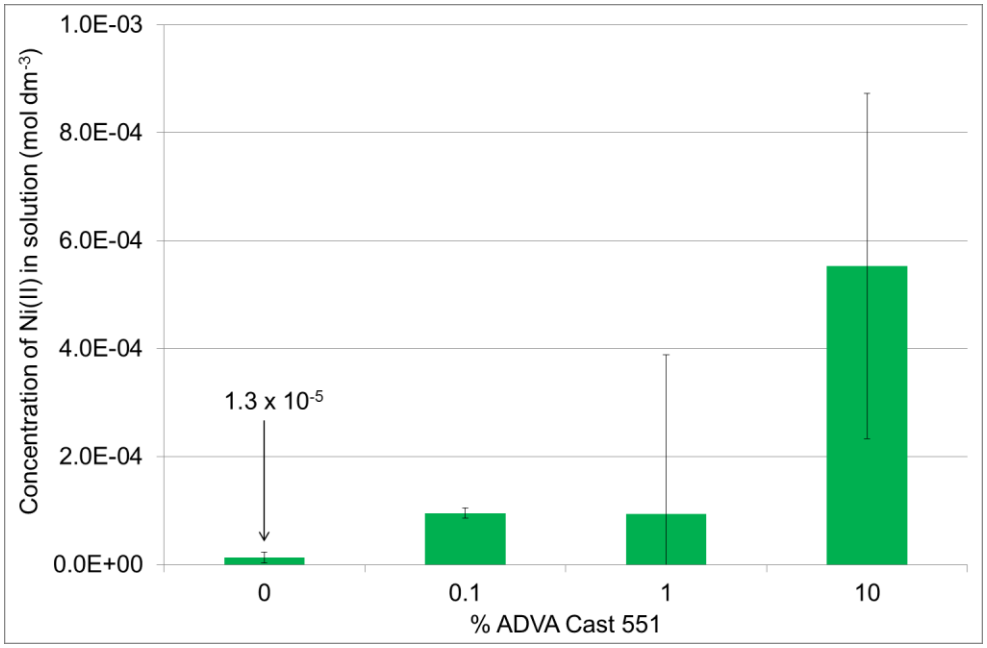

Figure 77 Final concentration of Ni (II) in OPC equilibrated water in the presence of ADVA Cast 551

Table 60 Ni (II) solubility in OPC equilibrated water in the presence of ADVA Cast 551

Solution	% ADVA Cast	Solubility (mol dm^{-3})	SEF
OPC	0	1.31E-05	1
	0.1	9.52E-05	7
	1	9.34E-05	7
	10	5.53E-04	42

3.3.6 *Summary of Experimental U (VI), Th (IV), Eu (III) and Ni (II) Solubility Data in the Presence of 'as received' ADVA Cast 551*

A summary of experimental solubility data and SEF values calculated for the presence of 1% ADVA Cast 551 are shown in Table 61.

Table 61 Summary of U (VI), Th (IV), Eu (III) and Ni (II) solubility results in the presence of 'as received' ADVA Cast 551

Aqueous Solution	pH	Baseline Solubility (Solubility in the absence of ADVA Cast 551) mol dm^{-3}				SEF in the presence of 1% ADVA Cast 551			
		U (VI)	Th (IV)*	Eu (III)	Ni (II)	U (VI)	Th (IV)*	Eu (III)	Ni (II)
95% Saturated $Ca(OH)_2$	12.5 ± 0.5	1E-07 ± 5E-09	1E-09	5E-07 ± 2E-08	8E-06 ± 4E-06	3152	3	936	6
0.1 mol dm^{-3} NaOH	12.5 ± 0.5	3E-05 ± 2E-05	1E-09	1E-06 ± 5E-08	5E-06 ± 1E-06	24	3	531	2
BFS:OPC Equilibrated Water	12.5 ± 0.5	2E-06 ± 3E-07	1E-09	1E-06 ± 1E-07	5E-06 ± 2E-06	125	4	338	30
PFA:OPC Equilibrated Water	12.5 ± 0.5	1E-05 ± 1E-05	1E-09	3E-06 ± 2E-07	2E-06 ± 1E-07	45	4	160	2
BFS Equilibrated Water	12.5 ± 0.5	1E-05 ± 1E-05	1E-09	1E-06 ± 1E-07	4E-06 ± 3E-06	17	5	340	68
PFA Equilibrated Water (pH adjusted)	12.5 ± 0.5	2E-06 ± 3E-07	1E-09	1E-06 ± 2E-07	7E-06 ± 2E-06	214	5	343	11
PFA Equilibrated Water (not pH adjusted)	10.5 ± 0.5	4E-04 ± 2E-06	-	-	-	NA	-	-	-
OPC Equilibrated Water	12.5 ± 0.5	2E-06 ± 3E-06	1E-09	1E-06 ± 2E-07	1E-05 ± 9E-06	186	6	42	7

* Th (IV) baseline solubility value is taken from the experimental work reported in (32,33,67).

3.4 Uptake of Superplasticiser onto Cement Surfaces

Several experiments were carried out as documented in 2.6 to investigate the interaction of superplasticiser with cement and the reversibility of that interaction or otherwise.

3.4.1 *Uptake of ADVA Cast 551 by BFS:OPC Crushed Grout*

The percentage uptake of ADVA Cast 551 onto BFS:OPC crushed grout is shown in Figure 78. The largest proportion of ADVA Cast 551 bound to the BFS:OPC grout was observed in the 0.2% samples. In this case, 17% of the ADVA Cast polymer in solution was taken up by the cement surface. In the 0.5% and 1% samples, percentage sorption was 11% and 5.5% respectively. This result suggests that the crushed grout becomes saturated with the superplasticiser since within errors, the actual amount of superplasticiser sorbed to the crushed grout in each case is the same (17% of 0.2% =0.034 while 11% of 0.5% =0.055 and finally 5.5% of 1% =0.055).

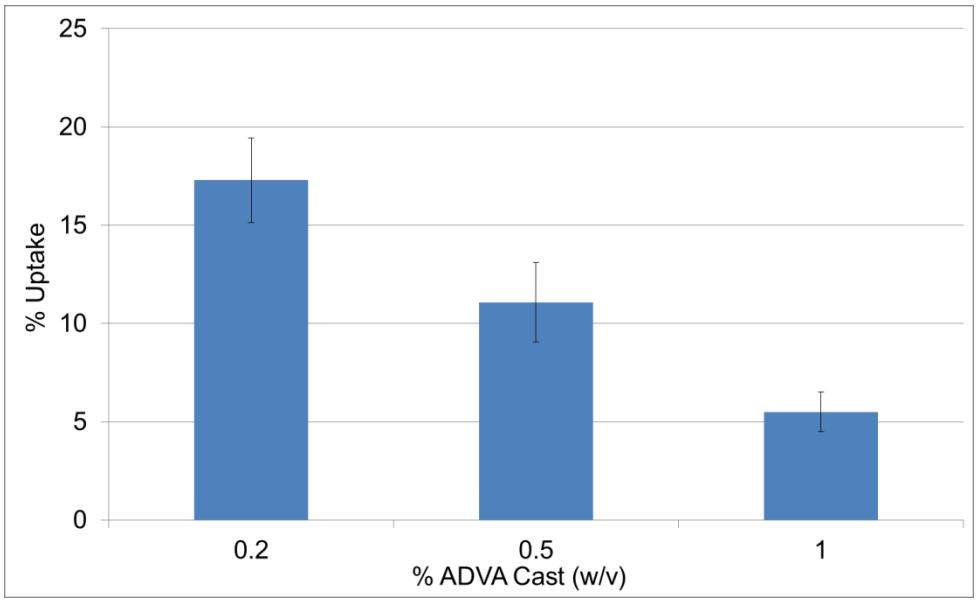

Figure 78 Uptake of ADVA Cast 551 by BFS:OPC crushed grout

3.4.2 *Uptake of ADVA Cast 551 by PFA:OPC Crushed Grout*

Percentage uptake of ADVA Cast 551 onto PFA:OPC crushed grout is shown in Figure 79.

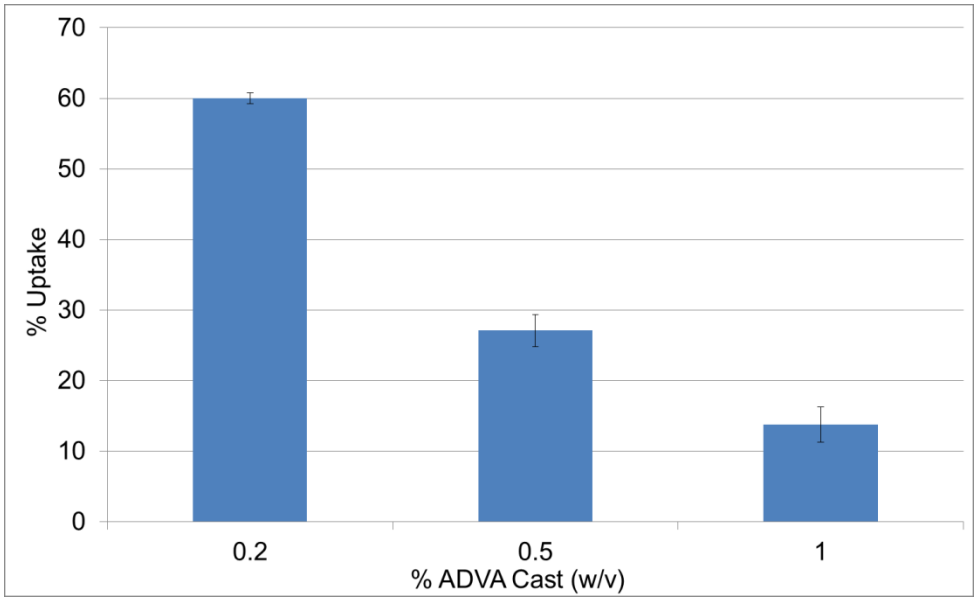

Figure 79 Uptake of ADVA Cast 551 by PFA:OPC crushed grout

In this case, 60% of the ADVA Cast polymer in solution was removed in the 0.2% samples, 28% was removed from the 0.5% samples and 12% removed from the 1% samples. This result suggests a similar trend where within errors, superplasticiser sorption to the grout reaches saturation at all concentrations of ADVA Cast 551 (60% of 0.2% =0.12 while 28% of 0.5% =0.14 and 12% of 1% =0.12). In this case however, a larger amount of superplasticiser is required for the crushed grout to reach saturation.

3.4.3 *Uptake of ADVA Cast 551 by OPC Powder*

BFS:OPC and PFA:OPC crushed grout show a different capacity for the uptake of superplasticiser. A larger amount of superplasticiser was required to saturate the PFA:OPC crushed grout compared to the BFS:OPC crushed grout. To try and identify the cement component most responsible for superplasticiser sorption, sorption experiments were also conducted on the individual cement component powders. Percentage sorption of ADVA Cast 551 onto OPC powder is shown in Figure 80.

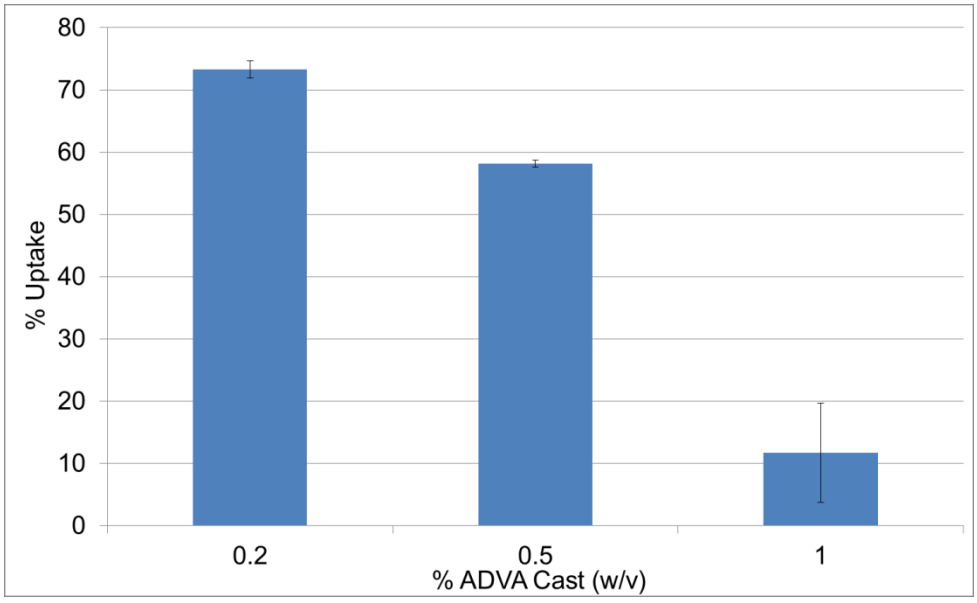

Figure 80 Uptake of ADVA Cast 551 by OPC powder

73% of superplasticiser was bound to OPC in the 0.2% samples, 58% was bound to OPC in the 0.5% samples and 12% superplasticiser was bound to OPC in the 1% samples. This demonstrates a similar trend to that of superplasticiser uptake by crushed grout where the OPC becomes saturated with the superplasticiser and within errors, the actual amount of superplasticiser sorbed is the same (73% of 0.2% =0.146 while 58% of 0.5% =0.29 and finally 12% of 1% =0.12).

3.4.4 *Uptake of ADVA Cast 551 by BFS and PFA Powder*

No uptake of ADVA Cast 551 was observed by BFS or PFA powder at any of the concentrations of superplasticiser investigated. This result shows that OPC is the component of the cement formulations that is responsible for the uptake of the superplasticiser. To validate this observation the TOC was measured of a solution of 0.5% ADVA Cast 551and also a solution of 0.5% ADVA Cast 551 in contact with the BFS and PFA solid. Figure 81 and Figure 82 show the concentration of ADVA Cast 551 measured in solution (ppm) with and without solid for BFS and PFA respectively.

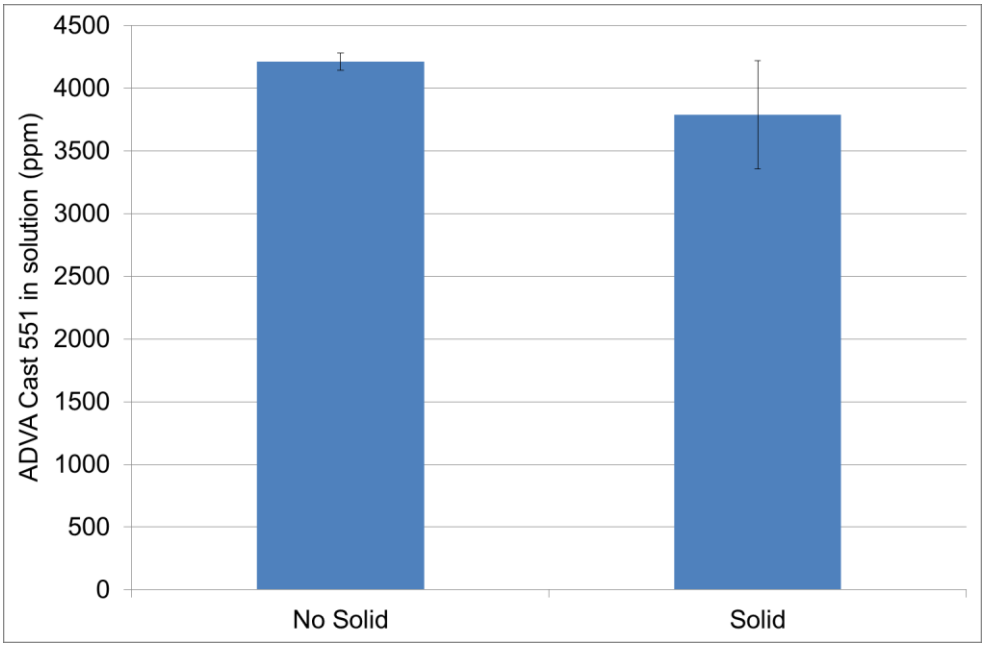

Figure 81 Concentration of ADVA Cast 551 (ppm) in a 0.5% superplasticiser solution with and without BFS solid

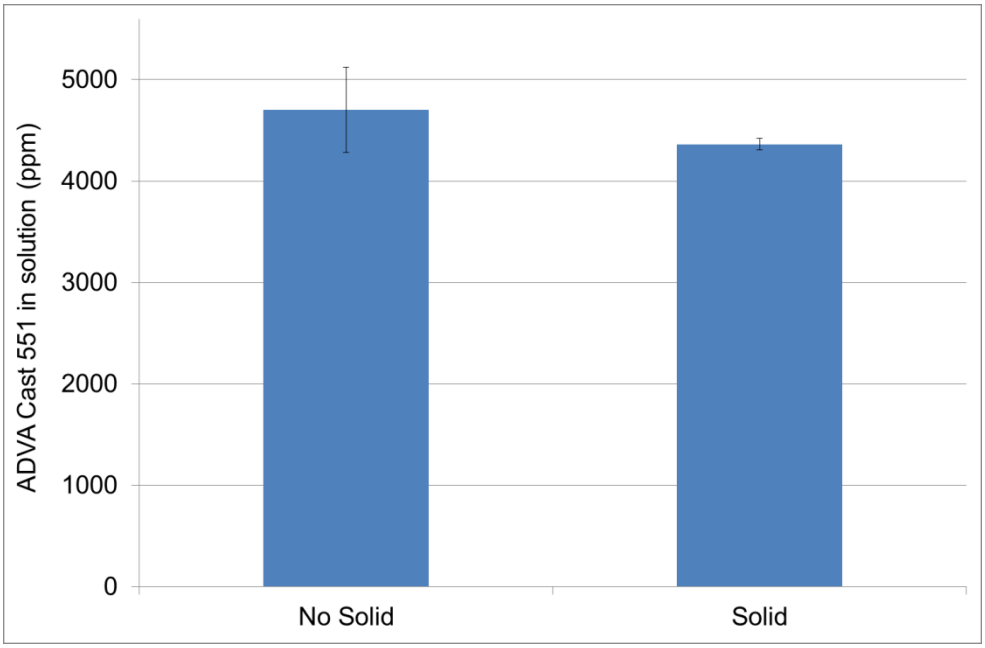

Figure 82 Concentration of ADVA Cast 551(ppm) in a 0.5% superplasticiser solution with and without PFA solid

Within errors (± the standard deviation of 4 sample replicates) the concentration of ADVA Cast (as TOC) measured in solution were the same irrespective of the presence of BFS or PFA solid.

3.4.5 *Reversibility of ADVA Cast 551 Uptake to Cement Materials*

To investigate the reversibility of superplasticiser uptake, de-sorption experiments were conducted as described in section 2.6.1. Table 62, Table 63 and Table 64 shows the reversibility of ADVA Cast 551 uptake to BFS:OPC, PFA:OPC and OPC powder respectively. No de-sorption experiment was carried out on PFA or BFS powder since no uptake of superplasticiser was observed to either powder in the original uptake experiment. The percentage of ADVA Cast 551 removed from each solid is minimal suggesting that superplasticiser binding to cement is irreversible. These results give further support to the theory proposed by Plank et al. (2006) that superplasticisers can intercalate into C_3A hydration products (68). This type of binding is known as chemisorption.

Table 62 Reversibilty of ADVA Cast 551 binding to BFS:OPC crushed grout

Sample	TOC originally bound to solid (ppm)	TOC in solution (ppm)	% Desorption
0.2%	1382.71	21	2
0.5%	3746.04	92	3
1%	7471.07	104	1

Table 63 Reversibility of ADVA Cast 551 binding to PFA:OPC crushed grout

Sample	TOC originally bound to solid (ppm)	TOC in solution (ppm)	% Desorption
0.2%	765.75	24.9	3
0.5%	3135.64	76.32	2
1%	7469.48	272.54	4

Table 64 Reversibility of ADVA Cast 551 binding to OPC powder

Sample	TOC originally bound to solid (ppm)	TOC in solution (ppm)	% Desorption
0.2%	533.55	11.99	2
0.5%	1891.29	27.97	2
1%	8192.11	308.16	4

3.5 Uptake of Metals onto Cement Surfaces in the Presence of Superplasticiser.

Section 3.3 shows that the presence of ADVA Cast 551 can have an enhancing effect on the solubility of metals. The solubility experiments conducted were 'free solution' experiments with no interaction of the superplasticiser or the metals with a surface such as cement.

It was hypothesised that a potential ternary system could form between a surface (in this case cement), superplasticiser and metal which, instead of increasing metal mobility, would aid in its retardation. Such ternary systems have been reported in the case of humic materials (69). To investigate the possibility of such ternary systems, two experiments were conducted. The first investigates the effect of the presence of superplasticiser *in solution* on the uptake of nickel or europium. The second investigates the effect of the presence of superplasticiser *in cement* on the uptake of nickel and europium.

Initial experiments were also conducted using uranium. The concentrations of uranium in the samples however were found to be below the limit of detection of the ICP-MS. The initial uranium inventory per sample was such that the solubility limit was not exceeded ($\approx 10^{-7}$ mol dm^{-3}). This is already near to the limit of detection of the instrument even before any metal uptake removes the uranium from solution. Further uranium experiments where therefore discontinued.

3.5.1 *Uptake of Metals onto Cement Prepared Without Superplasticiser*

Uptake of nickel and europium by BFS:OPC and PFA:OPC cement was investigated with increasing concentrations of ADVA Cast 551 present in solution using the method described in 2.7.1. No superplasticiser was used in the preparation of the crushed grout.

3.5.1.1 Ni (II) Uptake onto BFS:OPC Cement

Percentage uptake of Ni (II) onto crushed BFS:OPC grout with 0%, 0.2% 0.5% and 1% ADVA Cast 551 in solution respectively is shown in Figure 83.

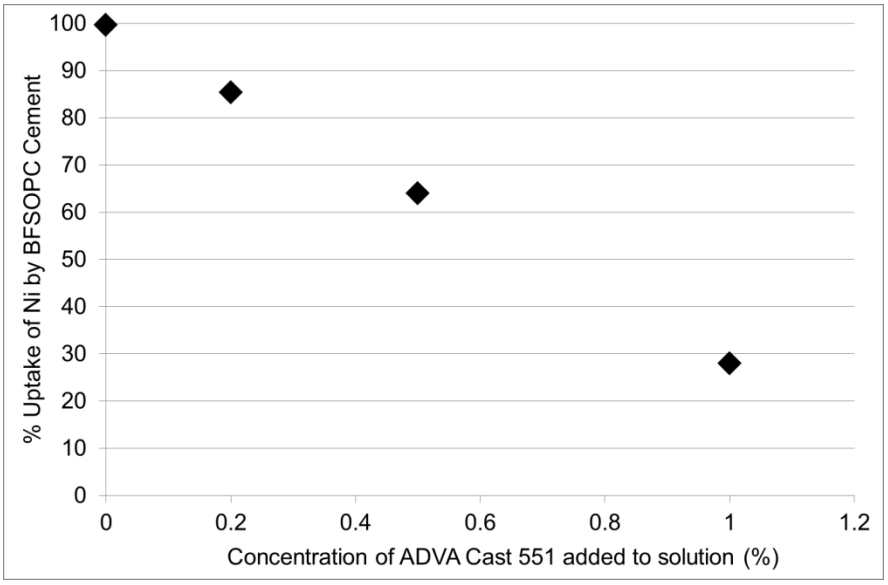

Figure 83 Uptake of Ni (II) to BFS:OPC crushed grout in the presence of ADVA Cast 551

By increasing the concentration of ADVA Cast 551 in solution, the amount of Ni (II) that binds to the cement surface is decreased. In the case of 1% ADVA Cast, only 28% of Ni (II) was bound to the cement while over 70% remained in solution and therefore potentially mobile.

3.5.1.2 Ni (II) Uptake onto PFA:OPC Cement

Percentage uptake of Ni (II) onto crushed PFA:OPC grout is shown in Figure 84.

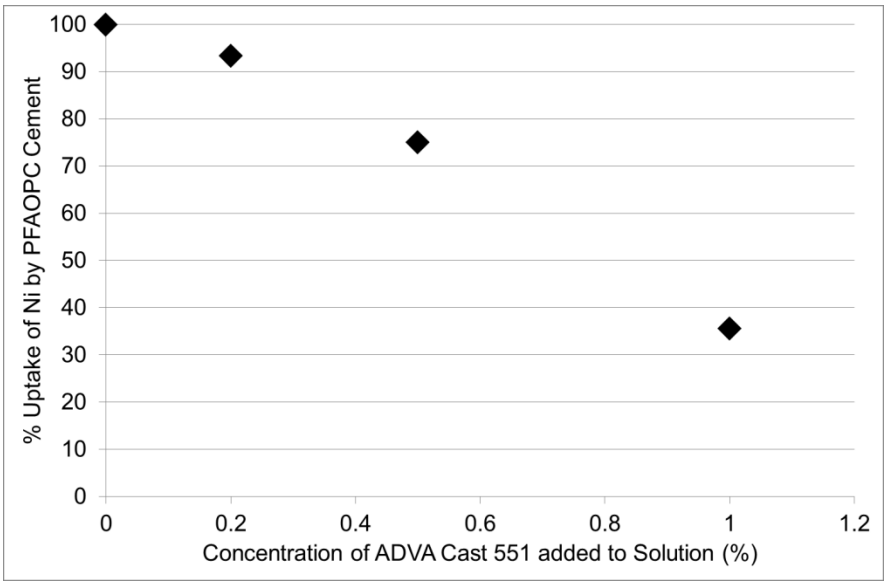

Figure 84 Uptake of Ni (II) to PFA:OPC crushed grout in the presence of ADVA Cast 551

A similar trend is observed to BFA:OPC grout with Ni (II) uptake decreasing as the concentration of ADVA Cast 551 increases. In this case, in the presence of 1% ADVA Cast 551, percentage uptake is 35%. This leaves 65% of Ni (II) in solution.

3.5.1.3 Eu (III) Uptake onto BFS:OPC Cement

Percentage uptake of Eu (III) onto crushed BFS:OPC is shown in Figure 85.

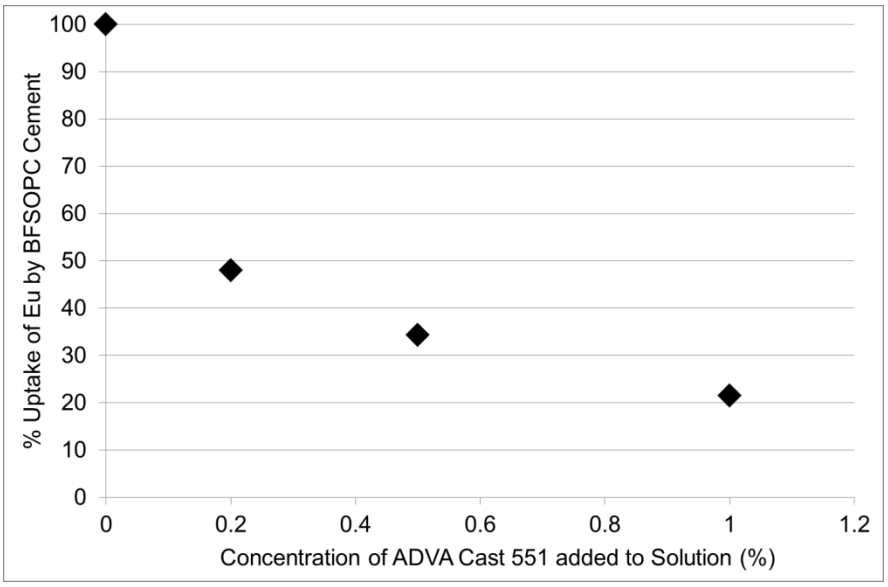

Figure 85 Uptake of Eu (III) to BFS:OPC crushed grout in the presence of ADVA Cast 551

In a similar trend to Ni (II), a reduction in Eu (III) uptake is noted with an increase in ADVA Cast 551 concentration. In this case, only 22% of the Eu (III) in solution is bound to the surface in the presence of 1% ADVA Cast 551.

3.5.1.4 Eu (III) Uptake onto PFA:OPC Cement

Percentage uptake of Eu (III) onto crushed BFS:OPC is shown in Figure 86.

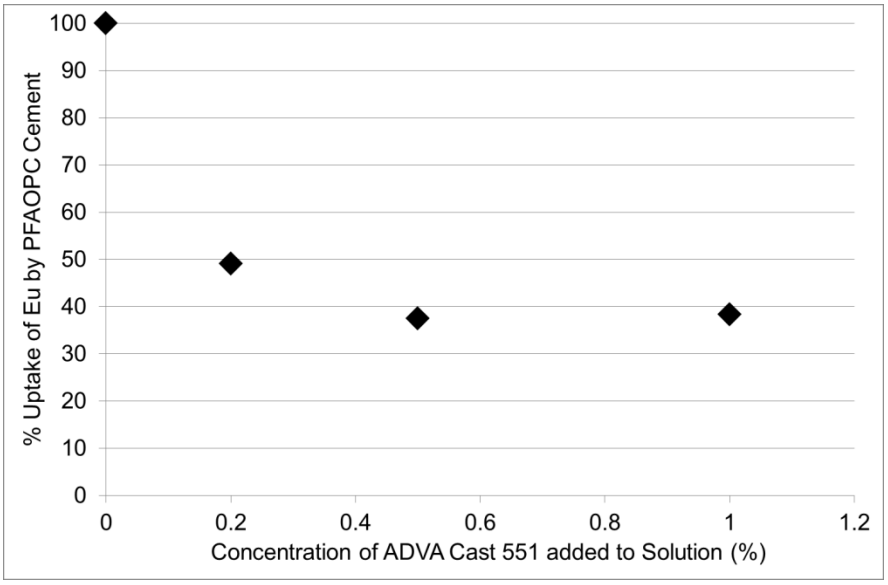

Figure 86 Uptake of Eu (III) to PFA:OPC crushed grout in the presence of ADVA Cast 551

The decrease in uptake is not as marked as that observed for crushed BFA:OPC; however, at both 0.5% and 1% ADVA Cast 551, the percentage uptake observed was 37% and 39% respectively. That means that over 60% of the added Eu (III) remains in solution.

It is important to ascertain the reversibility of metal binding to the cement, therefore a reversal experiment was also carried out on the same samples. Uptake reversibility experimental method is described in 2.7.3.

3.5.1.5 Reversibility of Ni (II) Uptake by BFS:OPC and PFA:OPC Crushed Grout

Table 65 and Table 66 show nickel removal from BFS:OPC and PFA:OPC crushed grout respectively. In both the 0.5% and 1% samples nearly all the nickel bound was re-suspended during the experiment (>98%). Errors quoted represent ± the standard deviation of 4 sample replicates. In the samples that contained no superplasticiser, less that 1% of the bound nickel was re-suspended. This result suggests that without the presence of the superplasticiser, metal binding is irreversible (at the same pH) while in the presence of the superplasticiser, the metal binding is more labile and easily re-suspended.

Table 65 Reversibility of Ni (II) uptake by BFS:OPC crushed grout

Sample	[Ni] Originally sorbed to cement (mol dm^{-3})	[Ni] De-sorbed (mol dm^{-3})	% Desorption
0% SP	$1.5 \times 10^{-9} \pm 5.8 \times 10^{-12}$	$1.1 \times 10^{-11} \pm 1.6 \times 10^{-12}$	0.7
0.2% SP	$1.3 \times 10^{-9} \pm 7.4 \times 10^{-12}$	$9.3 \times 10^{-10} \pm 6.9 \times 10^{-10}$	72
0.5% SP	$9.6 \times 10^{-10} \pm 5.4 \times 10^{-11}$	$9.4 \times 10^{-10} \pm 7.5 \times 10^{-11}$	98
1% SP	$4.3 \times 10^{-10} \pm 4.1 \times 10^{-11}$	$4.3 \times 10^{-10} \pm 2.9 \times 10^{-11}$	99

Table 66 Reversibility of Ni (II) uptake by PFA:OPC crushed grout

Sample	[Ni] Originally sorbed to cement (mol dm^{-3})	[Ni] De-sorbed (mol dm^{-3})	% Desorption
0% SP	$1.5 \times 10^{-9} \pm 5.2 \times 10^{-12}$	$9.2 \times 10^{-12} \pm 2.5 \times 10^{-12}$	0.6
0.2% SP	$1.4 \times 10^{-9} \pm 6.2 \times 10^{-12}$	$4.5 \times 10^{-10} \pm 1.9 \times 10^{-11}$	32
0.5% SP	$1.1 \times 10^{-9} \pm 2.5 \times 10^{-11}$	$1.1 \times 10^{-9} \pm 8.1 \times 10^{-11}$	99
1% SP	$5.3 \times 10^{-10} \pm 5.9 \times 10^{-12}$	$5.3 \times 10^{-10} \pm 1.4 \times 10^{-11}$	99

3.5.1.6 Reversibility of Eu (III) Uptake by BFS:OPC and PFA:OPC Crushed Grout

Table 67 and Table 68 show the reversibility of Eu (III) uptake by BFS:OPC and PFA:OPC crushed grout respectively. In the case in BFS:OPC >97% of bound Eu (III) was re-suspended in samples that had contained 0.2%, 0.5% and 1% ADVA Cast 551. Errors quoted represent ± the standard deviation of 4 sample replicates. Slightly less re-suspension was noted in the PFA:OPC samples nevertheless more than 60% of the originally sorbed metal were re-suspended.

Table 67 Reversibility of Eu (III) uptake by BFS:OPC crushed grout

Sample	[Eu] Originally sorbed to cement (mol dm^{-3})	[Eu] De-sorbed (mol dm^{-3})	% Desorption
0% SP	$1.4 \times 10^{-8} \pm 1.2 \times 10^{-12}$	$2.9 \times 10^{-13} \pm 1.9 \times 10^{-13}$	0.002
0.2% SP	$1.3 \times 10^{-10} \pm 5.3 \times 10^{-12}$	$1.3 \times 10^{-10} \pm 3.1 \times 10^{-12}$	99
0.5% SP	$9.4 \times 10^{-11} \pm 6.6 \times 10^{-12}$	$9.1 \times 10^{-11} \pm 6.4 \times 10^{-12}$	97
1% SP	$9.1 \times 10^{-11} \pm 2.4 \times 10^{-13}$	$8.9 \times 10^{-11} \pm 5.3 \times 10^{-11}$	97

Table 68 Reversibility of Eu (III) uptake by PFA:OPC crushed grout

Sample	[Eu] Originally sorbed to cement (mol dm^{-3})	[Eu] De-sorbed (mol dm^{-3})	% Desorption
0% SP	$2.8 \times 10^{-10} \pm 1.4 \times 10^{-12}$	$2.9 \times 10^{-13} \pm 1.9 \times 10^{-13}$	0.09
0.2% SP	$1.7 \times 10^{-10} \pm 7.3 \times 10^{-12}$	$1.3 \times 10^{-10} \pm 3.1 \times 10^{-12}$	81
0.5% SP	$1.5 \times 10^{-10} \pm 9.6 \times 10^{-12}$	$9.1 \times 10^{-11} \pm 6.4 \times 10^{-12}$	68
1% SP	$1.4 \times 10^{-10} \pm 3.1 \times 10^{-12}$	$8.9 \times 10^{-11} \pm 5.3 \times 10^{-11}$	60

3.5.2 *Uptake of Metals onto Cement Prepared with 0.5% (w/s) ADVA Cast 551*

Uptake of Ni (II) and Eu (III) by crushed BFS:OPC and PFA:OPC grout that was prepared with 0.5% (w/v) ADVA Cast 551 was investigated via the method described in 2.7.2. Table 69 shows Ni (II) uptake by BFS:OPC and PFA:OPC. In both cases >98% of Ni (II) was bound to the crushed grout. Table 70 shows Eu (III) uptake onto BFS:OPC and PFA:OPC. ^{152}Eu counts measured in solution were less than or equal to that of blank samples (containing no radioactivity) therefore [Eu] was below the limit of detection of the gamma spectrometer. The assumption is made therefore that all (>99%) of Eu (III) added to the samples was bound to the crushed grout. This observation demonstrates that ADVA Cast 551 does not have an effect on metal uptake when incorporated into the grout. The reduction in metal uptake only occurs when the superplasticiser is free in solution.

Table 69 Uptake of Ni (II) by BFS:OPC and PFA:OPC crushed grout prepared with 0.5% ADVA Cast 551

Sample	[Ni] Bound (mol dm^{-3})	[Ni] Solution (mol dm^{-3})	% Uptake
BFS:OPC (0.5% SP)	$2.7 \times 10^{-9} \pm 1.9 \times 10^{-11}$	$6.8 \times 10^{-11} \pm 5.8 \times 10^{-12}$	98
PFA:OPC (0.5% SP)	$2.6 \times 10^{-9} \pm 1.1 \times 10^{-11}$	$2.5 \times 10^{-10} \pm 1.1 \times 10^{-10}$	98

Table 70 Uptake of Eu (III) by BFS:OPC and PFA:OPC crushd grout prepared with 0.5% ADVA Cast 551

Sample	[Eu] Bound (mol dm^{-3})	[Eu] Solution (mol dm^{-3})	% Uptake
BFS:OPC (0.5% SP)	$3.8 \times 10^{-10} \pm 1.1 \times 10^{-12}$	<LOD	>99
PFA:OPC (0.5% SP)	$3.7 \times 10^{-10} \pm 2.9 \times 10^{-11}$	<LOD	>99

3.5.2.1 Reversibility of Metal Uptake by BFS:OPC and PFA:OPC Crushed Grout Prepared with 0.5% ADVA Cast 551

The reversibility of the uptake of both Ni (II) and Eu (III) from BFS:OPC and PFA:OPC was also analysed. Table 71 shows that very little Ni (II) (<0.1%) is re-suspended during the reversibility experiment while

Table **72** shows a similar trend for Eu (III). Eu (III) re-suspension is an order of magnitude higher than that for Ni (II) however this value is still <1%. Comparing these results to those in section 3.5.1.5 and 3.5.1.6 for Ni (II) and Eu (III) respectively, it is clear that the presence of ADVA Cast 551 in free solution has the greatest effect on the uptake behaviour of the metals. As mentioned previously, from the collected data it is not possible to determine whether this result is due to a solubility effect where the complexation of metals with the superplasticiser increases solubility and prevents sorption or the presence of the superplasticiser in solution saturates the sorption sites on the crushed grout surface thus preventing metal sorption.

Table 71 Reversibility of Ni (II) uptake by BFS:OPC and PFA:OPC crushed grout prepared with 0.5% ADVA Cast 551

Sample	[Ni] Originally Bound (mol dm^{-3})	[Ni] De-sorbed (mol dm^{-3})	% De-sorption
BFS:OPC (0.5% SP)	2.7×10^{-9}	$6.7 \times 10^{-13} \pm 4.1 \times 10^{-13}$	0.03
PFA:OPC (0.5% SP)	2.6×10^{-9}	$7.7 \times 10^{-13} \pm 1.6 \times 10^{-14}$	0.03

Table 72 Reversibility of Eu (III) uptake by BFS:OPC and PFA:OPC crushed grout prepared with 0.5% ADVA Cast 551

Sample	[Eu] Originally Bound (mol dm^{-3})	[Eu] De-sorbed (mol dm^{-3})	% De-sorption
BFS:OPC (0.5% SP)	3.8×10^{-10}	$1.14 \times 10^{-12} \pm 3.8 \times 10^{-13}$	0.3
PFA:OPC (0.5% SP)	3.7×10^{-10}	$7.48 \times 10^{-13} \pm 1.4 \times 10^{-13}$	0.2

3.6 Leaching of Superplasticiser and Metals from Hardened Cement Monoliths

3.6.1 *Leaching of ADVA Cast 551 from BFS:OPC and PFA:OPC Hardened Cement Monoliths*

Leaching experiments were prepared as described in section 2.8. The leach water was analysed for TOC (ppm) which was converted into a concentration of ADVA Cast 551 (ppm) via a calibration graph shown in APPENDIX 1 – Instrument Calibration Data.

Leaching experiments were also conducted on cement monoliths which did not contain superplasticiser. The TOC recorded in the leach water of these samples was assumed to be due to other organic materials present in the cement such as grinding agents. The TOC values for the samples containing superplasticiser were blank corrected using these values. After correction, all recorded TOC was assumed to be leached superplasticiser.

Table 73 ADVA Cast 551 leached from BFS:OPC and PFA:OPC

Sample	Total ADVA Cast 551 added (ppm)	Leached ADVA Cast 551 (ppm)	% of ADVA Cast leached
BFS:OPC 0.5% SP	5000	2.17	0.04
PFA:OPC 0.5% SP	5000	93.43	1.87

Table 73 demonstrates that of the total ADVA Cast 551 present in the samples on preparation, a very small proportion of superplasticiser is leached over 4 months (100 days). This is likely to be due to chemical binding and intercalation of the superplasticiser into the C_3A hydration phases on mixing that fixes the superplasticiser into organo-mineral phases of cement hydration products.

3.6.2 *Leaching of Metals from BFS:OPC Hardened Cement*

Leaching of Ni (II), U (VI) and Th (IV) from BFS:OPC prepared with and without superplasticiser is reported in Table 74. On preparation of BFS:OPC blocks it was noted that bleed water was present on the top of the blocks after the setting time of forty eight hours. The bleed was present in both the samples prepared with and without superplasticiser; however, there was substantially greater bleed in the samples that contained ADVA Cast 551

The bleed water was collected and analysed for the added metals by ICP- MS. It was found that in the cement monoliths prepared with superplasticiser, a significant proportion of the added metal was present in the bleed water and therefore not incorporated into the block. On preparation (method described in section 2.8.1.2), the metals were added to the aqueous portion of the cement mix to try to ensure a homogeneous mix of the metal throughout each sample. The presence of metal in the bleed indicates that the samples are not likely to be homogeneous.

Table 74 Leaching of metals from BFS:OPC

Sample	**Metal added (mol dm^{-3})**	**Metal in bleed water (mol dm^{-3})**	**% Metal in bleed water**	**Metal actually in block (mol dm^{-3})**	**Metal Leached (mol dm^{-3})**	**% Leach**
Ni No SP	1.47E-02	<LOD*	<0.0001	0.015	5.16E-07	0.004
Ni 0.5% SP	1.52E-02	2.85E-03	19	1.23E-02	2.34E-07	0.002
U No SP	3.36E-02	1.21E-06	0.004	3.36E-02	<LOD*	<0.0001
U 0.5% SP	3.49E-02	1.12E-02	32	2.37E-02	<LOD*	<0.0001

Th No SP	3.39E-03	8.07E-08	0.002	3.39E-03	<LOD*	<0.0001
Th 0.5% SP	3.53E-03	9.15E-04	26	2.62E-03	<LOD*	<0.0001

*ICP-MS LODs for U, Th and Ni are 8E-9 mol dm^{-3}, 4E-9 mol dm^{-3} and 6E-8 mol dm^{-3} respectively

In the case of U (VI), 32% of the original U (VI) inventory was in the bleed water of samples prepared with superplasticiser. Th (IV) and Ni (II) show a similar trend where 26% and 19% of the added Th (VI) and Ni (II) respectively was in the bleed water of samples with added superplasticiser. The samples prepared without superplasticiser had a much less significant proportion of metal in the bleed water; less that 1% in each case.

The homogeneity of the cement blocks was investigated using digital autoradiography and SEM to image the metal within the samples.

3.6.2.1 Imaging of U (VI) Th (IV) and Ni (II) in BFS:OPC

U (VI) and Th (IV) were imaged by digital autoradiography. The method for this type of imaging is described in 2.8.5.2. Figure 87 shows an autoradiography image and profile plot of U (VI) distribution in BFS:OPC cement containing 0.5% ADVA Cast 551.

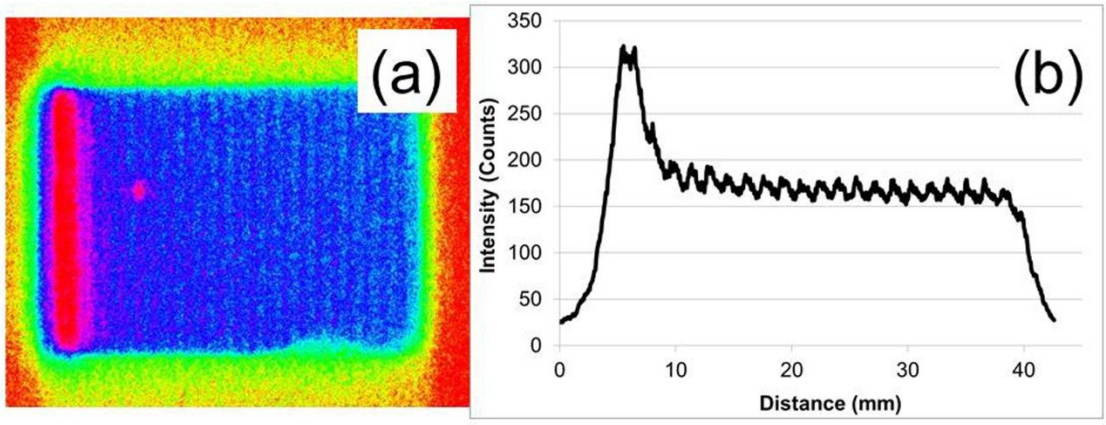

Figure 87 (a) Autoradiography image and (b) Profile Plot of BFS:OPC cement prepared with 0.5% ADVA Cast 551 and containing U (VI)

Activity is mapped using colour on the autoradiography images. The red/ pink areas on the image represent areas of higher concentration of radioactivity. The U (VI) distribution is not homogeneous and a very concentrated area of activity is present at the top of the block (left hand side of (a)). This result is consistent

with the high U (VI) concentration that was measured in the bleed water over the forty eight hour set time. The profile plot (b) represents the activity of the block as a cross section. The higher activity at the top of the block is shown with much higher counts in that area.

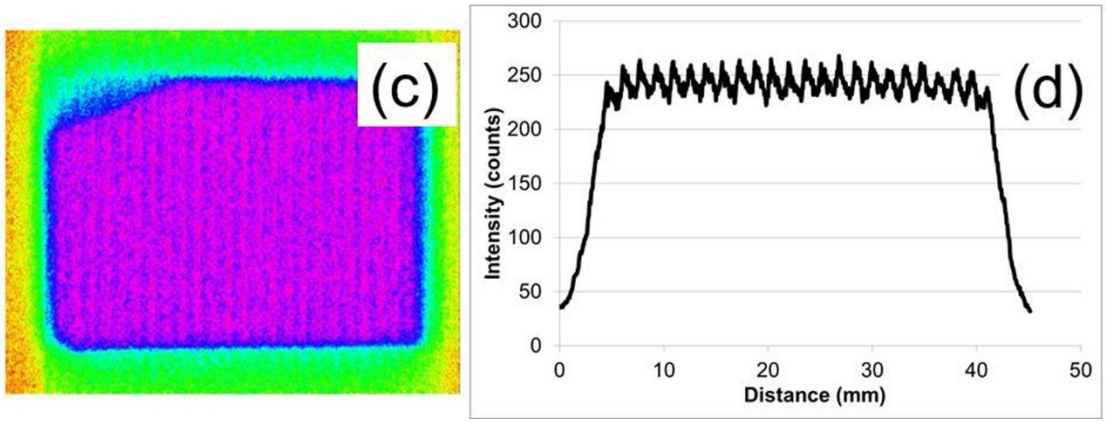

Figure 88 (c) Autoradiography image and (d) Profile Plot of BFS:OPC cement prepared with no superplasticiser and containing U (VI)

Figure 88 shows an autoradiography image and profile plot of U (VI) distribution in BFS:OPC cement prepared without superplasticiser. The autoradiography image and profile plot demonstrate a homogeneous distribution of activity throughout the sample with no specific areas of concentrated uranium.

BFS:OPC blocks containing Th were also imaged by autoradiography. Figure 89 shows an autoradiography image and profile plot of Th distribution in BFS:OPC cement prepared with 0.5% superplasticiser. A similar distribution of activity to the U (VI) block prepared with superplasticiser was observed. The lower activity of ^{232}Th compared with ^{238}U meant that exposure of the Th (IV) cement blocks to the autoradiography plate had to be extended from 1 week to 2 weeks. The longer exposure time reduces the resolution of the image; however, an area of higher intensity is clearly visible at the top (left hand side) of the block consistent with the high Th (IV) concentration in the bleed water. This area of high concentration of Th (IV) may also be seen on the profile plot (b) where an area of higher activity is recorded at the top of the block.

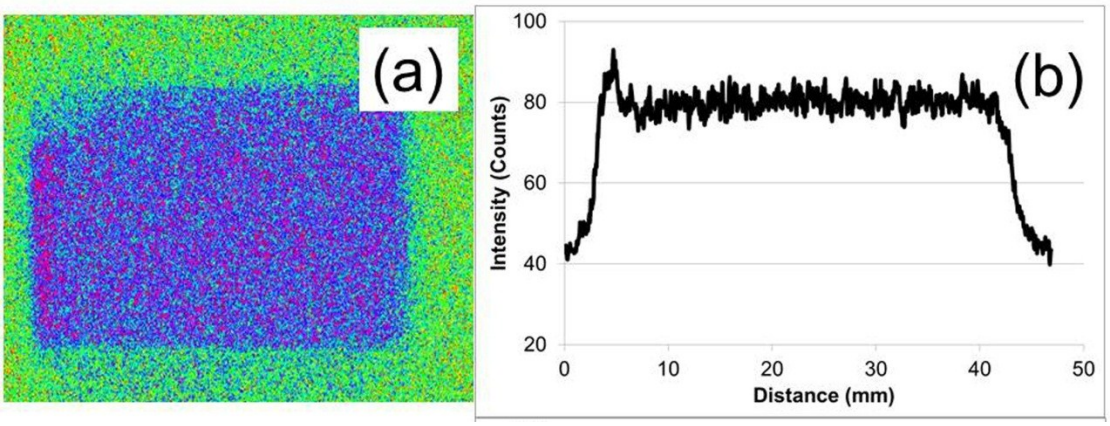

Figure 89 (a) Autoradiography image and (b) Profile Plot of BFS:OPC cement prepared with 0.5% ADVA Cast 551 and containing Th (IV)

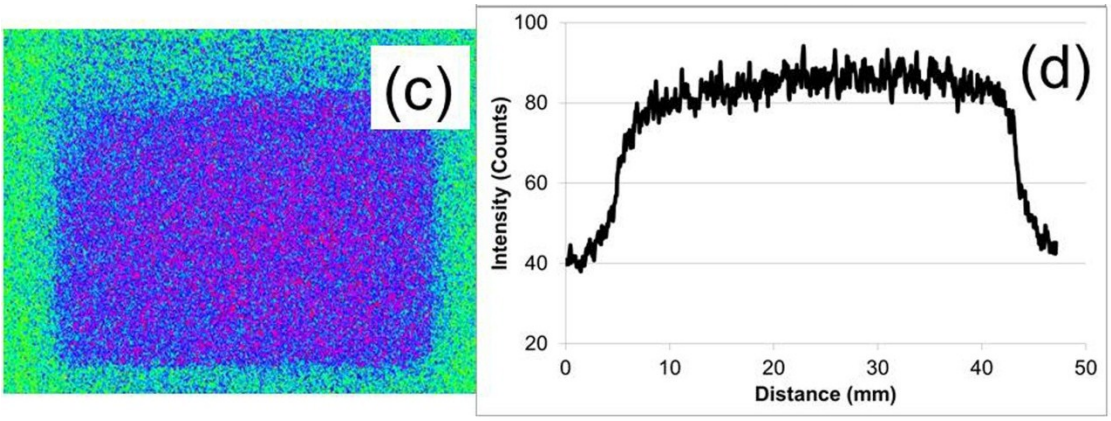

Figure 90 (c) Autoradiography image and (d) Profile Plot of BFS:OPC cement prepared with no superplasticiser and containing Th (IV)

An autoradiography image and profile plot for a BFS:OPC block containing Th (IV) with no superplasticiser is shown in Figure 90, in this case, the distribution of activity throughout the sample is homogeneous.

Since non- radioactive Ni (II) was used in the preparation of the cement blocks, it was not possible to map the Ni (II) containing blocks by autoradiography. SEM- EDX was therefore used to try and identify areas of high Ni (II) concentration within the sample. SEM is a microscopy technique and mapping of the entire sample was not possible in this way therefore areas were focused on at the top edge, middle and bottom edge of the block and an EDX spectrum taken to show the elements present in that area and try and identify a pattern

similar to that seen in the U (VI) and Th (IV) samples. The top edge of the sample that had been in contact with the bleed water was expected to have a higher proportion of Ni (II) than other areas of the sample. Unfortunately no nickel was detected in any areas of the sample suggesting that the concentration of nickel in the sample was below the limit of detection of the instrument.

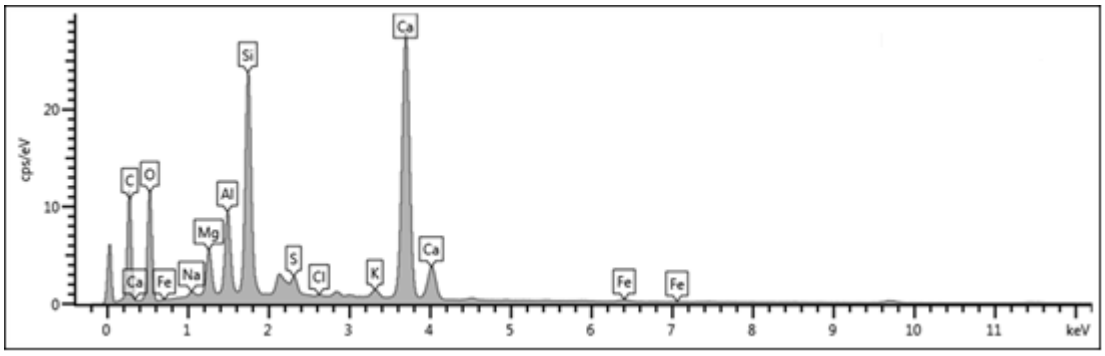

Figure 91 EDX Spectrum of the TOP EDGE of a BFS:OPC cement block containing 0.5% ADVA Cast 551 and Ni (II)

Figure 91 shows an example EDX spectrum of the top edge of the BFS:OPC cement block that contained 0.5% SP and Ni (II). All other EDX spectra corresponding to the BFS:OPC samples are shown in APPENDIX 2 – EDX Analysis Spectra.

3.6.3 *Leaching of Metals from PFA:OPC Hardened Cement*

Leaching of Ni (II), U (VI) and Th (IV) from PFA:OPC prepared with and without superplasticiser is shown in Table 75. No Th (IV) was detected in the leachate from the blocks with or without superplasticiser. This is not surprising due to the very low solubility of Th (IV) under these conditions. In the region of an order of magnitude more Ni (II) and U (VI) was leached from the blocks that contained superplasticiser compared to the samples that did not. In all cases <0.002% of the metal inventory was leached from the cement blocks. Interestingly however, the concentration of U (VI) measured in solution was close to the solubility measurements obtained in section 2.5.2.4 suggesting that U (VI) was close to its solubility limit. The presence of the superplasticiser in this case has increased uranium release.

Table 75 Leaching of metals from PFA:OPC

Sample	Metal added (mol dm^{-3})	Metal Leached (mol dm^{-3})	% Leach
Ni No SP	1.47E-02	1.80E-09	0.000012
Ni 0.5% SP	1.48E-02	2.71E-08	0.00018
U No SP	3.43E-02	2.59E-07	0.00076
U 0.5% SP	3.45E-02	6.42E-07	0.0019
Th No SP	3.31E-03	<LOD	<LOD
Th 0.5% SP	3.53E-03	<LOD	<LOD

3.6.3.1 Imaging of U (VI) Th (IV) and Ni (II) in PFA:OPC

In a similar fashion to the BFS:OPC samples, U (VI) and Th (IV) in PFA:OPC prepared with and without superplasticiser were imaged using autoradiography while Ni (II) was imaged using SEM- EDX. Unlike the BFS:OPC samples, there was no bleed associated with the cement on setting. It was therefore expected that these samples would be more homogeneous.

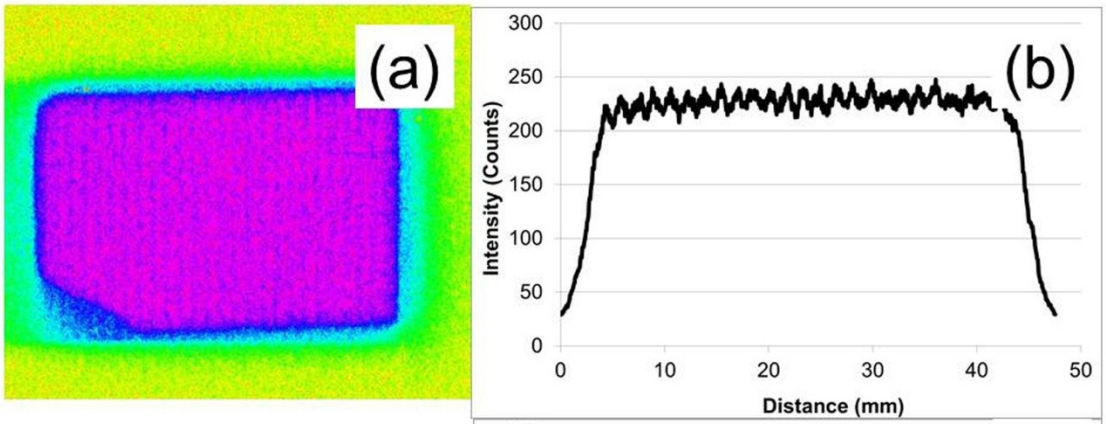

Figure 92 (a) Autoradiography image and (b) Profile Plot of PFA:OPC cement prepared with 0.5% ADVA Cast 551 and containing U (VI)

Figure 92 (a) shows the U (VI) distribution in a block of PFA:OPC cement prepared with 0.5% ADVA Cast 551. The radioactivity is distributed evenly throughout the sample and the profile plot (b) shows a constant intensity of activity throughout the cross section. In the case of PFA:OPC cement, the presence of the superplasticiser did not cause an increase in bleed during set time and in turn this has meant that a homogeneous sample was produced.

Figure 93 shows the autoradiography image and profile plot of a sample of PFA:OPC containing U (VI) but no superplasticiser. There is very little difference between (a) and (b) in Figure 92 and (c) and (d) in Figure 93. The intensity (counts) on the profile plot are the same which shows the same amount of activity is present in the two different samples. The PFA:OPC block prepared without superplasticiser is also homogeneous and U (VI) distribution is even.

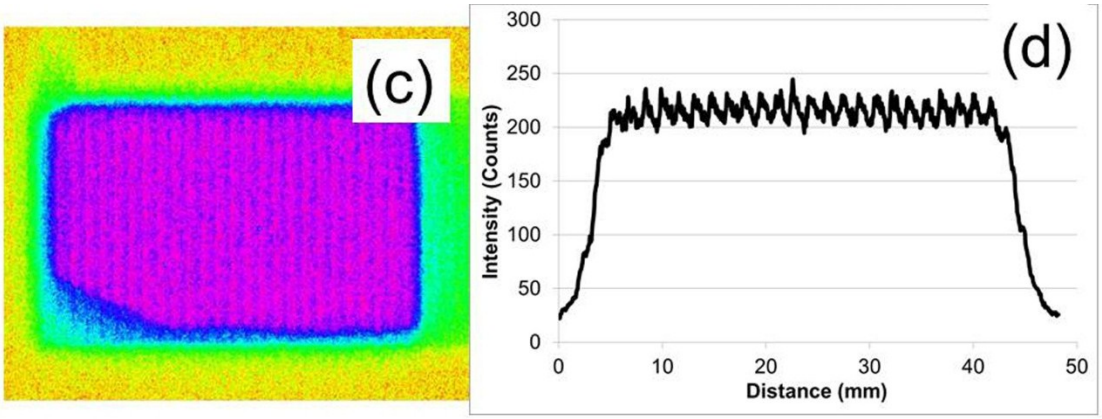

Figure 93 (c) Autoradiography image and (d) Profile Plot of PFA:OPC cement prepared with no superplasticiser and containing U (VI)

PFA:OPC blocks prepared with 0.5% ADVA Cast 551 and containing Th (IV) were also imaged using autoradiography. Figure 94 shows the autoradiography image and profile plot of a PFA:OPC sample containing 0.5% ADVA Cast 551. The Th (IV) distribution through the sample is homogeneous and the profile plot shows that the intensity of activity (counts) throughout the sample cross section is constant. Figure 95 shows a PFA:OPC sample that contained Th (IV) but no superplasticiser. As with the U (VI) PFA:OPC samples, there is little difference between the Th (IV) distribution in the blocks prepared with superplasticiser to those prepared without. This observation is attributed to the fact that the PFA:OPC samples did not produce any bleed so all water (containing both superplasticiser and the metal) was incorporated into the blocks during the set time.

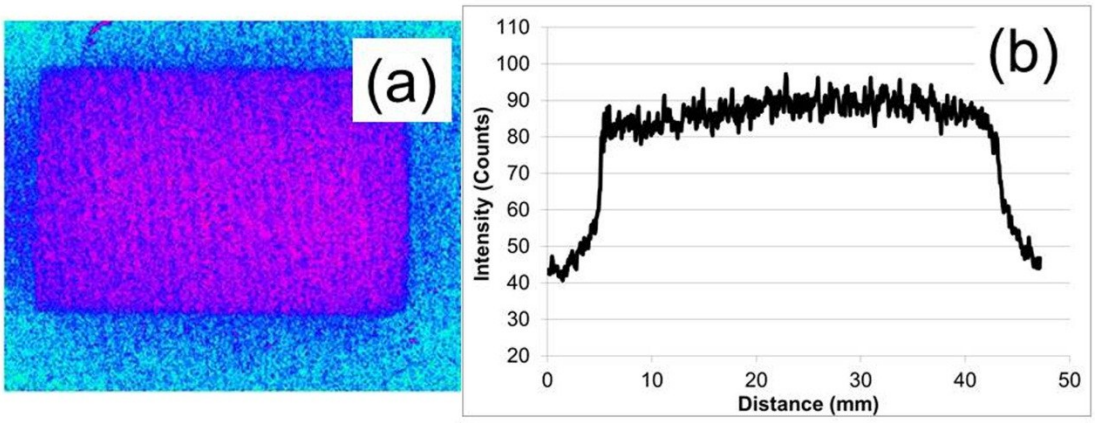

Figure 94 (a) Autoradiography image and (b) Profile Plot of PFA:OPC cement prepared with 0.5% ADVA Cast 551 and containing Th (IV)

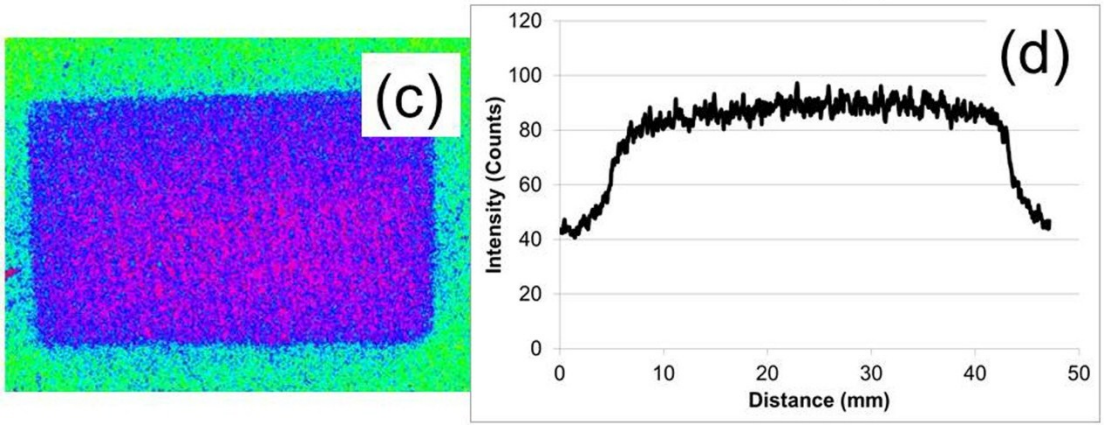

Figure 95 (c) Autoradiography image and (d) Profile Plot of PFA:OPC cement prepared with no superplasticiser and containing Th (IV)

Ni (II) in PFA:OPC was imaged using SEM- EDX. Like in the BFS:OPC samples, the amount of Ni (II) present was unfortunately below the limit of detection of the instrument therefore no conclusions could be drawn regarding the distribution of Ni(II) through the samples. An example EDX spectrum is shown in Figure 96 and shows the spectra from the top edge of a PFA:OPC sample containing Ni (II) and 0.5% ADVA Cast 551. All other SEM-EDX data are given in APPENDIX 2 – EDX Analysis Spectra.

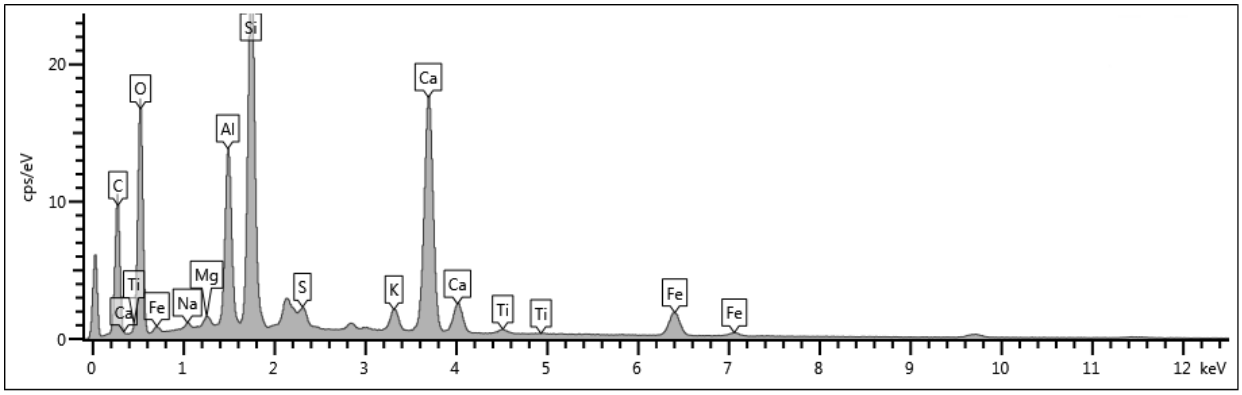

Figure 96 EDX Spectrum of the TOP EDGE of a PFA:OPC cement block containing 0.5% ADVA Cast 551 and Ni (II)

3.7 Stability of ADVA Cast 551

ADVA Cast 551 was subjected to a number of stability experiments as described in section 2.9. Analysing the resultant samples proved challenging; however, results and data collected are presented below.

3.7.1 *Observations*

During the stability experiments, ADVA Cast 551 underwent a number of visible changes. These changes were documented photographically for reference. Figure 97 shows a fresh ‘as received’ sample of ADVA Cast 551, a viscous yellow liquid. This is shown for comparison as the ‘starting material’.

Figure 97 'As Received' ADVA Cast 551

A sample of ADVA Cast that was subject to a temperature stability experiment is shown in Figure 98. There is a significant change in the colour of the ADVA Cast 551 to a dark brown along with an increase in the viscosity of the solution.

Figure 98 ADVA Cast 551 after the temperature stability experiment

ADVA Cast 551 that was irradiated to a total dose of 64 kGy is shown in Figure 99. There is a slight darkening in the colour of the solution however the viscosity remains similar to the original product.

Figure 99 ADVA Cast 551 after low dose irradiation

The most significant change in ADVA Cast 551 was observed on irradiation to a total dose of 220 kGy. Copolymerisation and crosslinking had occurred which in turn resulted in solidification of the sample. The sample in the vial appeared as an intact ‘plug’ of polymer. In order to remove the solid from the vial, the glass vial, and the polymer were broken up. The pieces of polymer are shown in the

photographs in Figure 100. The sample had also darkened and was amber like in colour.

Figure 100 ADVA Cast 551 after high dose irradiation

3.7.2 *Infrared Spectroscopy*

Analysis of the products of ADVA Cast 551 stability experiments was conducted by IR spectroscopy. IR analysis method is described in 2.3.2.1. The characterisation of fresh ADVA Cast 551 is described elsewhere (3.1.2.1) however for reference, the IR spectrum of a fresh sample of ADVA Cast 551 is shown below.

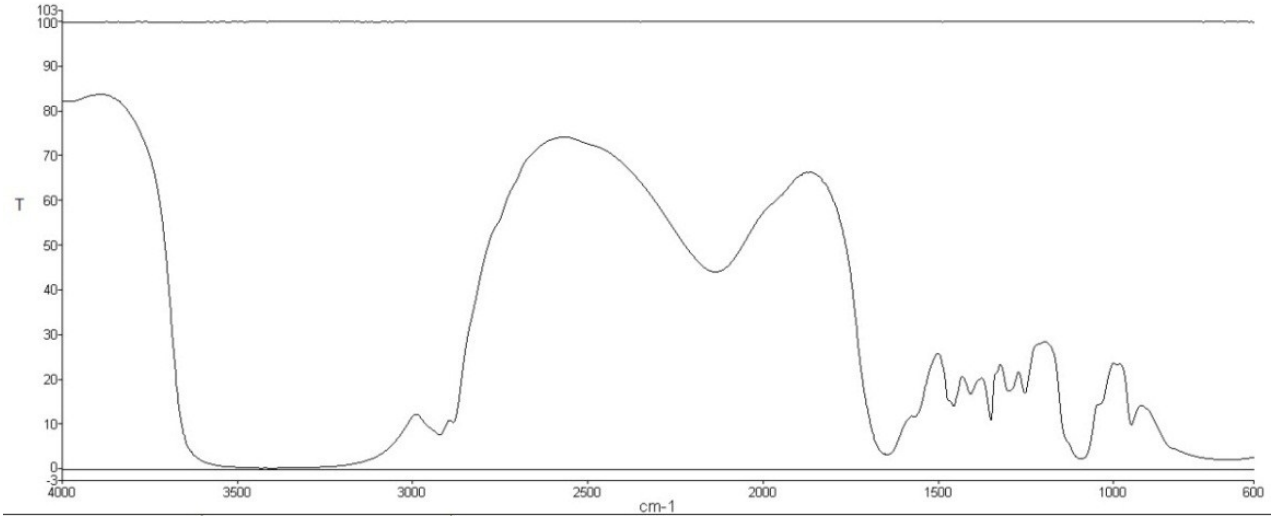

Figure 101 IR Spectrum of Fresh ADVA Cast 551

3.7.2.1 Stability of ADVA Cast 551 to Alkaline Conditions ($Ca(OH)_2$)

The IR spectrum of a 10% ADVA Cast 551 solution prepared in 95% saturated $Ca(OH)_2$ is shown in Figure 102. There is a broad peak at 3700cm^{-1} to 2700cm^{-1} which is associated with water in the sample. A peak exists at 1710cm^{-1} which corresponds to the C=O stretch of the carboxylic acid groups on the side chains: A smaller peak at 1094cm^{-1} is present which is due to the C-O stretch of the ether links on the side chains: A weak peak exists at 1350cm^{-1} which corresponds to the methyl 'umbrella' groups on the polymer backbone: Finally an unidentified peak is present at 2140cm^{-1}. This peak is also visible in the fresh ADVA Cast 551 spectrum but is much more intense than is observed here.

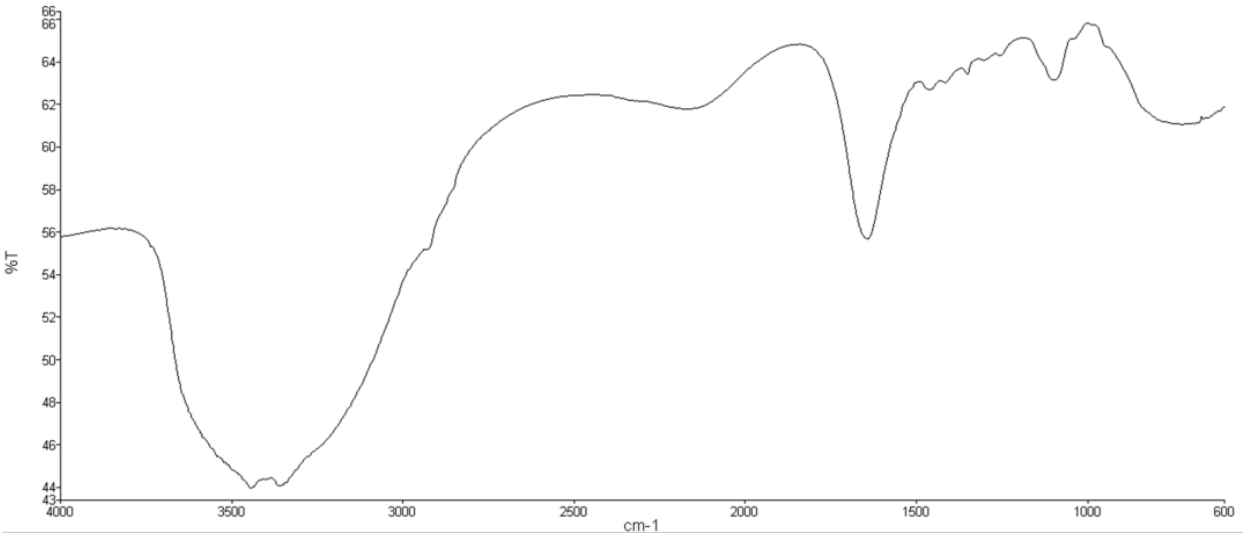

Figure 102 IR Spectrum of 10% ADVA Cast 551 prepared in 95% saturated $Ca(OH)_2$

3.7.2.2 Stability of ADVA Cast 551 to Alkaline Conditions (NaOH)

The IR spectrum of a 10% ADVA Cast 551 solution prepared in 0.1 mol dm^{-3} NaOH is shown in Figure 103.

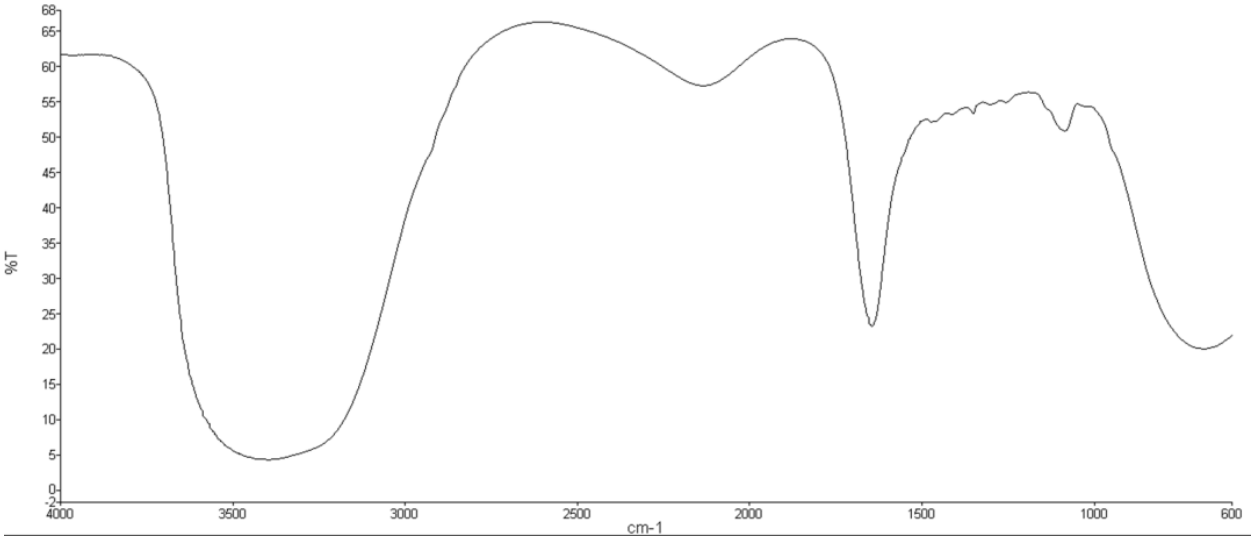

Figure 103 IR Spectrum of 10% ADVA Cast 551 prepared in 0.1 mol dm^{-3} NaOH

This spectrum is very similar to that observed for 10% ADVA Cast 551 in 95% saturated $Ca(OH)_2$. There is a broad peak at 3700cm^{-1} to 2700cm^{-1} associated with water in the sample: A strong peak at 1710cm^{-1} corresponding to the C=O stretch of the carboxylic acid groups on the side chains: A smaller peak at 1094cm^{-1} is present which is due to the C-O stretch of the ether links on the side chains: The unidentified peak at 2140cm^{-1} is also present with a slightly higher intensity than was noted in the $Ca(OH)_2$ sample.

3.7.2.1 Stability of ADVA Cast 551 to Elevated Temperature (80ºC)

The IR spectrum of a neat sample of ADVA Cast 551 that was subjected to elevated temperatures is shown in Figure 104.

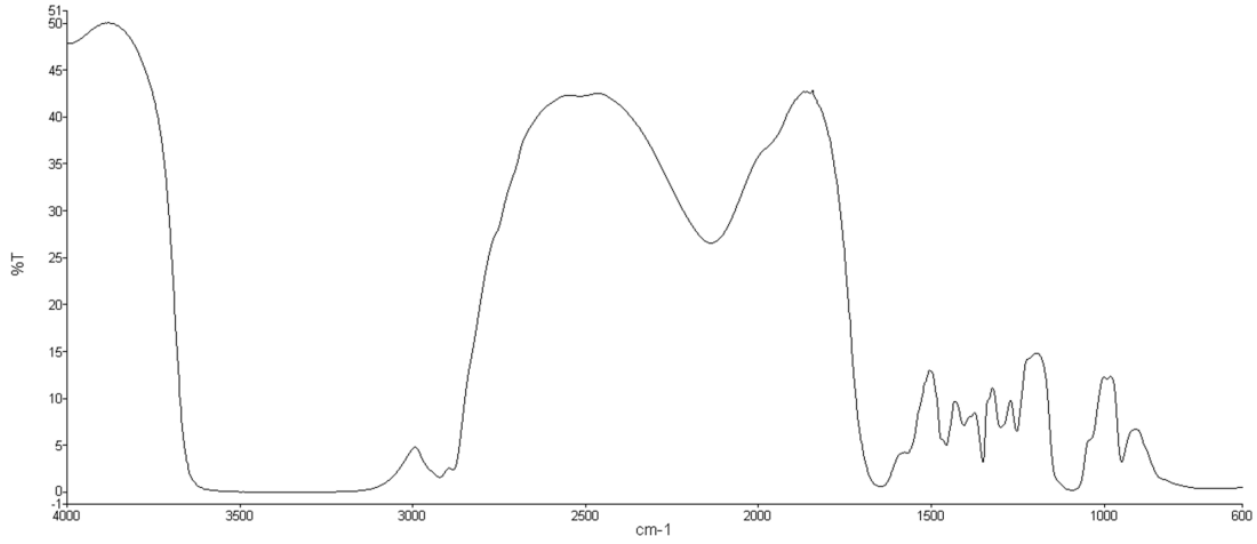

Figure 104 IR Spectrum of ADVA Cast 551 exposed to 80ºC

This spectrum is very similar to that of fresh ADVA Cast 551 with similar peaks observed at 1710cm^{-1} associated with C=O of the carboxylic acid: 1094cm^{-1} from the C-O ether links on the side chains and 1350cm^{-1} from the CH_3 umbrella on the polymer backbone: The unidentified peak of similar intensity to the fresh ADVA Cast 551 is present at 2140cm^{-1} and a broad peak associated with water in the sample is also present between 3700cm^{-1} and 2700cm^{-1}.

3.7.2.2 Stability of ADVA Cast 551 to Radiolysis

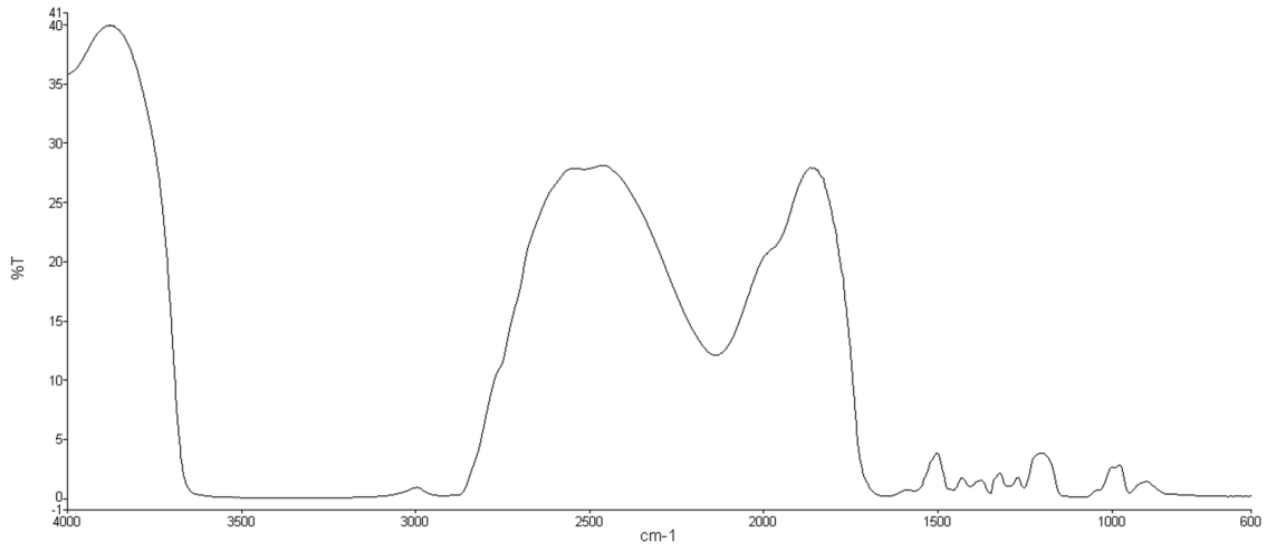

Figure 105 IR Spectrum of ADVA Cast 551 exposed to radiolysis (^{60}Co source)

Figure 105 shows an IR spectrum of neat ADVA Cast 551 that was exposed to a ^{60}Co source. This sample was exposed to the lower of the two doses investigated (3.23 Gy min^{-1} to a total dose of 64 kGy). At the higher dose rate, the sample solidified. It is thought that copolymerisation and crosslinking had occurred between the polymer chains as a result of radiation induced polymerisation. The IR spectrum obtained has the same peaks present as in the fresh sample of ADVA Cast 551 and the sample exposed to elevated temperatures. This means that the functionality on the polymer is still present however it is not possible to identify changes in the chain length and molecular size of the polymer.

3.7.3 *SEM*

SEM images of the copolymerised superplasticiser were taken at the British Geological Survey. The copolymerised superplasticiser was broken up easily by hand and images recorded at increasing magnification.

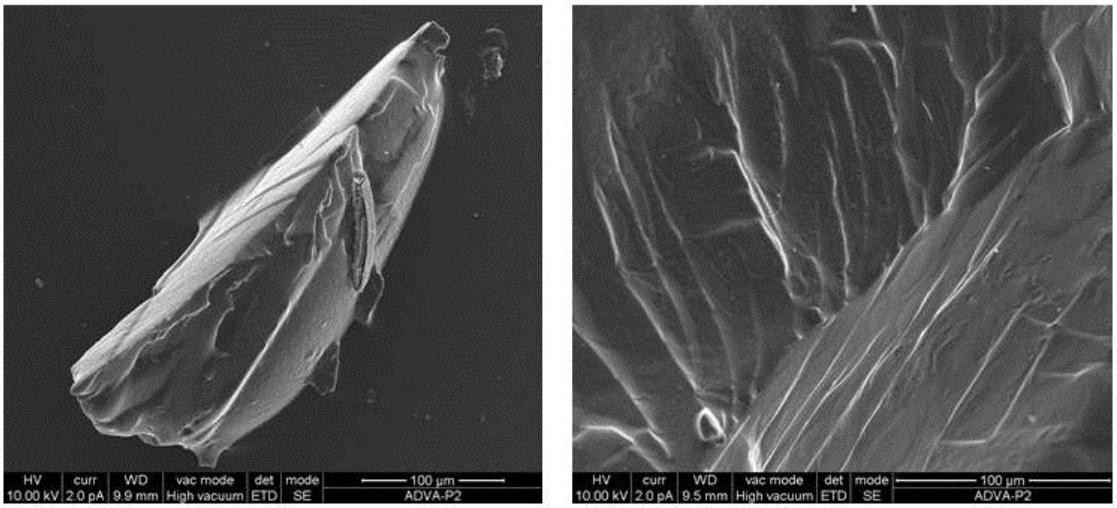

Figure 106 SEM Imaging of irradiated ADVA Cast 551 (A)

Figure 106 shows SEM images of irradiated ADVA Cast 551. Little structural information can be learnt from the images other than the observation of the smoothness of the copolymerised surfaces. Figure 107 shows SEM images taken at a higher magnification. The surface of the solid polymer has a ‘blistered’ topography and it is unclear what has caused this effect.

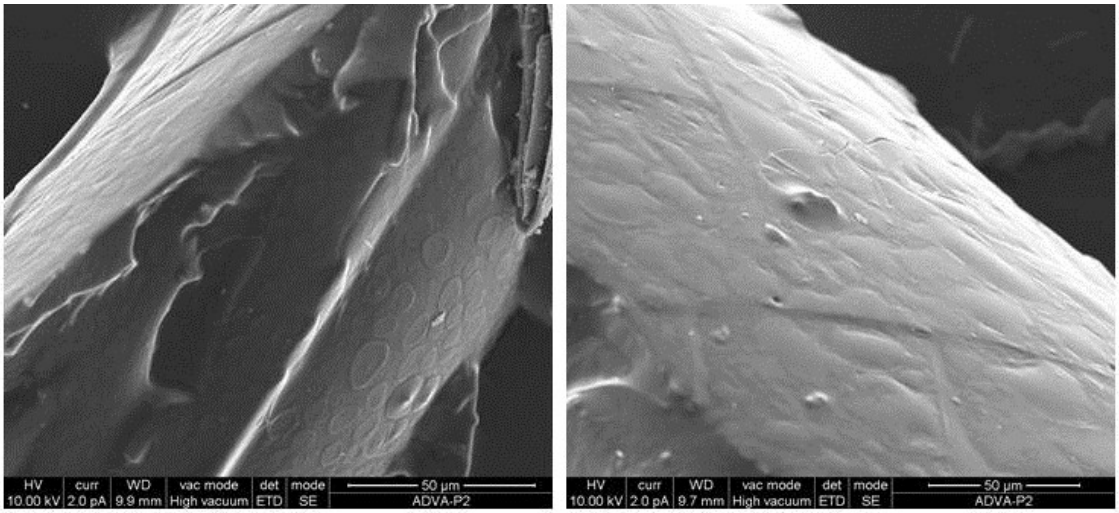

Figure 107 SEM Imaging of irradiated ADVA Cast 551 (B)

3.7.4 *ESI-MS*

Characterisation of fresh ADVA Cast 551 by ESI-MS is described elsewhere (3.1.2.4) however, for reference, the mass spectrum of fresh ADVA Cast 551 is shown below.

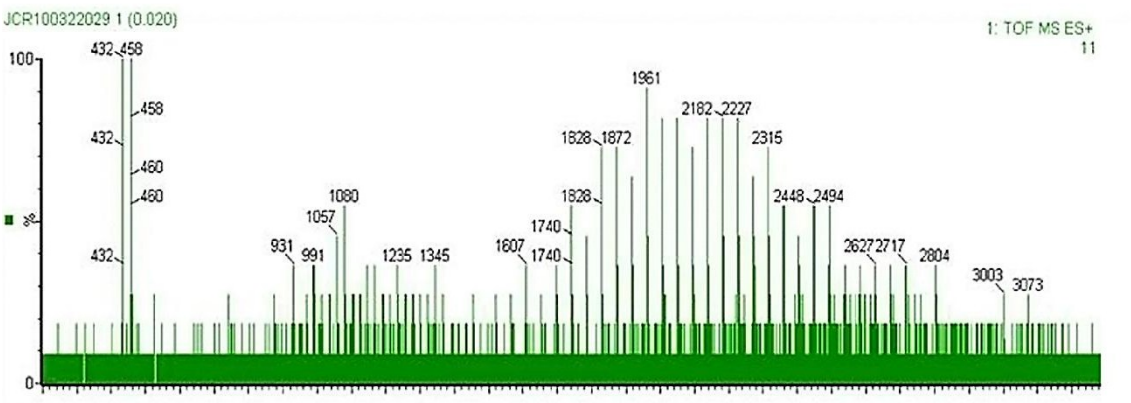

Figure 108 Mass Spectrum of an 'as received' sample of ADVA Cast 551

The mass spectrum of a fresh sample of ADVA Cast 551 shows numerous polymer distributions with varying chain length. It should be noted that the ESI-MS instrument is only efficient up to masses of around 3000 and the chains of ADVA Cast 551 are expected to be much longer than this (ca. 10,000). The technique therefore has limitations but can give an insight into the lower mass superplasticiser behaviour and identify trends in stability under different conditions.

3.7.4.1 Stability of ADVA Cast 551 to Alkaline Conditions ($Ca(OH)_2$)

The mass spectrum of ADVA Cast 551 prepared at 10% (w/v) in 95% saturated $Ca(OH)_2$ is shown in Figure 109. Some higher mass molecules are still present in the sample after exposure to the highly alkaline solution; however, there are a much higher proportion of low mass molecules. This suggests that ADVA Cast 551 has undergone some alkaline hydrolysis reactions in the $Ca(OH)_2$ solution which has resulted in a high proportion of molecules of decreased chain length.

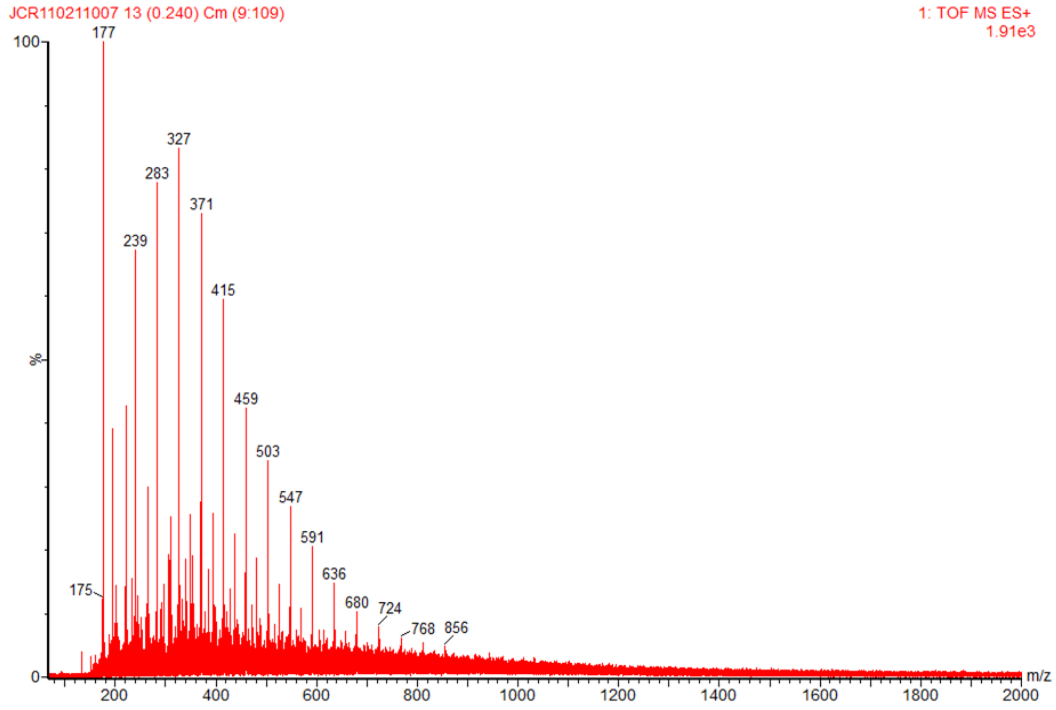

Figure 109 Mass Spectrum of ADVA Cast 551 prepared at 10% (v/w) in $Ca(OH)_2$

3.7.4.2 Stability of ADVA Cast 551 to Alkaline Conditions (NaOH)

The mass spectrum of ADVA Cast 551 prepared at 10% (w/v) in 0.1 mol dm^{-3} NaOH is shown in Figure 110.

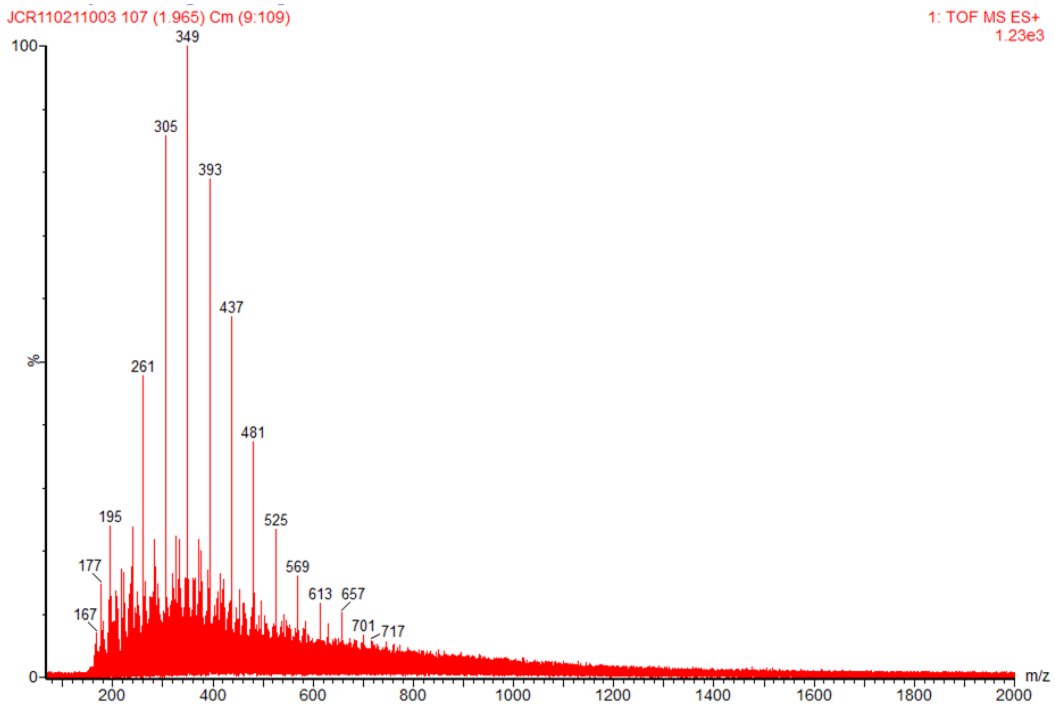

Figure 110 Mass Spectrum of ADVA Cast 551 prepared at 10% (w/v) in 0.1 mol dm^{-3} NaOH

The $Ca(OH)_2$ sample and the NaOH sample are similar. The presence of high molecular weight molecules is greatly reduced while the proportion of lower mass analogues is increased. This is further evidence to suggest alkaline hydrolysis results in some breakdown of the longer length polymer chains producing smaller and lower mass fragments.

3.7.4.1 Stability of ADVA Cast 551 to Elevated Temperature (80ºC)

The mass spectrum of a sample of ADVA Cast that was exposed to elevated temperatures is shown in Figure 111.

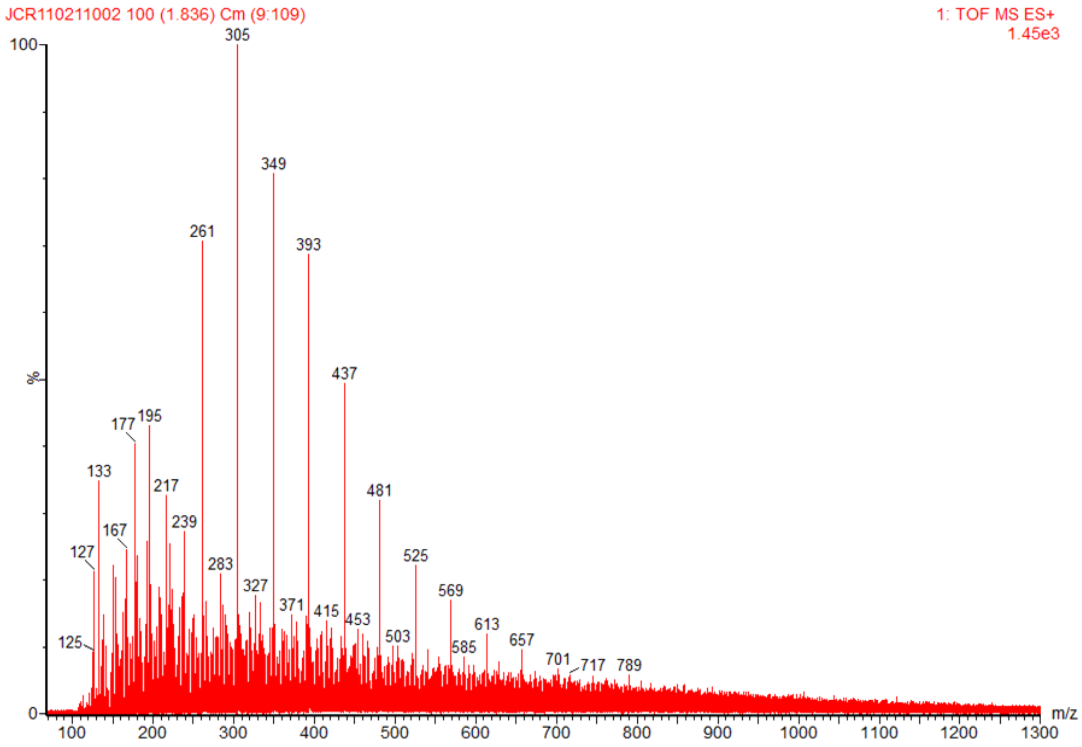

Figure 111 Mass Spectrum of neat ADVA Cast 551 that was exposed to elevated temperatures (80ºC)

The IR spectrum of the sample exposed to elevated temperatures did not show any significant changes to that of fresh ADVA Cast 551. In this case, the mass spectrum shows depletion in the higher molecular weight fractions but not such marked degradation in comparison to the $Ca(OH)_2$ and NaOH samples.

3.7.4.2 Stability of ADVA Cast 551 to Radiolysis

Of the two total radiation doses investigated, only the lower dose could be analysed by ESI-MS since the higher dose sample, as mentioned previously was solid and insoluble. The mass spectrum for a sample of ADVA Cast 551 exposed to 64 kGy is shown in Figure 112.

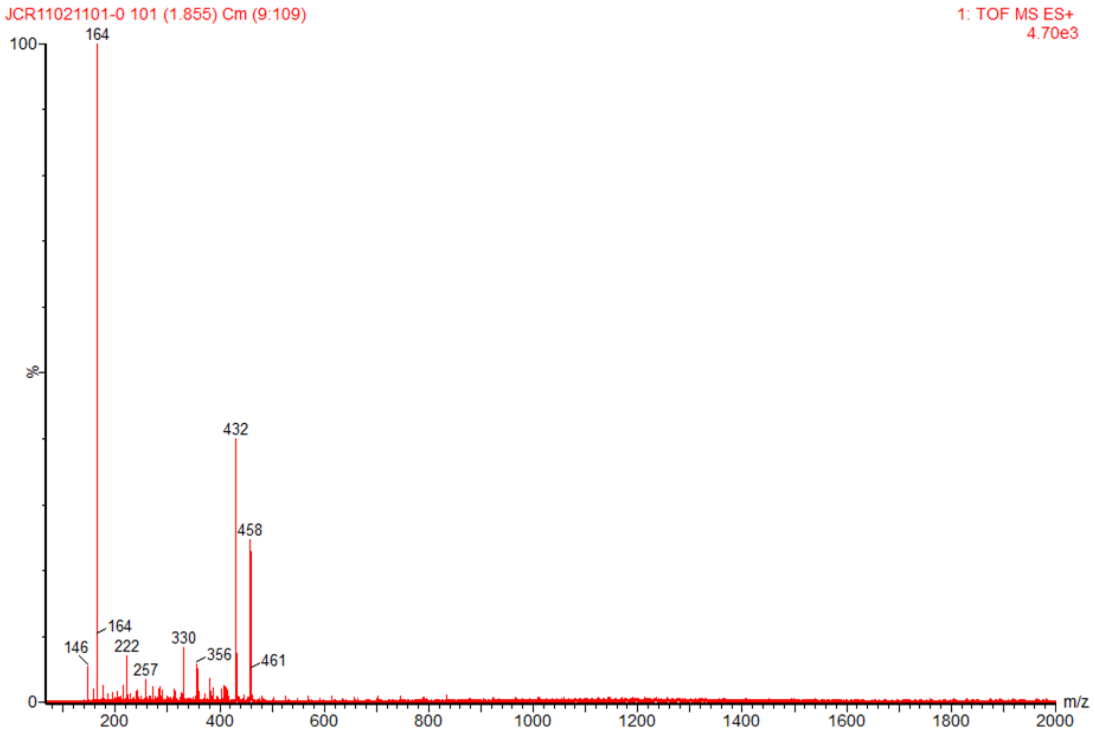

Figure 112 Mass Spectrum of ADVA Cast 551 exposed to radiolysis by a ^{60}Co source

The mass spectrum shows a range of molecular weights. Interestingly, there are few polymer fractions with molecular weights up to the instrumental limit of M_w ~3000. This confirms that radiation induced copolymerisation occurs on exposure to a ^{60}Co source and there is expected to be a large proportion of polymer species at much higher M_w that cannot be detected by the instrument. There are still some lower mass molecules which are likely to correspond to unreacted monomer units within the sample or are the product of polymer chain scission.

3.7.5 *Gel Permeation Chromatography*

The separation of ADVA Cast 551 and the products of stability experiments has proven to be a challenge. Results and data collected are shown below.

3.7.5.1 Stability of ADVA Cast 551 to Alkaline Conditions ($Ca(OH)_2$)

Good separation of the components of 'as received' ADVA Cast 551 was achieved by first vacuum drying the superplasticiser to remove solvent and re-suspending the solid in methanol (see section 2.3.2.5). Due to the nature of the chemical stability experiments, vacuum drying of the sample of superplasticiser

that was exposed to alkaline attack by $Ca(OH)_2$ was not possible. Therefore ADVA Cast 551 solution prepared at 10% (w/v) in 95% saturated $Ca(OH)_2$ and was injected without modification other than filtration through 0.45µm filters to remove any precipitated $Ca(OH)_2$ which could block the column. The chromatogram is shown in Figure 113. The aqueous nature of the sample means a large distorted peak associated with water is present in the sample and results in a large change in the recorded refractive index. A peak which is eluted at 9.676 minutes is visible and is shown more clearly in Figure 114 by magnification of the Y axis.

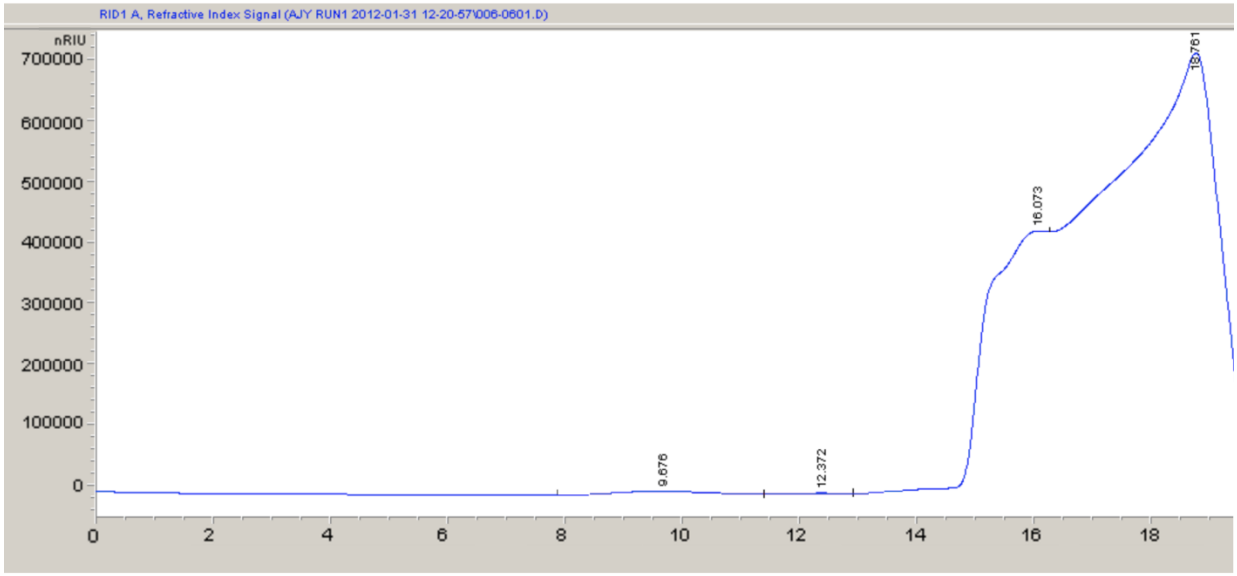

Figure 113 10% ADVA Cast 551 prepared in 95% saturated $Ca(OH)_2$

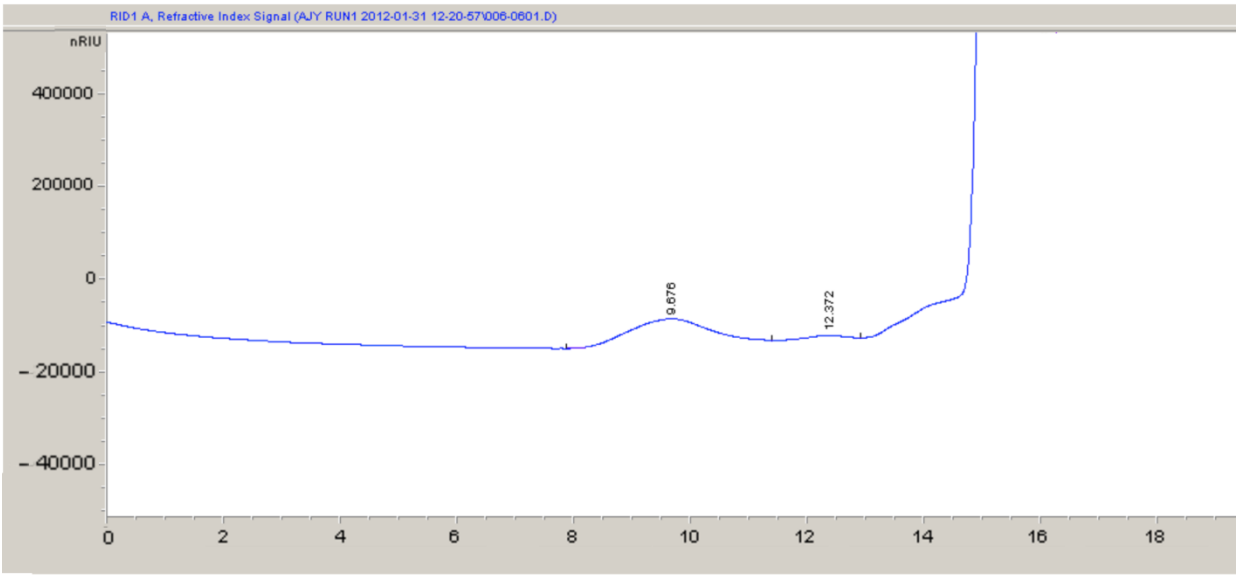

Figure 114 10% ADVA Cast 551 prepared in 95% saturated $Ca(OH)_2$ (magnified Y axis)

The presence of water in the sample causes such a significant change in refractive index that the resolution of the smaller peaks associated with the polymer is reduced. 10% ADVA Cast 551 solution prepared in $Ca(OH)_2$ was therefore diluted to 1% with methanol to try and reduce the effect of the presence of water on the sample elution. The resulting chromatogram is shown in Figure 115 and focuses on the peaks that are attributed to the superplasticiser. The molecular weights associated with each eluted peak are given in Table 76. These results show that a significant proportion of the polymer detected is within the molecular weight range of 115,757 to 467. This range is of lower molecular weight to that of the fresh ADVA Cast sample where the molecular weights eluted ranged from 780,601 to 1346. This is further evidence to suggest that degradation of the polymer chains is occurring as a result of exposure to alkaline conditions by alkaline hydrolysis of the superplasticiser chains.

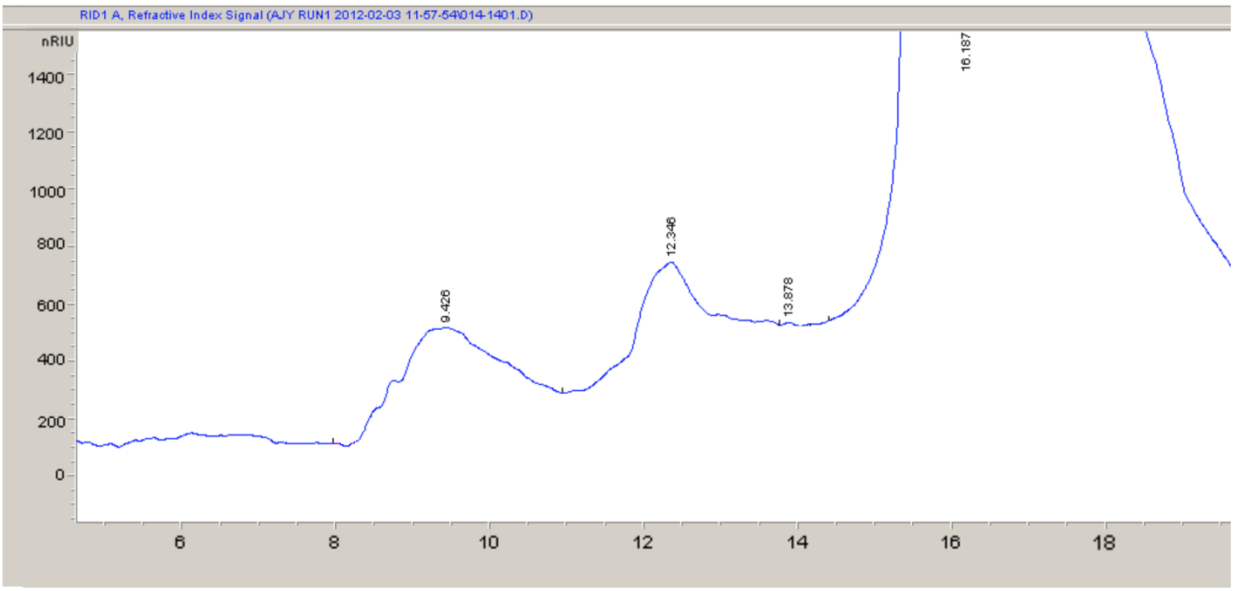

Figure 115 10% ADVA Cast 551 in 95% saturated $Ca(OH)_2$ diluted to 1% with methanol

Table 76 ADVA Cast 551 Alkaline Stability Experiment - $Ca(OH)_2$ GPC Peak Table

Peak Label	Start Time (min)	End Time (min)	Size Range (Mw)	Average (Mw)
9.426	8.4	11.0	115,757 to 467	58,112
12.346	11.3	13.0	247 to 7	127

3.7.5.2 Stability of ADVA Cast 551 to Alkaline Conditions (NaOH)

Similarly to the $Ca(OH)_2$ stability samples, the aqueous nature of the NaOH stability experiment meant that the 10% ADVA Cast 551 solution prepared in 0.1 mol dm^{-3} NaOH was unsuitable for vacuum drying. A sample of the solution was therefore filtered through 0.45µm syringe filters to remove any solid and injected into the instrument without further modification. The resulting chromatogram is shown in Figure 116 and is magnified in Figure 117.

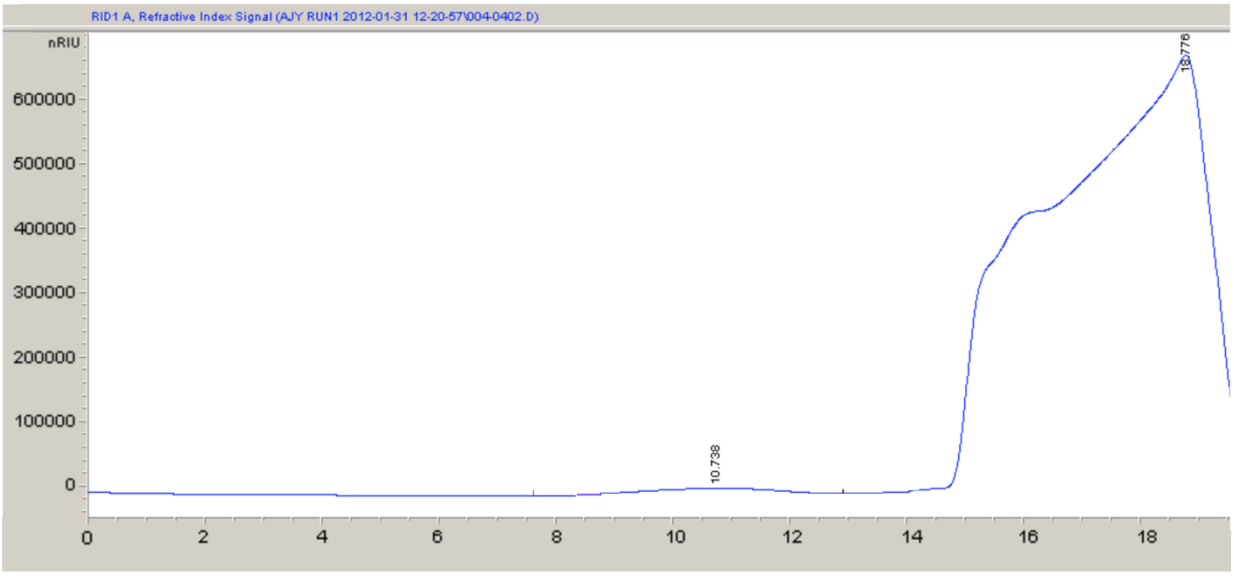

Figure 116 10% ADVA Cast 551 prepared in 0.1 mol dm^{-3} NaOH

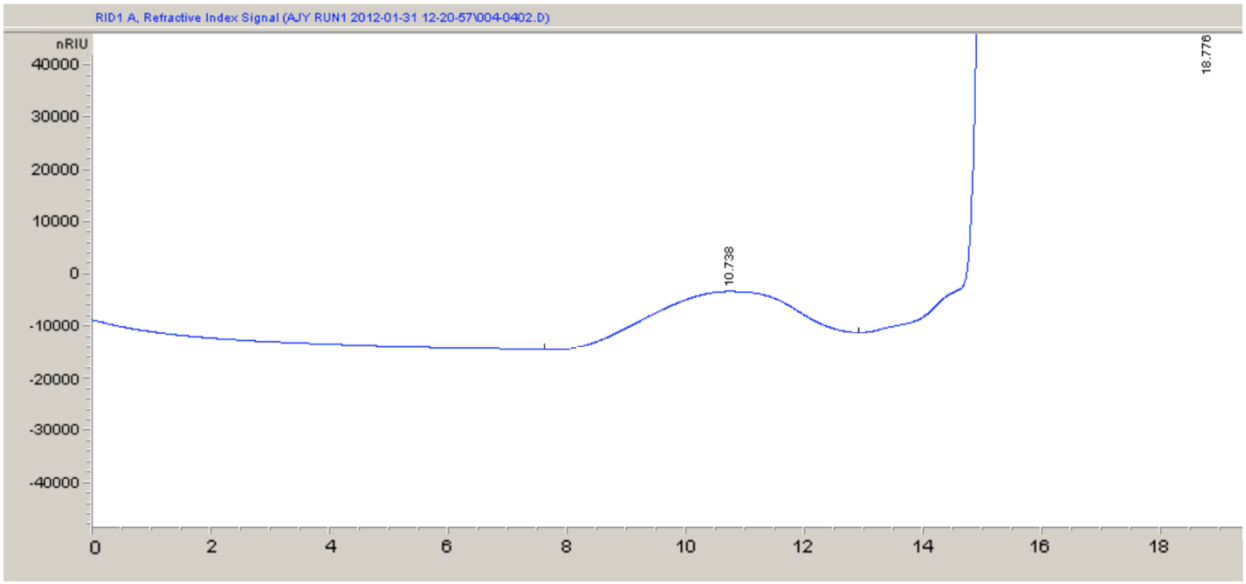

Figure 117 10% ADVA Cast 551 prepared in 0.1 mol dm^{-3} NaOH (magnified Y axis)

Again, the presence of water in the sample causes such significant refractive index response that the resolution of the peak associated with the polymer is reduced. The 10% ADVA Cast 551 solution prepared in 0.1 mol dm^{-3} NaOH was therefore diluted to 1% with methanol. The resulting chromatogram is shown in Figure 118. The Y axis is magnified to focus on the peak that is attributed to the superplasticiser. The molecular weight range associated with the peak is given in Table 77. A similar result is obtained to that in the $Ca(OH)_2$

experiment. The range of molecular weights in the resolved peak is extensive with an average molecular weight of 57,418. This value is very similar to that in the $Ca(OH)_2$ experiment where the average Mw was 58,112. This suggests that the effect of alkaline hydrolysis on the polymer is similar in both $Ca(OH)_2$ and NaOH.

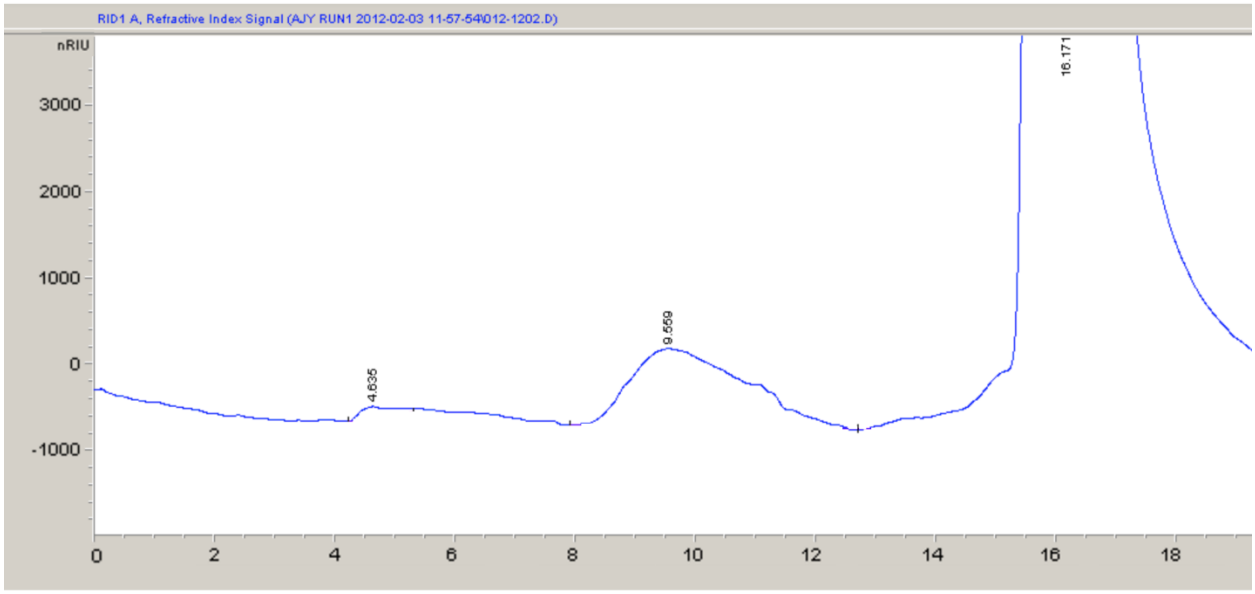

Figure 118 10% ADVA Cast 551 in 0.1 mol dm^{-3} NaOH diluted to 1% with methanol

Table 77 ADVA Cast 551 Alkaline Stability Experiment - NaOH GPC Peak Table

Peak Label	Start Time (min)	End Time (min)	Size Range (Mw)	Average (Mw)
9.559	8.4	12.5	114,815 to 20	57,418

3.7.5.1 Stability of ADVA Cast 551 to Elevated Temperature (80ºC)

Neat ADVA Cast 551 that had been exposed to elevated temperatures (80ºC) was dried by vacuum to remove the solvent and re-suspended at 1% (w/v) in methanol. The sample was injected into the GPC column and the resulting chromatogram is shown in Figure 119.

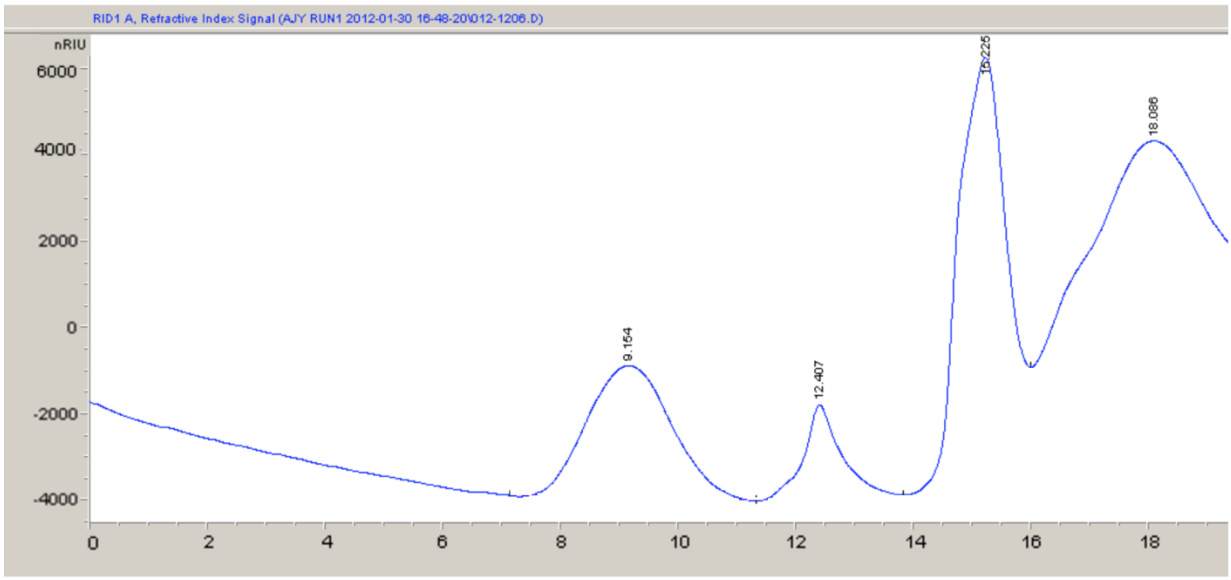

Figure 119 1% temperature degraded ADVA Cast 551 solid re-suspension in methanol

A peak out of the range of the calibration (smallest analyte is eluted before 14 minutes) is present at 18 minutes which cannot be attributed to the sample and is therefore discounted as an anomalous peak. Each sample injection was replicated four times and the peak at 18 minutes was present in each case but the cause is unclear. Although the sample was filtered to remove any solid, there may have been some contamination build up in the injection loop which was eluted as part of the sample. As the temperature stability sample was a particularly 'dirty' sample, the injector and loop was cleaned with methanol thoroughly before subsequent analysis. The molecular weight of the eluted polymer is shown in Table 78. There was less evidence of degradation in the temperature stability sample compared to the chemical stability experiments. The molecular weight range eluted was similar to that of the fresh ADVA Cast sample with an average molecular weight of the first peak of 338,261. The average molecular weight for the same peak in the fresh ADVA Cast 551 sample was 390,974. There was however, an increase in the low molecular weight molecules eluted suggesting that some degradation of the polymer had taken place. A large peak was observed between 11.25 minutes and 13.75 minutes which corresponds to the sample fraction with a molecular weight of <275. This may be attributed to unreacted monomer (that was also present in

the fresh sample) or a fraction of low molecular weight polymer degradation products. It is most likely that this fraction is due to a combination of the two.

Table 78 ADVA Cast 551 Temperature Stability Experiment GPC Peak Table

Peak Label	Start Time (min)	End Time (min)	Size Range (Mw)	Average (Mw)
9.154	7.5	11.25	776,247 to 275	338,261
12.407	11.25	13.75	275 to 0	138

3.7.5.2 Stability of ADVA Cast 551 to Radiolysis

A sample of neat ADVA Cast 551 that had been exposed to a total dose of 65 kGy by a ^{60}Co source was dried by vacuum and re-suspended to 1% (w/v) in methanol. This sample was exposed to the lower of the two total doses investigated and is the only sample suitable for GPC analysis since as mentioned previously, the higher dose rate same was solidified as a result of radiation exposure. The solid was insoluble and therefore analysis by GPC was not possible .The re-suspended lower dose sample was injected into the column and the chromatogram obtained is shown in Figure 120.

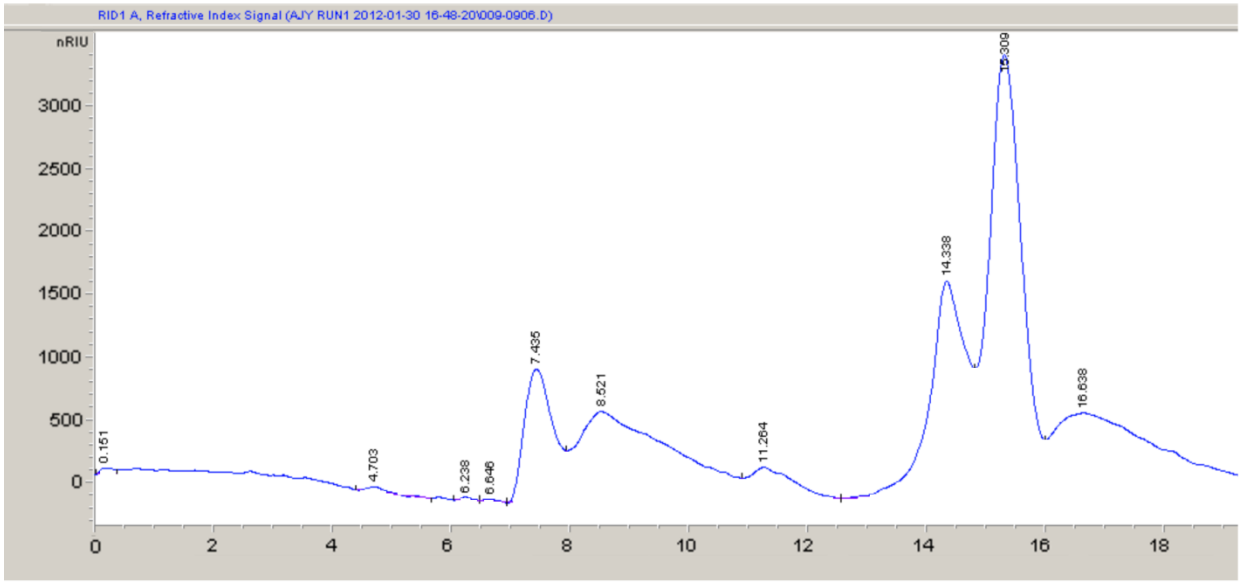

Figure 120 1% ADVA Cast 551(exposed to 65 kGy) solid re-suspension in methanol

A number of peaks were eluted including a peak at 14.338 minutes which was out of the calibration range but was also present in the fresh ADVA Cast 551

sample. This peak was attributed to low molecular weight impurities within the sample.

The peaks and their corresponding molecular weight ranges are given in Table 79. Much higher molecular weight ranges are recorded in the radiation exposed sample than any other. The molecular weight fractions eluted are higher than that of the fresh ADVA Cast 551. This observation provides evidence that radiation induced polymerisation has started to occur in this sample, increasing the molecular weight of the polymer chains. As observed in the higher dose sample, solidification occurs after exposure to a total dose of 220 kGy where the sample has cross-linked and co-polymerised. It is clear that this process has been initiated within this sample and it is likely that if exposure had continued, solidification of the sample would have occurred here also.

Table 79 ADVA Cast 551 Radiation Stability Experiment GPC Peak Table

Peak Label	Start Time (min)	End Time (min)	Size Range (Mw)	Average (Mw)
7.436	7.0	8.0	2,254,239 to 270,396	1,262318
8.521	8.0	11.0	270,396 to 467	135,418
11.264	11.0	12.5	467 to 20	244

3.8 Effect of Degraded Superplasticiser on Metal Solubilities

It is important to take into account the effect of ADVA Cast 551 that has been subjected to γ irradiation on the solubility of radionuclides. It is clear from the radiolysis stability tests, that ADVA Cast 551 undergoes significant chemical changes whilst subjected to radiation.

Irradiated-ADVA Cast 551 used in these experiments was exposed to a ^{60}Co source and received a total dose of 65 kGy. For brevity, ADVA Cast 551 will be referred to as Irradiated-ADVA Cast 551 in the text.

The method of solubility determination by oversaturation is described in section 2.5.1 while methods of metal analysis are explained in section 2.5.2. All errors quoted represent ± the standard deviation of 4 sample replicates.

ADVA Cast 551 concentrations investigated in this section were 0%, 0.1% 0.5% and 1% (w/v). This was due to space constraints within the ^{60}Co irradiation facility. This concentration range still represents the recommended dosage of ADVA Cast 551 that is between 0.3 and 0.8%.

3.8.1 *Uranium (VI) Solubility*

3.8.1.1 95% saturated $Ca(OH)_2$

The solubility of U (VI) was monitored over twenty eight days and samples taken for analysis at seven day intervals. The kinetic profile for the solubility of U (VI) in $Ca(OH)_2$ in the presence of Irradiated-ADVA Cast 551 is shown in Figure 121.

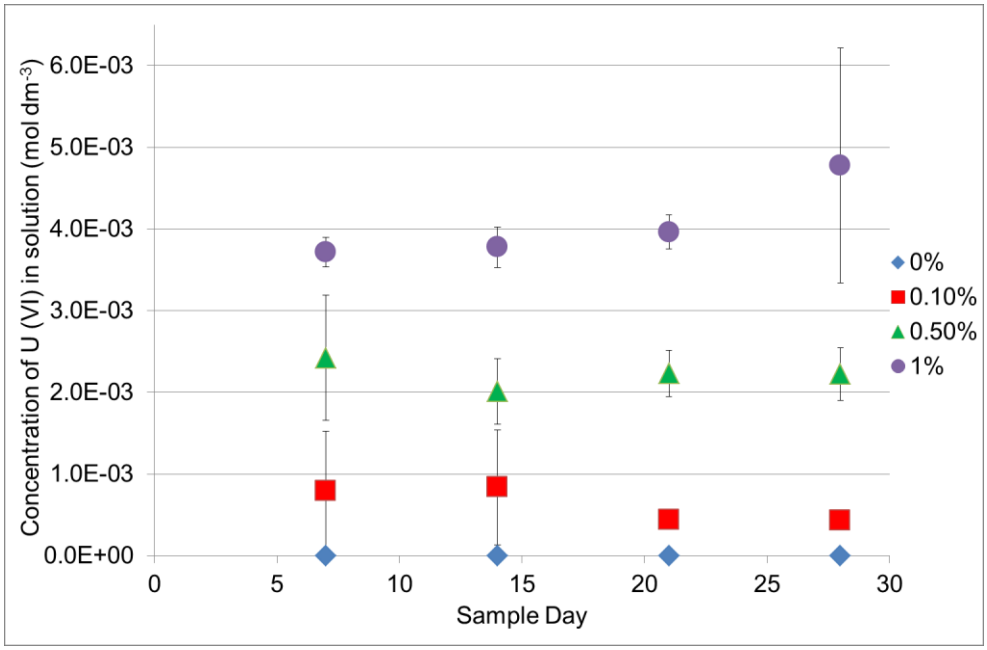

Figure 121 Kinetics of precipitation of U (VI) in the presence of irradiated-ADVA Cast 551 in 95% saturated $Ca(OH)_2$

The samples reached steady state by day 7. An increase in the concentration of U (VI) in solution is noted with the presence of increasing amounts of irradiated-ADVA Cast 551. The final concentration of U (VI) in solution is recorded in Figure 122 and shows an increase in solubility of several orders of magnitude. The solubility enhancement factors for each concentration of irradiated-ADVA Cast 551 are shown in Table 80. The SEF values in the case of irradiated-ADVA Cast 551 are much higher than those calculated in the 'as received'

experiment. At 1% irradiated-ADVA Cast 551 the SEF value recorded was 70561 compared to 3152 in the non-irradiated samples.

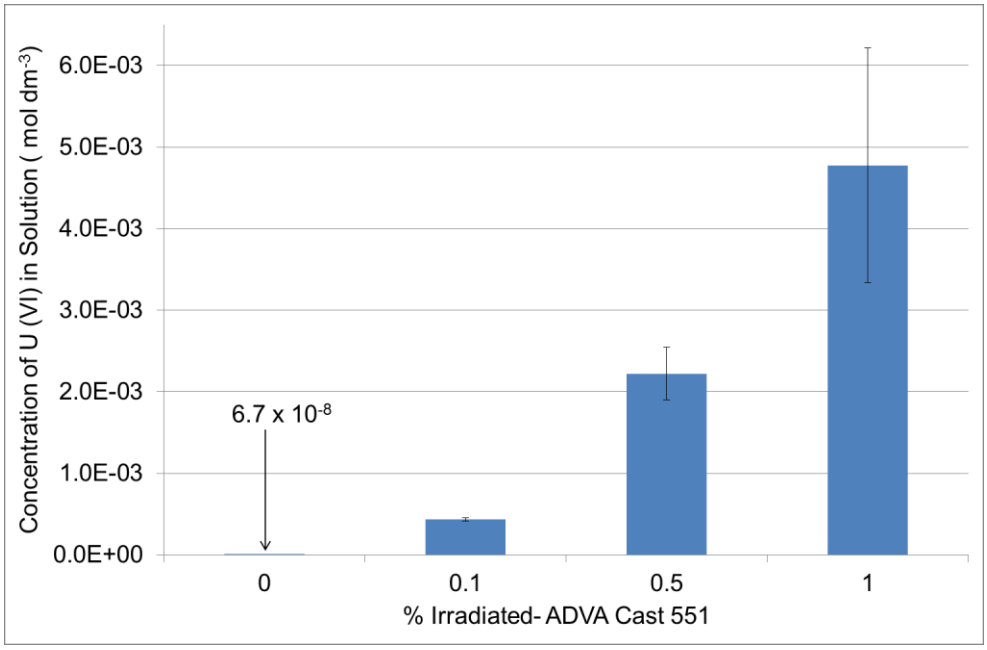

Figure 122 Final Concentration of U (VI) in 95% saturated $Ca(OH)_2$ in the presence of irradiated-ADVA Cast 551

Table 80 U (VI) solubility in 95% saturated $Ca(OH)_2$ in the presence of irradiated-ADVA Cast 551

Solution	% Irradiated-ADVA Cast	Solubility (mol dm^{-3})	SEF
$Ca(OH)_2$	0	6.77E-08	1
	0.1	4.33E-04	6401
	0.5	2.22E-03	32814
	1	4.78E-03	70561

3.8.1.1 0.1 mol dm^{-3} NaOH

Concentration of of U (VI) in 0.1 mol dm^{-3} NaOH as a function of time in the presence of irradiated-ADVA Cast 551 is shown in Figure 123. Steady state was reached by day 14 for 0%, 0.1% and 0.5% samples while the 1% samples reached steady state at day 21.

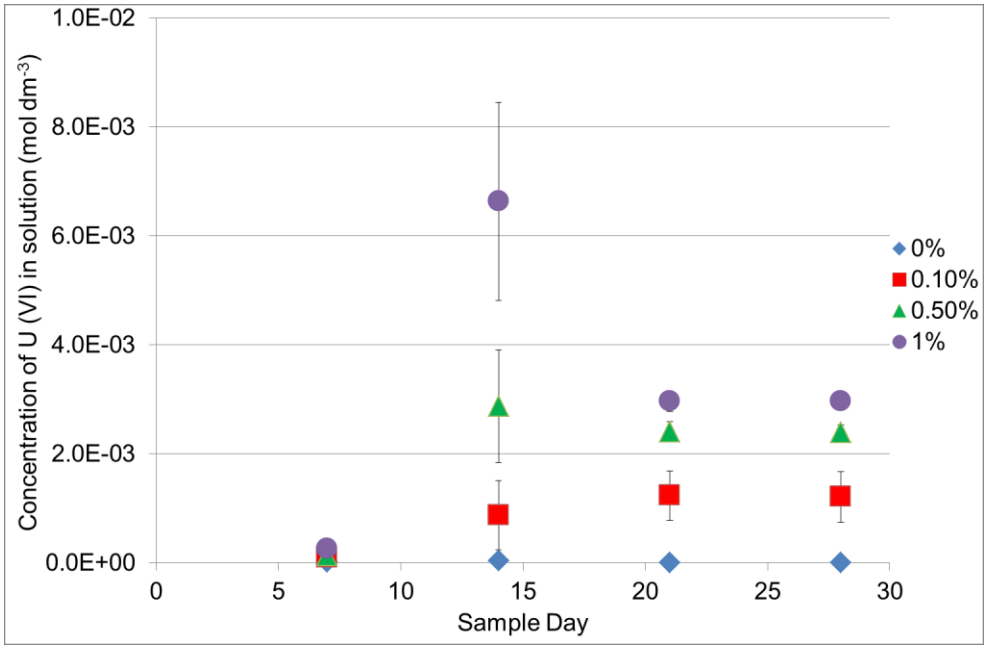

Figure 123 Kinetics of precipitation of U (VI) in the presence of irradiated-ADVA Cast 551 in 0.1 mol dm^{-3} NaOH

The final concentration of U (VI) in solution is recorded in Figure 124. A substantial increase in solubility is observed with increasing concentrations of irradiated ADVA Cast 551. SEF values are reported in Table 81 and although the observed values are much lower than that for $Ca(OH)_2$, there is a significant difference between values for the 'as received' and irradiated NaOH samples. The increase in solubility in the presence of irradiated-ADVA Cast 551 is within the region of 3 orders of magnitude.

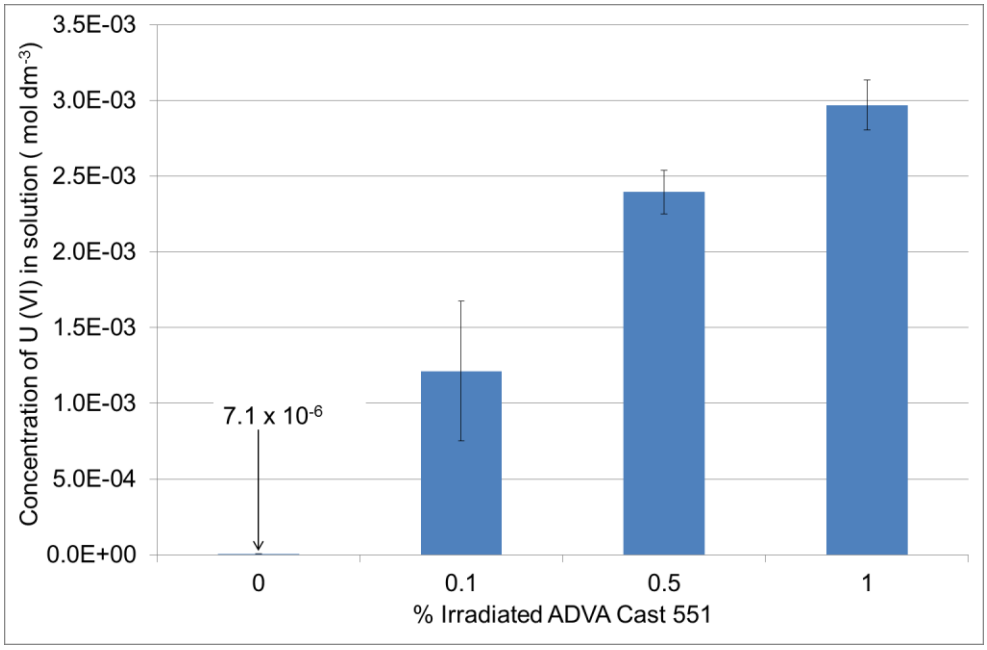

Figure 124 Final concentration of U (VI) in 0.1 mol dm^{-3} NaOH in the presence of irradiated-ADVA Cast 551

Table 81 U (VI) solubility in 0.1 mol dm^{-3} NaOH in the presence of irradiated-ADVA Cast 551

Solution	% Irradiated ADVA Cast	Solubility (mol dm^{-3})	SEF
NaOH	0	7.08E-06	1
	0.1	1.21E-03	171
	0.5	2.39E-03	338
	1	2.97E-03	419

3.8.1.1 BFS:OPC equilibrated water

The kinetics of precipitation of U (VI) in BFS:OPC equilibrated water in the presence of irradiated-ADVA Cast 551 is shown in Figure 125. Steady state is reached by day 14. The final concentration of U (VI) measured in solution is shown in Figure 126. A substantial increase in U (VI) solubility as ADVA Cast 551 concentration is observed. SEF values are reported in Table 82 and demonstrate a solubility increase over several orders of magnitude. In comparison to U (VI) solubility in the presence of 'as received' ADVA Cast 551, the increase in solubility is much greater. SEF values for 1% ADVA Cast 551 are calculated to be 125 and 31855 for 'as received' and irradiated ADVA Cast 551 respectively.

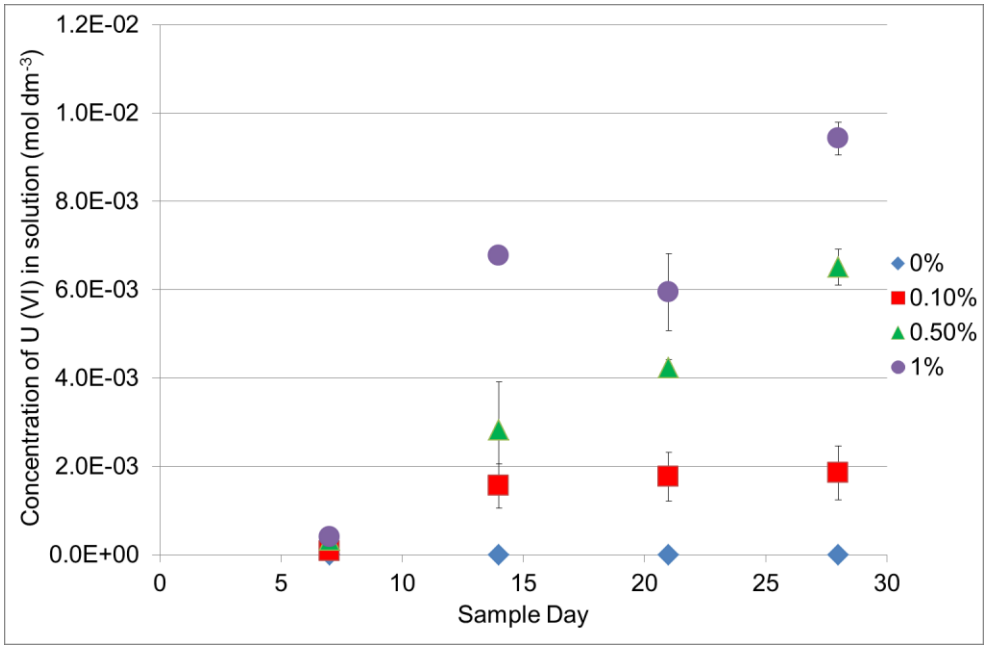

Figure 125 Kinetics of precipitation of U (VI) in the presence of irradiated-ADVA Cast 551 in BFS:OPC equilibrated water

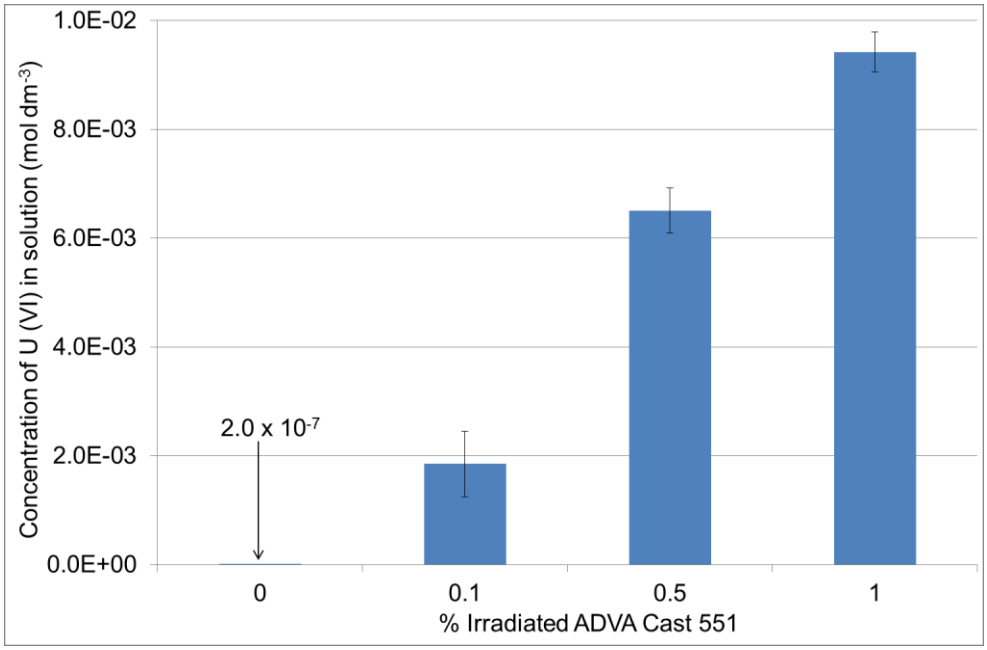

Figure 126 Final concentration of U (VI) in BFS:OPC equilibrated water in the presence of irradiated-ADVA Cast 551

Table 82 U (VI) solubility in BFS:OPC equilibrated water in the presence of irradiated-ADVA Cast 551

Solution	% Irradiated ADVA Cast	Solubility (mol dm^{-3})	SEF
BFS:OPC	0	2.04E-07	1
	0.1	1.85E-03	9065
	0.5	6.51E-03	31855
	1	9.42E-03	46114

3.8.1.2 PFA:OPC equilibrated water

U (VI) concentration in PFA:OPC equilibrated water over time in the presence of irradiated-ADVA Cast 551 is shown in Figure 127. Steady state was reached by day 14 for 0%, 0.1% and 1% irradiated-ADVA Cast 551 samples while the 0.5% samples had not reached steady state by day 28. A possible reason for these samples not reaching steady state is human error where the samples were knocked during their equilibration time which disturbed precipitate.

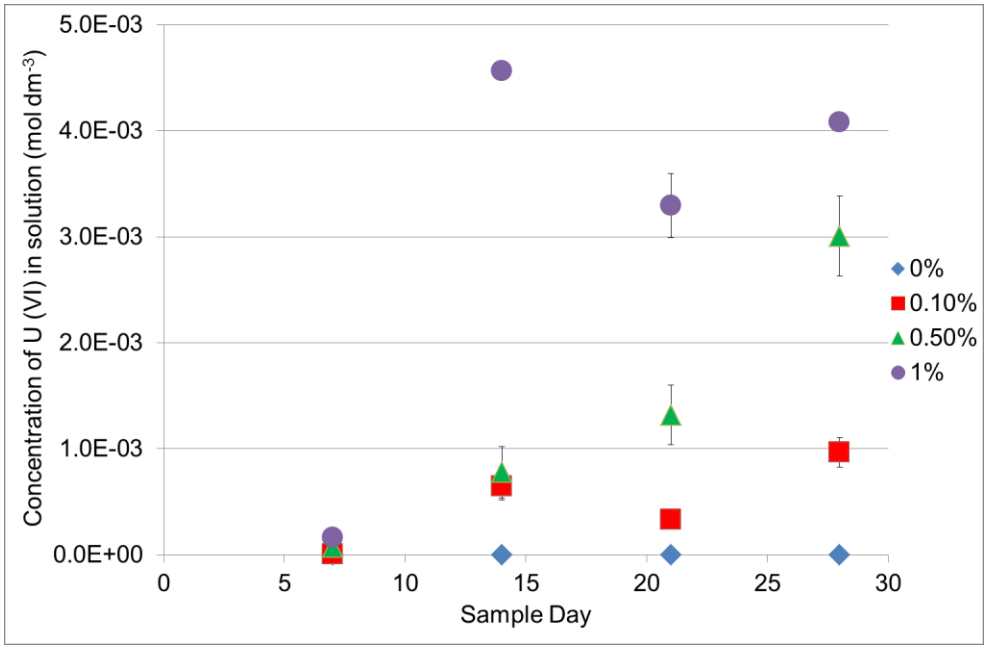

Figure 127 Kinetics of precipitation of U (VI) in the presence of irradiated-ADVA Cast 551 in PFA:OPC equilibrated water

The final concentration of U (VI) in solution is shown in Figure 128.

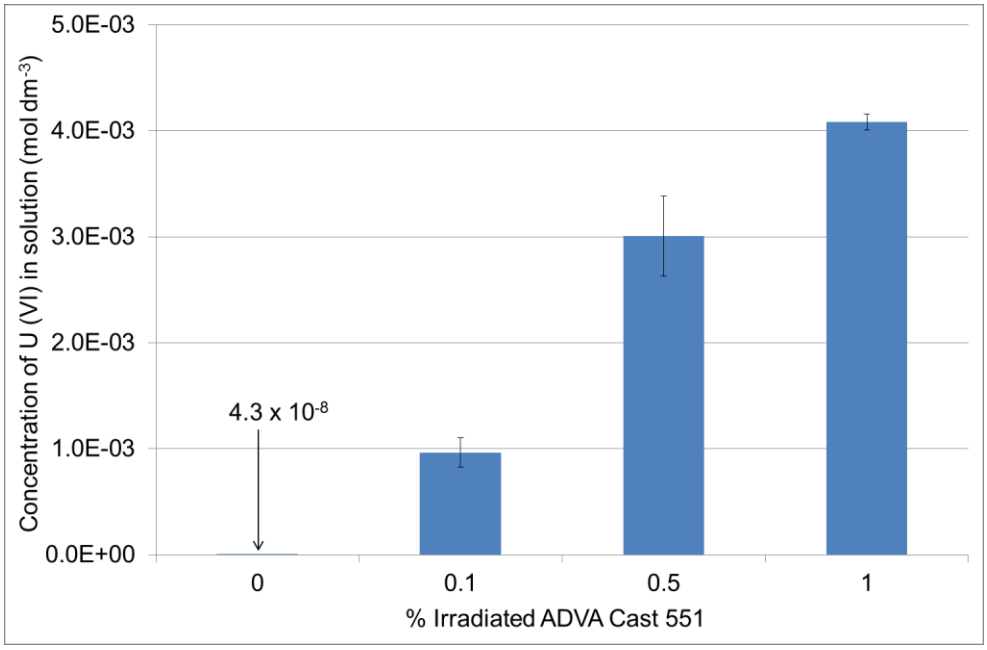

Figure 128 Final concentration of U (VI) in PFA:OPC equilibrated water in the presence of irradiated-ADVA Cast 551

Similarly to the BFS:OPC samples, there is a significant increase in concentration of U (VI) in solution with an increasing presence of irradiated ADVA Cast 551. This increase is much more evident in the irradiated samples than in the 'as received' samples. SEF values are shown in Table 83 and illustrate an increase in solubility in the region of 5 orders of magnitude. There is large difference between SEF values at 1% for the 'as received' and irradiated samples at 47 and 94447 respectively.

Table 83 U (VI) solubility in PFA:OPC equilibrated water in the presence of irradiated-ADVA Cast 551

Solution	% Irradiated ADVA Cast	Solubility (mol dm^{-3})	SEF
PFA:OPC	0	4.32E-08	1
	0.1	9.64E-04	22307
	0.5	3.01E-03	69568
	1	4.08E-03	94447

3.8.1.3 BFS equilibrated water

Kinetics of precipitation of U (VI) in BFS equilibrated water is shown in Figure 129 where steady state was reached by day 7 in all samples. There is an increase in solubility with increasing amounts of irradiated ADVA Cast 551

however this increase is not as marked as observed in other solutions such as PFA:OPC equilibrated water above.

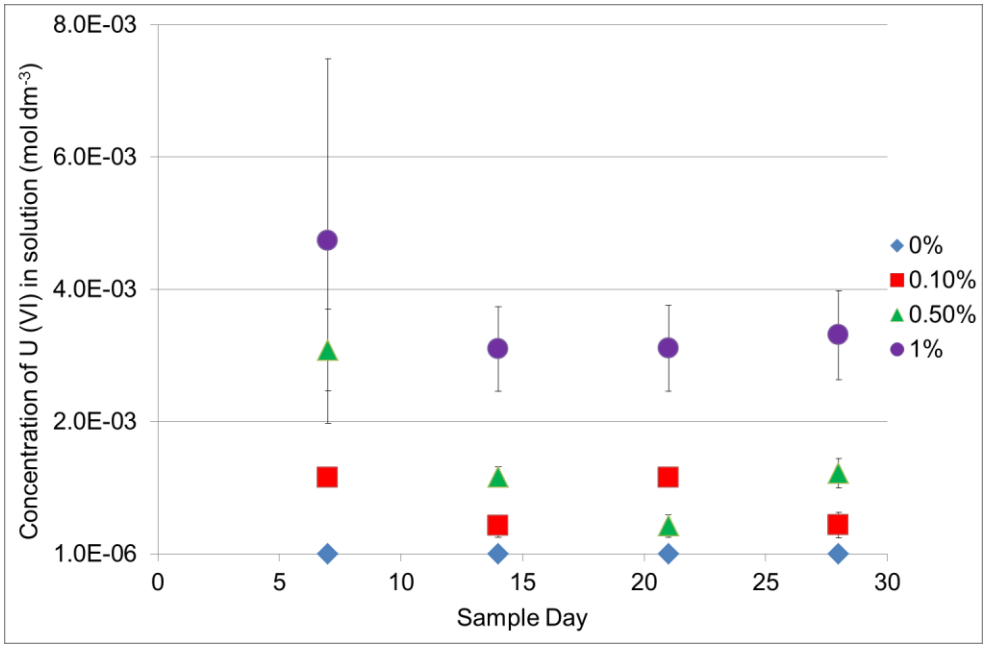

Figure 129 Kinetics of precipitation of U (VI) in the presence of irradiated-ADVA Cast 551 in BFS equilibrated water

The final concentration of U (VI) measured in solution is recorded in Figure 130 and the SEF values for each concentration of irradiated-ADVA Cast 551 are reported in Table 84. The increase in solubility is in the region of 3 orders of magnitude from the baseline and an SEF of 1631 is recorded for 1% irradiated ADVA Cast 551. The SEF values recorded here are higher than those recorded for ‘as received’ ADVA Cast 551 where the SEF at 1% in this case was 36.

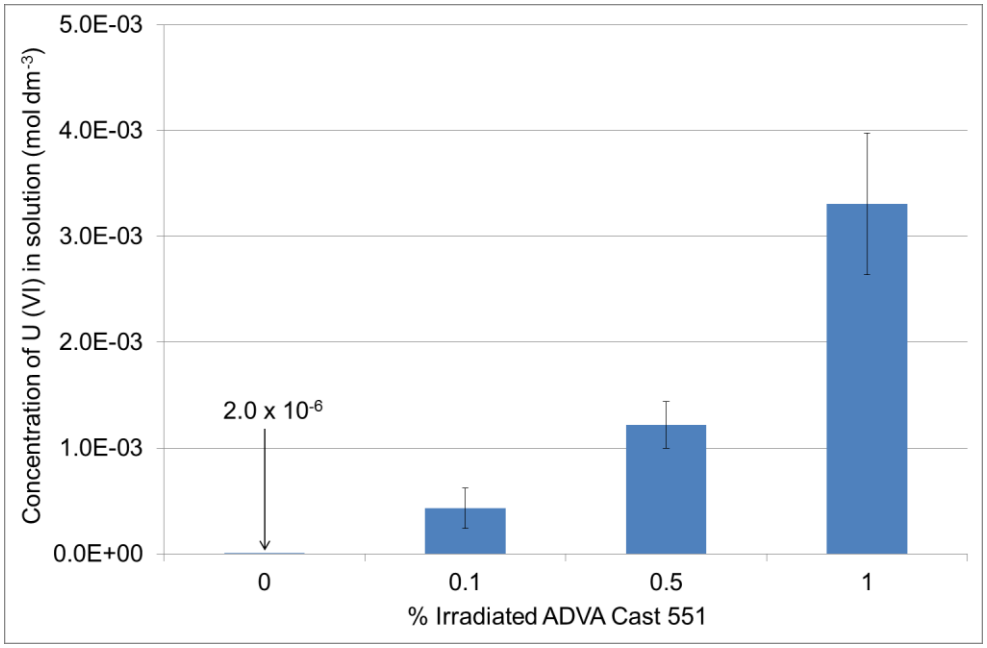

Figure 130 Final concentration of U (VI) in BFS equilibrated water in the presence of irradiated-ADVA Cast 551

Table 84 U (VI) solubility in BFS equilibrated water in the presence of irradiated-ADVA Cast 551

Solution	% Irradiated ADVA Cast	Solubility (mol dm^{-3})	SEF
BFS	0	2.03E-06	1
	0.1	4.34E-04	214
	0.5	1.22E-03	601
	1	3.31E-03	1631

3.8.1.4 PFA equilibrated water

The kinetics of precipitation for U (VI) in PFA equilibrated water is shown in Figure 131. All the samples had reached steady state by day 7. Enhancement in U (VI) solubility was observed with increasing concentration of irradiated ADVA Cast and the final concentration of U (VI) in solution is shown in Figure 132.

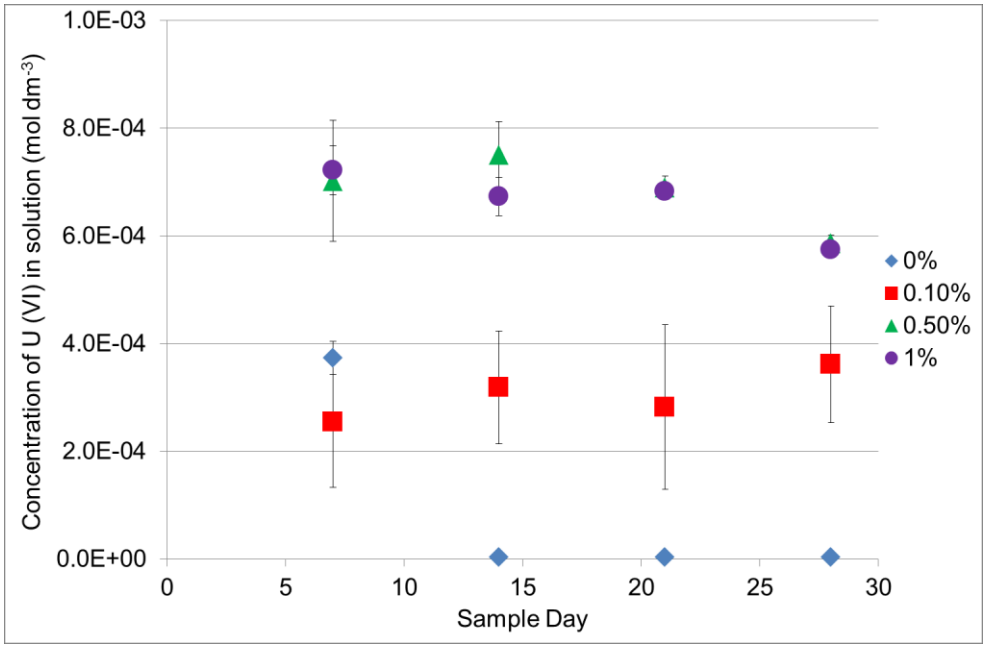

Figure 131 Kinetics of precipitation of U (VI) in the presence of irradiated-ADVA Cast 551 in PFA equilibrated water

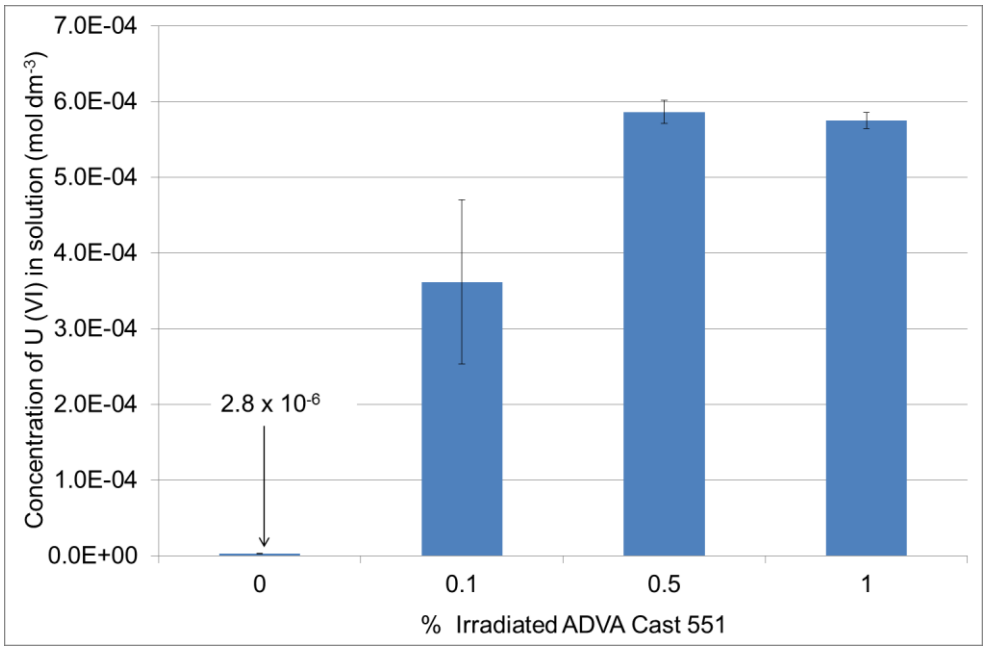

Figure 132 Final concentration of U (VI) in PFA equilibrated water in the presence of irradiated-ADVA Cast 551

The SEF values for the experiment are reported in Table 85. Values calculated here are low in comparison to other irradiated-ADVA Cast 551 experiments and are comparable to the SEF values recorded for 'as received' ADVA Cast 551 in the same solution. The solubility of U (VI) at 1% is recorded as 3.84 x 10^{-4} and

5.75 x 10^{-4} mol dm^{-3} for 'as received' and irradiated ADVA Cast 551 respectively.

Table 85 U (VI) solubility in PFA equilibrated water in the presence of irradiated-ADVA Cast 551

Solution	% Irradiated ADVA Cast	Solubility (mol dm^{-3})	SEF
PFA	0	2.83E-06	1
	0.1	3.62E-04	128
	0.5	5.86E-04	207
	1	5.75E-04	203

3.8.1.5 OPC equilibrated water

Concentration of U (VI) in OPC equilibrated water as a function of time is shown in Figure 133. The samples reached steady state by day 7 in all cases however an anomalous result was observed in the 1% samples on day 21. This anomaly was likely due to experimental error where the sample precipitate was disturbed during the sampling.

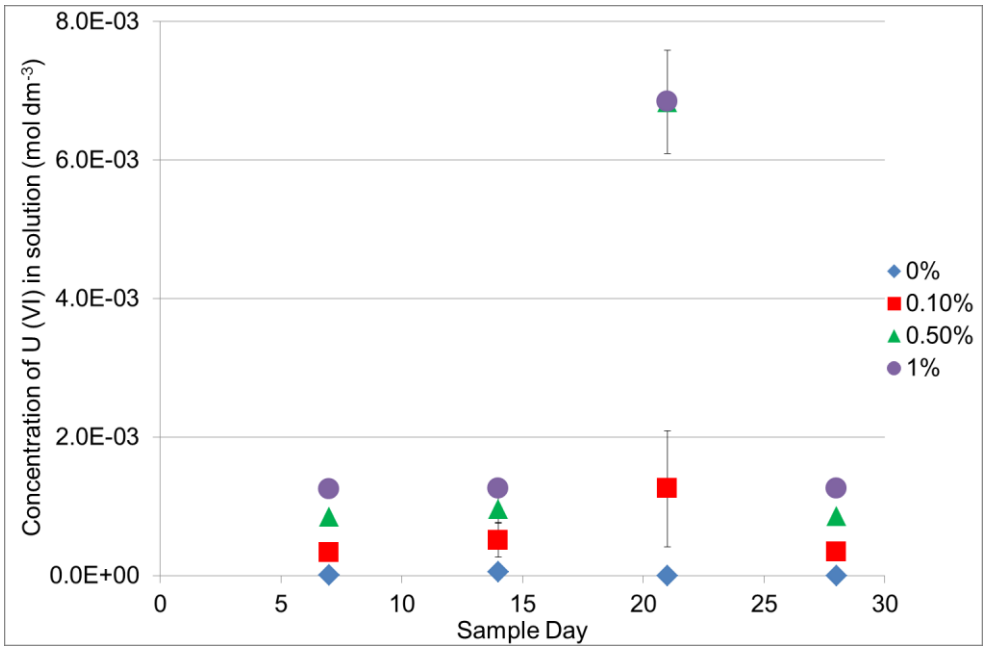

Figure 133 Kinetics of precipitation of U (VI) in the presence of irradiated-ADVA Cast 551 in OPC equilibrated water

The final concentration of U (VI) measured in solution is recorded in Figure 134. The same trend is followed as in all other aqueous solutions where the concentration of U (VI) in solution is increased with an increasing presence of

ADVA Cast 551. SEF values for U (VI) in OPC equilibrated water are reported in Table 86. The enhancement in solubility between 0% and 1% irradiated-ADVA Cast 551 is within the region of several orders of magnitude and in the presence of 1% irradiated- ADVA Cast 551 the SEF is calculated as 1935. This value is significantly higher than the SEF value calculated for 1% 'as received' ADVA Cast 551 in the same solution; 186.

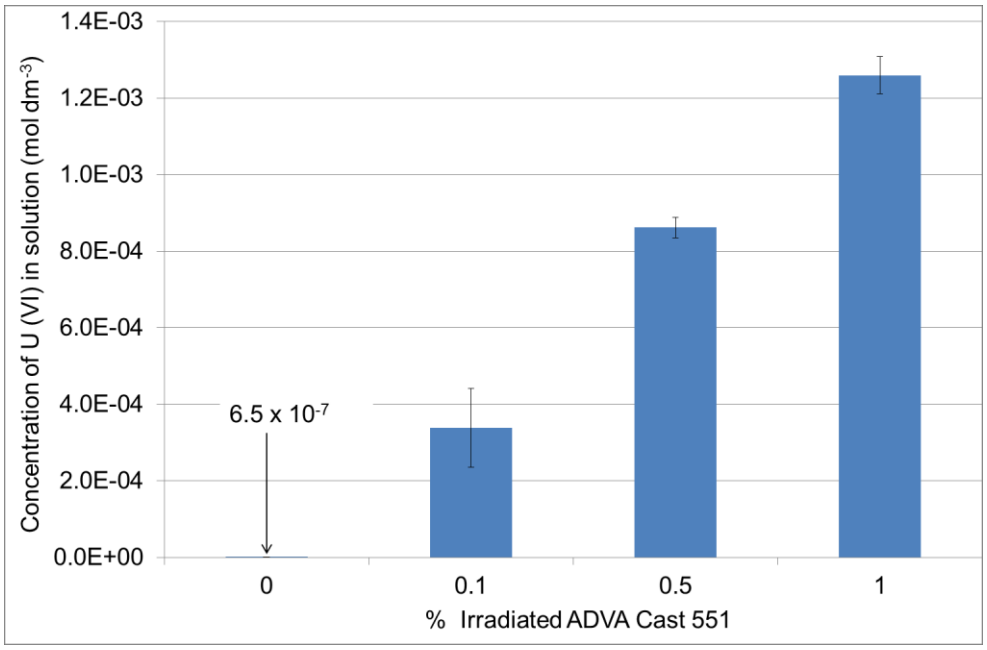

Figure 134 Final concentration of U (VI) in OPC equilibrated water in the presence of irradiated-ADVA Cast 551

Table 86 U (VI) solubility in OPC equilibrated water in the presence of irradiated-ADVA Cast 551

Solution	% Irradiated ADVA Cast	Solubility (mol dm^{-3})	SEF
OPC	0	6.51E-07	1
	0.1	3.38E-04	520
	0.5	8.62E-04	1324
	1	1.26E-03	1935

Overall, it may be said that the presence of irradiated-ADVA Cast 551 has a greater enhancement effect on U (VI) solubility than the 'as received' superplasticiser.

3.8.2 *Thorium (IV) Solubility*

Experimental methods for the determination of Th (IV) solubility are described in section 2.5.1. The baseline solubility of Th (IV) in each aqueous solutions investigated was below the limit of detection of the ICP-MS. To calculate SEF values for Th (IV) a representative baseline solubility value of $1x10^{-9}$ mol dm^{-3} was used as determined experimentally by Wierczinski et al. (1998), Neck et al. (2003) and Altmaier et al. (2008) (32,33,67).

3.8.2.1 95% Saturated $Ca(OH)_2$

Concentration of Th (IV) in 95% saturated $Ca(OH)_2$ in the presence of irradiated ADVA Cast 551 as a function of time is shown in Figure 135. Steady state was reached by day 14 in all samples.

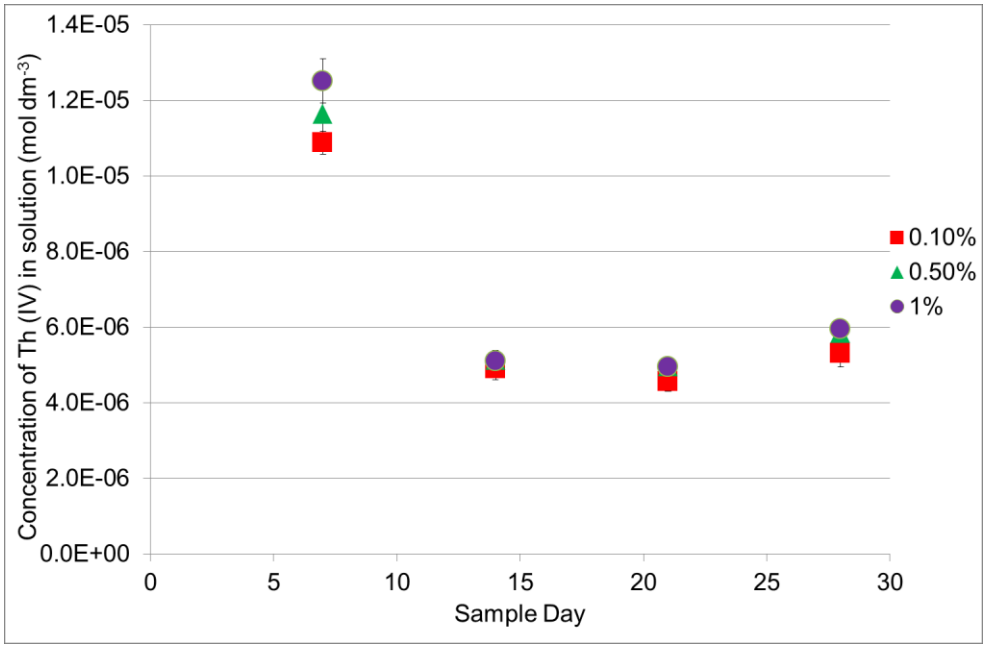

Figure 135 Kinetics of precipitation of Th (IV) in the presence of irradiated-ADVA Cast 551 in 95% saturated $Ca(OH)_2$

The final concentration of Th (IV) in solution is given in Figure 136 while SEF values are reported in Table 87. The solubility of Th (IV) measured in solution is similar at each concentration of ADVA Cast 551. This is also reflected in the SEF values. The increase in solubility with the presence of irradiated ADVA Cast 551 is much greater than that recorded with the 'as received' superplasticiser. SEF values in the presence of 1% irradiated-ADVA Cast 551 were recorded as 3 and 5953 for 'as received' and irradiated ADVA Cast 551

respectively. This is a very significant result showing much more solubilisation of Th (IV) by the irradiated superplasticiser.

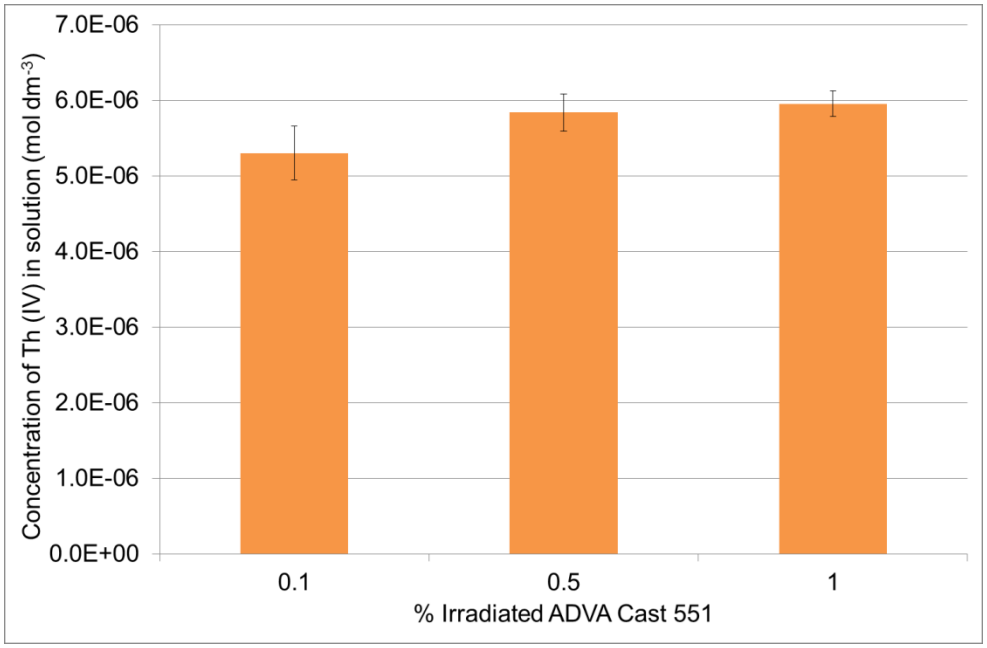

Figure 136 Final Concentration of Th (IV) in 95% saturated $Ca(OH)_2$ in the presence of irradiated-ADVA Cast 551

Table 87 Th (IV) solubility in 95% saturated $Ca(OH)_2$ in the presence of irradiated-ADVA Cast 551

Solution	% Irradiated ADVA Cast	Solubility (mol dm^{-3})	SEF
$Ca(OH)_2$	0	1.00E-09	1
	0.1	5.30E-06	5301
	0.5	5.84E-06	5839
	1	5.95E-06	5953

3.8.2.2 0.1 mol dm^{-3} NaOH

Figure 137 shows the kinetics of precipitation of Th (IV) in 0.1 mol dm^{-3} NaOH in the presence of irradiated-ADVA Cast 551. In all samples, steady state was achieved by day 14. In a similar trend to that observed in $Ca(OH)_2$ there is little variation in solubility enhancement between the different concentrations of irradiated ADVA Cast 551. The final concentration of Th (IV) measured in solution is recorded in Figure 138 demonstrating that within errors the concentration of Th (IV) in solution is the same irrespective of irradiated ADVA Cast 551 concentration.

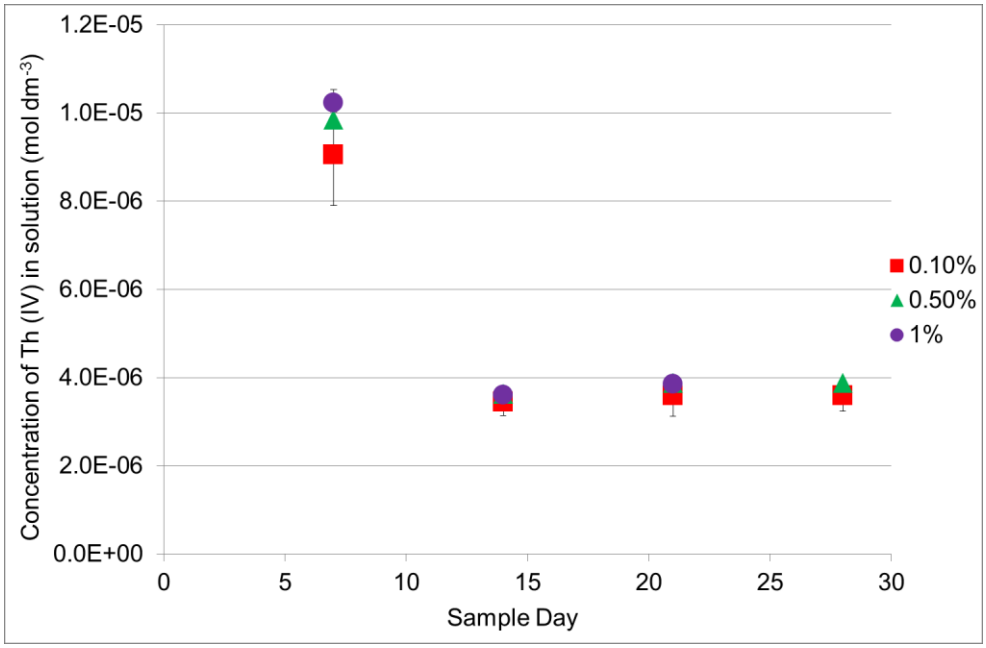

Figure 137 Kinetics of precipitation of Th (IV) in the presence of irradiated-ADVA Cast 551 in 0.1 mol dm^{-3} NaOH

SEF values were calculated and are reported in Table 88. The SEF values are very similar for each concentration of irradiated-ADVA Cast 551; solubility enhancement is within the range of 3 orders of magnitude. Since comparatively very little solubility enhancement was observed for Th (IV) in the presence of 'as received' ADVA Cast 551, this is a significant result.

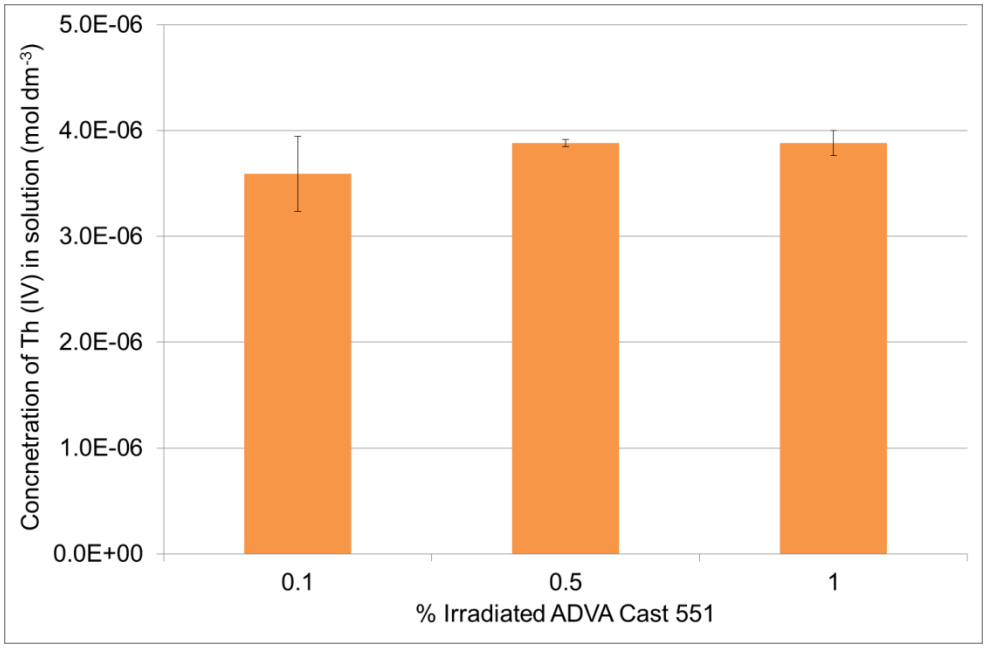

Figure 138 Final Concentration of Th (IV) in 0.1 mol dm^{-3} NaOH in the presence of irradiated-ADVA Cast 551

Table 88 Th (IV) solubility in 0.1 mol dm^{-3} NaOH in the presence of irradiated-ADVA Cast 551

Solution	% Irradiated ADVA Cast	Solubility (mol dm^{-3})	SEF
NaOH	0	1.00E-09	1
	0.1	3.59E-06	3591
	0.5	3.88E-06	3881
	1	3.88E-06	3884

3.8.2.3 BFS:OPC equilibrated water

The kinetics of precipitation of Th (IV) in BFS:OPC equilibrated water is shown in Figure 139. Steady state was reached by day 14 in all samples. A slight increase in Th (IV) solubility enhancement with increasing amounts of ADVA Cast 551is observed. This is shown in the final concentration of Th (IV) measured in solution reported in Figure 140. The solubility values are all within the same order of magnitude and have similar SEF values as reported in Table 89. Solubility enhancement in all cases is in the region of 3 orders of magnitude. In a similar trend to that observed in NaOH and $Ca(OH)_2$, there is a much more significant Th (IV) solubility enhancement in the presence of the irradiated superplasticiser than with 'as received' superplasticiser.

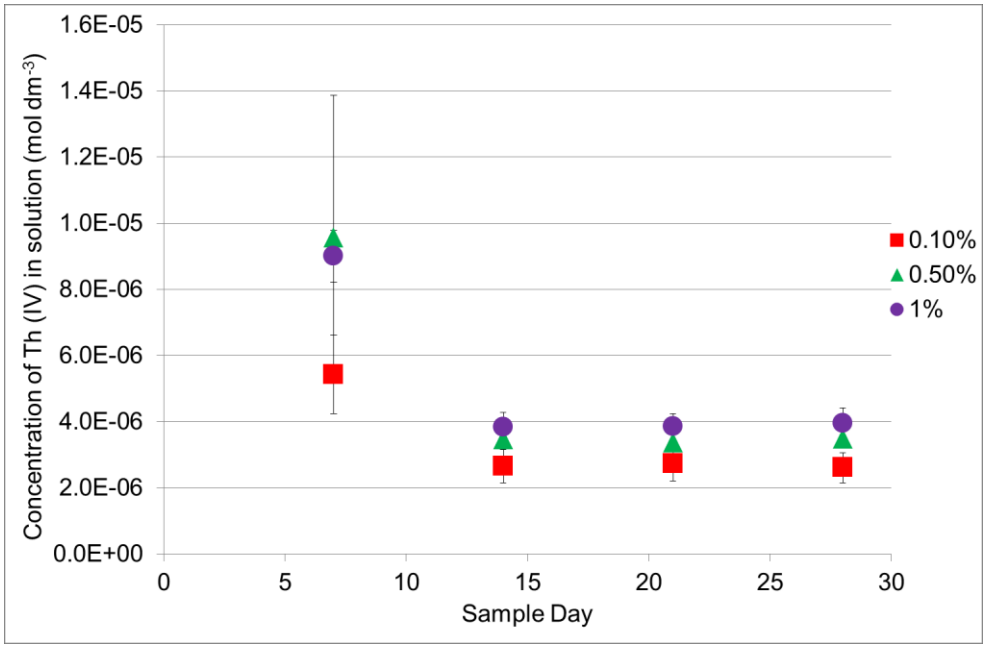

Figure 139 Kinetics of precipitation of Th (IV) in the presence of irradiated-ADVA Cast 551 in BFS:OPC equilibrated water

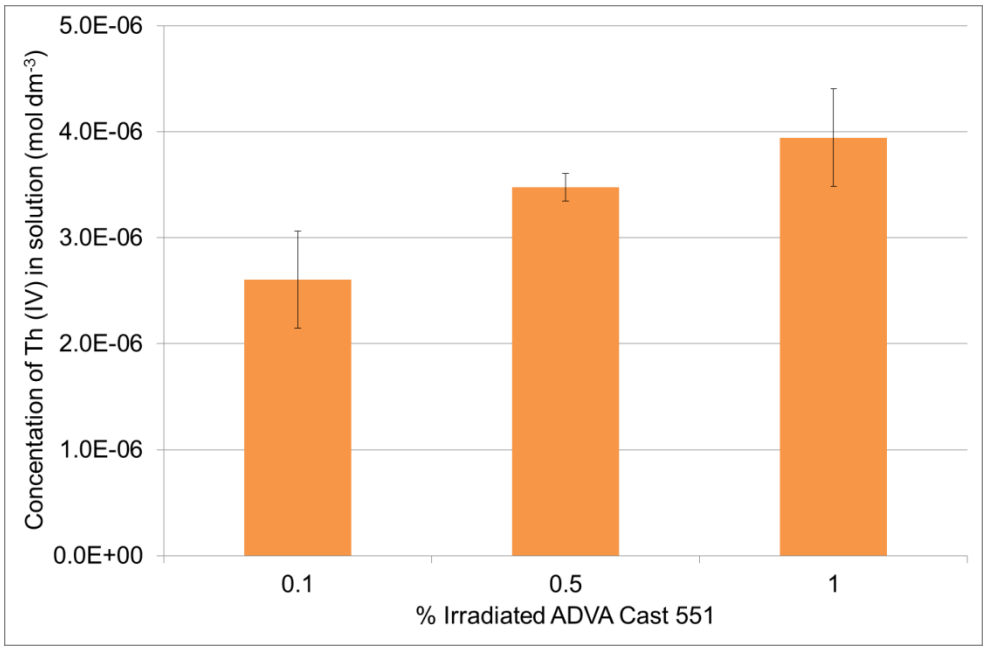

Figure 140 Final concentration of Th (IV) in BFS:OPC equilibrated water in the presence of irradiated-ADVA Cast 551

Table 89 Th (IV) solubility in BFS:OPC equilibrated water in the presence of irradiated-ADVA Cast 551

Solution	% Irradiated ADVA Cast	Solubility (mol dm^{-3})	SEF
BFS:OPC	0	1.00E-09	1
	0.1	2.61E-06	2605
	0.5	3.48E-06	3477
	1	3.95E-06	3946

3.8.2.4 PFA:OPC equilibrated water

Figure 141 shows the concentration of Th (IV) in PFA:OPC equilibrated water over time. All samples reached steady state by day 14. Similar enhancement in Th (IV) solubility is noted at all concentrations of ADVA Cast 551. Figure 142 demonstrates that within errors the solubility of Th (IV) in the presence of 0.5% and 1% irradiated ADVA Cast 551 is equivalent. Th (IV) solubility in the presence of 0.1% irradiated ADVA Cast 551 is slightly lower, nevertheless a substantial increase in Th (IV) measured in solution is observed.

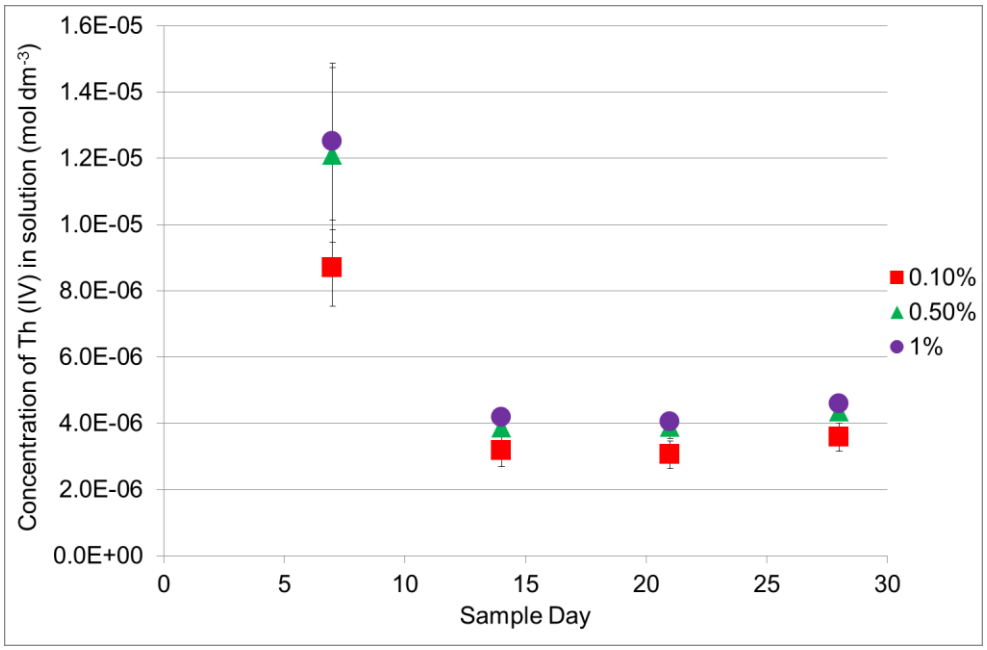

Figure 141 Kinetics of precipitation of Th (IV) in the presence of irradiated-ADVA Cast 551 in PFA:OPC equilibrated water

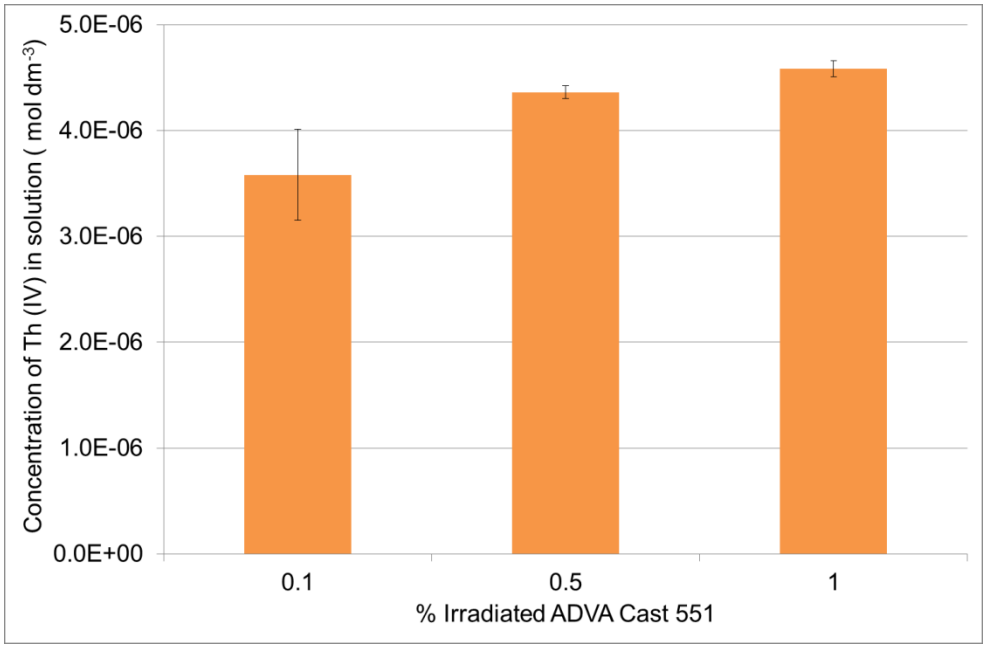

Figure 142 Final concentration of Th (IV) in PFA:OPC equilibrated water in the presence of irradiated-ADVA Cast 551

The SEF values for Th (IV) in PFA:OPC equilibrated water are recorded in Table 90. The solubility enhancement observed is in the region of 3 orders of magnitude and SEF values are significantly higher than those calculated for 'as received' ADVA Cast 551.

Table 90 Th (IV) solubility in PFA:OPC equilibrated water in the presence of irradiated-ADVA Cast 551

Solution	% Irradiated ADVA Cast	Solubility (mol dm^{-3})	SEF
PFA:OPC	0	1.00E-09	1
	0.1	3.58E-06	3582
	0.5	4.36E-06	4363
	1	4.58E-06	4583

3.8.2.5 BFS equilibrated water

The kinetics of precipitation of Th (IV) in BFS equilibrated water is shown in Figure 143 where steady state is achieved by day 14 in all samples. The final concentration of Th (IV) measured in solution is shown in Figure 144 and demonstrates that Th (IV) concentration was similar irrespective of the concentration of irradiated ADVA Cast 551. The solubility enhancement observed was in the region of 3 orders of magnitude from the baseline solubility.

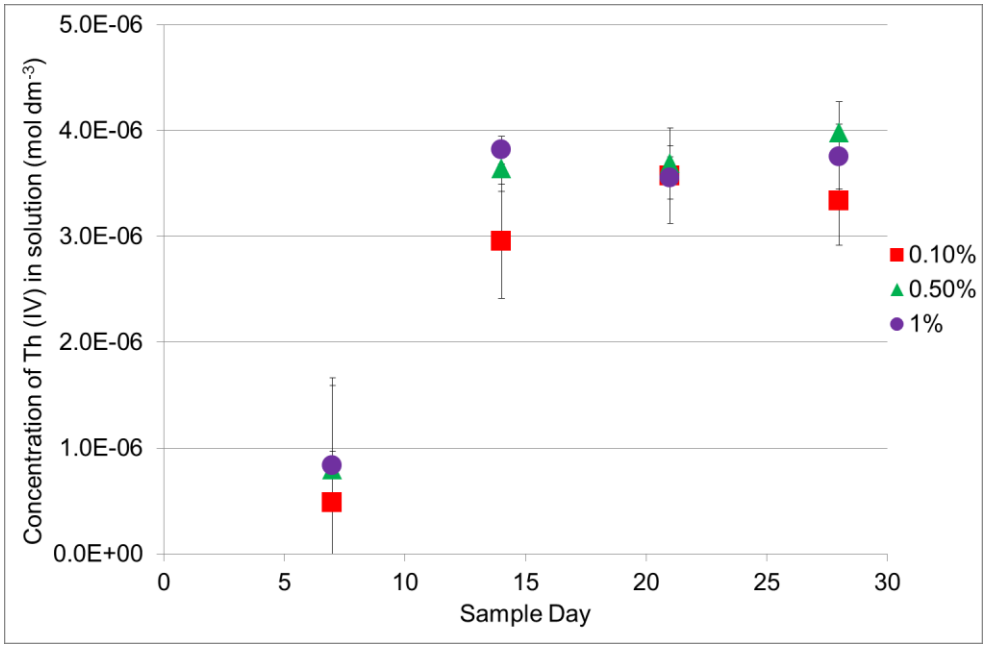

Figure 143 Kinetics of precipitation of Th (IV) in the presence of irradiated-ADVA Cast 551 in BFS equilibrated water

The calculated SEF values for Th (IV) are shown in Table 91 and emphasise that the solubility of Th (IV) at each concentration of ADVA Cast 551 is, within errors, equivalent and again, much higher than the solubility recorded in the presence of 'as received' ADVA Cast 551.

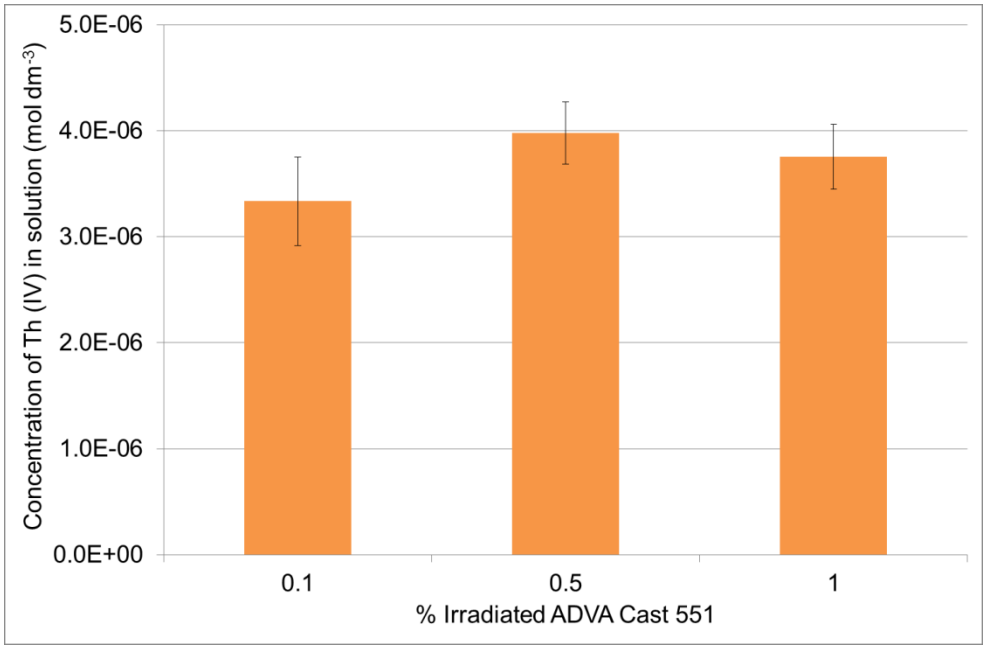

Figure 144 Final concentration of Th (IV) in BFS equilibrated water in the presence of irradiated-ADVA Cast 551

Table 91 Th (IV) solubility in BFS equilibrated water in the presence of irradiated-ADVA Cast 551

Solution	% Irradiated ADVA Cast	Solubility (mol dm^{-3})	SEF
PFA:OPC	0	1.00E-09	1
	0.1	3.33E-06	3335
	0.5	3.98E-06	3980
	1	3.75E-06	3755

3.8.2.6 PFA equilibrated water

Figure 145 shows the concentration of Th (IV) in PFA equilibrated water as a function of time and demonstrates that steady state was reached in all samples by day 14. As was observed in all other solutions investigated, the concentration of Th (IV) measured in solution is similar irrespective of the concentration of ADVA Cast 551. This is demonstrated in Figure 146 where within errors, Th (IV) remains constant with increasing amount of irradiated ADVA Cast 551. The solubility enhancement is in the region of 3 orders of magnitude with SEF values of around 3000 at each concentration of irradiated ADVA Cast 551 these values are recorded in Table 92. As mentioned previously, these SEF values are significantly higher than those recorded for Th (IV) in the same solutions with 'as received' ADVA Cast 551.

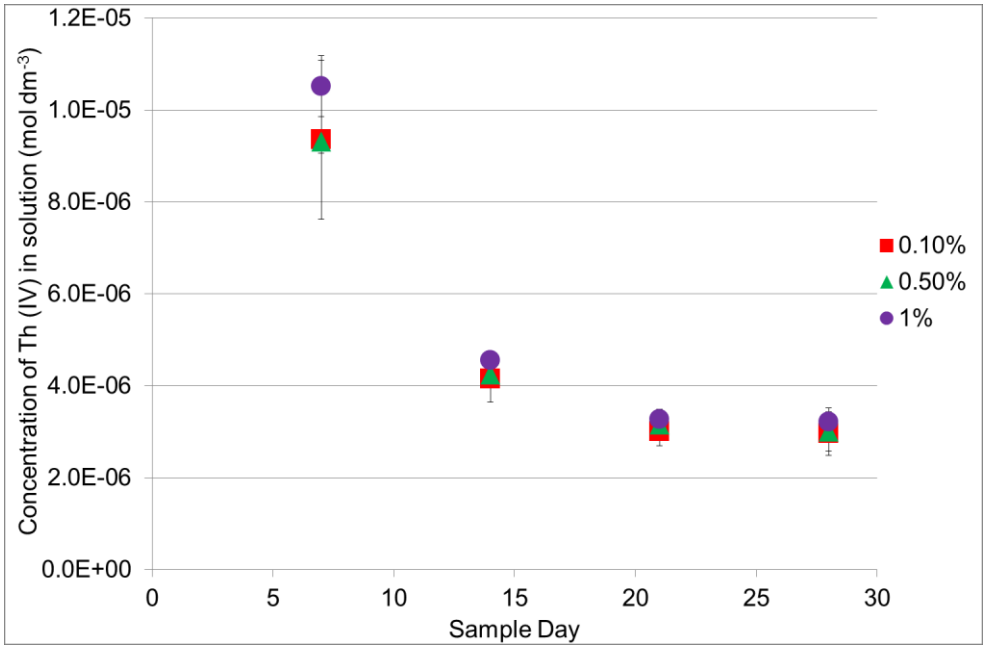

Figure 145 Kinetics of precipitation of Th (IV) in the presence of irradiated-ADVA Cast 551 in PFA equilibrated water

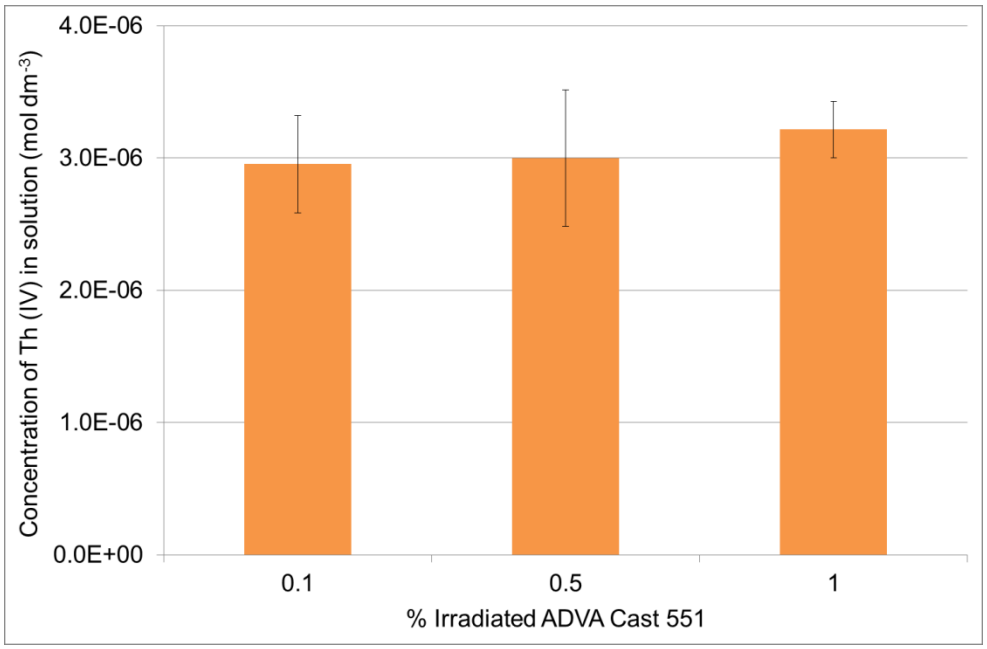

Figure 146 Final concentration of Th (IV) in PFA equilibrated water in the presence of irradiated-ADVA Cast 551

Table 92 Th (IV) solubility in PFA equilibrated water in the presence of irradiated-ADVA Cast 551

Solution	% Irradiated ADVA Cast	Solubility (mol dm^{-3})	SEF
PFA:OPC	0	1.00E-09	1
	0.1	2.95E-06	2954
	0.5	3.00E-06	2999
	1	3.21E-06	3215

3.8.2.7 OPC equilibrated water

Th (IV) kinetics of precipitation in OPC equilibrated water is shown in Figure 147 where steady state is achieved by day 14 in all samples. Again, as demonstrated in Figure 148, the concentration of Th (IV) measured in solution, is enhanced equivalently, irrespective of the amount of irradiated ADVA Cast 551 in solution.

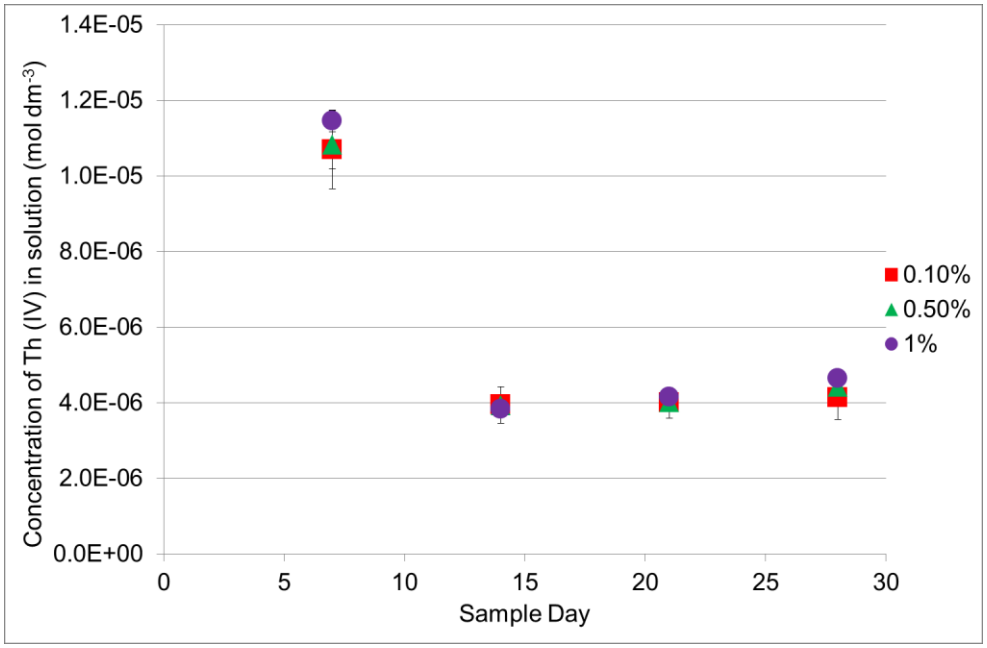

Figure 147 Kinetics of precipitation of Th (IV) in the presence of irradiated-ADVA Cast 551 in OPC equilibrated water

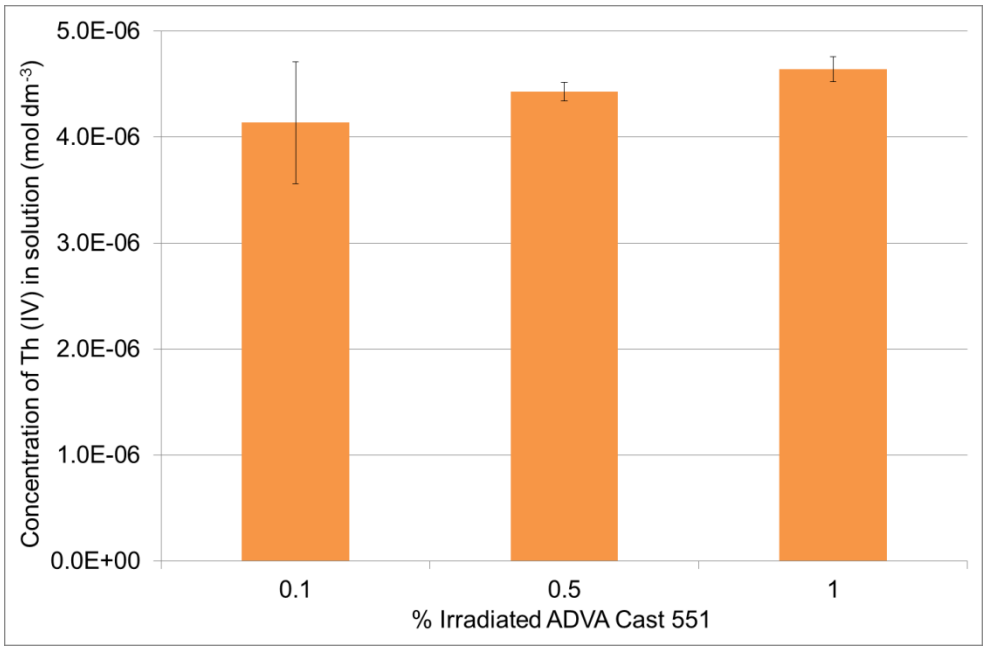

Figure 148 Final concentration of Th (IV) in OPC equilibrated water in the presence of irradiated-ADVA Cast 551

SEF values calculated are recorded in Table 93 and show Th (IV) solubility enhancement over 3 orders of magnitude. And SEF values of around 4000 were calculated in the presence of each concentration of irradiated-ADVA Cast 551.

Table 93 Th (IV) solubility in OPC equilibrated water in the presence of irradiated-ADVA Cast 551

Solution	% Irradiated ADVA Cast	Solubility (mol dm^{-3})	SEF
PFA:OPC	0	1.00E-09	1
	0.1	4.14E-06	4137
	0.5	4.43E-06	4429
	1	4.64E-06	4640

3.8.3 *Europium (III) Solubility*

3.8.3.1 95% Saturated $Ca(OH)_2$

The concentration of Eu (III) in 95% saturated $Ca(OH)_2$ as a function of time is shown in Figure 149 where steady state is achieved by day 14 in all samples. In comparison to Th (IV), there is a much more marked increase in Eu (III) solubility within increasing concentration of irradiated ADVA Cast 551. The final concentration of Eu (III) measured in solution is shown in Figure 150 while calculated SEF values are reported in Table 94. Comparing these values to those obtained for 'as received' ADVA Cast 551, the concentration of Eu (III) measured in solution at the end of the experiment is very similar in both experiments. The observed solubility enhancement is over several orders of magnitude in both cases.

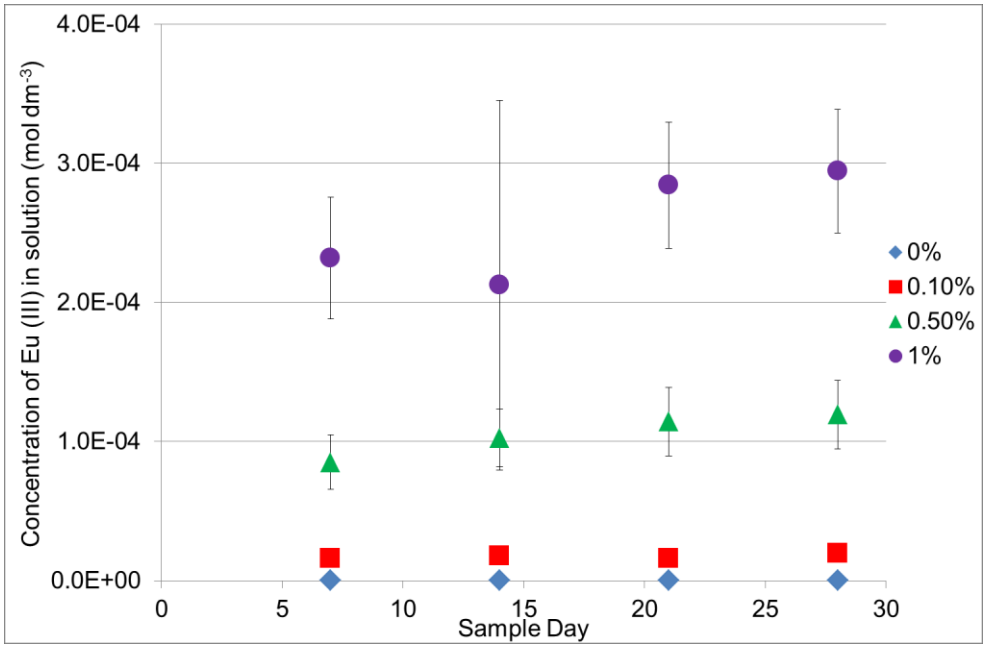

Figure 149 Kinetics of precipitation of Eu (III) in the presence of irradiated-ADVA Cast 551 in 95% saturated $Ca(OH)_2$

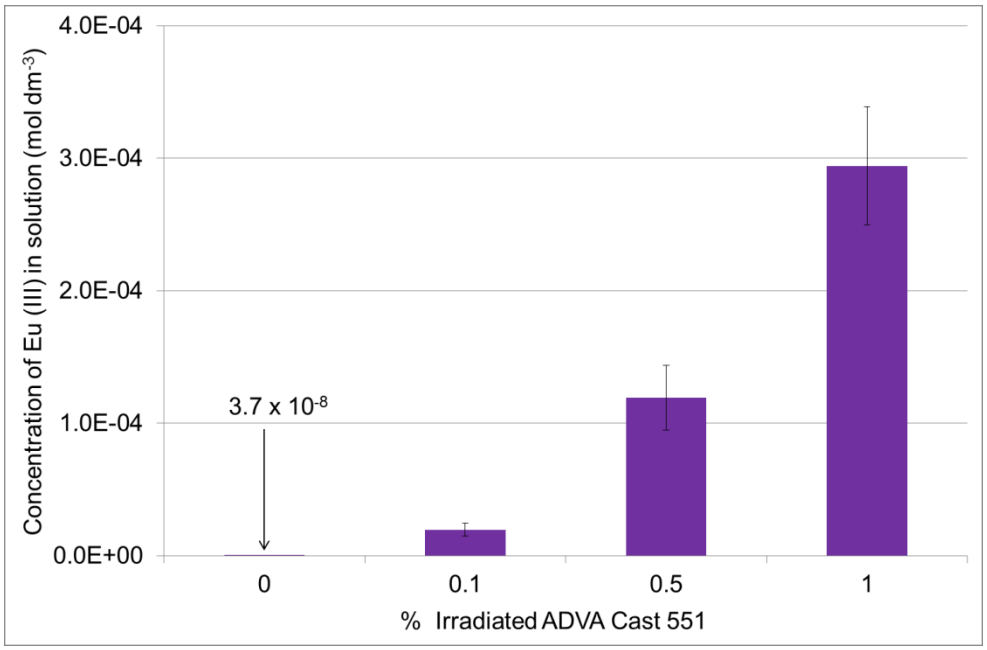

Figure 150 Final concentration of Eu (III) in 95% saturated $Ca(OH)_2$ in the presence of irradiated-ADVA Cast 551

Table 94 Eu (III) solubility in 95% saturated $Ca(OH)_2$ in the presence of irradiated-ADVA Cast 551

Solution	% Irradiated ADVA Cast	Solubility (mol dm^{-3})	SEF
$Ca(OH)_2$	0	3.73E-08	1
	0.1	1.97E-05	528
	0.5	1.19E-04	3198
	1	2.94E-04	7883

3.8.3.2 0.1 mol dm^{-3} NaOH

The kinetics of precipitation for Eu (III) in 0.1 mol dm^{-3} NaOH is shown in Figure 151 where steady state is achieved at day 7 by all samples. An increase in Eu (III) concentration in solution with increasing concentrations of irradiated ADVA Cast 551 is observed however this increase is not so marked as was observed in $Ca(OH)_2$. Figure 152 shows the final concentration of Eu (III) measured in solution while Table 95 gives SEF values for Eu (III) in the presence of each concentration of irradiated-ADVA Cast 551. The Eu (III) solubility enhancement in this case is within the range of 2 orders of magnitude and is in fact a lower enhancement than was observed in the same solution with the presence of 'as received' ADVA Cast 551.

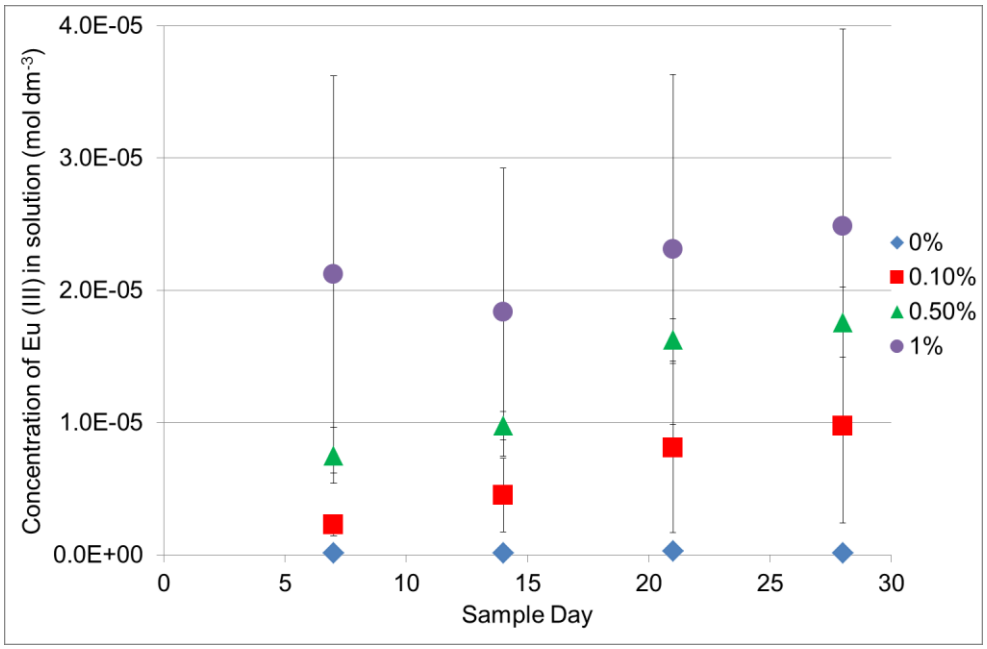

Figure 151 Kinetics of precipitation of Eu (III) in the presence of irradiated-ADVA Cast 551 in 0.1 mol dm^{-3} NaOH

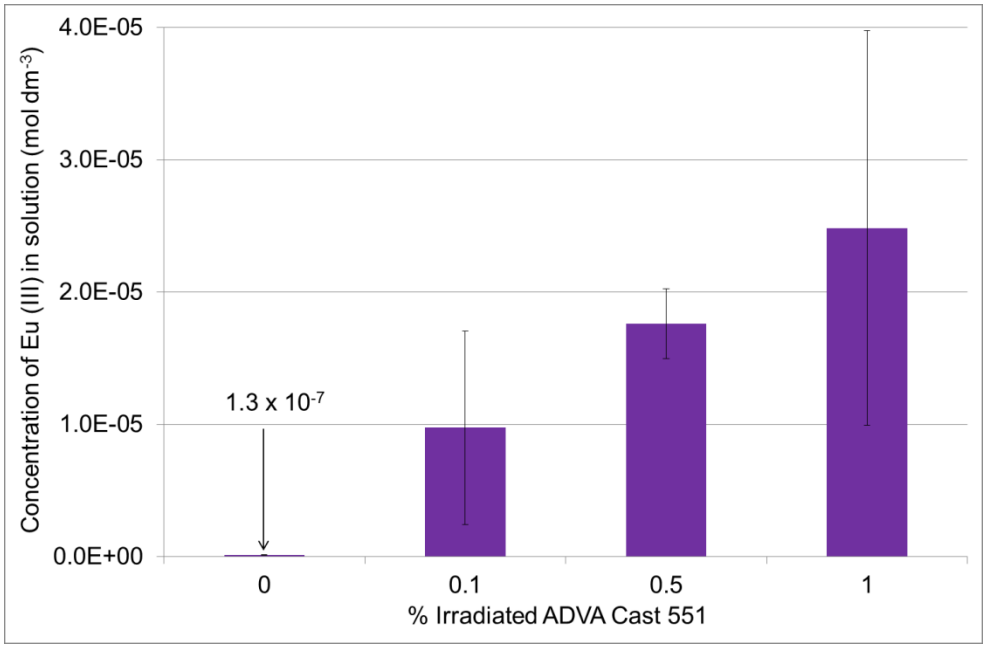

Figure 152 Final concentration of Eu (III) in 0.1 mol dm^{-3} NaOH in the presence of irradiated-AVDA Cast 551

Table 95 Eu (III) solubility in 0.1 mol dm^{-3} NaOH in the presence of irradiated-ADVA Cast 551

Solution	% Irradiated ADVA Cast	Solubility (mol dm^{-3})	SEF
NaOH	0	1.25E-07	1
	0.1	9.74E-06	78
	0.5	1.76E-05	141
	1	2.48E-05	199

3.8.3.3 BFS:OPC equilibrated water

Figure 153 shows the concentration of Eu (III) in BFS:OPC equilibrated water as a function of time where steady state is reached by day 7 of the experiment. The final concentration of Eu (III) in solution is shown in Figure 154 and demonstrates an increase in Eu (III) concentration in solution with increasing concentration of irradiated ADVA Cast 551.

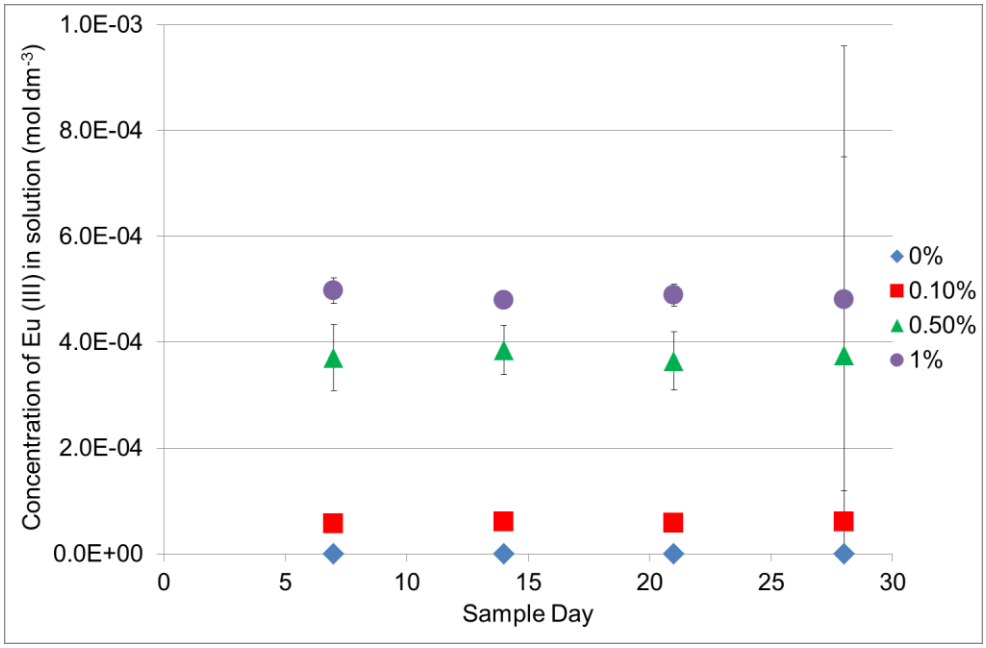

Figure 153 Kinetics of precipitation of Eu (III) in the presence of irradiated-ADVA Cast 551 in BFS:OPC equilibrated water

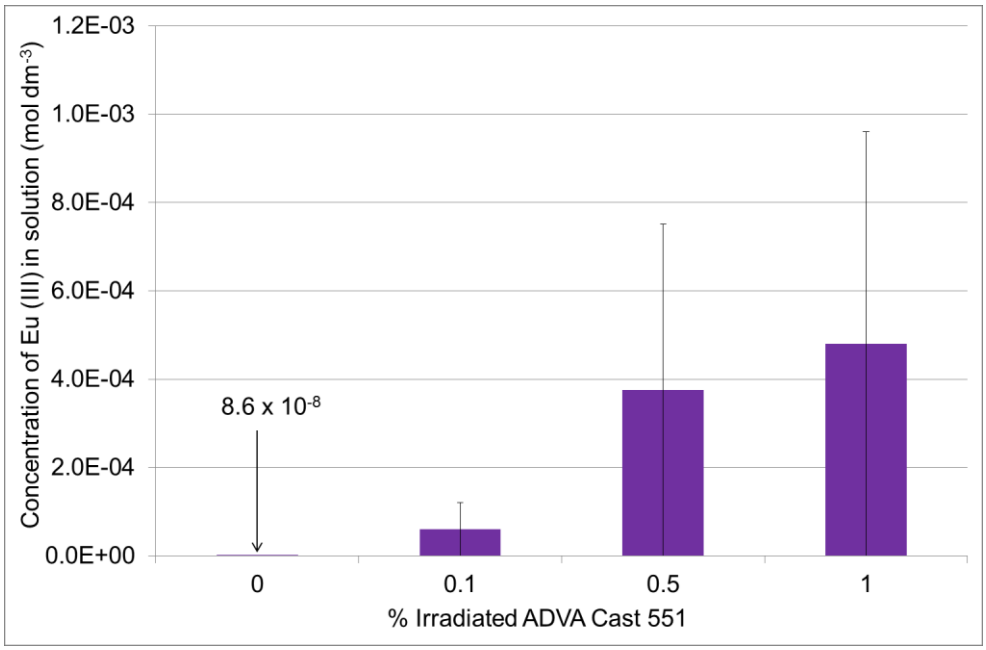

Figure 154 Final concentration of Eu (III) in BFS:OPC equilibrated water in the presence of irradiated-ADVA Cast 55

SEF values are reported in Table 96 and show an increase in Eu (III) solubility over several orders of magnitude. In the presence of 1% irradiated ADVA Cast 551, the concentration of Eu (III) measured in solution was 4.8 x 10^{-4}mol dm^{-3}. This is very similar to the Eu (III) concentration measured in BFS:OPC solution in the presence of 1% 'as received' ADVA Cast 551 at 4.6 x 10^{-4} mol dm^{-3}. In both cases, this value is close to the inventory of Eu (III) added to the sample

indicating that almost all of the metal is solubilised in the presence of the superplasticiser (both 'as received' and irradiated).

Table 96 Eu (III) solubility in BFS:OPC equilibrated water in the presence of irradiated-AVDA Cast 551

Solution	% Irradiated ADVA Cast	Solubility (mol dm^{-3})	SEF
BFS:OPC	0	8.61E-08	1
	0.1	6.00E-05	697
	0.5	3.75E-04	4360
	1	4.80E-04	5577

3.8.3.4 PFA:OPC equilibrated water

Figure 155 shows the kinetics of precipitation for Eu (III) in PFA:OPC equilibrated water. An increase in Eu (III) concentration in solution is observed with increasing concentration of irradiated ADVA Cast 551. Steady state was achieved by day 7 by all samples.

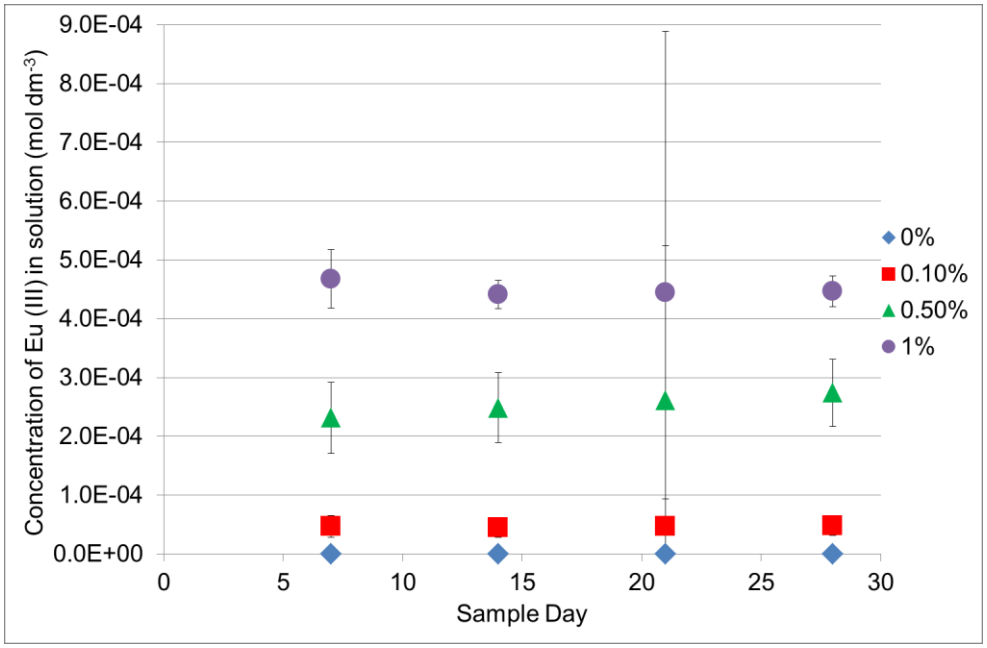

Figure 155 Kinetics of precpitation of Eu (III) in the presence of irradiated-ADVA Cast 551 in PFA:OPC equilibrated water

The final concentration of Eu (III) measured in solution is given in Figure 156 while SEF values are recorded in Table 97. The solubility enhancement observed is within the range of several orders of magnitude. In the presence of 1% irradiated ADVA Cast 551, the concentration of Eu (III) is close to the

inventory added which means nearly all added metal has been solubilised in the presence of irradiated ADVA Cast 551.

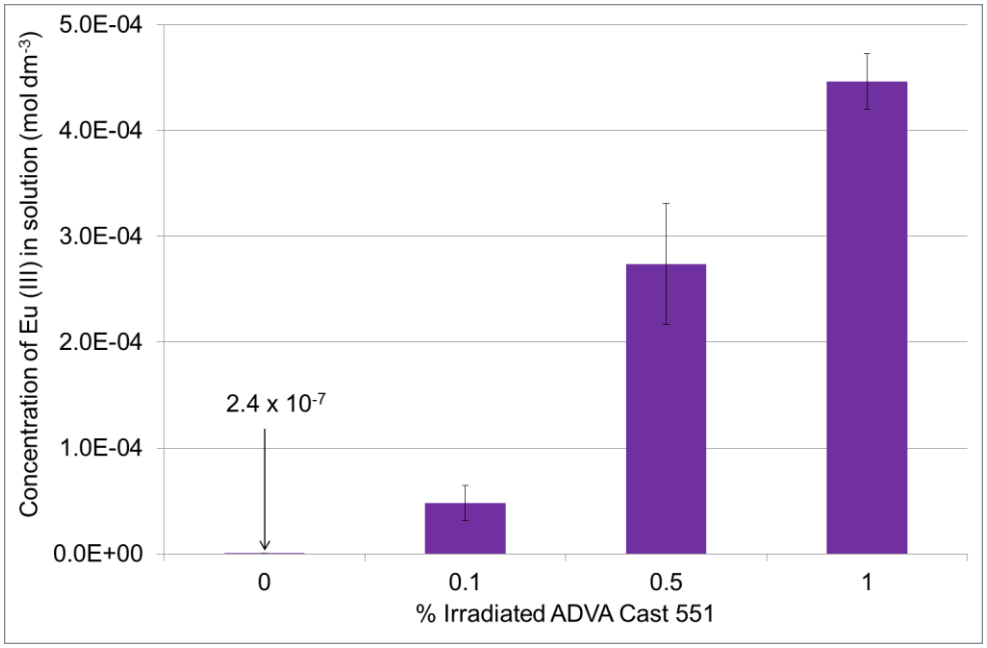

Figure 156 Final concnetration of Eu (III) in PFA:OPC equilibrated water in the presence of irradiated-ADVA Cast 551

Table 97 Eu (III) solubility in PFA:OPC equilibrated water in the presence of irradiated-ADVA Cast 551

Solution	% Irradiated ADVA Cast	Solubility (mol dm^{-3})	SEF
PFA:OPC	0	2.42E-07	1
	0.1	4.80E-05	198
	0.5	2.74E-04	1130
	1	4.46E-04	1840

3.8.3.5 BFS equilibrated water

Kinetics of precipitation of Eu (III) in BFS equilibrated water is shown in Figure 157 where steady state is observed to be achieved by day 7. Figure 158 records the final concentration of Eu (III) measured in solution and demonstrates a significant increase in solubility in samples containing 0.5% and 1% irradiated ADVA Cast 551. In both cases the concentration of Eu (III) measured in solution is close to the inventory limit. SEF values reported in Table 98 illustrate an enhancement in Eu (III) solubility over several orders of magnitude at all concentrations of irradiated ADVA Cast 551 while in particular, SEF values of 4000+ are recorded for the 0.5% and 1% samples.

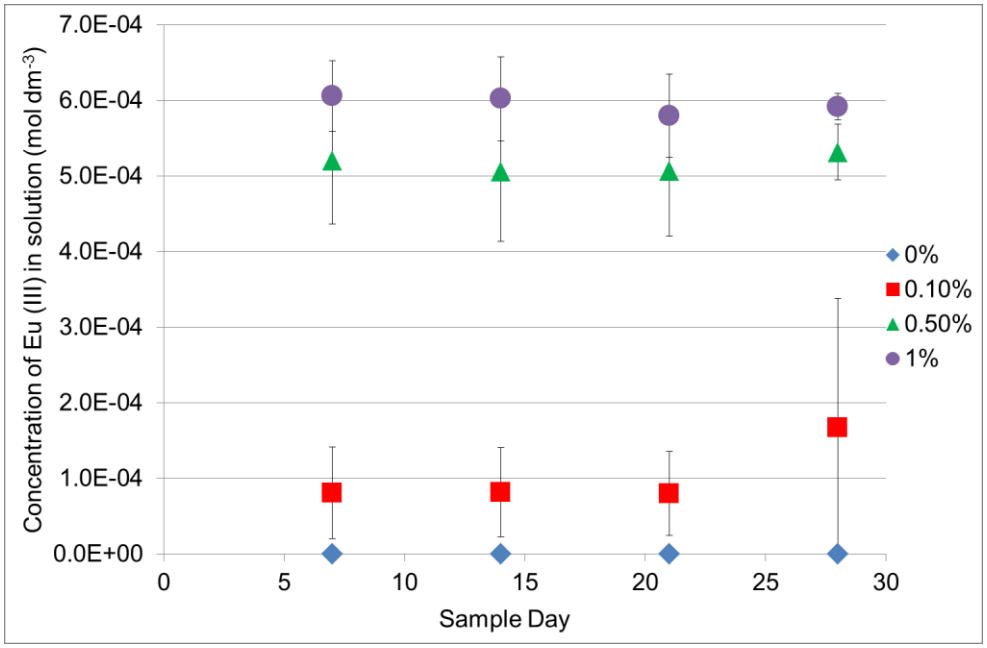

Figure 157 Kinetics of precipitation of Eu (III) in the presence of irradiated-ADVA Cast 551 in BFS equilibrated water

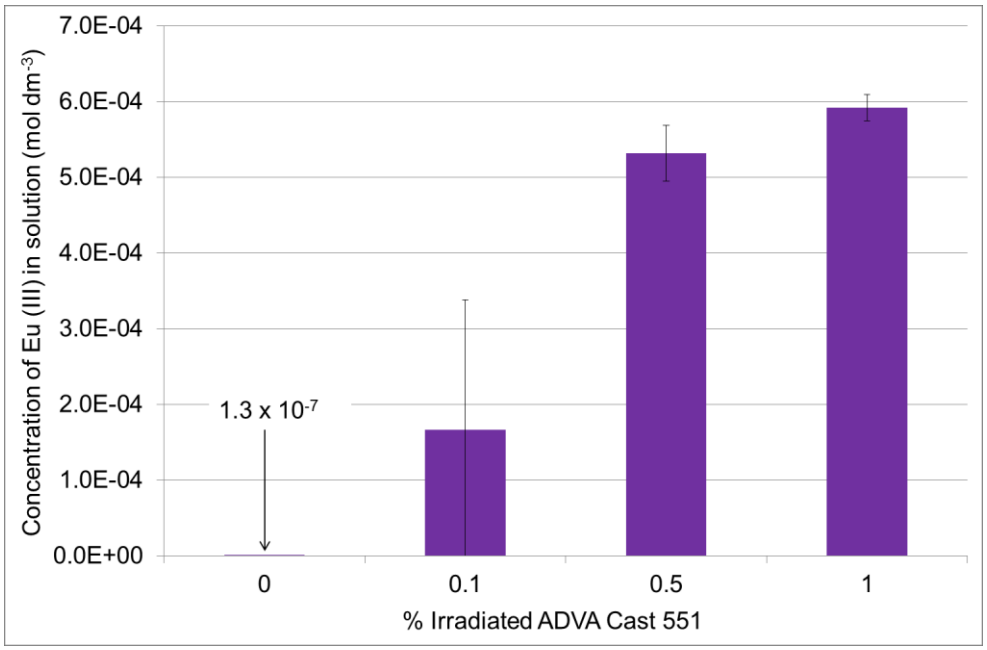

Figure 158 Final concentration of Eu (III) in BFS equilibrated water in the presence of irradiated-ADVA Cast 551

Table 98 Eu (III) solubility in BFS equilibrated water in the presence of irradiated-ADVA Cast 551

Solution	% Irradiated ADVA Cast	Solubility (mol dm^{-3})	SEF
BFS	0	1.33E-07	1
	0.1	1.67E-04	1259
	0.5	5.32E-04	4012
	1	5.92E-04	4466

3.8.3.6 PFA equilibrated water

The concentration of Eu (III) in PFA equilibrated water reached steady state by day 7 at all concentrations of ADVA Cast 551 as demonstrated in Figure 159 which shows the concentration of Eu (III) in solution as a function of time.

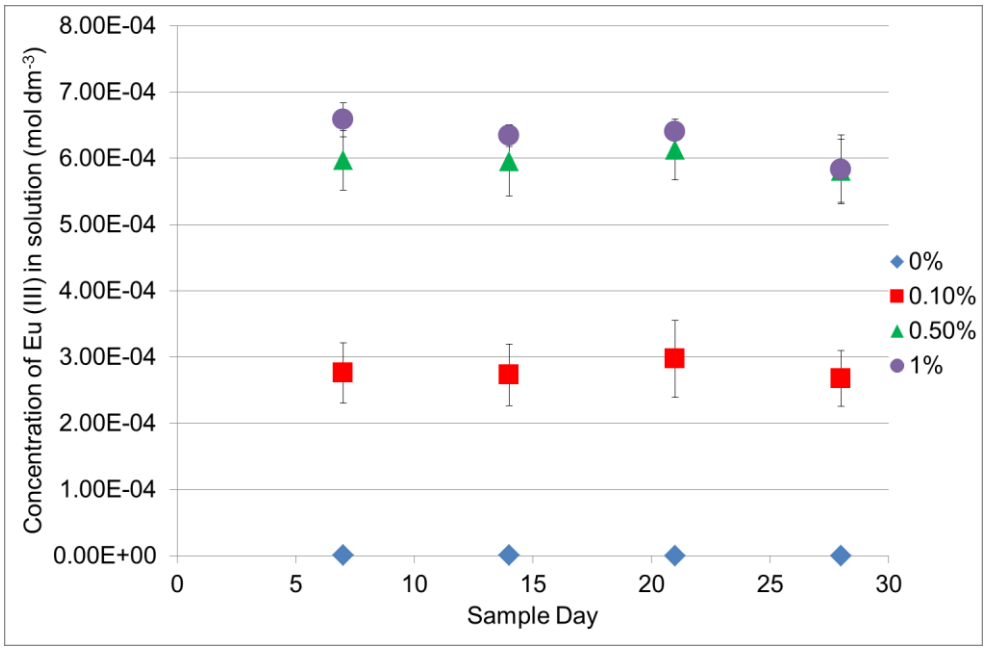

Figure 159 Kinetics of precipitation of Eu (III) in the presence of irradiated-ADVA Cast 551 in PFA equilibrated water

The concentration of Eu (III) measured in solution was significantly affected by the presence of both 0.5% and 1% ADVA Cast 551 where Eu (III) solubility reached the inventory limit in both cases as shown in Figure 160. This solubility enhancement was within the range of several orders of magnitude and SEF values are given in Table 99. A Eu (III) Solubility enhancement that reached the inventory limit was also observed in the presence of 'as received' ADVA Cast 551 in PFA equilibrated water.

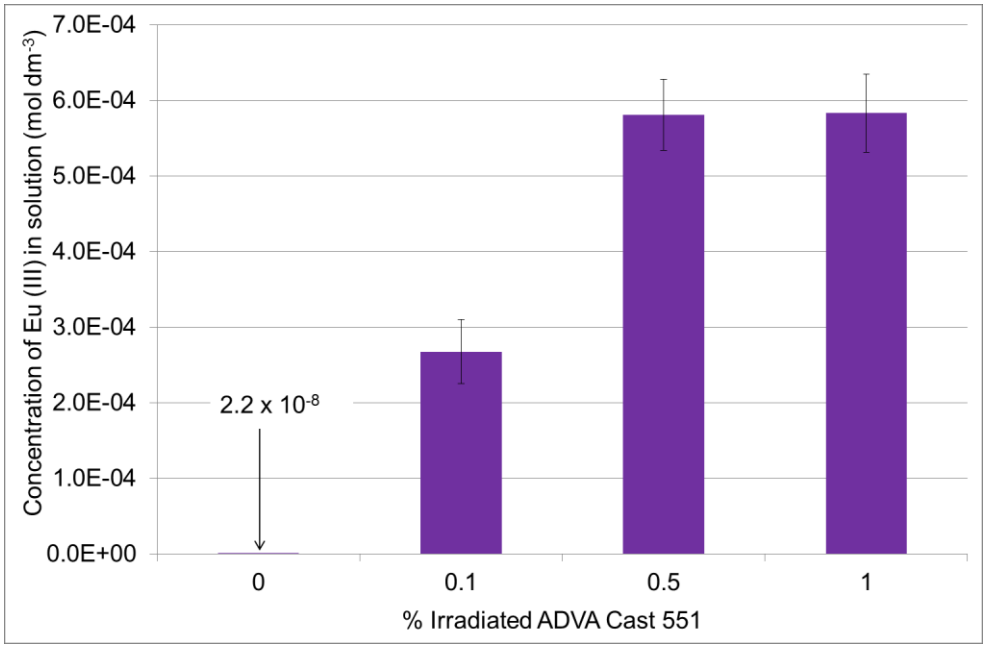

Figure 160 Final concentration of Eu (III) in PFA equilibrated water in the presence of irradiated-ADVA Cast 551

Table 99 Eu (III) solubility in PFA equilibrated water in the presence of irradiated-ADVA Cast 551

Solution	% Irradiated ADVA Cast	Solubility (mol dm^{-3})	SEF
PFA	0	2.18E-07	1
	0.1	2.67E-04	1226
	0.5	5.81E-04	2665
	1	5.83E-04	2675

3.8.3.7 OPC equilibrated water

Kinetics of precipitation of Eu (III) in OPC equilibrated water is shown in Figure 161 where steady state was achieved in all samples by day 7.

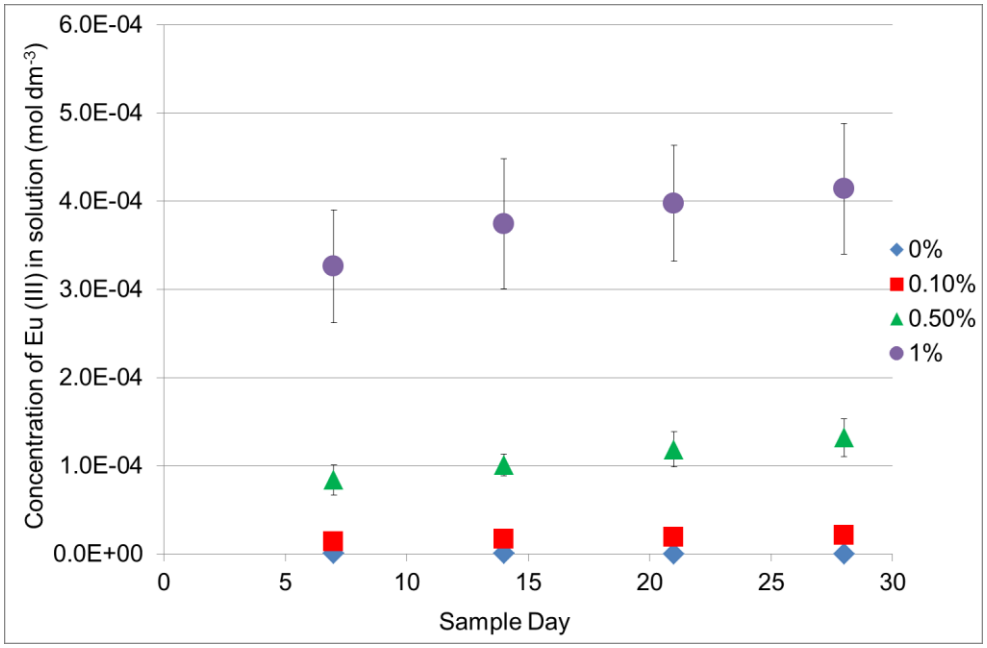

Figure 161 Kinetics of precipitation of Eu (III) in the presence of irradiated ADVA Cast 551 in OPC equilibrated water

There is a significant increase in Eu (III) solubility with increasing concentration of irradiated ADVA Cast 551. The final Eu (III) concentration in solution is recorded in Figure 162. In the presence of 1% irradiated ADVA Cast, the concentration of Eu (III) in solution is close to the inventory added. This is a similar result to that obtained for 10% 'as received' ADVA Cast 551 in the same solution. Table 100 reports SEF values which indicate an increase in solubility over several orders of magnitude. In this case however, calculated SEF values are lower than those recorded in the other high aqueous solutions investigated.

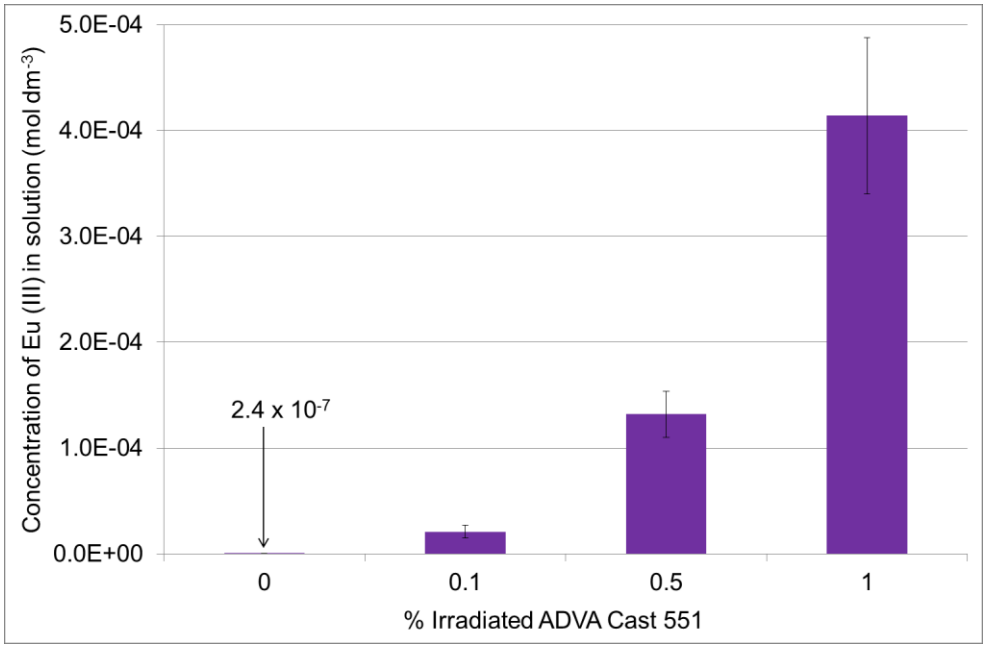

Figure 162 Final concentration of Eu (III) in OPC equilibrated water in the presence of irradiated-ADVA Cast 551

Table 100 Eu (III) solubility in OPC equilibrated water in the presence of irradiated ADVA Cast 551

Solution	% Irradiated ADVA Cast	Solubility (mol dm^{-3})	SEF
OPC	0	2.43E-07	1
	0.1	2.11E-05	87
	0.5	1.32E-04	543
	1	4.14E-04	1705

3.8.4 *Nickel Solubility*

3.8.4.1 95% Saturated $Ca(OH)_2$

Kinetics of precipitation of Ni (II) in 95% saturated $Ca(OH)_2$ in the presence of irradiated ADVA Cast 551 is shown in Figure 163. Steady state was reached by day 7 for all samples except the 0.5% set which had not achieved steady state by the end of the experiment. It is likely the reason for this is experimental error in the handling of the samples which disturbed the precipitate. This anomaly is also reflected in Figure 164 which shows the final concentration of Ni (II) measured in solution. The concentration is highest in the 0.5% samples whereas 0.1% and 1% contained a similar concentration of Ni (II) in solution.

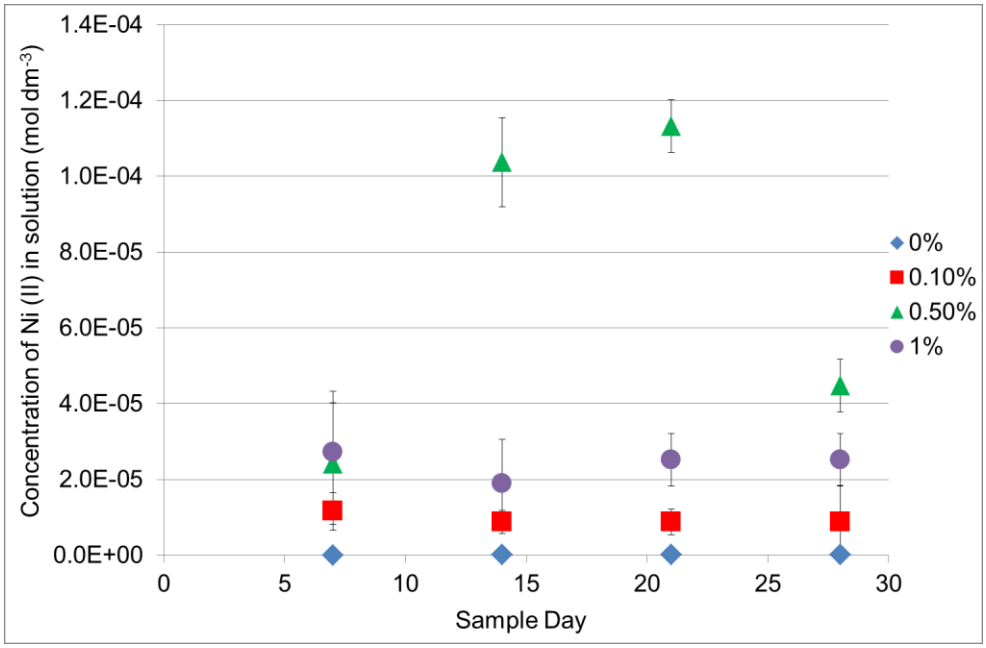

Figure 163 Kinetics of precipitation of Ni (II) in the presence of irradiated-ADVA Cast 551 in 95% saturated $Ca(OH)_2$

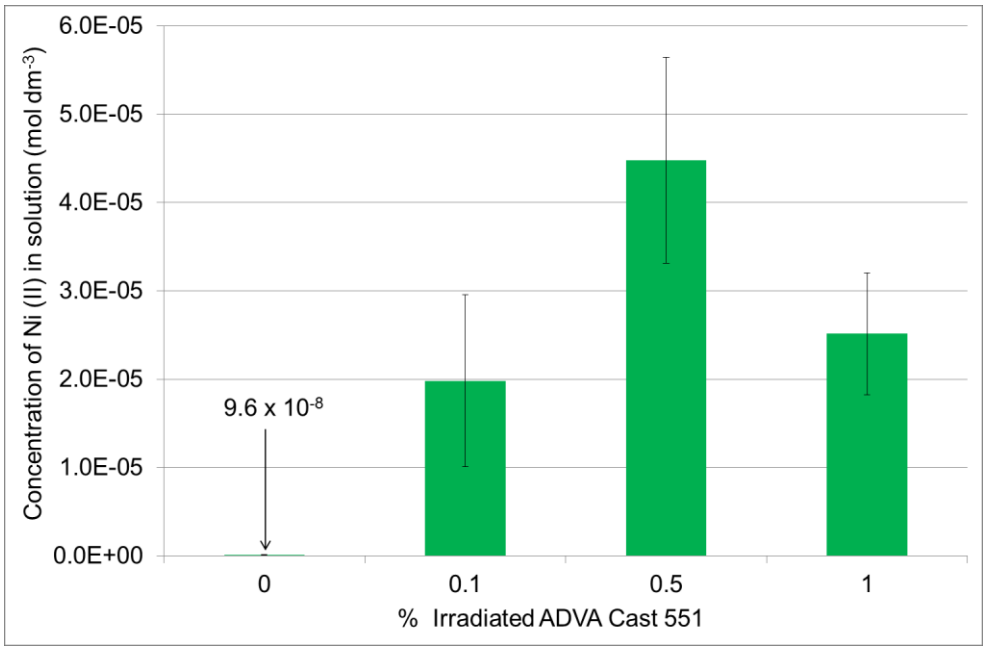

Figure 164 Final concentration of Ni (II) in 95% saturated $Ca(OH)_2$ in the presence of irradiated-ADVA Cast 551

SEF calculations are reported in Table 101 and show a significant increase in Ni (II) solubility from the baseline in all cases. The concentration of Ni (II) in

solution with the presence of 1% irradiated ADVA Cast however is similar to that observed with 'as received' ADVA Cast 551.

Table 101 Ni (II) solubility in 95% saturated $Ca(OH)_2$ in the presence of irradiated-ADVA Cast 551

Solution	% Irradiated ADVA Cast	Solubility (mol dm^{-3})	SEF
$Ca(OH)_2$	0	9.60E-08	1
	0.1	1.98E-05	206
	0.5	4.48E-05	466
	1	2.52E-05	262

3.8.4.2 0.1 mol dm^{-3} NaOH

Figure 165 shows the concentration of Ni (II) in 0.1 mol dm^{-3} NaOH as a function of time. Steady state is reached by day 21 in all samples. The final concentration of Ni (II) measured in solution is recorded in Figure 166 and shows a significant increase in Ni (II) solubility as a result of increasing the concentration of irradiated-ADVA Cast 551. Ni (II) solubility increases over several orders of magnitude with the addition of 1% irradiated-ADVA Cast 551. Ni (II) solubility enhancement in the presence of irradiated ADVA Cast 551 is greater than that for 'as received' ADVA Cast 551 and this is reflected in the SEF calculations are reported in Table 102.

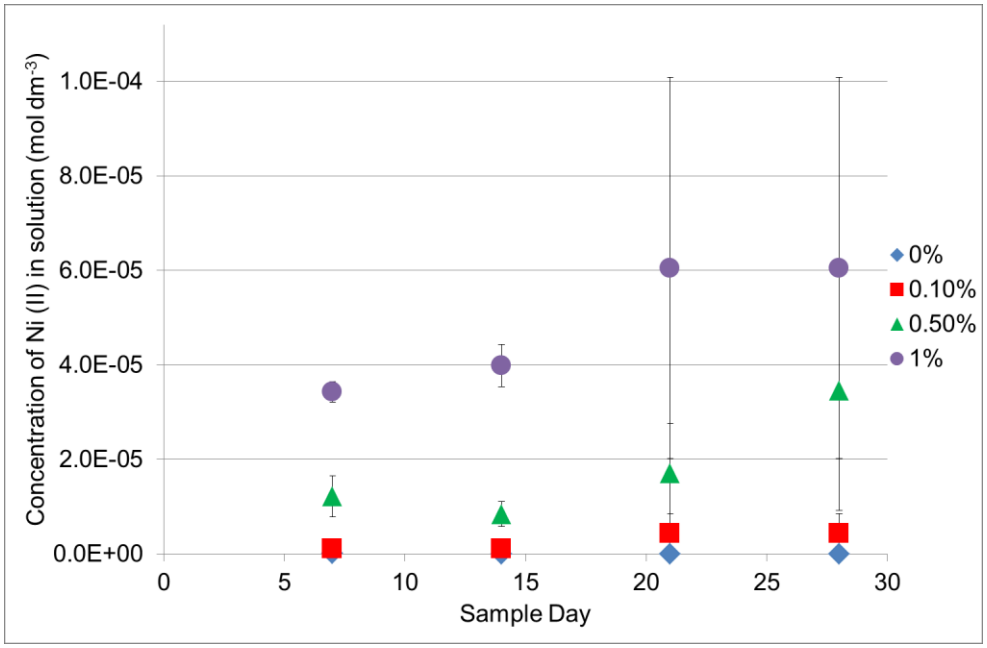

Figure 165 Kinetics of precipitation of Ni (II) in the presence of irradiated-ADVA Cast 551 in 0.1 mol dm^{-3} NaOH

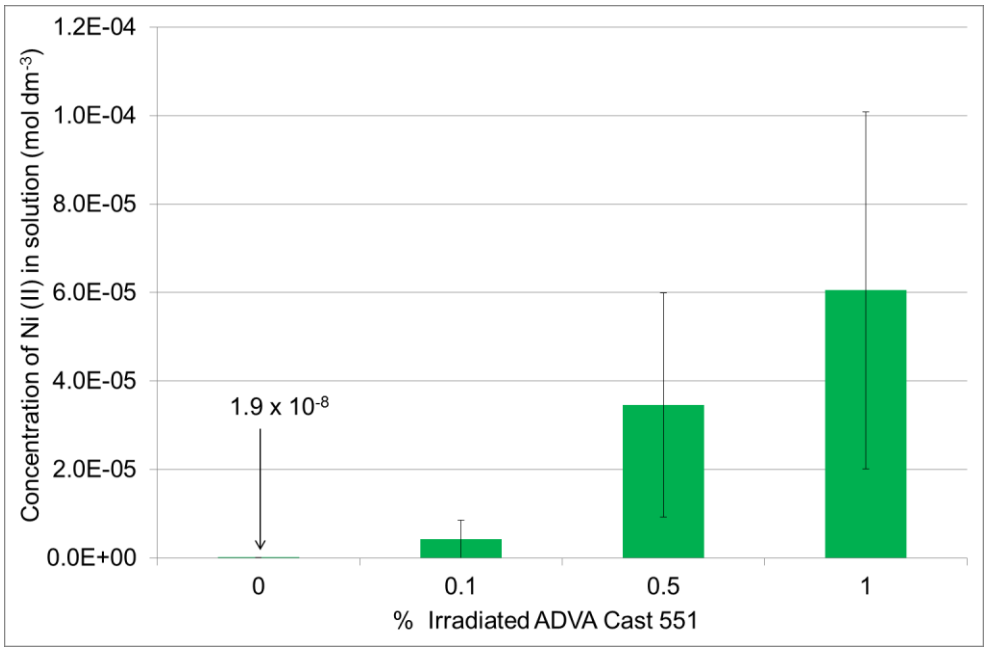

Figure 166 Final concentration of Ni (II) in 0.1 mol dm^{-3} NaOH in the presence of irradiated-ADVA Cast 551

Table 102 Ni (II) solubility in 0.1 mol dm^{-3} NaOH in the presnce of irradiated-ADVA Cast 551

Solution	% Irradiated ADVA Cast	Solubility (mol dm^{-3})	SEF
NaOH	0	1.99E-08	1
	0.1	4.27E-06	214
	0.5	3.45E-05	1736
	1	6.05E-05	3041

3.8.4.3 BFS:OPC equilibrated water

Kinetics of precipitation for Ni (II) in BFS:OPC equilibrated water is shown in Figure 167. Steady state is reached in the 0% and 0.1% samples by day 7 while the 0.5% and 1% samples achieved steady state by day 21. Throughout the experiment, the concentration of Ni (II) in solution in the presence of 0.5% and 1% irradiated ADVA Cast 551 is similar. This is demonstrated in the final concentration of Ni (II) measured in solution in Figure 168. Within errors, Ni (II) concentration is equivalent in the presence of 0.5% and 1% irradiated-ADVA Cast 551. As shown in Table 103, Ni (II) solubility increases over several orders of magnitude with the presence of ADVA Cast 551 and as mentioned, 0.5% and 1% irradiated ADVA Cast 551 have a similar effect on Ni (II) solubility with SEF values of 2022 and 2060 respectively. The solubilities recorded in this case are lower than those recorded for the 'as received' ADVA Cast 551 where final Ni (II) concentration was 1 x 10^{-4} mol dm^{-3} in the presence of 1% ADVA Cast 551.

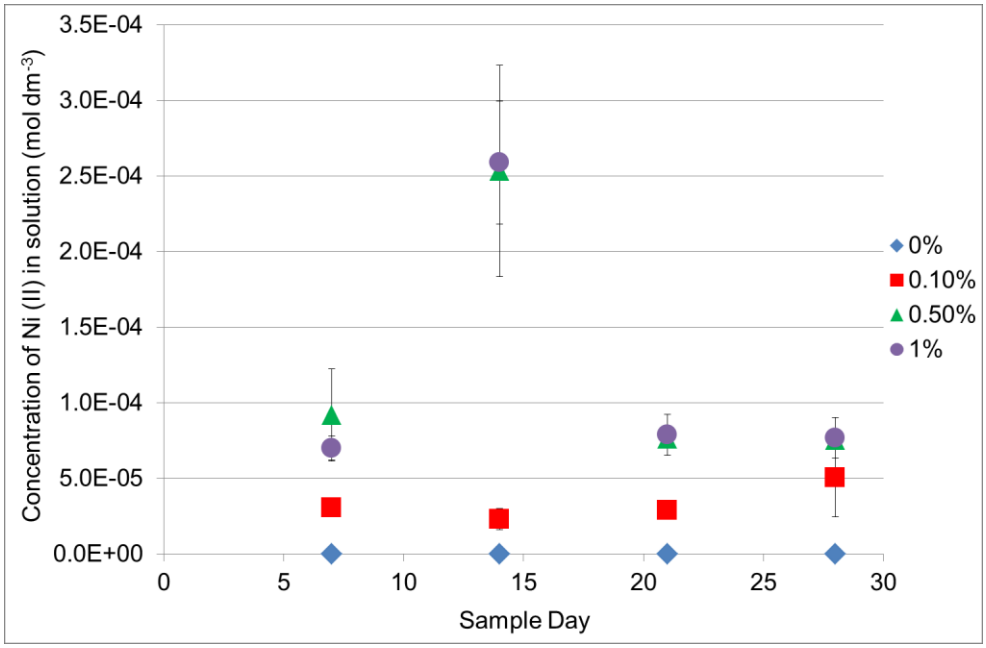

Figure 167 Kinetics of precipitation of Ni (II) in the presence of irradiated-ADVA Cast 551 in BFS:OPC equilibrated water

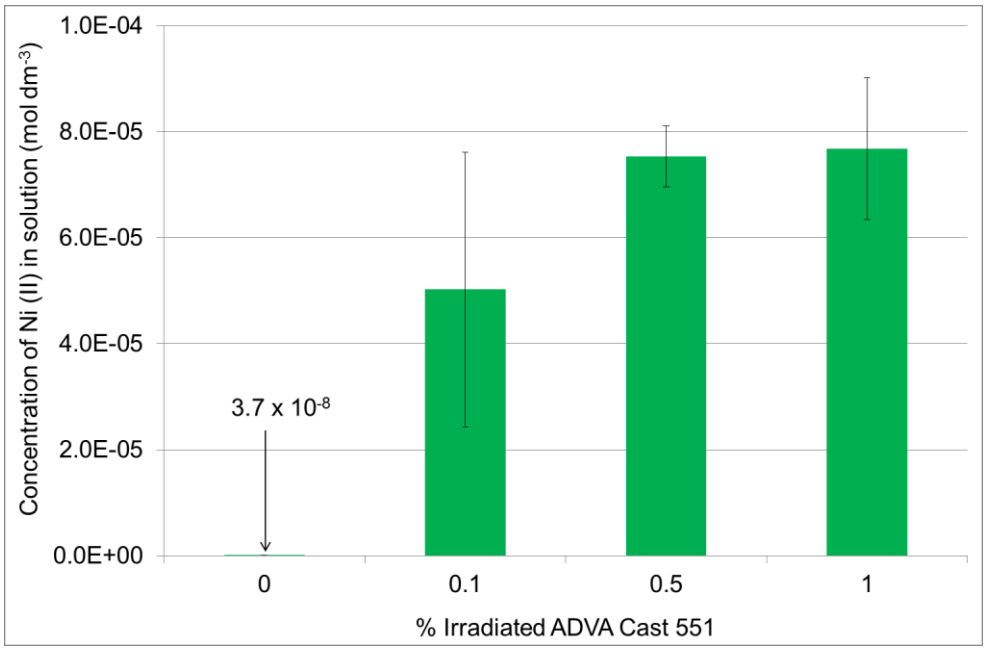

Figure 168 Final concentration of Ni (II) in BFS:OPC equilibrated water in the presence of irradiated-ADVA Cast 551

Table 103 Ni (II) solubility in BFS:OPC equilibrated water in the presence of irradiated-ADVA Cast 551

Solution	% Irradiated ADVA Cast	Solubility (mol dm^{-3})	SEF
BFSOPC	0	3.73E-08	1
	0.1	5.02E-05	1348
	0.5	7.53E-05	2022
	1	7.68E-05	2060

3.8.4.1 PFA:OPC equilibrated water

As demonstrated in Figure 169, Ni (II) concentration in PFA:OPC equilibrated water reached steady state by day 7 in the presence of 0% and 0.1% irradiated ADVA Cast 551. However, the 0.5% and 1% samples did not reach steady state throughout the duration of the experiment. A true solubility value of Ni (II) in these cases cannot therefore be given. As was true in BFS:OPC equilibrated water, the concentration of Ni (II) measured in the presence of 0.5% and 1% ADVA Cast 551 were similar. Figure 170 gives the final concentration of Ni (II) in solution and shows within errors the 0.5% and 1% yield the same Ni (II) aqueous concentration.

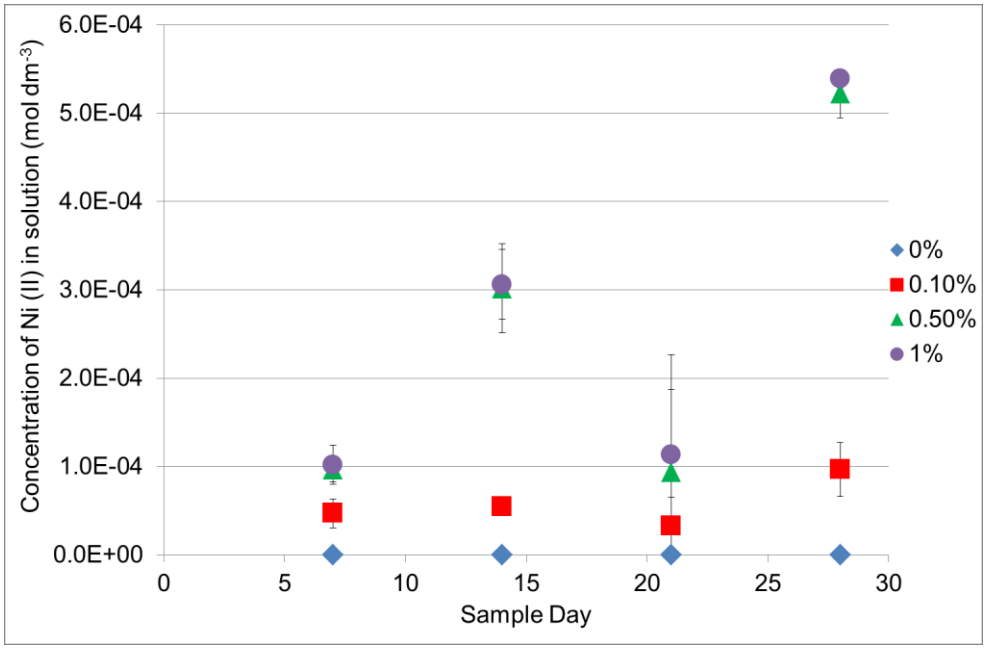

Figure 169 Kinetics of precipitation of Ni (II) in the presence of irradiated-ADVA Cast 551 in PFA:OPC equilibrated water

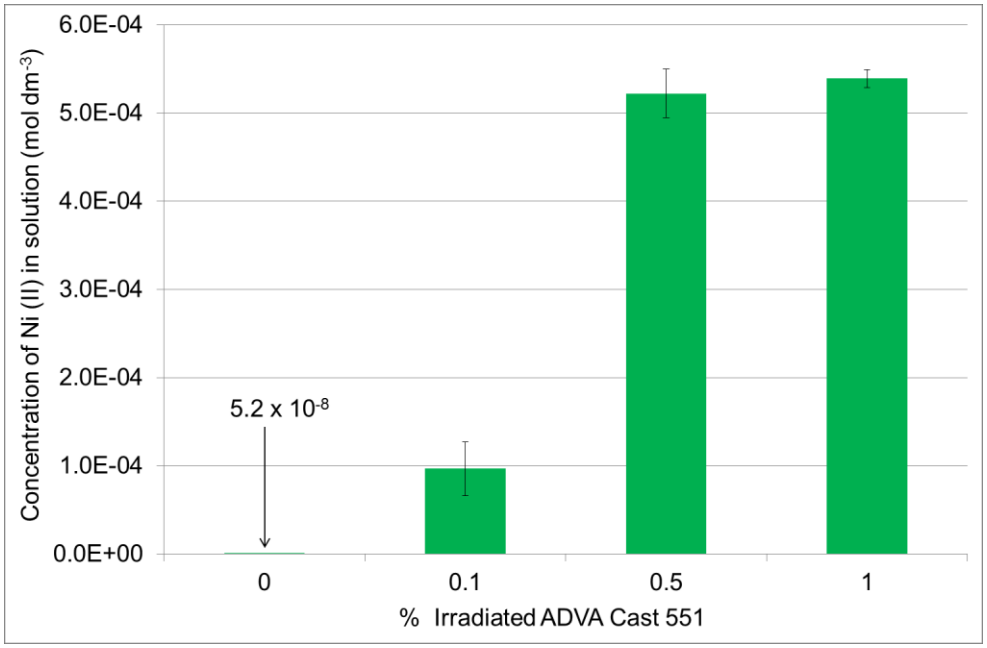

Figure 170 Final concentration of Ni (II) in PFA:OPC equilibrated water in the presence of irradiated-ADVA Cast 551

Ni (II) solubility enhancement in the presence of 0.5% and 1% irradiated ADVA Cast 551 is substantial with an increase over several orders of magnitude. The values for 0.5% and 1% irradiated-ADVA Cast 551 should however be treated with caution since these samples did not reach steady state. A true solubility value may be obtained in this case by extending the duration of the experiment to allow the samples to equilibrate for longer.

Table 104 Ni (II) solubility in PFA:OPC equilibrated water in the presence of irradiated-ADVA Cast 551

Solution	% Irradiated ADVA Cast	Solubility (mol dm^{-3})	SEF
PFAOPC	0	5.20E-08	1
	0.1	9.66E-05	1858
	0.5	5.22E-04	10046
	1	5.39E-04	10368

3.8.4.2 BFS equilibrated water

Ni (II) concentration in BFS equilibrated water did not reach steady state in the presence of 0.1%, 0.5% or 1% irradiated ADVA Cast 551. The only samples to reach steady state were the baseline (0%) samples. The final concentration of Ni (II) in solution shown in Figure 172 cannot therefore be represented as a true solubility. A significant solubility enhancement it observed over several orders

of magnitude in the presence of all concentrations of irradiated-ADVA Cast 551 and representative SEF values are reported in Table 105. The concentrations of Ni (II) in solution in the presence of 1% irradiated-ADVA Cast 551 are similar to that observed with 'as received' ADVA Cast 551 where the final Ni (II) concentrations were recorded as 2.7 x 10^{-4} mol dm^{-3} and 5.0 x 10^{-4} mol dm^{-3} for 'as received' and irradiated-ADVA Cast 551 respectively.

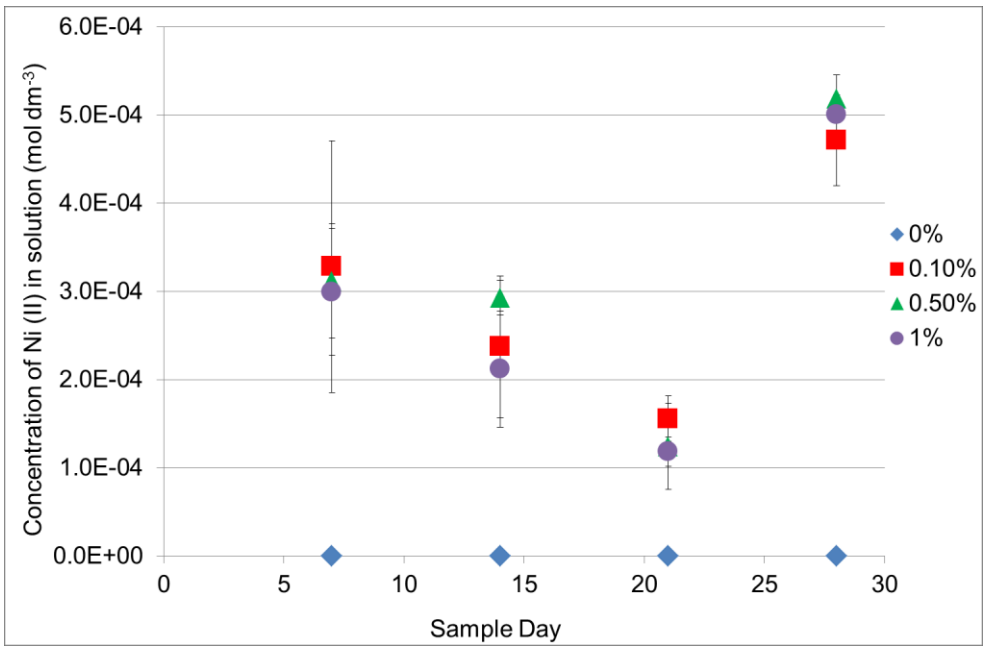

Figure 171 Kinetics of precipitation of Ni (II) in the presence of irradiated-ADVA Cast 551 in BFS equilibrated water

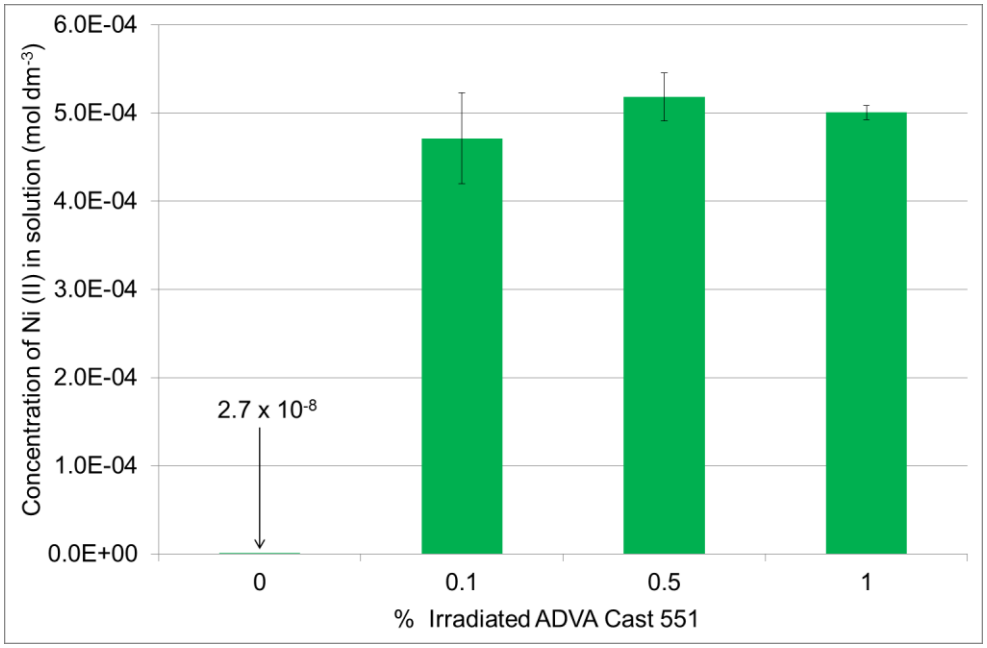

Figure 172 Final concentration of Ni (II) in BFS equilibrated water in the presence of irradiated-ADVA Cast 551

Table 105 Ni (II) solubility in BFS equilibrated water in the presence of irradiated-ADVA Cast 551

Solution	% Irradiated ADVA Cast	Solubility (mol dm^{-3})	SEF
BFS	0	2.72E-08	1
	0.1	4.71E-04	17309
	0.5	5.18E-04	19036
	1	5.00E-04	18381

3.8.4.3 PFA equilibrated water

Kinetics of precipitation of Ni (II) in PFA equilibrated water is shown in Figure 173 where the samples reached steady state by day 7. At day 28, a slight increase in solubility in the presence of all concentrations of superplasticiser is observed; however, this increase is within an order of magnitude compared to the Ni (II) concentrations measured at day 21. Figure 174 records the final concentration of Ni (II) measured in solution and demonstrates a similar Ni (II) solubility enhancement in the presence of all concentrations of superplasticiser.

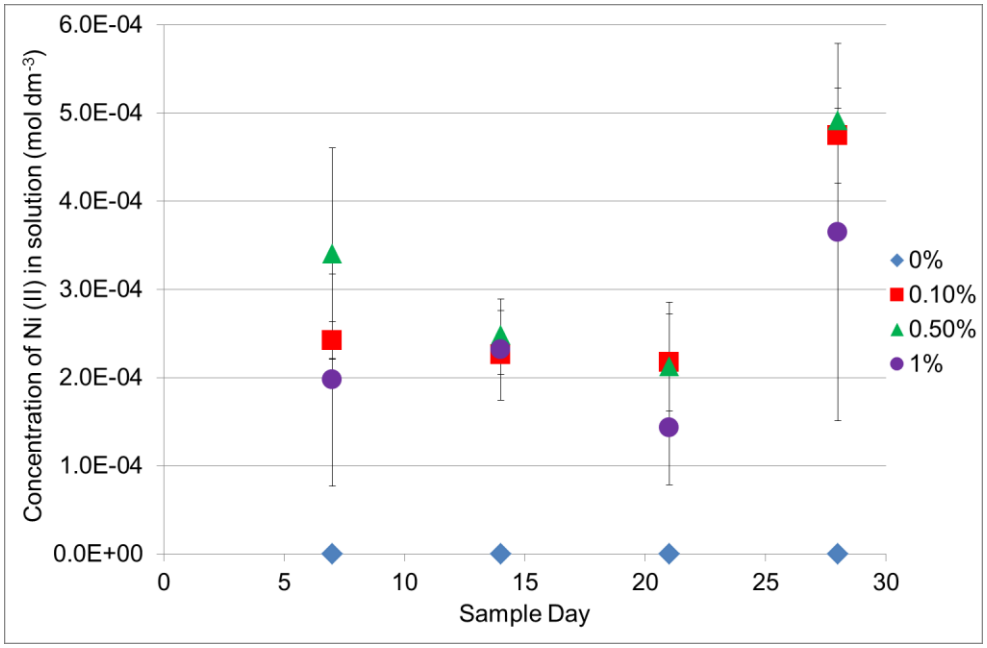

Figure 173 Kinetics of precipitation of Ni (II) in the presence of irradiated-ADVA Cast 551 in PFA equilibrated water

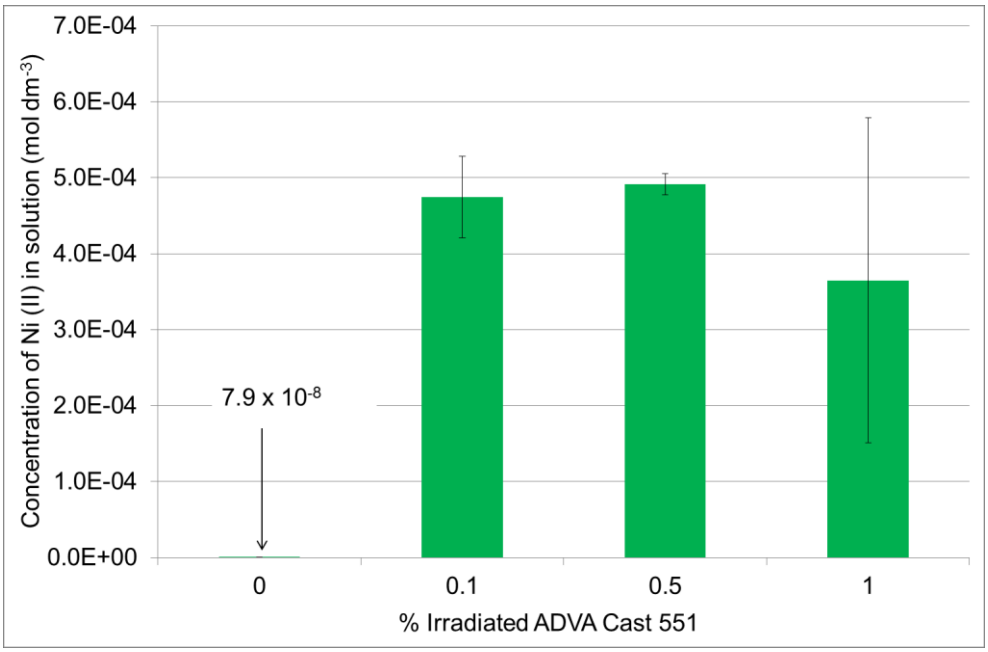

Figure 174 Final concentration of Ni (II) in PFA equilibrated water in the presence of irradiated-ADVA Cast 551

SEF values are reported in Table 106 and show an increase in Ni (II) solubility over several orders of magnitude in the presence of all concentrations of

irradiated-ADVA Cast 551. The effect of irradiated ADVA Cast 551 is slightly higher than recorded in the 'as received' superplasticiser experiment.

Table 106 Ni (II) solubility in PFA equilibrated water in the presence of irradiated-ADVA Cast 551

Solution	% Irradiated ADVA Cast	Solubility (mol dm^{-3})	SEF
PFA	0	7.96E-08	1
	0.1	4.74E-04	5963
	0.5	4.91E-04	6176
	1	3.65E-04	4584

3.8.4.4 OPC equilibrated water

Concentration of Ni (II) in OPC equilibrated water as a function of time is shown in Figure 175 where Ni (II) concentration reaches steady state by day 7 for 0%, 0.1% and 1% irradiated-ADVA Cast 551 samples while the 0.5% samples are slightly less stable with an increase in Ni (II) concentration measured at day 28. The final concentration of Ni (II) in solution is recorded in Figure 176 and shows the highest concentration of Ni (II) measured is in the 0.5% irradiated ADVA Cast 551 samples. This corresponds with the anomalous increase in solubility noted in the kinetic profile which is likely due to human error. Nevertheless, the increase in Ni (II) solubility in the presence of irradiated ADVA Cast 551 is overs several orders of magnitude. SEF values are reported in Table 107. The concentration of Ni (II) measured in the presence of the irradiated superplasticiser is within the same order or magnitude of that measured in the 'as received' ADVA Cast 551 experiment.

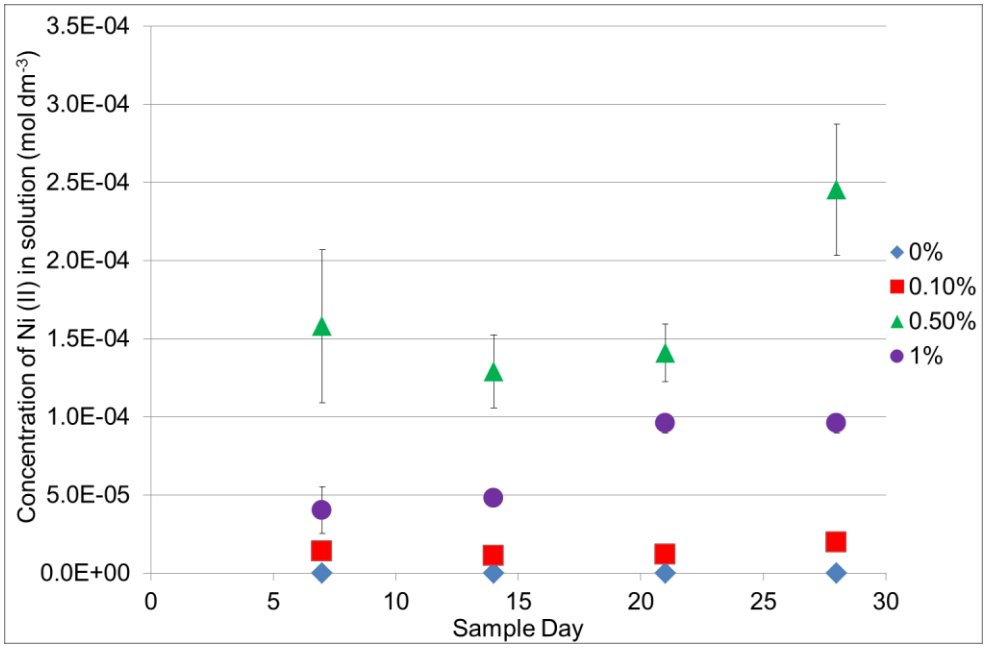

Figure 175 Kinetics of precipitation of Ni (II) in the presence of irradiated-ADVA Cast 551 in OPC equilibrated water.

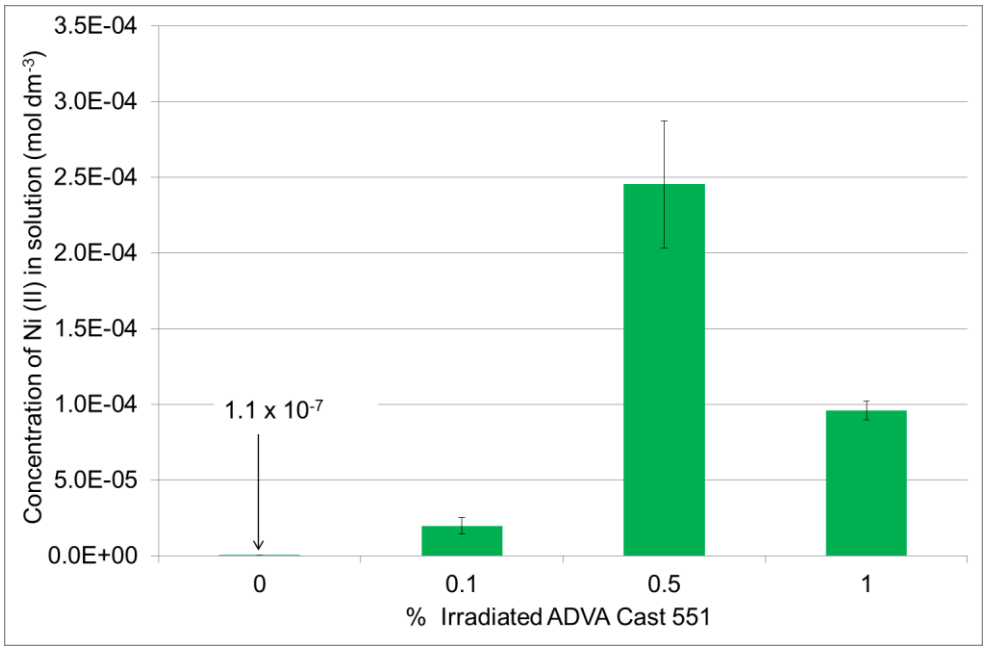

Figure 176 Final concentration of Ni (II) in OPC equilibrated water in the presence of irradiated-ADVA Cast 551

Table 107 Ni (II) solubility in OPC equilibrated water in the presence of irradiated-ADVA Cast 551

Solution	% Irradiated ADVA Cast	Solubility (mol dm^{-3})	SEF
OPC	0	1.05E-07	1
	0.1	1.98E-05	188
	0.5	2.45E-04	2331
	1	9.58E-05	910

3.8.5 *Summary of Experimental U (VI), Th (IV), Eu (III) and Ni (II) Solubility Data in the Presence of Irradiated ADVA Cast 551*

A summary of experimental solubility data and SEF values calculated for the presence of 1% irradiated-ADVA Cast 551 are shown in

Table **108**

Table 108 Summary of U (VI), Th (IV), Eu (III) and Ni (II) solubility results in the presence of irradiated-ADVA Cast 551

Aqueous Solution	pH	Baseline Solubility (Solubility in the absence of irradiated-ADVA Cast 551) mol dm^{-3}				SEF in the presence of 1% irradiated-ADVA Cast 551			
		U (VI)	Th (IV)*	Eu (III)	Ni (II)	U (VI)	Th (IV)*	Eu (III)	Ni (II)
95% Saturated $Ca(OH)_2$	12.5 ± 0.5	7E-08 ± 1E-08	1E-09	4E-08 ± 1E-08	9E-08 ± 4E-09	70561	5953	7883	262
0.1 mol dm^{-3} NaOH	12.5 ± 0.5	7E-06 ± 6E-07	1E-09	1E-07 ± 1E-08	2E-08 ± 1E-08	419	3884	199	23041
BFS:OPC Equilibrated Water	12.5 ± 0.5	2E-07 ± 6E-08	1E-09	9E-08 ± 3E-08	4E-08 ± 5E-09	46114	3946	5577	2060
PFA:OPC Equilibrated Water	12.5 ± 0.5	4E-08 ± 7E-09	1E-09	2E-07 ± 1E-08	5E-08 ± 5E-09	94447	4583	1840	10368
BFS Equilibrated Water	12.5 ± 0.5	2E-06 ± 3E-08	1E-09	1E-07 ± 2E-08	3E-08 ± 2E-08	1631	3755	4466	18381
PFA Equilibrated Water (pH adjusted)	12.5 ± 0.5	3E-06 ± 4E-07	1E-09	2E-07 ± 6E-08	8E-08 ± 1E-07	203	3215	2675	4584
OPC Equilibrated Water	12.5 ± 0.5	7E-07 ± 7E-08	1E-09	2E-07 ± 2E-08	1E-07 ± 1E-07	1935	4640	1705	910

* Th (IV) baseline solubility value is taken from the experimental work reported in (32,33,67)

4 Discussion and Concluding Remarks

The results presented in this research describe the behaviour of a range of metals in the presence of cement superplasticiser whilst also considering the behaviour and stability of the superplasticiser itself.

4.1 Effect of Superplasticiser on Metal Solubility

4.1.1 *Effect of 'as received' ADVA Cast 551 on the Solubility of U (VI), Th (IV), Eu (III) and Ni (II)*

As shown in JCHESS speciation predictions (section 4.1.3) metal speciation in high pH aqueous solution is dominated by hydroxyl complexes e.g. $UO_2(OH)_3^-$, $Ni(OH)_3^-$, $Th(OH)_4$ and $Eu(OH)_3$. It is therefore postulated, that mixed complexes are formed by the displacement of hydroxyl groups from the metal species by the ligand (the superplasticiser). A similar effect was reported using different types of superplasticiser (46). The formation of these soluble mixed complexes therefore may be said to be responsible for the observed solubility enhancement of the metals investigated.

The assumed equilibrium for the mixed complex formation may be given by Equation 9.

$$M(OH)_x + Lig = M(OH)_{x-n}Lig + nOH^-$$

Equation 9 Equilibrium for the formation of mixed complexes

The binding constant corresponding to this equilibrium is given in Equation 10.

$$K_{comp} = \frac{[M(OH)_{x-n}Lig]\,[OH^-]^n}{[Lig]\,[M(OH)_x]}$$

Equation 10 Binding constant for the formation of mixed complexes

And finally, solubility of the metal may be given by Equation 11.

$$[Sol] = [M(OH)_x] + [M(OH)_{x-n}Lig]$$

Equation 11 Metal Solubility

Variation in the extent of solubility enhancement may be due to the effects of the hard-soft acid-base theory (70). One functional group which has been shown to coordinate metals through a hard oxygen donor atom is carboxylate. There are a number of potential carboxylate donor sites located on the superplasticiser that are available for coordination.

The hardness of an acid is characterised in general by a small atomic radius, a high effective nuclear charge and low polarizability. Actinides and Lanthanides (U (VI), Th (IV) and Eu (III)) are classed as hard acids and have a high affinity towards the hard oxygen base. This high affinity would explain the large solubility enhancement observed for U (IV) and Eu (III) but Th (IV) does not fit the trend so well. Ni (II) is a transition metal and is classified as a borderline or soft acid and therefore has less affinity towards the hard O donor and explains the lower enhancements in solubility observed in the Ni samples.

Th (IV) solubility predicted by JCHESS (the dominant aqueous Th species is $Th(OH)_4$ (aq)) is in the region of 1×10^{-12} mol dm^{-3}. This solubility value is in the region of 3 orders of magnitude lower than the experimental results reported here (3.3.2) and by Wierczinski et al. (1998), Neck et al. ((2003) and Altmaier et al. (2008). The most likely reason for this difference is the effect of the crystallinity of the thorium precipitate. Amorphous and colloidal precipitates of $Th(OH)_4$ have been reported which have much higher solubility limit than the crystalline ThO_2 (33). In this case, the authors suggest that during their experimental time scales of a year and at pH values above the onset of hydrolysis, precipitation of monomeric or polynuclear hydroxide complexes on the surface of the crystalline AnO_2 (cr) will result in an amorphous surface layer which is responsible for the observed Th(IV) solubility being higher than modelling calculations. This observation highlights the importance of experimental data versus model calculations and assumptions in the performance assessment of the long term behaviour of metals within the GDF system.

The differences in reported solubilities between authors can result due to; differences in experimental methods, experimental temperature, pH and the formation history and aging of the experimental solid phase (95). Solubility data based on the formation of crystalline solid phases are not appropriate to the experimental timescales of days such as those reported in this research. Here, steady state is achieved between aqueous solution and an amorphous or metastable precipitate. This type of precipitate gives rise to higher aqueous concentrations of metal than if the solid were crystalline. An 'active' form of a precipitate (one which is very fine and has a disordered lattice) is usually formed incipiently from an oversaturated solution and the solid may remain in metastable equilibrium with the aqueous phase and/or convert slowly into a 'inactive', more stable, crystalline form over time. This process is known as aging (96). Solubility of the metal species generally decreases with aging as the crystal lattice becomes more ordered.

Thermodynamic equilibrium data generally exists only for the stable crystalline form of the solids. Only in a geochemical context dealing with equilibrium over geological timescales are the crystalline solids more prevalent. This means therefore that estimations of stability constants for complexation of these metals with ligand (in this case superplasticiser) are limited by basing calculations on a number of assumptions. These include the validity of Ksp values where an amorphous precipitate is present experimentally and the uncertainty and reliability of superplasticiser structure (i.e. binding sites) and therefore the method of binding.

4.1.2 *Effect of Irradiated ADVA Cast 551 on the Solubility of U (VI), Th (IV), Eu (III) and Ni (II)*

In contrast to what was observed with 'as received' ADVA Cast 551, the solubility of Th (IV) is enhanced significantly in the presence of irradiated-ADVA Cast 551. U (VI) also shows a greater enhancement in the presence of the irradiated superplasticiser while Eu (III) and Ni (II) show enhancement similar to that observed in the non- irradiated samples. The formation of similar mixed complexes between the aqueous metal hydroxyl species and the superplasticiser are likely to be responsible for the observed enhancement in

solubility, however it is not conclusive why Th (IV) and U (VI) are more affected by the irradiated superplasticiser than the non-irradiated form.

The hard acid/ hard base principle applies in this case as it did in the 'as received' superplasticiser experiment with hard acids U (VI) Th (IV) and Eu (III) solubility enhanced more significantly than the borderline/ soft Ni (II) due to their greater affinity for the hard oxygen donor of the carboxylic acid group on the superplasticiser polymer.

4.1.3 *JCHESS Metal Speciation*

JCHESS (71) is a useful modelling tool and was used along with the HATCHES (72) and NIST (73) thermodynamic databases, in this case, to predict the speciation of U (VI), Th (IV), Eu (III) and Ni (II) in saturated $Ca(OH)_2$ and 0.1 mol dm^{-3} NaOH.

4.1.3.1 U (VI) Speciation in Saturated $Ca(OH)_2$

The concentration of Ca^{2+} and OH^- present in a saturated solution of $Ca(OH)_2$ was calculated using the solubility product equilibrium constant K_{sp} according to the scheme shown in Figure 177.

$$Ca(OH)_2 \overset{H_2O}{\rightleftharpoons} Ca^{2+}(aq) + 2OH^-(aq)$$

$$K_c = \frac{[Ca^{2+}][OH^-]^2}{[Ca(OH)_2]}$$

$$[Ca^{2+}][OH^-]^2 = K_c \times [Ca(OH)_2]$$

$$K_{sp} = [Ca^{2+}][OH^-]^2 = 5.02 \times 10^{-6}$$

$$[OH\text{-}] = 2[Ca^{2+}]$$

$$K_{sp} = [Ca^{2+}](2Ca^{2+})^2$$

$$K_{sp} = 4[Ca^{2+}]^3 = 5.02 \times 10^{-6}$$

$$[Ca^{2+}]^3 = \frac{5.02 \times 10^{-6}}{4} = 1.255 \times 10^{-6}$$

$$[Ca^{2+}] = \sqrt[3]{1.233 \times 10^{-6}} = 0.011 \text{ mol dm}^{-3}$$

$$[OH^-] = 2[Ca^{2+}] = 2 \times 0.011 = 0.022 \text{ mol dm}^{-3}$$

Figure 177 $Ca(OH)_2$ solubility product, K_{sp}

By inputting the following data into the JCHESS model, a list of species, their concentration in mol dm^{-3} and the final solution pH were calculated and are shown in Table 109.

$[Ca^{2+}]$ = 0.011 mol dm^{-3}

$[OH^-]$ = 0.022 mol dm^{-3}

UO_2^{2+} = 1 x 10^{-3} mol dm^{-3}

NO_3^- = 2 x 10^{-3} mol dm^{-3}

pH = 12.16

Table 109 U (VI) speciation in saturated $Ca(OH)_2$

	mol dm^{-3}	**Species**
OH^-	0.0169	Aqueous
Ca^{2+}	0.0088	Aqueous
NO_3^-	0.00195	Aqueous
CaOH-	0.00113	Aqueous
$CaNO_3^+$	4.68 x 10^{-5}	Aqueous
H^+	7.86 x 10^{-13}	Aqueous
$UO_2(OH)_3^-$	8.62 x 10^{-14}	Aqueous
$UO_2(OH)_4^{2-}$	3.14 x 10^{-15}	Aqueous
$CaUO_4$	0.001	Mineral/Colloid

A prediction of U (VI) solubility can be made by the sum of all aqueous uranium species and is in the region of 9 x 10^{-14} mol dm^{-3}. The JCHESS model is based on the assumption that the system is in equilibrium. In this case, the solid phase (precipitate) is predicted to be $CaUO_4$, a crystalline solid. As suggested by Duff et al. (2002) and Opel et al. (2007) a uranium hydroxide species such as schoepite, $UO_3 \cdot 2H_2O$ (am), may be a more representative precipitate present in solution (74,75). On aging, uranium hydroxide species can increase in crystallinity such that UO_3 (cr) is formed. Crystalline solids are much less soluble than amorphous precipitates. The U (VI) solubility predicted here is much lower than the results observed in section 3.3.1 and this is probably due to the amorphous nature of the precipitate formed experimentally. The experimental period of twenty eight days is not long enough for sufficient crystallinity to be achieved to have U (VI) solubility as low as predicted in the model.

4.1.3.2 U (VI) Speciation in 0.1 mol dm^{-3} NaOH

The following data were input into JCHESS to produce a list of predicted species, their concentration and the final solution pH.

NaOH = 0.1 mol dm^{-3}

UO_2^{2+} = 1 x 10^{-3} mol dm^{-3}

NO_3^- = 2 x 10^{-3} mol dm^{-3}

pH = 12.88

Table 110 U (VI) speciation in 0.1 mol dm^{-3} NaOH

	mol dm^{-3}	**Species**
Na^+	0.098	Aqueous
OH^-	0.096	Aqueous
NO_3^-	0.002	Aqueous
NaOH (aq)	0.00093	Aqueous
$UO_2(OH)_3^-$	1.89 x 10^{-7}	Aqueous
$UO_2(OH)_4^{2-}$	4.69 x 10^{-8}	Aqueous
$UO_2(OH)_2$ (aq)	1.57 x 10^{-11}	Aqueous
H^+	1.65 x 10^{-13}	Aqueous
$Na_2U_2O_7$	0.0005	Mineral/Colloid

In this case, the predicted concentration of U (VI) in solution is 2.4 x 10^{-7} mol dm^{-3} which is within the range of experimental data collected in section 3.3.1.

4.1.3.3 Th (IV) Speciation in Saturated $Ca(OH)_2$

The following data was input into JCHESS to produce a list of predicted species, their concentration and the final solution pH.

$[Ca^{2+}]$ = 0.011 mol dm^{-3}

$[OH^-]$ = 0.022 mol dm^{-3}

Th^{4+} = 1 x 10^{-9} mol dm^{-3}

NO_3^- = 4 x 10^{-9} mol dm^{-3}

pH = 12.25

Table 111 Th (IV) speciation in saturated $Ca(OH)_2$

	mol dm^{-3}	**Species**
OH^-	0.021	Aqueous
Ca^{2+}	0.0095	Aqueous
$CaOH^-$	0.0015	Aqueous
NO_3^-	3.81×10^{-9}	Aqueous
$CaNO_3^+$	9.69×10^{-11}	Aqueous
H^+	6.53×10^{-13}	Aqueous
$Th(OH)_4$ (aq)	6.62×10^{-15}	Aqueous
ThO_2 (Thorianite)	9.77×10^{-10}	Mineral/Colloid

The predicted solubility of Th (IV) in this case is 6.6×10^{-15} mol dm^{-3}, a value far below the limit of detection for ICP-MS. Neck et al (2003) (33) have shown experimentally that precipitation of ThO_2 does not occur above pH 3 as predicted in this model. A more likely precipitate is a thorium hydroxide species $ThO_2 \cdot xH_2O$ (am) which has a higher solubility than the crystalline phase.

4.1.3.4 Th (IV) Speciation in 0.1 mol dm^{-3} NaOH

The following data were input into JCHESS to predict the thorium species formed and final pH in 0.1 mol dm^{-3} NaOH

NaOH = 0.1 mol dm^{-3}

Th^{4+} = 1×10^{-9} mol dm^{-3}

NO_3^- = 4×10^{-9} mol dm^{-3}

pH = 12.89

Table 112 Th (IV) speciation in 0.1 mol dm^{-3} NaOH

	mol dm^{-3}	**Species**
Na^+	0.099	Aqueous
OH^-	0.099	Aqueous
NaOH (aq)	0.00097	Aqueous
NO_3^-	3.91×10^{-9}	Aqueous
H^+	1.6×10^{-13}	Aqueous
$Th(OH)_4$ (aq)	6.62×10^{-15}	Aqueous
ThO_2 (Thorianite)	9.77×10^{-10}	Mineral/Colloid

Similarly to that shown in $Ca(OH)_2$, the dominant aqueous species is $Th(OH)_4$ which has solubility much lower than the limit of detection for ICP-MS. It is likely that the solid phase present in the samples is not crystalline thorianite but a more soluble amorphous $ThO_2 \cdot xH_2O$ species.

4.1.3.5 Eu (III) Speciation in Saturated $Ca(OH)_2$

The data below were entered into JCHESS to produce a speciation list and final solution pH:

$[Ca^{2+}] = 0.011$ mol dm^{-3}

$[OH^-] = 0.022$ mol dm^{-3}

$Eu^{3+} = 1 \times 10^{-3}$ mol dm^{-3}

$Cl^- = 3 \times 10^{-3}$ mol dm^{-3}

pH = 12.18

Table 113 Eu (III) speciation in saturated $Ca(OH)_2$

	mol dm^{-3}	**Species**
OH^-	0.018	Aqueous
Ca^{2+}	0.0097	Aqueous
Cl^-	0.0029	Aqueous
$CaOH^+$	0.0013	Aqueous
$CaCl^+$	3.04×10^{-6}	Aqueous
EuO_2^-	1.22×10^{-7}	Aqueous
$CaCl_2$	7.39×10^{-9}	Aqueous
$Eu(OH)_3$ (aq)	1.63×10^{-9}	Aqueous
$Eu(OH)_4^-$	9.95×10^{-10}	Aqueous
EuO_2H	8.34×10^{-11}	Aqueous
$Eu(OH)_2^+$	2.32×10^{-12}	Aqueous
H^+	7.55×10^{-13}	Aqueous
EuO^+	7.75×10^{-14}	Aqueous
$Eu(OH)_3$	0.00098	Mineral/Colloid

Predicted solubility of Eu (III) is the sum of all aqueous europium species and is in the region of 1 x 10^{-9} mol dm^{-3} which is within the range of experimental solubility values measured in section 3.3.3.

4.1.3.1 Eu (III) Speciation in 0.1 mol dm^{-3} NaOH

The following data were inputted into JCHESS and a species list plus a final solution pH were predicted as follows:

NaOH = 0.1 mol dm^{-3}

Eu^{3+} = 1 x 10^{-3} mol dm^{-3}

Cl^- = 3 x 10^{-3} mol dm^{-3}

pH = 12.88

Table 114 Eu (III) speciation in 0.1 mol dm^{-3} NaOH

	mol dm^{-3}	**Species**
Na^+	0.099	Aqueous
OH^-	0.096	Aqueous
Cl^-	0.0029	Aqueous
NaOH (aq)	0.00094	Aqueous
NaCl (aq)	2.99 x 10^{-5}	Aqueous
EuO_2^-	6.60 x 10^{-7}	Aqueous
$Eu(OH)_4^-$	5.37 x 10^{-9}	Aqueous
$Eu(OH)_3$ (aq)	1.63 x 10^{-9}	Aqueous
EuO_2H (aq)	8.34 x 10^{-11}	Aqueous
$Eu(OH)_2^+$	5.06 x 10^{-13}	Aqueous
H^+	1.65 x 10^{-13}	Aqueous
EuO^+	1.69 x 10^{-14}	Aqueous
$Eu(OH)_3$	0.001	Mineral/Colloid

The total concentration of Eu (III) predicted in solution is 6.6 x 10^{-7} mol dm^{-3} which, again, is within the range of Eu (III) solubility measured experimentally in section 3.3.3.

4.1.3.2 Ni (II) Speciation in Saturated $Ca(OH)_2$

The following data were put into JCHESS and a list of predicted species plus the final solution pH was generated.

$[Ca^{2+}]$ = 0.011 mol dm^{-3}

$[OH^-]$ = 0.022 mol dm^{-3}

Ni^{2+} = 1 x 10^{-3} mol dm^{-3}

NO_3^- = 2 x 10^{-3} mol dm^{-3}

pH = 12.20

Table 115 Ni (II) speciation in saturated $Ca(OH)_2$

	mol dm^{-3}	**Species**
OH^-	0.019	Aqueous
Ca^{2+}	0.0096	Aqueous
NO_3^-	0.002	Aqueous
$CaOH^+$	0.0013	Aqueous
$CaNO_3^+$	4.98 x 10^{-5}	Aqueous
$Ni(OH)_3^-$	5.66 x 10^{-7}	Aqueous
$Ni(OH)_2$ (aq)	2.96 x 10^{-8}	Aqueous
Ni^{2+}	2.18 x 10^{-12}	Aqueous
H^+	7.19 x 10^{-13}	Aqueous
$NiNO_3^+$	5.65x 10^{-15}	Aqueous
NiO (Bunsenite)	0.001	Mineral/Colloid

The combined Ni (II) aqueous species concentration is predicted to be within the region of 5.9 x 10^{-7} mol dm^{-3} which is within the range of Ni (II) solubility determined experimentally in section 3.3.5.

4.1.3.3 Ni (II) Speciation in 0.1 mol dm^{-3} NaOH

The following data were input into JCHESS to produce a speciation list and prediction of solution pH is given below:

NaOH = 0.1 mol dm^{-3}

Ni^{2+} = 1 x 10^{-3} mol dm^{-3}

NO_3^- = 2 x 10^{-3} mol dm^{-3}

pH = 12.88

Table 116 Ni (II) speciation in 0.1 mol dm^{-3} NaOH

	mol dm^{-3}	**Species**
Na^+	0.099	Aqueous
OH^-	0.097	Aqueous
NO_3^-	0.002	Aqueous
NaOH (aq)	0.00095	Aqueous
$Ni(OH)_3^-$	2.94×10^{-6}	Aqueous
$Ni(OH)_2$ (aq)	2.96×10^{-8}	Aqueous
H^+	1.63×10^{-13}	Aqueous
Ni^{2+}	1.32×10^{-13}	Aqueous
NiO (Bunsenite)	0.001	Mineral/Colloid

The total concentration of predicted Ni (II) species is 2.9 x 10-6 mol dm-3 which is within the experimentally measured Ni (II) concentrations described in section 3.3.5.

Although JCHESS has proven to be a useful predictive tool for metal solubilities in high pH solution, it is important to take into account the fact that the programme assumes the system has achieved equilibrium and that in some cases; the solubility limiting phase formed is crystalline. Under the experimental times scales investigated here, the precipitates formed are unlikely to be crystalline therefore observed concentrations of metal in solution are higher than predicted (due to a higher solubility of amorphous phases). JCHESS therefore underestimates the solubility of metals and care should be taken when using the data to predict metal behaviour.

4.2 Uptake of Superplasticiser and Metals by Cement

4.2.1 *Superplasticiser Uptake onto Cement Surfaces*

The mechanism of cement dispersion by a polycarboxylated superplasticiser involves adsorption onto the solid phase (the cement particles) while the extension of the polyethylene oxide side chains prevents cement agglomeration by steric repulsion (76)(23). Although steric repulsion is the dominant dispersive force for this type of superplasticiser, there is also evidence to suggest that short range electrostatic forces between the side chains may also contribute (13).

Polycarboxylated superplasticisers are said to bond chemically via their carboxyl and hydroxyl groups to calcium and aluminium ions on the cement surface (23). It has also been proposed more recently that this type of superplasticiser can intercalate into C_3A cement hydration products. In particular the layered double hydroxide $[Ca_4Al_2(OH)_{12}](SO_4)\cdot 6H_20$ (AF_m) which forms during the hydration of tricalcium aluminate phase with sulphate present in the cement (68). The result is an organo-mineral phase with a layered structure and a wider interlayer distance, depending on the size of the superplasticiser and the length of its side chains (25).

Mineral phases with a negative or neutral zeta potential do not adsorb large amounts of superplasticiser (25). A positive zeta potential therefore is key for superplasticiser sorption. This suggests that since ADVA Cast 551 adsorbs most significantly to OPC, it has the most positive zeta potential while BFS or PFA may have a negative or neutral zeta potential since no sorption is observed. To investigate this theory, zeta potential measurements of active slurry of each cement component were measured.

4.2.1.1 Zeta Potential of Cement Slurry

The zeta potential of a 1% active cement slurry in water was measured after one week intermittent shaking as described in section 2.6.2. Results are shown in Table 117.

Table 117 Zeta Potential of cement suspensions

Sample	Zeta Potential (mV)
BFS:OPC	-6.1 ± 0.3
PFA:OPC	-6.2 ± 0.5
PFA	-6.7 ± 0.3
BFS	-6.9 ± 0.4
OPC	-6.2 ± 0.6

The zeta potential results for each cement are very similar and not in keeping with the observed differences in superplasticiser sorption therefore they are inconclusive. The likely reason for this is method design and execution. Some of the cement slurry samples settled within the measurement cell therefore reducing the accuracy of the zeta potential measurement. Further method development is required before an accurate cement zeta potential may be

obtained. In comparison, Nagele (1986) and Nagele and Schneider (1989) (77,78) measured the zeta potential of BFS, PFA and Portland Cements at pH 12 and their results are shown in Table 118. These results support the theory and the experimental results that a negative zeta potential leads to no polycarboxylated sorption, whereas a positive zeta potential promotes significant sorption.

Table 118 Zeta Potential of BFS, PFA and Portland Cements

Cement Component	Zeta Potential (mV)	Reference
BFS	-5	(77)
PFA	-18	(77)
Portland Cement	+12	(78)

A further proposal for the effectiveness of superplasticiser sorption was put forward by Plank and Hirsch (2007)(25). They suggest the importance of the formation of the early cement hydration product ettringite (Af_t) or ($[Ca_6Al_2(OH)_{12}](SO_4)_3 \cdot 26H_2O$). With a positive zeta potential (+4.5 mV) the ettringite is able to sorb high quantities of the anionic superplasticiser.

Another factor in superplasticiser sorption is the specific surface area of the cement component. Table 20 (Page 51) gives the BET measurements for each cement and shows that BFS:OPC and PFA:OPC crushed grout have the highest surface area at 7.0966 and 4.0845 m^2/g respectively area while OPC is relatively low at 0.9898 m^2/g. This demonstrates that although a high surface area promotes superplasticiser sorption, zeta potential is the driving factor and a positive zeta potential is vital for polycarboxylated sorption.

4.2.2 *Extent of Metal Binding to Cement in the Presence of Superplasticiser*

Schlegel et al. (2004) suggest that Eu (III) uptake by C-S-H may be explained by Eu (III) surface complexation and Ca substitution within the structure (79). Ca substitution is possible due to the similarity in ionic radia between Eu and Ca in seven fold coordination (1.01 and 1.06 Å respectively) (80).

One reason for the decrease in both Ni (II) and Eu (III) uptake with increasing concentrations of ADVA Cast 551 is a solubility effect. Sections 2.5.2.1 and 2.5.2.2 show increases in solubility in the presence of ADVA Cast for Ni (II) and

Eu (III) respectively in free solution oversaturation experiments. The complexation of metal with the superplasticiser in solution could prevent metal binding to the cement surface by increasing the metal solubility.

As shown in 3.4.1 and 3.4.2, ADVA Cast 551 binds significantly to BFS:OPC and PFA:OPC grout respectively. The superplasticiser may therefore saturate the cement solid surface and block uptake sites that would have otherwise been available to the metal.

It is unlikely that high concentrations of ADVA Cast 551 (1%) will be available in the pore water of cement or concrete. At lower concentrations (0.2% ADVA Cast 551) Ni (II) uptake is affected less with a reduction is binding of only 15% and 5% for BFS:OPC and PFA:OPC respectively. Eu (III) however shows a reduction in uptake of at least 50% in both cases of BFS:OPC and PFA:OPC with the presence of 0.2% ADVA Cast. This is a significant finding, since uptake by cementitious materials is one of the key engineered barriers to radionuclide migration in the design of the GDF.

Results for the reversibility of Ni (II) and Eu (III) uptake shows that with no superplasticiser present in free solution, metal binding is irreversible, while in the presence of superplasticiser, metal binding is much more labile. >98% of metal was re-suspended in both cases of PFA:OPC and BFS:OPC where 0.5% and 1% superplasticiser was present in the original solution (it should be noted that no superplasticiser was added to solution during the de-sorption experiment).

In the case of uptake of Ni (II) and Eu (III) to cement prepared with superplasticiser, metal uptake is >98% in both cases to BFS:OPC and PFA:OPC. The binding is not reversible on the most part with a negligible amount of superplasticiser re-suspended during the reversibility experiment. The absence of free ‘ligand’ precludes solubility enhancement but, equally, the superplasticiser (0.5% ADVA Cast 551) is obviously not effective at blocking metal binding sites when incorporated into the cement. Interactions between the superplasticiser and the cement during the early stages of hydration lead to the polymer becoming incorporated into cement hydration phases and, therefore, unavailable for subsequent interactions with the metals. Direct

evidence that the first few seconds in the crystallisation of cement are crucial to its development has recently been obtained using *in situ* synchrotron X-ray diffraction by (81).

4.3 Leaching of Superplasticiser and Metals from Hardened Cement Monoliths

Leaching experiments showed a small proportion of superplasticiser leaches from hardened cement over the investigated time period of 4 months. Low leaching of superplasticiser is attributed to chemisorption and intercalation of the polymer into organo-mineral cement phases, formed during the cement hydration process.

At the very early stages of the hydration process, polycarboxylated superplasticiser retards cement hydration. This occurs by the adsorption of the anionic superplasticiser onto the positively charged C_3A phases. Retardation occurs as the adsorbed polymer hinders the reaction between C_3A and sulphate ions to form ettringite (81). As the reactions proceed, the superplasticiser chains are incorporated into the cement hydration products.

Transport of contaminants (leaching) may be considered in terms of cement permeability and as such it is well recognised that transport occurs through a continuous network of cement pores. Pore structure within cement defines the paths along which liquid preferentially moves. The source of matrix porosity that contributes to permeability is associated with the residual space between cement grains that was originally filled with water. The water is consumed via incorporation into the cement hydration products (e.g. CSH).

In the metal leaching experiment, the only metal to leach in a measurable concentration from BFS:OPC cement was Ni (II), however <0.01% of the total added Ni was detected. Ni (II) and U (VI) were observed to leach from PFA:OPC during the leach test and a significantly higher amount of metal was leached from cement that contained superplasticiser. The porosity of cement in the presence of polycarboxylated superplasticiser is thought to be lower than cement prepared without cement (25,26) therefore it may be expected that less metal transport (leaching) would be observed in cement prepared with the superplasticiser. This was not observed to be the case and suggests that it is

not only cement permeability that controls leaching but also the consequences of the superplasticiser interaction with the metal (complexation). Permeability of cement is generally considered to decrease with time as hydration reactions proceed. It would be beneficial to investigate the kinetics of metal leaching to observe any relationships between metal leaching and time (with and without the presence of superplasticiser). It may then be possible to understand the role of the superplasticiser in metal leaching and thus the implications of the addition of the superplasticiser to cement for the encapsulation of radioactive contaminants.

4.3.1 *Significance of Cement Bleed in Metal Leaching Experiments*

An interesting observation was made on the preparation of BFS:OPC cement where a significant amount of cement bleed was observed over 48 hours. A similar observation was made by Morgan and Constable (2008) (53) where much more bleed and segregation was observed in a 9:1 BFS:OPC than a 3:1 PFA:OPC cement mix prepared with 0.3% and 0.8% ADVA Cast 551. It was stipulated that this phenomenon is due to deflocculation of the cement particles due to the presence of the superplasticiser. This in turn leads to a greater packing density of powders on curing. This hypothesis however has not been confirmed. Analysis of this bleed water indicated a large proportion of the added metals were present. The amount of metal in the bleed water was significantly higher in the samples that contained superplasticiser.

Autoradiography of the cement blocks showed that U (VI) and Th (IV) accumulated at the top surface of the block that was in contact with the bleed water during the set time. In samples that were prepared with no superplasticiser, autoradiography showed that the activity (or metal) distribution was homogenous throughout the sample. The significant leach of metal in the bleed is associated with the effect of superplasticiser on the metal solubility. The formation of mixed complexes associated between the metal and the aqueous metal hydroxide species keep the metal in solution (the bleed water) which in turn means the sample will not be homogenous.

4.4 Stability of Superplasticiser

4.4.1 *Superplasticiser Analysis*

Characterisation of the products of ADVA Cast 551 stability experiments has identified changes in the chemical and physical properties of ADVA Cast 551, under conditions representative of the geological disposal facility. Several techniques were used to analyse and characterise ADVA Cast 551 with varied success. UV spectroscopy and Gas Chromatography- Mass Spectrometry were discounted from further experiments as no information regarding the polymer was gained using these techniques. Structural information regarding the polymer's functionality was obtained from IR data while molecular weight information was obtained using both Electrospray Ionisation–Mass Spectrometry and Gel Permeation Chromatography with Refractive Index detection.

4.4.2 *Superplasticiser Stability*

Under alkaline conditions, some degree of alkaline hydrolysis takes places which results in the presence of lower molecular weight polymer fragments, however instrumental limitations (ESI-MS) have meant that identification of the very high molecular weight polymer fractions was not possible. GPC has presented some results which give molecular weight ranges, but not to a high resolution. There is little degradation of the sample observed under the temperature stability test, despite the visible change in colour between the fresh and temperature stability samples. Radiolysis has the greatest effect on the superplasticiser, with visible evidence of polymerisation occurring in the presence of ionising radiation at a total dose of 220 kGy. At the lower dose of 64 kGy, GPC evidence suggests polymerisation has been initiated in the sample since a molecular weight fraction higher than that of the 'as received' material is observed.

4.4.2.1 Radiation Induced Polymerisation

Polymerisation initiated by ionising radiation can be carried out by both a free radical and an ionic mechanism. The determining factor is the nature of the end of the growing chain. In the case of ADVA Cast 551 the end of the growing

chain may be the methacrylate backbone or the poly ether comb type polymer side chains.

The formation of radiation induced free radicals which initiate polymerisation is explained by Ivanov (82). Monomer, M, ionisation can occur due to Compton's effect where inelastic scattering of photons in matter, results in a decrease in gamma ray energy and part of this energy is transferred to a scattering electron. The electrons recoils and is ejected from its atom. This effect forms an electron which can induce secondary ionisation processes (Equation 12)

Equation 12 Monomer Ionisation

This primary electron e is transformed into a 'thermal' electron which means it attains thermal equilibrium with the medium. The thermal electron is trapped by ions formed from monomers M^+ through their conversion to activated molecules, M* via Equation 13.

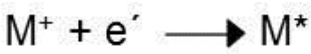

Equation 13 Monomer conversion to an activated molecule.

The activated monomer M* is in an excited state and has an energy reserve of ca. 8-15 eV which exceeds the strength of a covalent bond in an organic molecule (around 3 eV). Decomposition occurs and the formation of a free radical, which in turn is responsible for initiating polymerisation (Equation 14).

Equation 14 Formation of free radicals

If the monomer M is not exposed to sufficient radiation energy to attain ionisation, a similar activated monomer M** may be generated directly, also via Compton's effect (Equation 15).

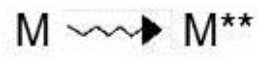

Equation 15 Direct generation of an activated monomer

This activated monomer M** can then undergo free radical decomposition as shown in Equation 16. The probability of the formation of M* or M** are equal.

Equation 16 Free radical decomposition of an activated monomer

An example of primary reactions of methyl methacrylate polymerisation (a polymer with similar functionality to ADVA Cast 551) is given by Lipscomb and Weber (83) and is shown in Table 119 along with the rate expression for each step.

K_x is the rate constant, M is the monomer, R· is a radical, RM· is the result of a monomer reacting with a free radical and P is a growing polymer chain.

Table 119 Polymerisation of methyl methacrylate

Reaction	Equation	Rate Expression
Primary Initiation	k_1 $M + \gamma \longrightarrow R\cdot$	$-d[M]/dt = k_1[M]$
Chain Initiation	k_2 $R\cdot + M \longrightarrow RM\cdot$	$d[RM\cdot]/dt = k_2[R\cdot][M]$
Propagation	k_3 $RM_n\cdot + M \longrightarrow RM\cdot_{n+1}$	$d[M\cdot_{n+1}]/dt = k_3[RM_n\cdot][M]$
Transfer	$RM_n\cdot + MH \rightarrow RM_nH + M\cdot$	-
	$RM_n\cdot + PH \rightarrow RM_nH + P\cdot$	-
Termination	k_4 $RM_n\cdot + RM_n\cdot \rightarrow RM_nM_nR$	$-d[RM_n\cdot]/dt = k_4[RM_n\cdot]^2$
	k_4' $RM_n\cdot + R\cdot \longrightarrow RM_nR$	$-d[RM_n\cdot]/dt = k_4'[RM_n\cdot][R\cdot]$

In the past, a number of superplasticisers have been discounted for use in a radioactive waste disposal context due to complexation of metals with the polymers (as described in Section 1.5.2). In comparison to HS-100 and HS-700 (HS-100 is a naphthalene sulphonic acid condensation and lignin sulphuric acid derivative polymer while HS-700 is a polycarboxylated superplasticiser with a similar structure to ADVA Cast 551), and using the example of U(VI), ADVA Cast 551 has a significantly higher solubilising effect than either of the two polymers. The solubility enhancement in the presence of ADVA Cast 551 is orders of magnitude more at all concentrations of ADVA Cast 551 investigated here. Since ADVA Cast 551 and HS-700 are both grouped within the 'Polycarboxylate Superplasticisers', this suggests that although the polymers may be based on a similar structure, the exact nature of their interactions with aqueous species are different and should be considered and assessed separately.

In contrast, in comparison to Sulphonated naphthalene formaldehyde polymers and sulphonated melamine formaldehyde polymers (also described in section 1.5.2), the solubility enhancement of ADVA Cast 551 is much lower than observed for those types of polymers.

As the development of superplasticiser technology continues, novel superplasticiser should be assessed thoroughly before application in a radioactive waste context. It is possible to make estimations of stability constants of complexes between superplasticiser and metals however these calculations have a number of limitations. These include the availability of reliable thermodynamic equilibrium data for the equilibrium between dissolved species and the solid phase – numerous sources of K_{sp} for the equilibrium between metal precipitates and dissolved species are available relevant to high pH however they are applicable to crystalline solid phases and not the amorphous precipitates that are present experimentally on the time scales presented here. There is also uncertainty relating to the superplasticiser structure and therefore binding mechanisms and availability of binding sites are also calculated speculatively. Predictive modelling of interactions of superplasticiser with metals can therefore only be considered with supplemented experimental data.

4.5 Recommendations for Further Work

It has been widely documented, that the addition of organics to radioactive waste matrixes can cause an increase in radionuclide solubility and migration and should, if possible be avoided. However, in the case of superplasticiser, there are so many benefits associated with the addition of these organic polymers to cement, that research in to the consequences of their addition should continue.

To gain further knowledge on the behaviour of radionuclides in the presence of ADVA Cast 551, it is important to assess the solubility of higher activity actinides such as Am (III) and Pu (IV) which are important contributors to the UK waste inventory. Some work has been conducted by Clacher et al (2009, 2010) where solubility of the metals is measured in $Ca(OH)_2$ or NaOH (84,85).

$Ca(OH)_2$ and NaOH provide a simple solution in which to measure metal solubility at high pH, however the presence of a range of elements at varying concentration that will be present in cement pore water should be taken into account. In this research, cement equilibrated water is used as representative solution similar to that of cement pore water. Other authors have used produced artificial cement pore water to investigate metal solubility (86). There is uncertainty in the composition of cement equilibrated water compared to that of actual cement pore water. It would be beneficial, to extract the pore water from cured cement and complete solubility experiments using the extracted fluid.

A proposed method for this experimental process is given below:

4.5.1 *Solubility of Metals in Pore Squeeze Cement Water*

There are a number of methods for the mechanical extraction of cement pore water reported in the literature (87-89). The main limitation to these methods is that a large amount of hardened cement is required to produce a sufficient amount of pore water for the experiments. The aim of the experiment in this case would be to measure the solubility of metals in squeeze pore water of cement prepared with and without superplasticiser. This would give an opportunity not only to investigate the consequence of superplasticiser addition

on metal solubility but also gain knowledge on the fate of superplasticisers within the hardened cement.

For this experiment, two grout formulations containing ADVA Cast 551 at 0.5% (v/w) should be prepared. A 9:1 BFS:OPC grout and a 3:1 PFA:OPC grout both having a water to solids ratio of 0.36. The grouts will be prepared and cured for 100 days in >90% humidity before the pore squeeze process. Blank grouts not containing superplasticiser should also be prepared in order to investigate the quantity of superplasticiser (either whole or as degradation products) that has been expressed in the pore fluid.

A high pressure, pore solution expression device is available in the Department of Materials at Loughborough University. For the pore expression, cylindrical samples of each grout should be cast with dimensions of 49 mm diameter and 75 mm length.

For extraction, the specimen is placed on the base of the pore press and the pressure increased through the piston to 150 MPa gradually. Using this method, around 3 cm^3 of solution may be collected from each specimen. Although pore solution expression can be a tedious process, the resulting expressed fluid has a uniform composition. It is possible to avoid the pore solution coming into contact with air by using a hypodermic needle to collect the expressed fluid thus reducing the effects of carbonation.

Additionally, the effect of irradiation on the composition of cement pore water and in turn the solubility of metals in the pore squeeze solution may be investigated by preparation of cement as above, and irradiation of the blocks at a ^{60}Co facility. This type of experiment would enable to fate of superplasticiser in cement pore water after radiolysis to be investigated. Since crosslinking and copolymerisation of the polymer was observed on radiolysis of a neat sample, it would be interesting to characterise the size range of the organic products present in the pore solution after radiolysis.

4.5.2 *Further Characterisation of Superplasticiser and Products Resulting from Stability Experiments.*

This research has demonstrated the challenges faced in the characterisation of superplasticiser and in particular the products that result from stability experiments. Although the gel permeation chromatography results obtained were encouraging, it would be beneficial to increase the resolution obtained during separation of the superplasticiser size fractions. GPC has been applied to the length sorting and purification of DNA wrapped carbon nanotubes (DNA-CNT) which processes the fractions into uniform length. This is achieved by passing the sample through several columns with different pore sizes (90). A similar application may be made to superplasticiser separation and would be particularly useful for the molecular weight determination of degradation products.

Another area of interest is the design and synthesis of a novel superplasticiser that is tailored to the requirements of radioactive waste disposal. This could be a superplasticiser which is effective in cement dispersion but does not increase the solubility of radionuclides. The design of such a polymer would determine and reduce the functionality of the polymer that is responsible for metal coordination whilst giving the opportunity for the establishment of a performance envelope for superplasticiser quality (including limits for impurities within the raw material). The commercial nature of superplasticiser research means that little is available on superplasticiser synthesis in the literature. However, Zhang et al. (2008) and Lu et al. (2010) (91)(92) report methods of superplasticiser production. In these cases, the methods are tailored to producing superplasticiser with optimized molecular structure for such this paste fluidification, cement workability or an increase in mechanical properties of cement. It may be possible however to tailor superplasticiser structure to specific requirements for use in radioactive waste disposal.

4.5.3 *Leaching Behaviour of Radionuclides from Hardened Cement*

The success of autoradiography in the imaging of activity in cement blocks could be utilised further. Since SEM was proven to be an unsuccessful technique for the determination/ imaging of non-active Ni in cement. The

leaching experiment and subsequent imaging could be repeated using radioisotopes. This could be extended further to other isotopes of interest such as europium, caesium and strontium.

BFS:OPC cement showed excessive bleed when prepared with 0.5% (w/s) ADVA Cast 551. This bleed water was found to contain a high proportion of the metal intended to be encapsulated in the hardened cement. Experiments to investigate the optimisation of superplasticiser dosage to BFS:OPC cement formulations may reduce this associated bleed water and allow a more homogenous cement to be produced; again, autoradiography may be employed to confirm the homogeneity of the samples.

5 References

(1) Defra. Managing Radioactive Waste Safely: A framework for Implementing Geological Disposal.
A White Paper by Defra, BERR and the devolved administrations for Wales and Northern Ireland. 2008.

(2) CoRMW. Managing our Radioactive Waste Safely - CoRWM's Recommendations to Government. 2006;CoRWM Document 700.

(3) Poyry Energy Ltd. The 2010 UK Radioactive Waste Inventory; Report produced for the Department of Energy and Climate Change (DECC) and the Nuclear Decommissioning Authority (NDA). 2011;URN 10D/987 NDA/ST/STY(11)006.

(4) Glasser F. Mineralogical aspects of cement in radioactive waste disposal. Mineral Mag 2001 65(5):621-633.

(5) Taylor H.F.W. Cement Chemistry. 2nd ed. London: Thomas Telford; 1997.

(6) Lea F.M., Desch C.H. The Chemistry of Cement and Concrete. Edward Arnold; 1970.

(7) Bogue R.H. The Chemistry of Portland Cement. 2nd ed. New York, USA: Reinhold Publishing Corporation; 1955.

(8) Environment Agency. Blast furnace slag (BFS): A technical report on the manufacturing of blast furnace slag and materials status in the UK. 2007.

(9) Williams R.P., van Riessen A. Determination of the reactive component of fly ashes for geopolymer production using XRF and XRD RID. Fuel 2010 89(12):3683-3692.

(10) Joshi R.C., Lohtia R.P. Fly Ash in Concrete: Production Properties and Uses. Netherlands: Gordon and Breach Science Publishers; 1997.

(11) Pavia S., Condren E. Study of the Durability of OPC versus GGBS Concrete on Exposure to Silage Effluent. Journal of Materials in Civil Engineering 2008;20:313.

(12) Mindess S., Young J.F. Concrete. Englewood Cliffs, NJ: Prentice- Hall; 1981.

(13) Jolicoeur C., Simard M. Chemical Admixture-Cement Interactions: Phenomenology and Physico-chemical Concepts. Cement and Concrete Composites 1998 20(2-3):87-101.

(14) Glasser F.P. Chemistry of Cement-Solidified Waste Forms. In: Spence RD, editor. Chemistry and Microstructure of Solidified Waste Forms Boca Raton, USA: Lewis Publishers; 1993.

(15) Evans N.D.M. Binding Mechanisms of Radionuclides to Cement. Cement and Concrete Research 2008 38(4):543-553.

(16) Bayliss S., Howse R.M, McCrohon R, Oliver P, Smith-Briggs J.L, Thomason H.P. Near Field Sorption Studies: UK Nirex Report. 2000;AEAT/ERRA-0073.

(17) Glasser F. P. Characterisation of the Barrier Performance of Cements. Scientific Basis for Nuclear Waste Management Xxv 2002;713:721-732.

(18) Peiwei G., Min D., Naiqian F. The Influence of Superplasticizer and Superfine Mineral Powder on the Flexibility, Strength and Durability of HPC. Cement and Concrete Research 2001 31(5):703-706.

(19) Ramachandran V.S- Editor. Concrete Admixtures Handbook. 2nd ed. New Jersey, USA: Noyes Publications; 1995.

(20) Hewlett P.C.- Editor. Lea's Chemistry of Cement and Concrete. 4th ed. New York, USA: John Wiley & Sons Inc.; 1998.

(21) Yamada K., Takahashi T., Hanehara S., Matsuhisa M. Effects of the Chemical Structure on the Properties of Polycarboxylate-type Superplasticizer. Cement and Concrete Research 2000 30(2):197-207.

(22) Hanehara S., Yamada K. Interaction between Cement and Chemical Admixture from the Point of Cement Hydration, Absorption Behaviour of Admixture and Paste Rheology. Cement and Concrete Research 1999 29(8):1159-1165.

(23) Yoshioka K., Sakai E., Daimon M., Kitahara A. Role of Steric Hindrance in the Performance of Superplasticizers for Concrete. Journal of the American Ceramic Society 1997 80(10):2667-2671.

(24) Mollah M., Adams W., Schennach R., Cocke D. A Review of Cement-Superplasticizer Interactions and their Models. Advances in Cement Research 2000 OCT;12(4):153-161.

(25) Plank J., Hirsch C. Impact of Zeta Potential of Early Cement Hydration Phases on Superplasticizer Adsorption. Cement and Concrete Research 2007 37(4):537-542.

(26) Puertas F., Santos H., Palacios M., Martinez-Ramirez S. Polycarboxylate Superplasticiser Admixtures: Effect on Hydration, Microstructure and Rheological Behaviour in Cement Pastes. Advances in Cement Research 2005 17(2):77-89.

(27) Choppin G.R, Liljenzin J., Rydberg J. Radiochemistry and Nuclear Chemistry. 3rd ed.: Butterworth Heinemann; 2001.

(28) Argonne National Laboratory. Human Health Fact Sheet - Nickel. 2005; Available at: http://www.ead.anl.gov/pub/doc/nickel.pdf. Accessed 28th March, 2012.

(29) Sutton M. Uranium Solubility, Speciation and Complexation at high pH; PhD Thesis, Loughborough University 1999.

(30) Fujiwara K., Yamana H., Fujii T., Kawamoto K., Sasaki T., Moriyama H. Solubility Product of Hexavalent Uranium Hydrous Oxide. Journal of Nuclear Science and Technology 2005 42(3):289-294.

(31) Ewart F.T. The Solubility of Actinides in a Cementitious Near-Field Environment. Waste Management 1992 12(2-3):241-252.

(32) Wierczinski B., Helfer S., Ochs M., Skarnemark G. Solubility Measurements and Sorption Studies of Thorium in Cement Pore Water. Journal of Alloys and Compounds 1998 12;271:272-276.

(33) Neck V., Altmaier M., Muller R., Bauer A., Fanghanel T., Kim J. Solubility of Crystalline Thorium Dioxide. Radiochimica Acta 2003 91(5):253-262.

(34) Ochs M., Hager D., Helfer S., Lothenbach B. Solubility of Radionuclides in Fresh and Leached Cementitious Systems at 22 degrees C and 50 degrees C. Scientific Basis for Nuclear Waste Management 1998 506:773-780.

(35) Aldridge S. Some Aspects of Near Field Chemistry in a Nuclear Waste Repository, PhD Thesis, Loughborough University 2005.

(36) Ramirez-Garcia J.J., Jimenez-Reyes M., Solache-Rios M., Fernandez-Ramirez E., Lopez-Gonzalez H., Rojas-Hernandez A. Solubility and First Hydrolysis Constants of Europium at Different Ionic Strength and 303 K. Journal of Radioanalytical and Nuclear Chemistry 2003 257(2):299-303.

(37) Jimenez-Reyes M., Solache-Rios M., Rojas-Hernandez A. Application of the Specific Ion Interaction Theory to the Solubility Product and First Hydrolysis Constant of Europium. Journal of Solution Chemistry 2006 35(2):201-214.

(38) Mattigod S.V., Rai D., Felmy A.R., Rao L.F. Solubility and Solubility Product of Crystalline Ni(OH)(2). Journal of Solution Chemistry 1997 26(4):391-403.

(39) Felmy A. R., Qafoku O. An Aqueous Thermodynamic Model for the Complexation of Nickel with EDTA valid to High Base Concentration. Journal of Solution Chemistry 2004 33(9):1161-1180.

(40) Palmer D.A., Gamsjaeger H. Solubility Measurements of Crystalline Beta-Ni(OH)(2) in Aqueous Solution as a Function of Temperature and pH. Journal of Coordination Chemistry 2010 63(14-16):2888-2908.

(41) Hummel W., Anderegg G., Puigdomenech I., Rao L., Tochiyama O. The OECD/NEA TDB Review of Selected Organic Ligands. Radiochimica Acta 2005 93(11):719-725.

(42) Warwick P., Evans N., Lewis T. Effect of "As Disposed" Complexants on the Solubility of Nickel (II), Thorium (IV) and Uranium (VI). 2008 NR3256A.

(43) Cetiner Z.S. Initial Assessment of Hydrous Thorium(IV) Solubility and Speciation in Geological Environments: An Experimental Approach in the Presence of Organic Ligands. Asian Journal of Chemistry 2007 19(4):3228-3238.

(44) McCrohon R., Williams S.J. Effect of Sikament 10 Superplasticiser on Radionuclide Solubility: A report produced for UK Nirex Ltd. 1997.

(45) Boult K., McCrohon R., Williams S.J. Further Experiments on the Effects of Sikament 10 and Sikament N on Plutonium Solubility: A report produced for UK NIREX Ltd. 1998

(46) Greenfield B., Ilett D., Ito M., McCrohon R., Heath T., Tweed C., et al. The Effect of Cement Additives on Radionuclide Solubilities. Radiochimica Acta 1998 82:27-32.

(47) Palardy D, Onofrei M, Ballivy G. Microstructural Changes due to Elevated Temperature in Cement Based Grouts. Advanced Cement Based Materials 1998 8(3-4):132-138.

(48) Ruckstuhl S., Suter M., Kohler H., Giger W. Leaching and Primary Biodegradation of Sulfonated Naphthalenes and their Formaldehyde Condensates from Concrete Superplasticizers in Groundwater affected by Tunnel Construction. Environmental Science and Technology 2002 1;36(15):3284-3289.

(49) Yilmaz V., Odabasoglu M., Icbudak H., Olmez H. The Degradation of Cement Superplasticizers in a High Alkaline-Solution Cement and Concrete Research 1993 23(1):152-156.

(50) Colak A. Properties of Plain and Latex Modified Portland Cement Pastes and Concretes with and without Superplasticizer. Cement and Concrete Research 2005 35(8):1510-1521.

(51) Chandler K., Constable M., Dawson J., Morgan S. Gamma Irradiation Testing of Grout and Aqueous Samples Containing ADVA Cast 550: A report produced for Magnox Electric Ltd. (North). 2008;4510177929 (14-2007/08N).

(52) Baillie L.A. Determination of Liquid Scintillation Counting Efficiency by Pulse Height Shift. International Journal of Applied Radiation and Isotopes 1960 8:1-7.

(53) Morgan S., Constable M. Superplasticiser Irradiation Trials: Preparation and Evaluation Testing of Grout Samples Containing ADVA Cast 551. A report produced for Magnox Electric Ltd (North). 2008;4510177929 (14-2007/08N additional task).

(54) Dean J.R. Methods for Environmental Trace Analysis. Vol 12 of Analytical Techniques in the Sciences ed. USA: Wiley; 2003.

(55) Kemp S.J., Turner G., Wagner D. Initial Testing and a Laboratory Manual for the Micromeritics Gemini VI Physisorption System. 2009;IR/08/086.

(56) Thomas J.J, Jennings H.M., Allen A.J. The Surface Area of Hardened Cement Paste as Measured by Various Techniques. 1999;1:45-64.

(57) Grace Construction Products Ltd. Material Safety Data Sheet: ADVA Cast 551. 2009.

(58) Yoshioka K., Tazawa E., Kawai K., Enohata T. Adsorption Characteristics of Superplasticizers on Cement Component Minerals. Cement and Concrete Research 2002 32(10):1507-1513.

(59) Ran Q., Somasundaran P., Miao C., Liu J., Wu S., Shen J. Effect of the Length of the Side Chains of Comb-like Copolymer Dispersants on Dispersion and Rheological Properties of Concentrated Cement Suspensions. Journal of Colloid and Interface Science 2009 15;336(2):624-633.

(60) Sutton M., Warwick P., Hall A., Jones C. Carbonate Induced Dissolution of Uranium Containing Precipitates under Cement Leachate Conditions. Journal of Environmental Monitoring 1999 1(2):177-182.

(61) Takahashi S., Sakai E., Sugiyama T. Study on Leaching of Hexavalent Chromium from Hardened Concretes Using Tank Leaching Test. Journal of Advanced Concrete Technology 2007 5(2):201.

(62) Conner J.R. Chemical Fixation and Solidification of Hazardous Wastes. USA: Van Nostrand Reinhold; 1990.

(63) Amemiya Y., Miyaharal J. Imaging Plate Illuminates Many Fields. Nature 1988 3;336(6194):89-90.

(64) Azenha M., Faria R., Ferreira D. Identification of Early-age Concrete Temperatures and Strains: Monitoring and numerical simulation. Cement and Concrete Composites 2009 7;31(6):369-378.

(65) Sivaji K., Murty, G. S. R. N. Kinetics of Sulfite Oxidation Reaction. Industrial and Engineering Chemistry Fundamentals 1982;21:344-352.

(66) Satake H., Hisano T., Ikeda S. The Rapid Determination of Sulfide, Thiosulfate, and Polysulfide in the Lixiviation Water of Blast-furnace Slag by Means of Argentimetric Potentiometric Titration. Bulletin of the Chemical Society of Japan 1981;54(7):1968 - 1971.

(67) Altmaier M., Neck V., Fanghaenel T. Solubility of Zr(IV), Th(IV) and Pu(IV) Hydrous Oxides in CaCl(2) Solutions and the Formation of Ternary Ca-M(IV)-OH Complexes. Radiochimica Acta 2008 96(9-11):541-550.

(68) Plank J., Dai Z., Andres P.R. Preparation and Characterization of new Ca-Al-Polycarboxylate Layered Double Hydroxides. Materials Letters 2006 60(29-30):3614-3617.

(69) Kaplan D.I., Serkiz S.M., Allison J.D. Europium Sorption to Sediments in the Presence of Natural Organic Matter: A laboratory and modeling study. Applied Geochemistry 2010 25(2):224-232.

(70) Pearson R. Hard and Soft Acids and Bases. Journal of the American Chemical Society 1963 85(22):3533-&.

(71) Van der Lee J., JCHESS 2.0. Ecole des Mines de Paris, Centre d'Informatique Geologique, Paris, 2000, http://chess.geosciences.ensmp.fr/

(72) Bond K.A., Moreton A.D., Heath T.G. The HATCHES User Manual. 1992.

(73) Chase M.W., Sauerwein J.C. NIST Standard Reference Data Products Catalog 1994. NIST Special Publication 782.

(74) Duff M., Coughlin J., Hunter D. Uranium Co-precipitation with Iron Oxide Minerals. Geochimica Cosmochimica Acta 2002 66(20):3533-3547.

(75) Opel K., Weiss S., Huebener S., Zaenker H., Bernhard G. Study of the Solubility of Amorphous and Crystalline Uranium Dioxide by Combined Spectroscopic Methods. Radiochimica Acta 2007 95(3):143-149.

(76) Mikanovic N., Jolicoeur C. Influence of Superplasticizers on the Rheology and Stability of Limestone and Cement Pastes. Cement and Concrete Research 2008 38(7):907-919.

(77) Nagele E., Schneider U. The Zeta-Potential of Blast-Furnace Slag and Fly-Ash. Cement and Concrete Research 1989 19(5):811-820.

(78) Nagele E. The Zeta-Potential of Cement.2. Effect of Ph-Value. Cement and Concrete Research 1986 16(6):853-863.

(79) Schlegel M., Pointeau I., Coreau N., Reiller P. Mechanism of Europium Retention by Calcium Silicate Hydrates: An EXAFS study RID G-4731-2010. Environmental Science and Technology 2004 15;38(16):4423-4431.

(80) Shannon R. Revised Effective Ionic-Radii and Systematic Studies of Interatomic Distances in Halides and Chalcogenides. Acta Crystallographica Section A 1976;32(1):751-767.

(81) Schlegel M., Sarfraz A., Müller U., Panne U., Emmerling F. First Seconds in a Building?s Life?In?Situ Synchrotron X-Ray Diffraction Study of Cement Hydration on the Millisecond Timescale. Angewandte Chemie International Edition 2012;51(20):4993-4996.

(82) Ivanov V.S., Radiation Chemistry in Polymers: Volume 5 of New Concepts in Polymer Science. Netherlands: Kononklijke Wohmann B. V.; 1992.

(83) Lipscomb N., Weber E. Kinetics of Gamma-Radiation-Induced Low Temperature Polymerization of Methyl Methacrylate. Journal of Polymer Science Part A-General Papers 1965 3(1PA):55.

(84) Clacher A., Cowper M. Effect of ADVA Cast 551 on the Solubility of Plutonium (IV) and Uranium (VI). 2009.

(85) Clacher A., Marshall T, Swanton S. Solubility Studies: Effect of ADVA Cast 551 in Low Concentration. 2010;SERCO/TCS/004249/001.

(86) Wieland E., Tits J., Ulrich A., Bradbury M. Experimental Evidence for Solubility Limitation of the Aqueous Ni(II) Concentration and Isotopic Exchange of Ni-63 in Cementitious Systems. Radiochimica Acta 2006;94(1):29-36.

(87) Bjork F., Eriksson C.A. Measurement of Alkalinity in Concrete by a Simple Procedure, to Investigate Transport of Alkaline Material from the Concrete Slab to a Self-levelling Screed. Construction and Building Materials 2002 16(8):535-542.

(88) Tritthart J. Chloride binding in cement I. Investigations to Determine the Composition of Porewater in Hardened Cement. Cement and Concrete Research 1989 7;19(4):586-594.

(89) Dehwah H.A.F., Maslehuddin M., Austin S.A. Effect of Cement Alkalinity on Pore Solution Chemistry and Chloride-induced Reinforcement Corrosion. ACI Materials Journal 2002 99(3):227-233.

(90) Huang X.Y., McLean R.S., Zheng M. High-resolution Length Sorting and Purification of DNA-wrapped Carbon Nanotubes by Size-Exclusion Chromatography. Analytical Chemistry 2005 77(19):6225-6228.

(91) Zhang R., Li Q., Zhang A., Liu Y., Lei J. The Synthesis Technique of Polyacrylic Acid Superplasticizer. Journal of Wuhan University of Technology-Materials Science Edition 2008 23(6):830-833.

(92) Lu S., Liu G., Ma Y., Li F. Synthesis and Application of a New Vinyl Copolymer Superplasticizer. Journal of Applied Polymer Science 2010 117(1):273-280.

(93) Petit J., Wirquin E., Duthoit B. Influence of Temperature on Yield Value of Highly Flowable Micromortars made with Sulfonate-based Superplasticizers. Cement and Concrete Research 2005 35(2):256-266.

(94) Plank J., Schroefl C., Gruber M., Lesti M., Sieber R. Effectiveness of Polycarboxylate Superplasticizers in Ultra-High Strength Concrete: The Importance of PCE Compatibility with Silica Fume. Journal of Advanced Concrete Technology 2009 7(1):5-12.

(95) Stumm W., Morgan J. J., Aquatic Chemistry; Chemical Equilibria and Rates in Natural Waters, 3rd Edition, John Wiley &Sons Inc, New York, 1996

(96) Dyer J. A., Scrivner N. C., Dentel S. K., A Practical Guide for Determining the Solubility of Metal Hydroxides and Oxides in Water, Environmental Progress 2006 7 (1)

6 APPENDIX

6.1 APPENDIX 1 – Instrument Calibration Data

6.1.1 *ICP-OES*

6.1.1.1 Aluminium

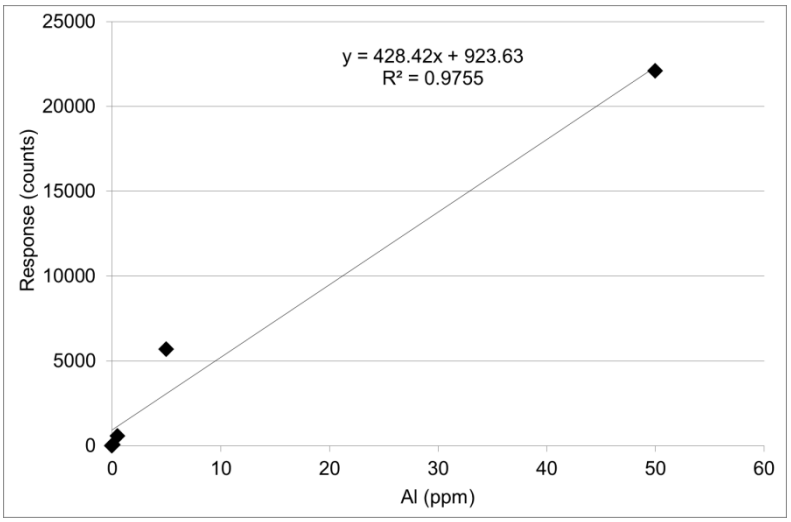

6.1.1.2 Arsenic

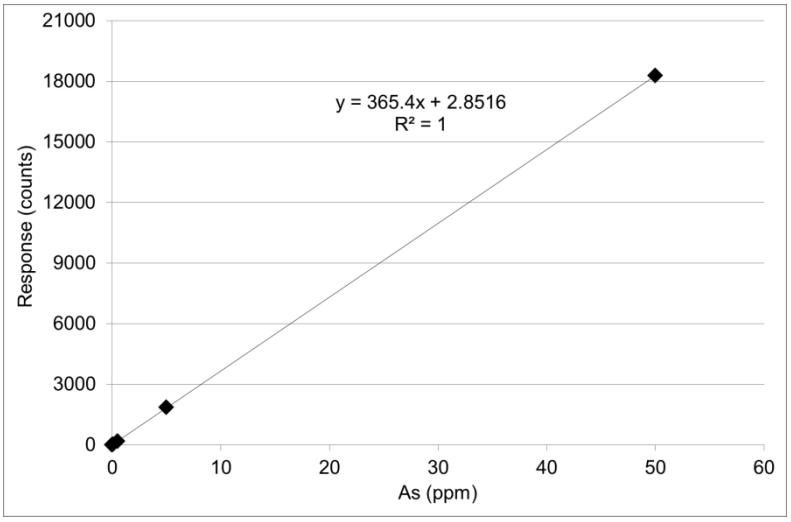

6.1.1.3 Barium

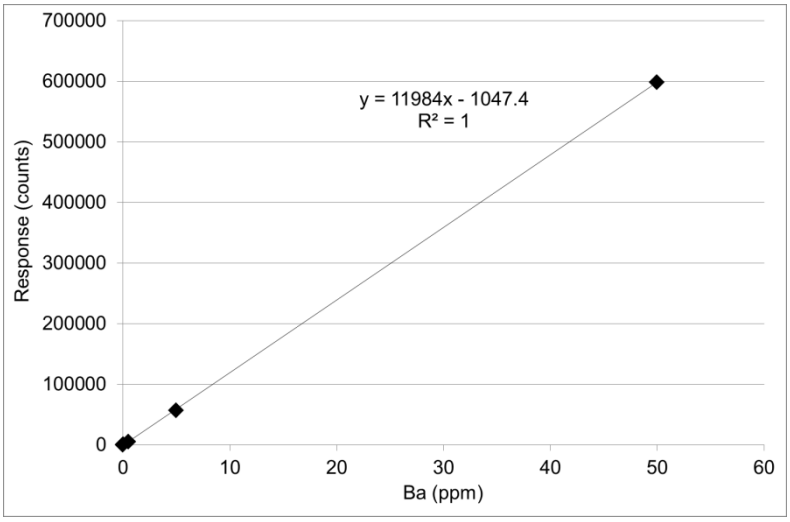

6.1.1.4 Calcium

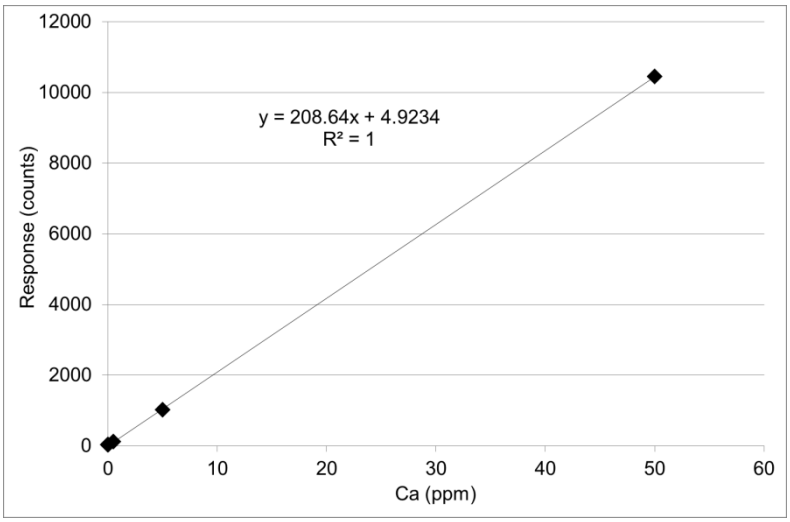

6.1.1.5 Cobalt

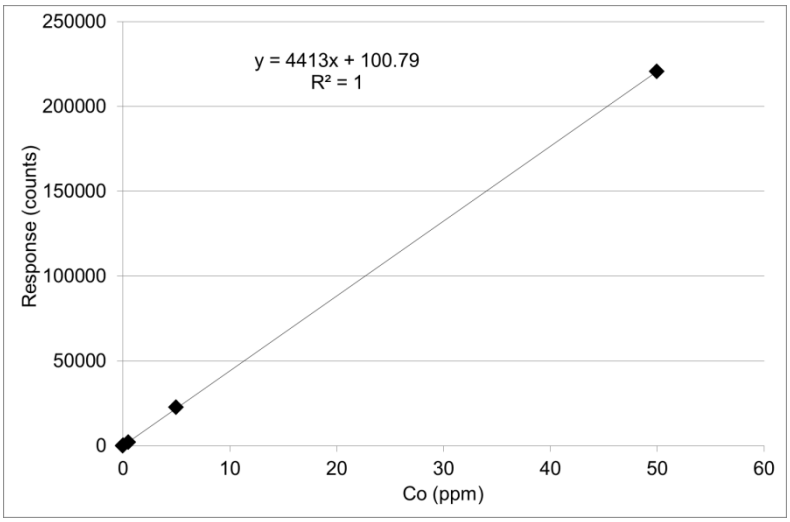

6.1.1.6 Chromium

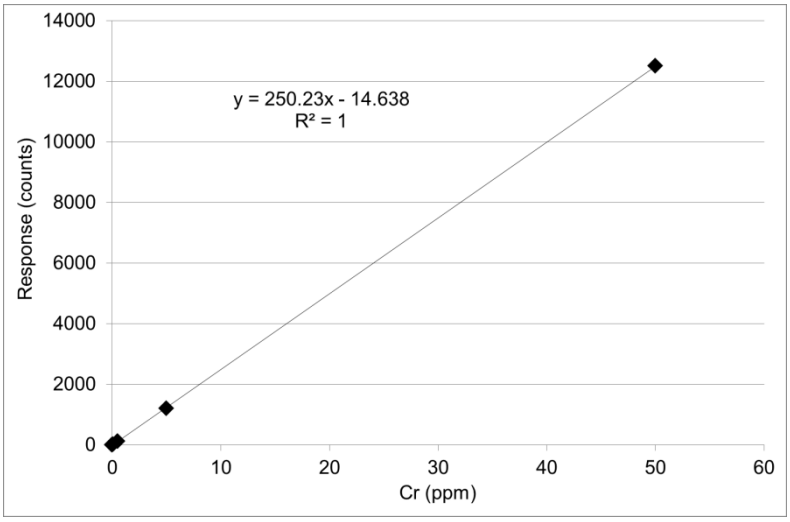

6.1.1.7 Copper

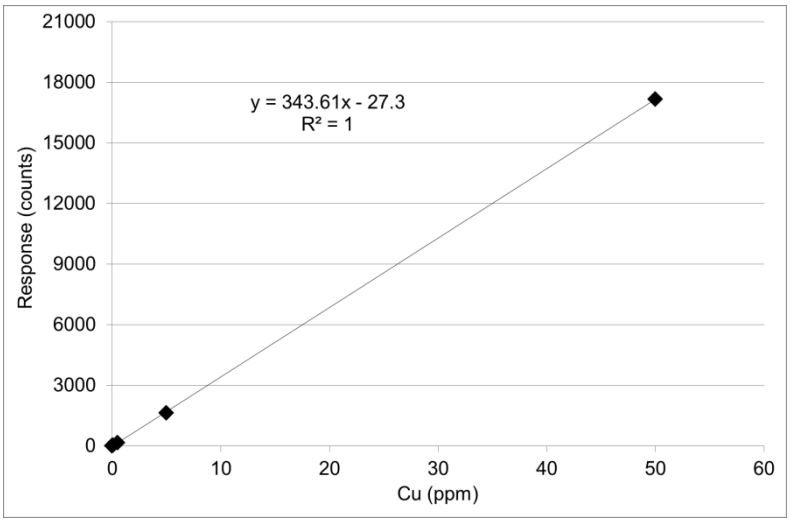

6.1.1.8 Iron

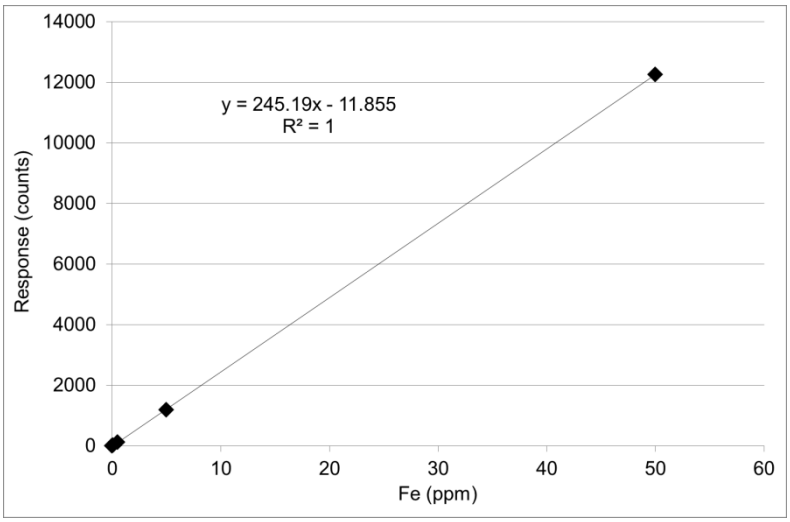

6.1.1.9 Potassium

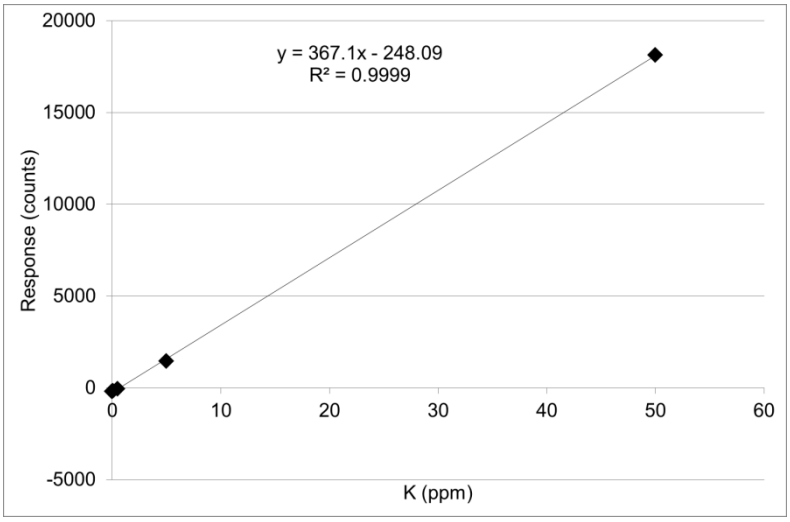

6.1.1.10 Magnesium

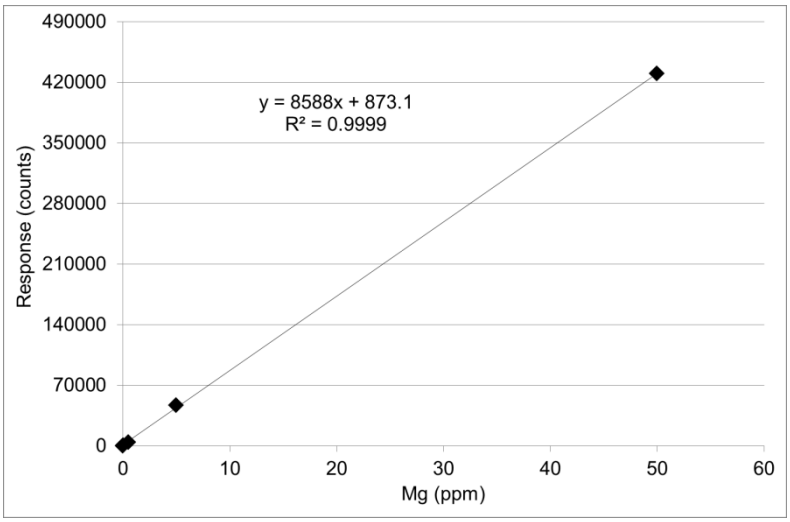

6.1.1.11 Manganese

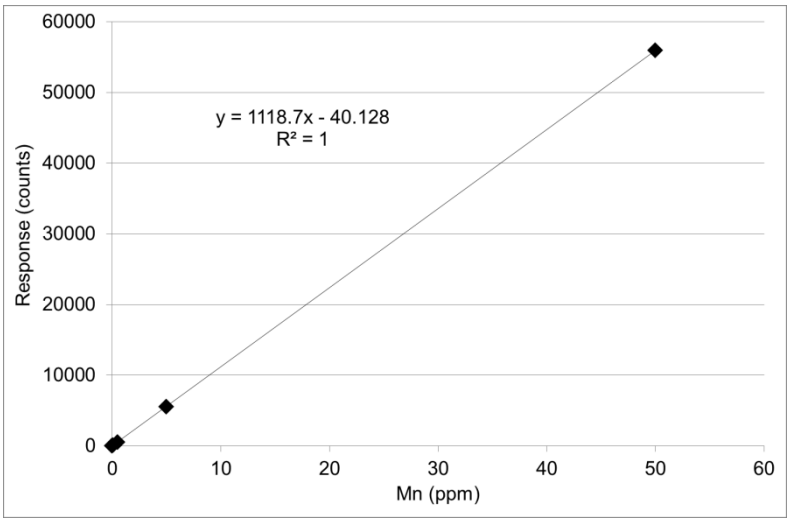

6.1.1.12 Sodium

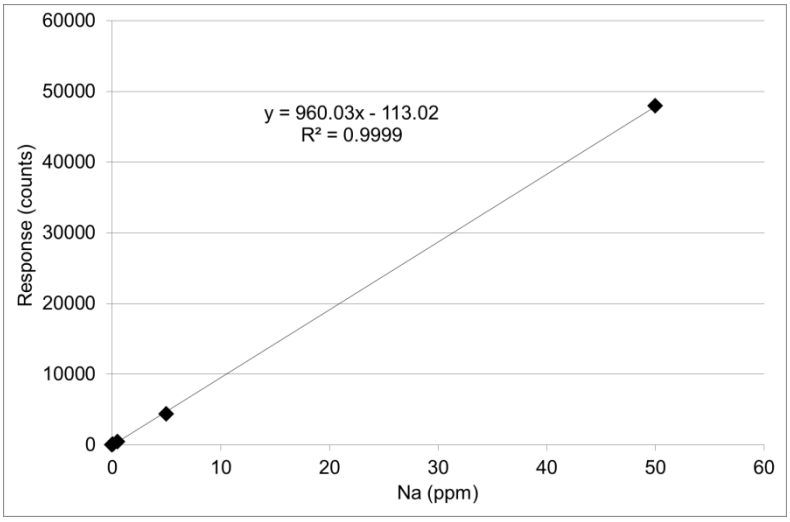

6.1.1.13 Niobium

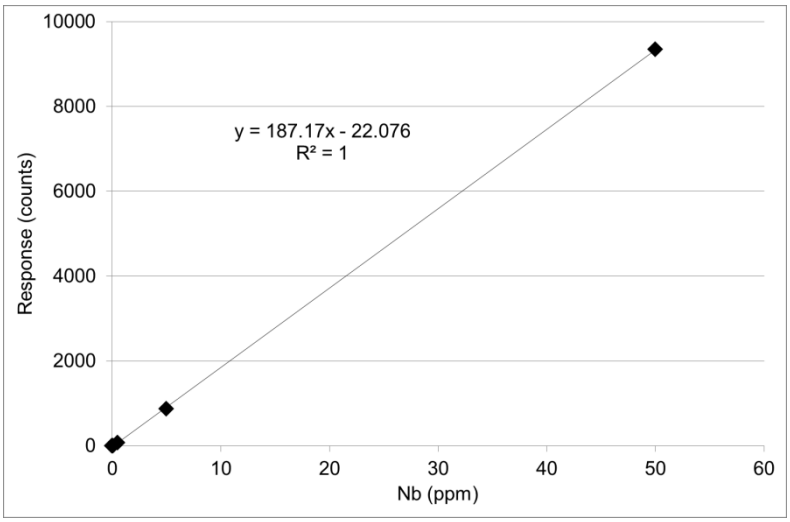

6.1.1.14 Nickel

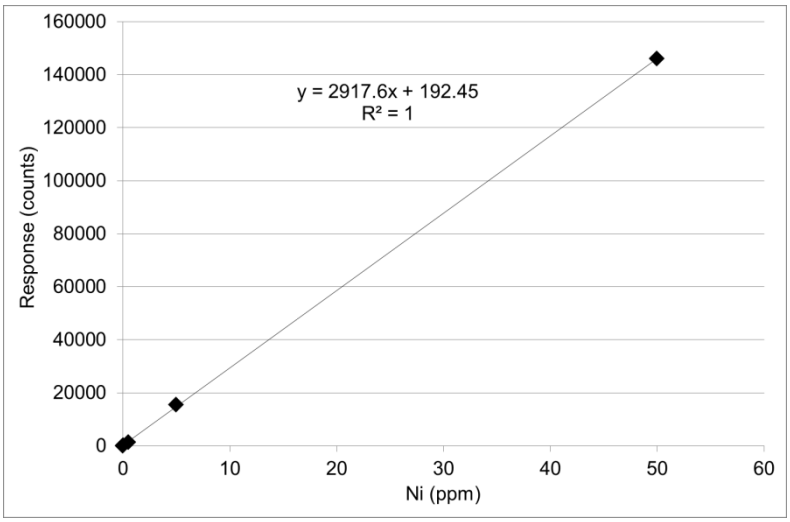

6.1.1.15 Phosphorus

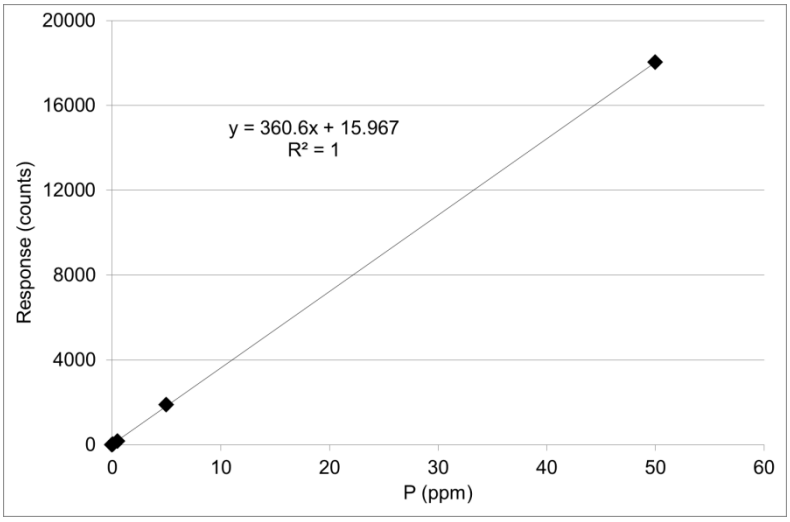

6.1.1.16 Lead

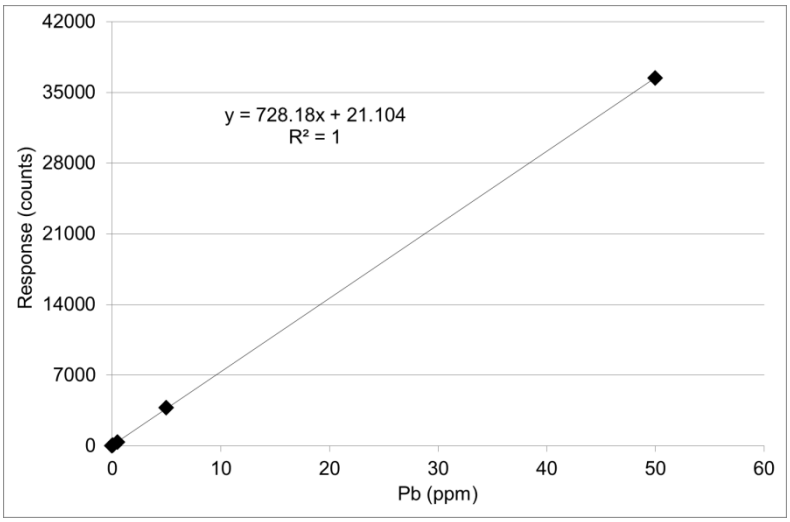

6.1.1.17 Sulphur

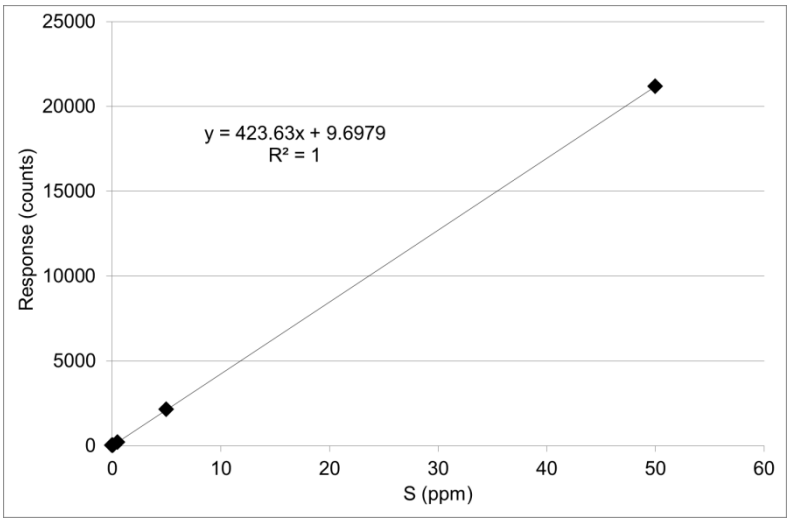

6.1.1.18 Strontium

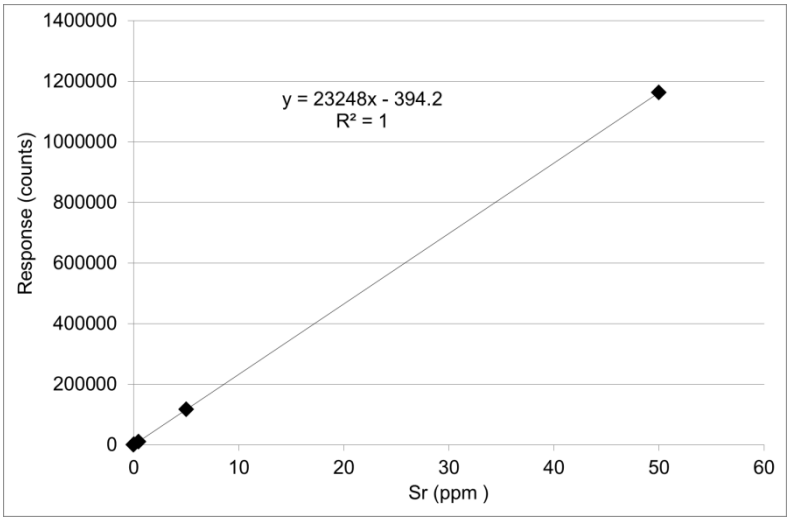

6.1.1.19 Titanium

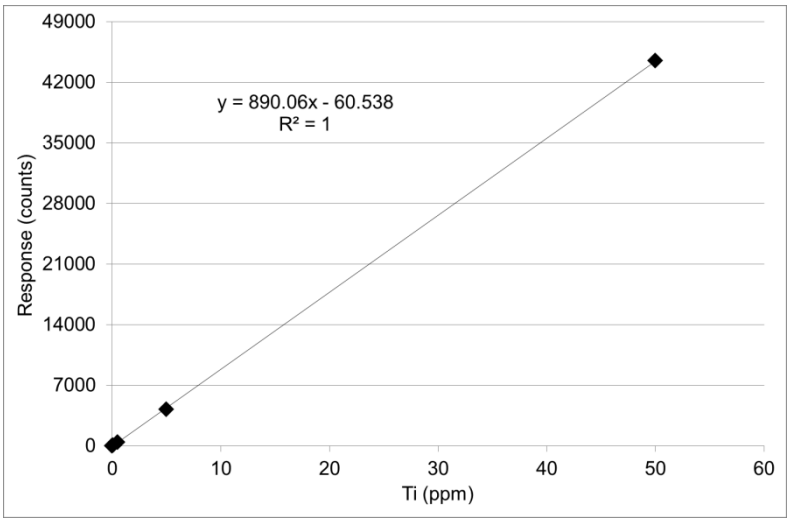

6.1.1.20 Uranium

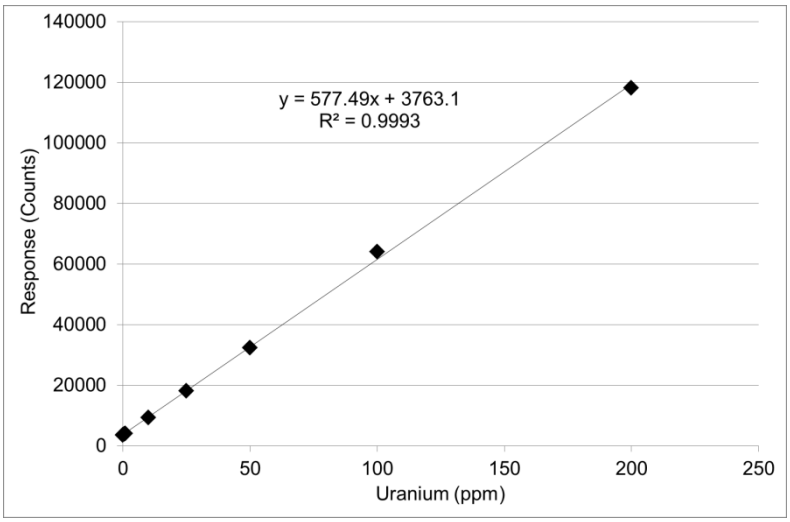

6.1.1.21 Vanadium

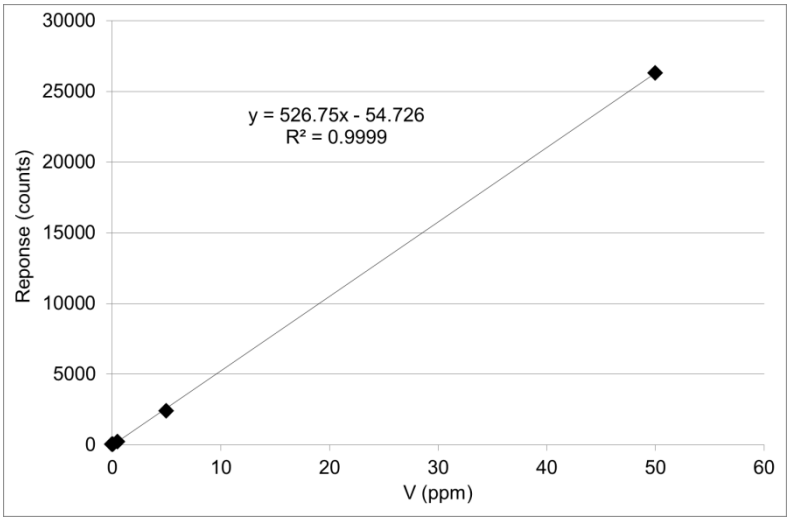

6.1.1.22 Zinc

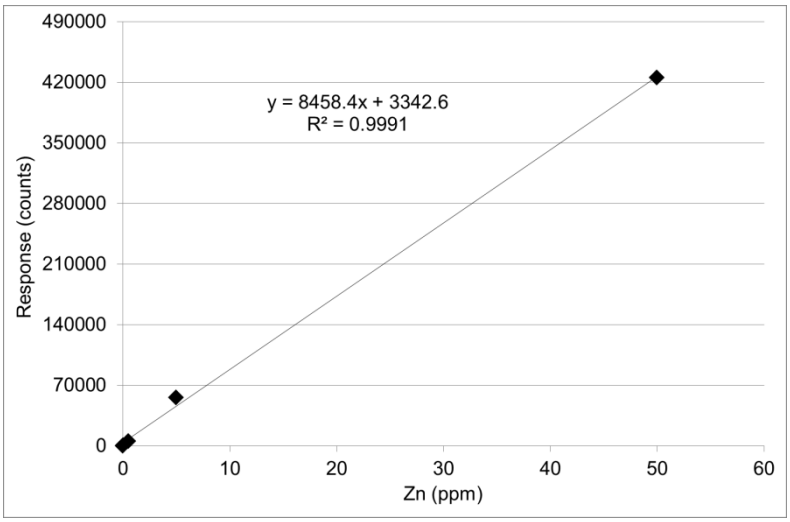

6.1.1.23 Zirconium

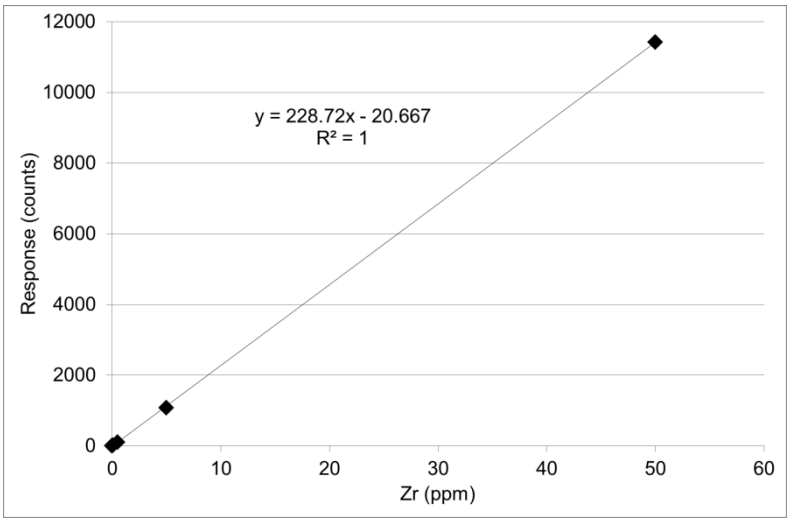

6.1.2 *ICP-MS*

6.1.2.1 Nickel

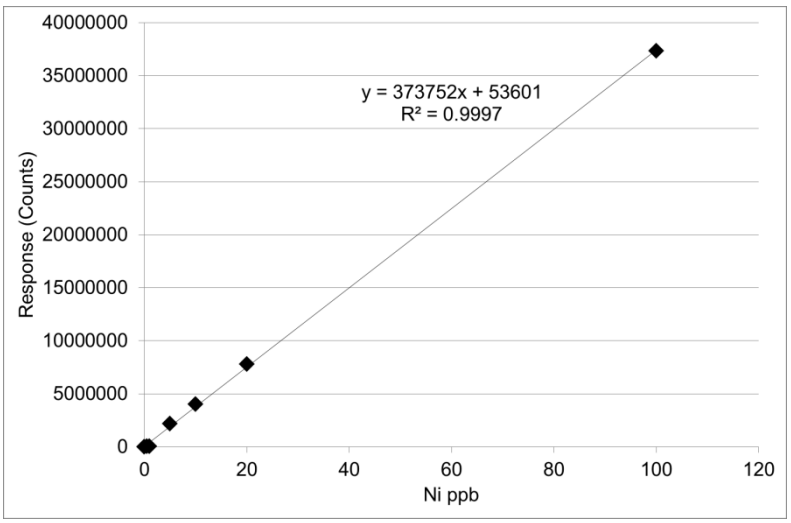

6.1.2.2 Silica

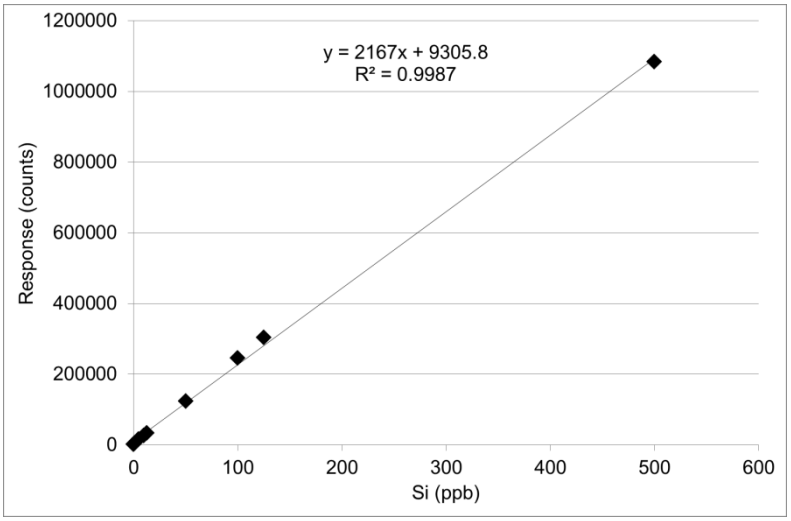

6.1.2.3 Thorium

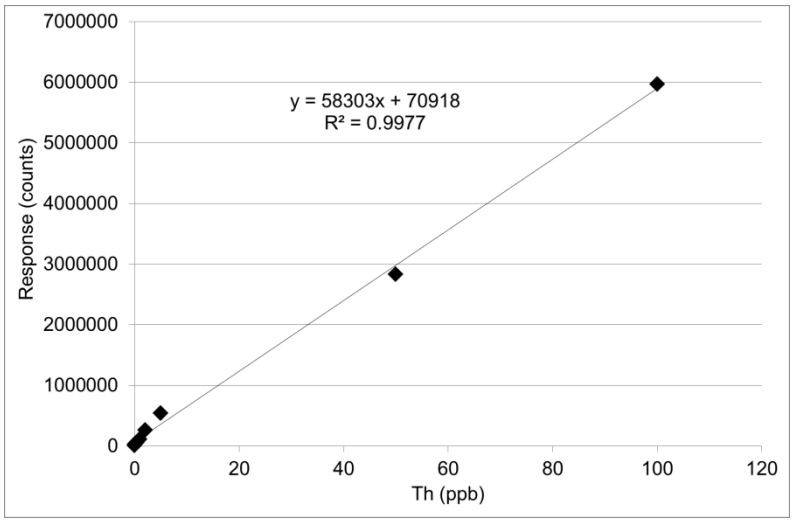

6.1.2.4 Uranium

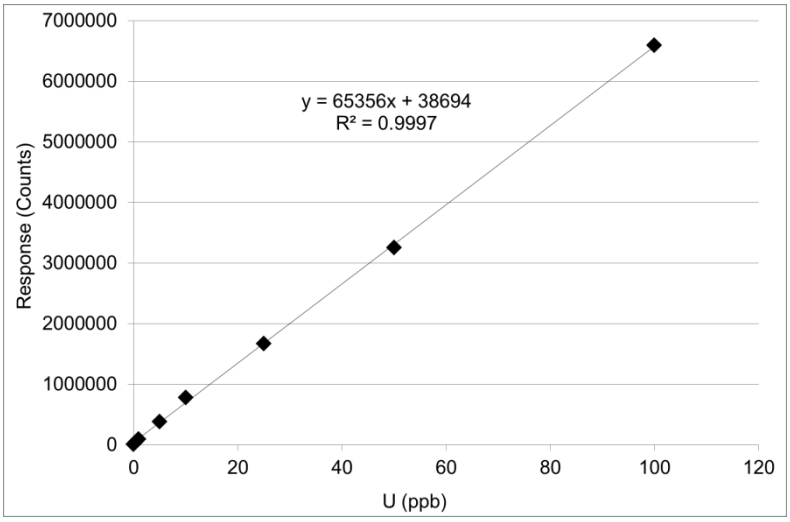

6.1.3 *Dionex Ion Chromatography*

6.1.3.1 Chloride

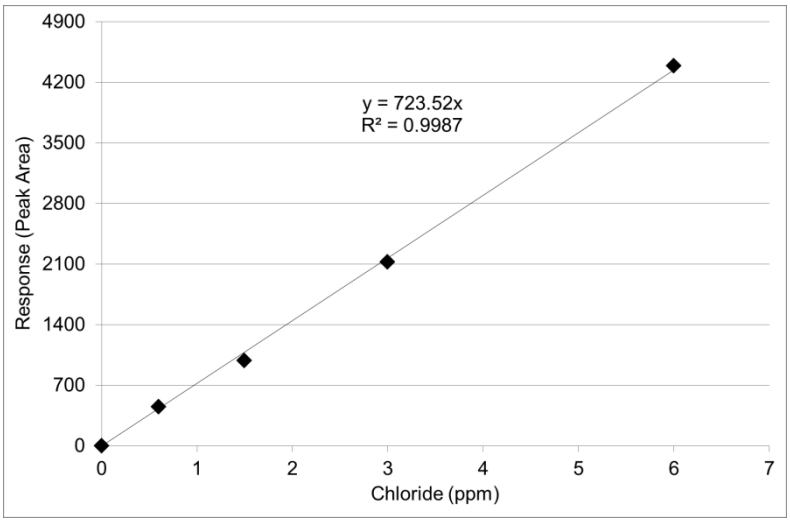

6.1.3.2 Nitrate

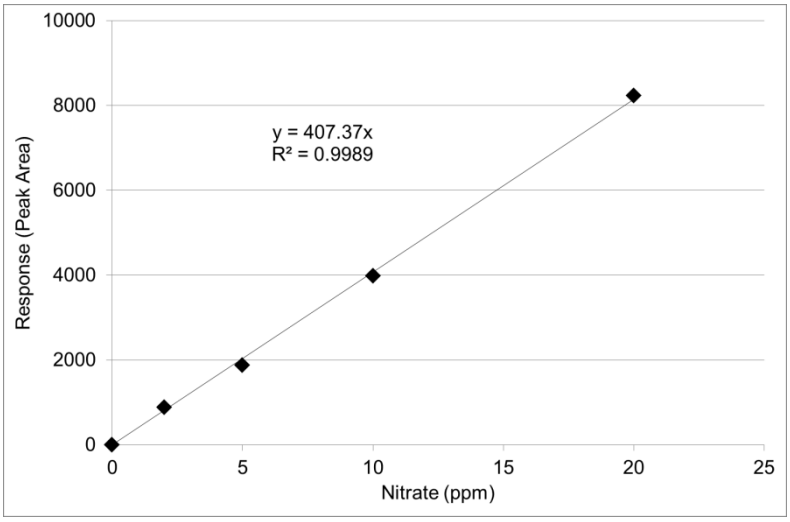

6.1.3.3 Sulphate

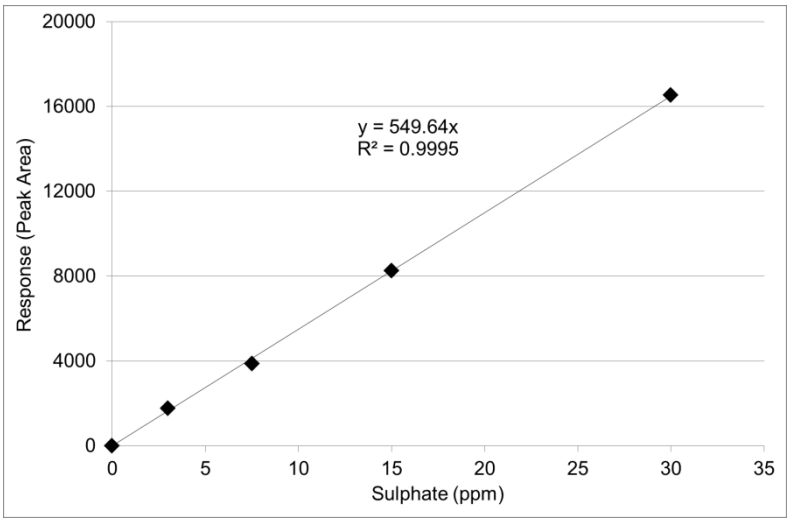

6.1.3.4 Sulphite

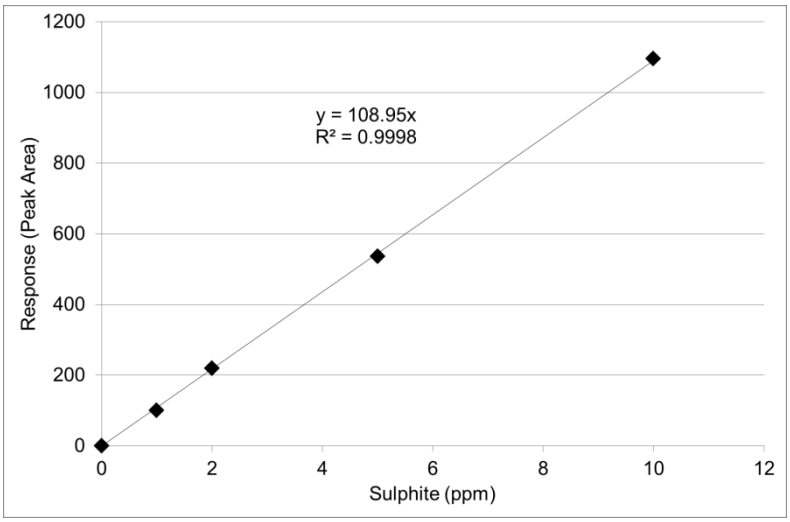

6.1.3.5 Thiosulphate

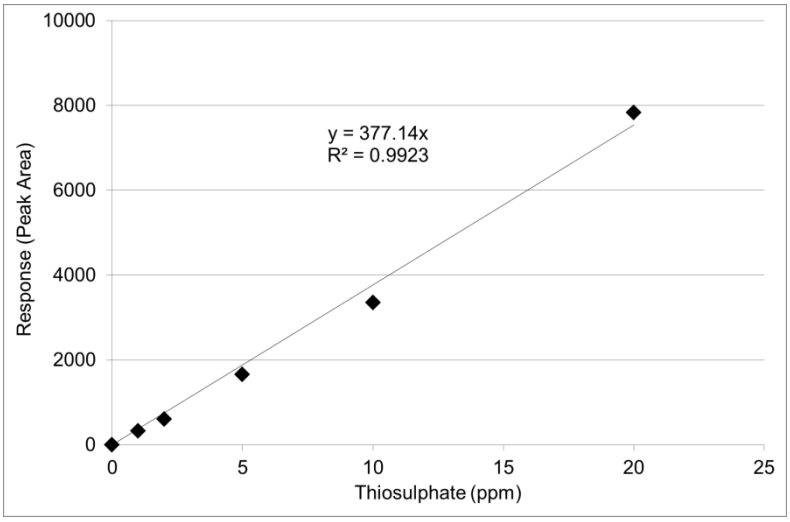

6.1.4 *TOC Analyser*

6.1.4.1 ADVA Cast 551

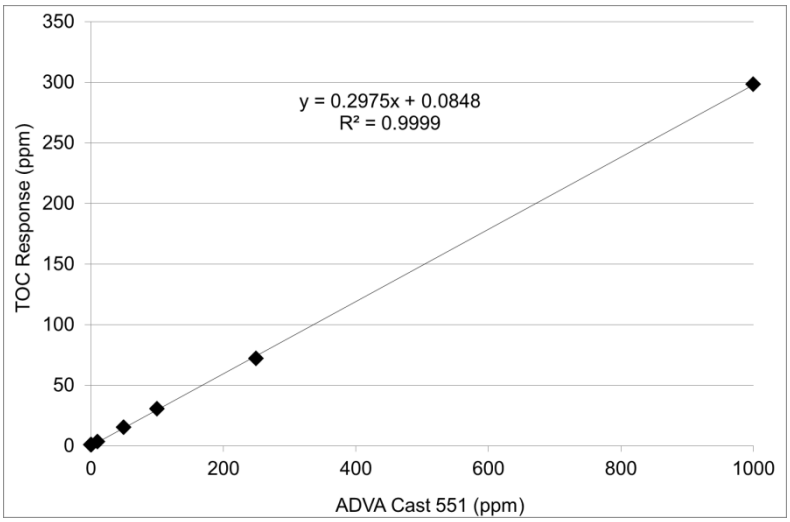

6.2 APPENDIX 2 – EDX Analysis Spectra

6.2.1 *BFS:OPC*

6.2.1.1 BFS:OPC + 0.5% SP + Ni. Top Edge

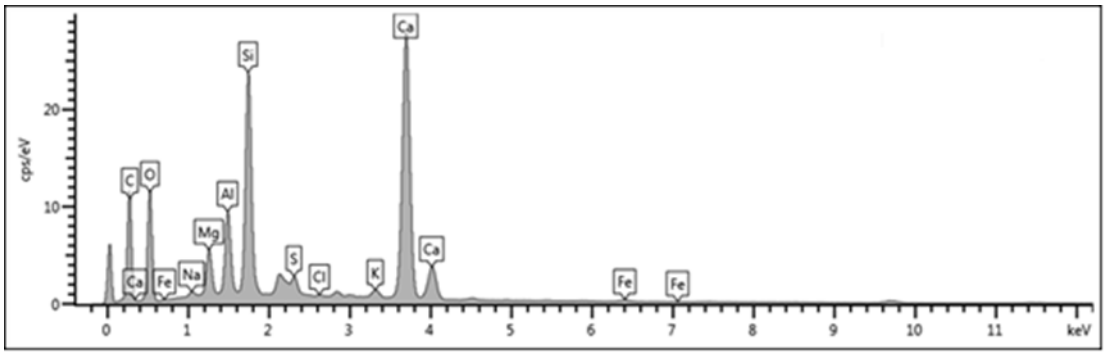

6.2.1.2 BFS:OPC + 0.5% SP + Ni. Middle

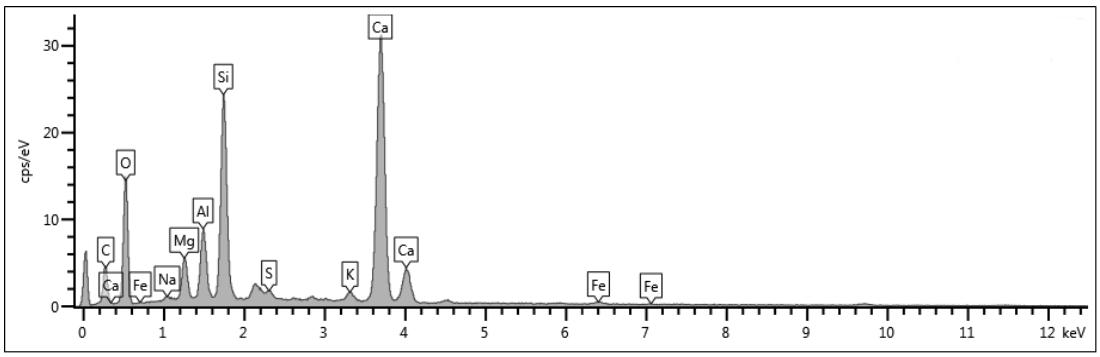

6.2.1.3 BFS:OPC + 0.5% SP + Ni. Bottom Edge

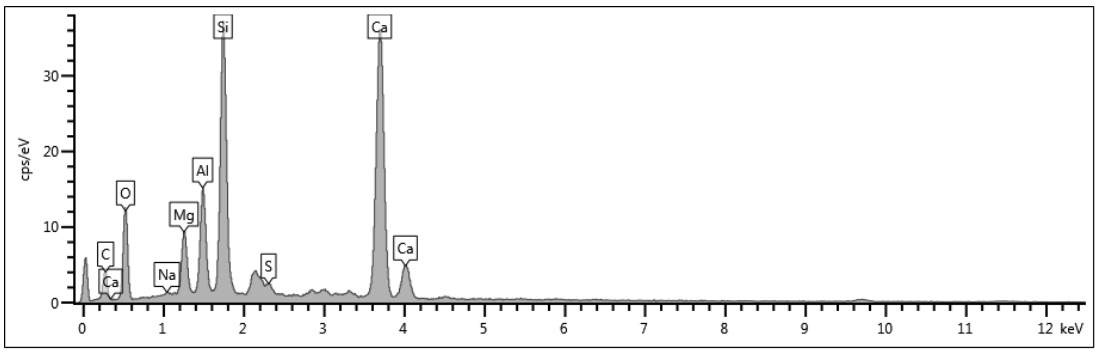

6.2.1.4 BFS:OPC + No SP + Ni. Top Edge

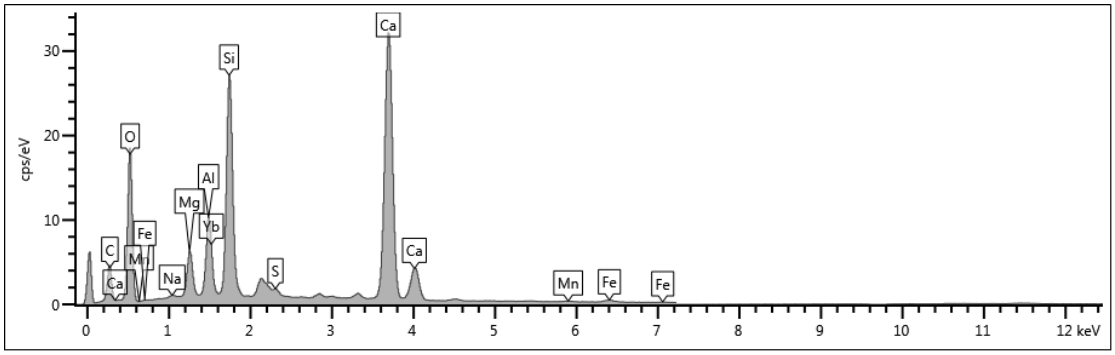

6.2.1.5 BFS:OPC + No SP + Ni. Middle

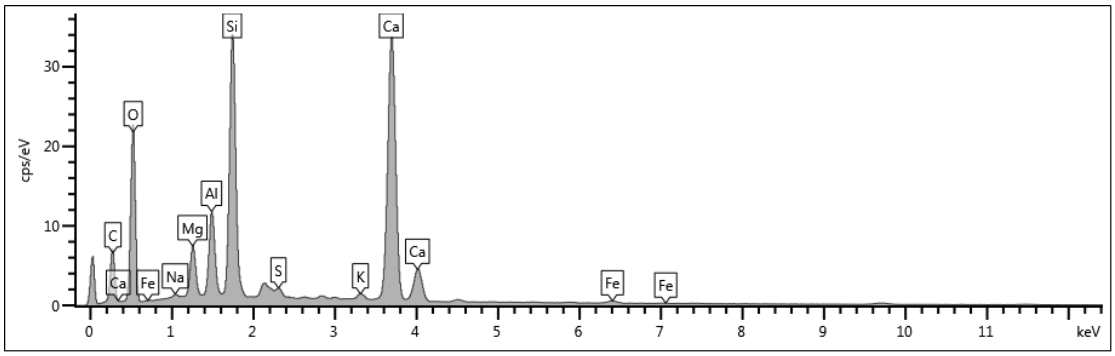

6.2.1.6 BFS:OPC + No SP + Ni. Bottom Edge

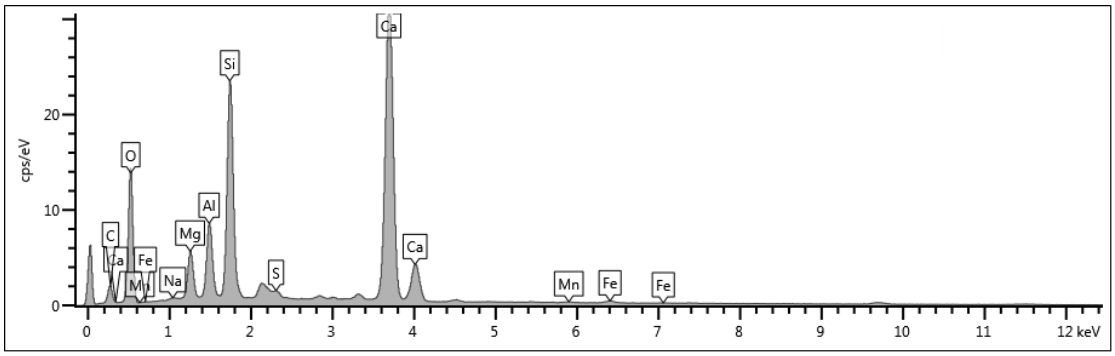

6.2.2 *PFA:OPC*

6.2.2.1 PFA:OPC + 0.5% SP + Ni. Top Edge

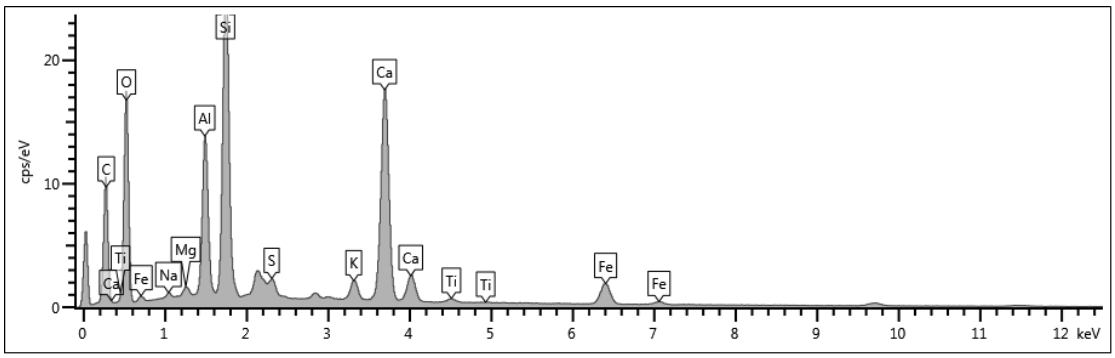

6.2.2.2 PFA:OPC + 0.5% SP + Ni. Middle

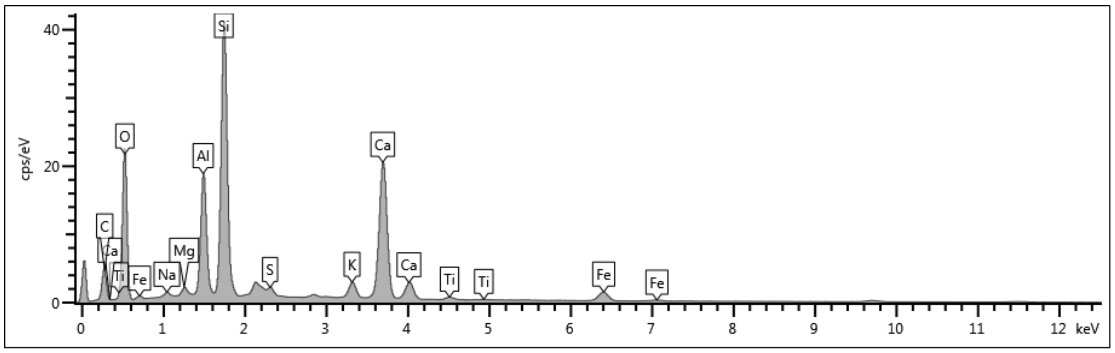

6.2.2.3 PFA:OPC + 0.5% SP + Mi. Bottom Edge

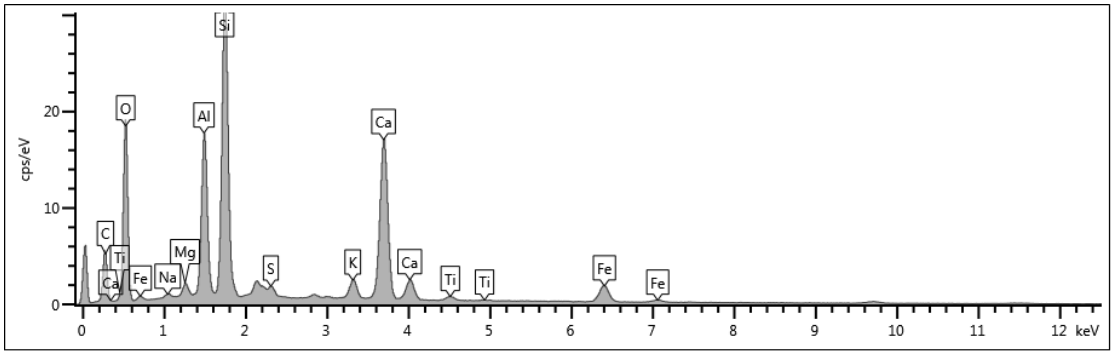

6.2.2.4 PFA:OPC + No SP + Ni. Top Edge

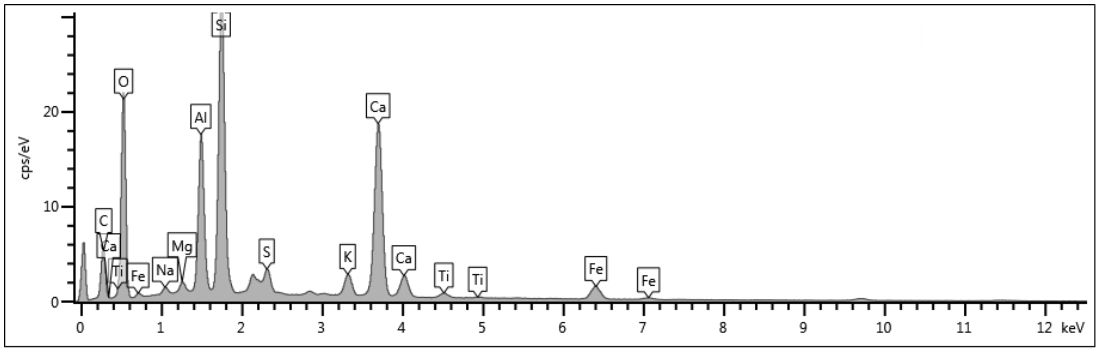

6.2.2.5 PFA:OPC + No SP + Ni. Middle

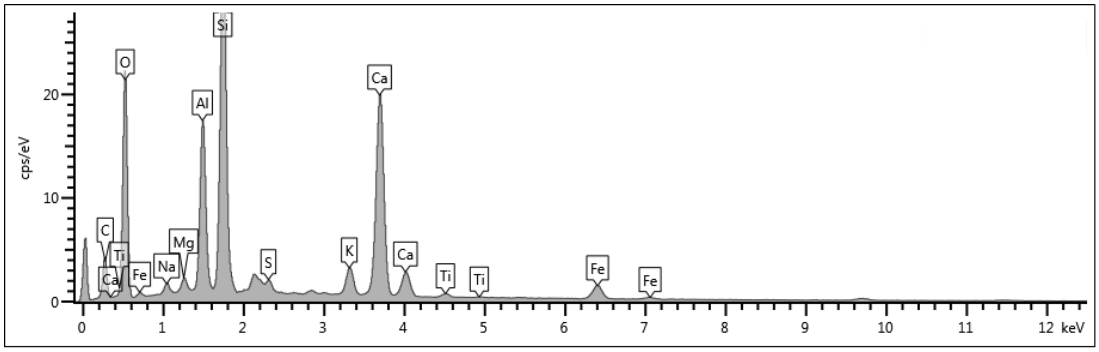

6.2.2.6 PFA:OPC + No SP + Ni. Bottom Edge

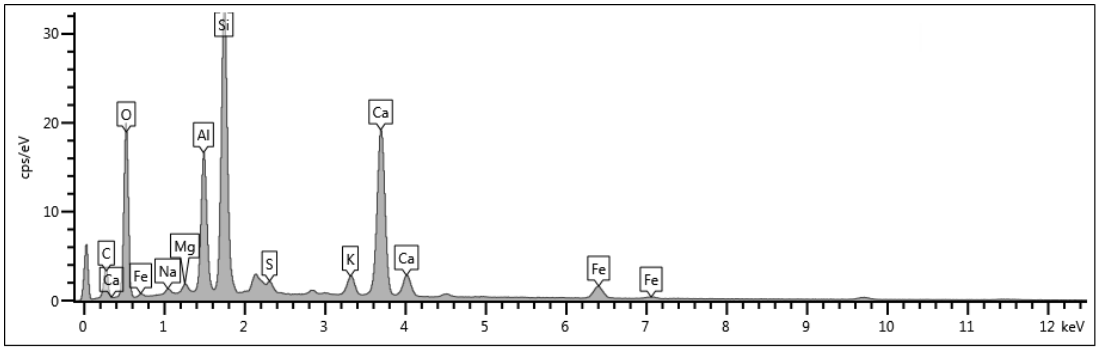

6.3 APPENDIX 3 – Paper Submitted to 'Advances in Cement Research'

Submitted to 'Advances in Cement Research' - 14th May 2012

Behaviour of Radionuclides in the Presence of Superplasticiser

Amy J. Young, Loughborough University

Peter Warwick, Enviras Ltd

Antoni Milodowski, British Geological Survey

David Read, Loughborough University

Abstract

Superplasticisers are used to improve the flow properties of fresh cement and offer undoubted benefits to the construction sector. There is concern in the nuclear industry, however, that organic additives may increase the solubility of radionuclides when in contact with cementitious grouts or backfill. This paper describes the effect of a commercial, polycarboxylated, polyether comb-type superplasticiser on the behaviour of selected metals in blended cements through a series of batch and monolith leach experiments. Results of batch experiments show that the presence of free superplasticiser in solution reduces uptake of nickel (^{63}Ni) and europium (^{152}Eu) by both Blast Furnace Slag and Pulverised Fly Ash - amended Ordinary Portland Cement. Further, metal bound in the presence of free superplasticiser is readily remobilised on exposure to fresh cement solution. Conversely, metal uptake is quantitative and irreversible when exposed to hardened cements prepared with superplasticiser as part of the original mix. Monolithic slag cement samples prepared with superplasticiser suffered from bleed with the surplus water containing a significant proportion of the metals added, including uranium and thorium. Digital autoradiography revealed heterogeneous distribution of activity in the monoliths and demonstrated that the metals had not been effectively encapsulated. The mobility of thorium may indicate similar behaviour by other tetravalent actinide species, notably Pu(IV).

Introduction

The United Kingdom has accumulated a substantial legacy of radioactive waste, much of it arising from civil nuclear power generation over the past sixty years. In the event that new nuclear power plants enter service, as is currently envisaged, waste created by the new facilities will also need to be managed and disposed of safely.

Current government policy suggests that deep geological disposal preceded by secure interim storage is the best option for dealing with the UK's inventory of nuclear waste. Geological disposal is a multi-barrier, multi-phased approach based on placing suitably packaged and contained waste in an underground repository. Interim surface storage provides a secure store for packaged waste throughout the period during which the geological disposal facility is in the planning, (3)development and licensing stage (3,3)(Poyry Energy Ltd 2011).

Concrete and cement will inevitably play an important role in the construction of a geological disposal facility (GDF). Standard techniques used for underground construction will be employed and therefore concrete will be used for the walls, floors and ceilings of the vaults, shafts and tunnels. According to current designs, intermediate (ILW) and longer-lived low level (LLW) waste will be placed in standardised stainless steel or concrete-lined stainless steel containers and mixed with a cement-based grout. The waste packages will then be stored in engineered vaults within the host geological environment. These packages could remain underground until the vault is full, which could take many decades, and the decision made to either leave the vault open, with the option of retrieving the waste in the future, or to backfill the vault, the shafts and tunnels with cement grout in order to permanently immobilise the waste.

The cement backfill is designed to provide an important chemical barrier to radionuclide migration; firstly, by providing a high surface area available for radionuclide uptake and secondly, by chemically conditioning the cement pore water to high pH (4). The presence of $Ca(OH)_2$ (portlandite), with a solubility of ~1 g dm^{-3} at 25ºC, buffers the cement pore water to pH 12.5, conditions under

which the actinides tend to display low solubility and may precipitate as salts. Uptake of radionuclides by cements may also retard migration via ion exchange and adsorption on, or incorporation in, mineral phases.

It is important to understand the implications of using cement-based materials in the construction of a GDF. Many types of cement matrix exist, with the partial substitution of pozzolans, such as Pulverised Fly Ash (PFA), or latent hydraulic materials, for example, Blast Furnace Slag (BFS), for Ordinary Portland Cement (OPC). Additives, primarily retarders and superplasticisers, present specific benefits to the nuclear industry in terms of workability but they also introduce uncertainty regarding the potential fate of radioactive species.

Superplasticisers belong to a group of cement additives known as high range water reducers. They are polymeric molecules and are widely used in the construction industry to improve flow characteristics whilst reducing the water content of a cement formulation by around 30%, providing higher compressive strength (19,21). Superplasticisers are synthetic chemicals consisting of high molecular weight, water-soluble organic polymers. Solubility is ensured by the presence of adequate hydroxyl, sulfonate or carboxylate groups attached to the main organic repeat unit, which is usually anionic in nature (20).

Many organic molecules, for example EDTA, used as a decontamination agent in radioactive waste streams, are able to complex radionuclides (39,42,43). Some superplasticisers (sulphonated melamine formaldehyde and sulphonated naphthalene formaldehyde) have also been shown to increase the solubility of radionuclides (including U(VI) and Pu(IV)) in high pH solutions representative of cement pore water (44,46). Consequently, their use in a radioactive waste disposal context has been discounted. More recently, highly effective superplasticisers based on polycarboxylated polyether comb polymers have been developed. These are now being considered for use within a GDF, though little is yet known of their complexation potential. This paper focuses on one such polycarboxylated superplasticiser, ADVA Cast 551, the structure of which is shown in Figure 1.

The behaviour of selected radioactive metals in cements is compared in the presence and absence of superplasticiser from two view points;

i) By regarding the superplasticiser as a 'ligand' where batch experiments of metal uptake on crushed cement are carried out with increasing concentrations of free superplasticiser in solution.
ii) By investigating metal uptake in cements prepared with superplasticiser already present. The subsequent leaching of metal from hardened cements prepared with and without superplasticiser is then assessed.

The objectives above also impact on the ability of superplasticiser-amended cement to act as a grout since reactions immediately after water addition can have a major bearing on subsequent performance (93)((81).

Experimental

Two cement formulations were investigated: BFS:OPC (9:1) and PFA:OPC (3:1). Blast Furnace Slag (BNFL Specification 7th revision) was supplied by Civil and Marine. Pulverised Fly Ash (Class S, Category B, manufactured to comply with the requirements of BS EN:2005 to BNFL specification 6th revision) was supplied by Cemex. Ordinary Portland Cement (BNFL specification 7th revision, manufactured to comply with the requirements of BS EN 197-1:2000 type CEM I, Portland Cement Strength Class 42, 5N) was supplied by Castle Cement.

The following metal salts were used in the experiments – $UO_2(NO_3)_2$ (BDH Laboratory Reagents), $Ni(NO_3)_2$ (Sigma Aldrich), $EuCl_3$ (Acros Organics) and $Th(NO_3)_4$ (Fluka). In the metal uptake experiments, a further radioactive spike of nickel and europium was used in the form of ^{63}Ni and ^{152}Eu (both supplied by Eckert and Ziegler). ADVA Cast 551 was supplied by Grace Construction Products.

For the first set of experiments, involving the uptake of nickel and europium by crushed BFS:OPC and PFA:OPC, the cement powders, without superplasticiser, were weighed into a plastic beaker according to the compositions shown in Table 1 and mixed thoroughly. Water was added slowly over 2 minutes with stirring. The mix was stirred for a further 4 minutes before pouring into a plastic mould (53), covered with parafilm and left for 24 hours before de-moulding. The specimens were then cured at >90% humidity for 28 days. After curing, the samples were allowed to dry for 24 hours, then crushed,

sieved and the <180 μm fraction used for the experiments. 0.5 g of solid were weighed into plastic vials.

Solutions of $Ni(NO_3)_2$, and $EuCl_3$ were prepared at a concentration of 10^{-9} mol dm^{-3} using the appropriate cement equilibrated water. This concentration was chosen to be lower than the estimated solubility limit for each metal at high pH (6×10^{-8} mol dm^{-3} for Ni (39) and 6×10^{-7} mol dm^{-3} for Eu (35). ADVA Cast 551 was added in solution at 0, 0.2, 0.5 and 1% (w/v) to assess the effect of increasing concentration of superplasticiser on the uptake of the metals by the cement. A spike of either ^{63}Ni or ^{152}Eu was added to bring the activity of each sample to 3 kBq. The samples were allowed to equilibrate on a flat-bed shaker for 28 days.

Desorption experiments were carried out to investigate the reversibility of metal uptake when superplasticiser is present in solution. All of the supernatant was removed from the cement solid and 10 cm^3 of fresh cement-equilibrated water added. The samples were then shaken on a flatbed shaker for a further 28 days.

In the second set, uptake of metals onto crushed BFS:OPC and PFA:OPC prepared with ADVA Cast 551 were measured. Cements were prepared with the addition of 0.5% (w/s) superplasticiser, then cured and crushed prior to the experiment as described above; 0.5 g of the crushed cements were weighed into plastic vials. The compositions of the cements are given in Table 2.

Nickel and europium solutions at a concentration of 10^{-9} mol dm^{-3} were prepared in the relevant cement equilibrated water and 10 cm^3 solution added to the weighed cement solid. The samples were allowed to equilibrate on a flatbed shaker for 28 days.

The reversibility of metal uptake was investigated by conducting a desorption experiment similar to that described above. All the supernatant was removed from the cement solids and 10 cm^3 of fresh cement equilibrated solution added before equilibration on a flatbed shaker for a further 28 days.

The leaching behaviour of U (VI), Th and Ni from BFS:OPC and PFA:OPC, prepared with and without the addition of 0.5% (w/s) superplasticiser, was also

investigated using monolithic samples. They were prepared by adding $UO_2(NO_3)_2$, $Th(NO_3)_4$ and $Ni(NO_3)_2$ respectively to the water of each cement mix to give a loading of 200ppm (w/w). The metal nitrates are soluble in water at near neutral pH thus, adding them before mixing with the cement powders should result in homogeneous monoliths. The composition of the cement monoliths is given in Table 3.

The design of the leaching experiment was based on the 'Tank Leach Test' as described by Conner (62) and Takahashi *et al*. (61). The extent of metal leaching is dependent upon: fixation of the elements by amorphous and microcrystalline phases (largely. calcium silicate hydrogel, CSH) produced during the hydration of the cement, the formation of metal hydroxides at high pH and metal diffusion. Cement prepared with superplasticiser has a lower porosity; therefore, a decrease in metal diffusion due to a reduced pore volume may be expected.

After mixing, the cements were poured into plastic moulds, covered with parafilm, and allowed to set for 48 hours. After this time, the samples were de-moulded and the ends of each block sealed with paraffin wax. The blocks were then submerged in a known volume of the appropriate equilibrated water (either BFS:OPC or PFA:OPC) and sealed in screw-top Pyrex jars. The samples were left for 4 months before aliquots of the leachate solution were removed for analysis.

In the case of the BFS:OPC samples, bleed water was present on the surface after the 48 hour set time, particularly in those samples that contained superplasticiser. The water was collected and analysed for the metals of interest by Inductively Coupled Plasma- Mass Spectrometry (ICP-MS). The quantity of metal leached in the bleed water was taken into account in the calculations.

Aliquots of the supernatant were removed from the samples and analysed for the metals of interest after filtering through 0.45 μm. Nickel (^{63}Ni) was analysed by liquid scintillation counting (LSC) using a Tri-Carb 2750 TR/LL Packard Liquid Scintillation Counter. 1 cm^3 of supernatant were added to 10 cm^3 of GoldStar LSC cocktail (Meridian), the samples shaken on a whirl-mixer and

allowed to settle for 1 hour before counting. Europium (^{152}Eu) samples were analysed by gamma counting using a Cobra II Auto Gamma Spectrometer (Packard). Uranium was measured by ICP-MS using a 770x Series Quadrupole ICP-MS (Agilent Technologies). The supernatant was acidified with 0.5% analytical grade HNO_3 before analysis. The ICP-MS Instrument was calibrated on a daily basis using a uranium standard solution (Fisher). Sample vials were washed three times with 0.5% HNO_3 to check for adsorption to the vial walls; no loss of metal was observed.

The homogeneity of the cement monoliths was assessed by Scanning Electron Microscopy (Field Emission Gun SEM), in the case of nickel, and digital autoradiography for uranium and thorium (63). The cement blocks were removed from the leachate solutions and cut axially with a diamond circular blade saw. Wet/dry sand paper was used to smooth the cut surface of the blocks before imaging. For autoradiography, the cement blocks were placed onto Eu^{2+} doped BaFBr storage phosphor autoradiography plates (Fuji) and sealed in a light tight box. The U and Th-containing blocks were exposed for 7 and 14 days, respectively and the images recorded by a STORM 860 Laser Photostimulated Fluorescence Scanner (Amersham Biosciences).

Results

Effect of free ADVA Cast 551 on nickel and europium uptake by crushed cements

The uptake of nickel onto BFS:OPC grout as a function of free superplasticiser in solution is shown in Figure 2. In the absence of ADVA Cast 551, uptake is effectively quantitative but decreases linearly with increasing concentration of ADVA Cast 551 such that, at 1% superplasticiser, less than 30% of the nickel inventory is bound. The effect is reversible, though there is discernible hysteresis (Figure 2). With no superplasticiser present, <1% of the Ni bound is re-suspended but the addition of even a small amount (0.2%) of ADVA Cast 551 has a marked impact on the ability of the cement to retain the metal. In the samples containing ≥0.5% ADVA Cast 551, more than 98% of the bound Ni was re-suspended.

Nickel uptake onto PFA:OPC grout displays similar trends (Figure 3). However, in comparison to BFA:OPC, more metal is bound and less released at corresponding concentrations of ADVA Cast 551. The differences are most marked at 0.2% superplasticiser (a typical commercial dosage), where the reduction in Ni uptake is only 5%. Again, at higher concentrations of superplasticiser more than 99% of the bound metal was re-suspended when exposed to fresh cement solution.

The percentage uptake of Eu onto crushed BFS:OPC and PFA:OPC is shown in Figures 4 and 5, respectively. The behaviour of trivalent europium broadly follows that of nickel although some trends are more pronounced. The proportion of metal bound is sharply reduced by superplasticiser even at low concentrations; only 0.2% ADVA Cast 551 is sufficient to reduce Eu uptake by half for both cement formulations. Thereafter, the slag samples show little change, uptake stabilising at around 40% of the metal added. In contrast, proportional uptake continues to decrease with PFA:OPC grout, reaching 20% with 1% superplasticiser present in solution. Differences in desorption behaviour are also apparent. More than 97% of the metal was re-suspended during the desorption experiment on BFS:OPC at all concentrations of ADVA Cast (Figure 4). In contrast, desorption of Eu from the fly ash grout reaches a peak at 0.2% superplasticiser (Figure 5), implying that a fraction of the metal is irreversibly bound.

Uptake of nickel and europium by crushed cements prepared with superplasticiser

Uptake of nickel and europium to crushed cements prepared with 0.5% superplasticiser is shown in Tables 4 and 5, respectively. Nickel uptake is 98% for both the slag and fly ash grouts. Europium uptake is even greater (>99%) as levels in the residual solution were below detection. These data demonstrate that ADVA Cast 551 does not affect uptake of the metals when already incorporated in the grout, in marked contrast to when the superplasticiser is free in solution. Desorption was also investigated (Tables 6 and 7). The results show that (<1%) is re-suspended in each case.

Leaching of nickel, uranium and thorium from cement monoliths prepared with and without superplasticiser

Results for leaching of Ni , U (VI) and Th from BFS:OPC are shown in Table 8. As noted previously, bleed water was found on the BFS:OPC cement blocks; however, there was substantially greater bleed in the samples containing ADVA Cast 551. This water was collected and analysed by ICP-MS. It is apparent that a significant proportion of the metals added are present in the bleed above the cement prepared with superplasticiser. In the case of U, 32% of the original inventory was found in the bleed water, the corresponding values for thorium and nickel are 26% and 19%, respectively. In the case of slag cement prepared without superplasticiser, less than 1% of the original metal inventory was found in the bleed (Table 8). No bleed was associated with the PFA:OPC cement on setting.

On subsequent leaching, the concentrations of U and Th released from the BFS:OPC monoliths are very low (Table 8). With nickel, a similar concentration of metal (within a factor of two) was leached from the cement irrespective of whether the block contained superplasticiser. Therefore, short-term behaviour in the form of bleed appears to have little impact on longer term trends, in this case leaching over a period of four months.

Leaching of the same metals from the PFA:OPC blend is shown in Table 9. As for the slag samples, no thorium was leached from the blocks prepared with or without superplasticiser. In the case of nickel, approximately 15x more metal was leached from the blocks that contained superplasticiser, suggesting that it may have enhanced metal release. Nevertheless, absolute concentrations are still lower than those for BFS:OPC (Table 8) and the fractional release is very small. A small amount of uranium was detected in the fly ash tests (Table 9). Slightly more metal is released in the presence of ADVA Cast, in this case by a factor of 2.5, but at such low concentrations the difference is unlikely to be significant.

The distribution of U and Th in the cement blocks was investigated using digital autoradiography. Figure 6 compares autoradiographic images and depth profile

plots of U distribution in BFS:OPC cement made with and without superplasticiser (0.5% ADVA Cast 551). The exposure time was one week and darker areas represent regions of higher radioactivity. The uranium distribution in the sample prepared with superplasticiser is concentrated in the first 5mm of the block (Figure 6a, b); *i.e.* the zone that was in contact with uranium-rich bleed water during set. The remainder of the block contains relatively little uranium. In the absence of superplasticiser, the distribution of activity is homogeneous throughout the sample (Figure 6c, d). The latter demonstrates that the samples were mixed sufficiently prior to moulding.

Similar findings were obtained with thorium (Figure 7). The exposure time was increased to two weeks owing to the lower activity of ^{232}Th. Image resolution is poorer but nevertheless, an area of higher activity is discernible in the region where thorium was detected in the bleed water from superplasticiser-amended BFS:OPC (Figure 7a, b). The distribution of activity throughout the sample is again homogeneous in the cement prepared without ADVA Cast (Figure 7 c, d). These data confirm that the presence of ADVA Cast inhibits encapsulation.

Unlike the BFS:OPC samples, there was no bleed water associated with the PFA:OPC cements, implying that all of the water added, containing both superplasticiser and the metal, was incorporated into the monoliths during the set time. There is also very little difference in autoradiographic images for uranium (Figure 8) and thorium (Figure 9), irrespective of the presence of superplasticiser (0.5% ADVA Cast 551). This finding can only be attributed to compositional differences between the fly ash and slag blends.

Stable nickel was used in preparing the cement monoliths and so recourse was made to SEM-EDX in an attempt to identify areas of enhanced accumulation. Nickel concentrations in the samples were found to be below the detection limit of the instrument and so no firm conclusions concerning the distribution of this metal can be drawn. However, it is noted that nickel was detected in bleed water from BFS:OPC monoliths prepared with ADVA Cast 551 (Table 8).

Discussion

These results establish the extent to which a commercial superplasticiser, in this case ADVA Cast 551, can inhibit the encapsulation of metals by cement and, additionally, suggest means by which the impact can be mitigated. The findings are significant since uptake by cement is one of the key engineered barriers to radionuclide migration in the design of a GDF.

In the absence of superplasticiser, binding of Ni (II) and Eu (III) is quantitative and irreversible (at the same pH). Schlegel *et al*. (79), suggest that Eu uptake by CSH may be explained by substitution for calcium within the structure due to their similar ionic radii in seven-fold coordination (1.01 and 1.06 Å, respectively; (80). As the gel crystallises, the trace metal becomes trapped within the lattice. However, free superplasticiser in solution substantially reduces uptake by both BFS:OPC and PFA:OPC blends. Moreover, when exposed to fresh cement water, the metals are labile and easily re-suspended. Almost all of the bound metals were recovered from BFS:OPC cement when ≥0.5% superplasticiser was present in the original solution. Factors thought to be responsible include; formation of mixed complexes between the superplasticiser and the metal resulting in increased solubility of the metal (44) and binding of the polymer itself onto the cement surface, thereby blocking sites that are normally available to the metals (81). In these experiments, trivalent europium is affected more that nickel, displaying ≥50% reduction in uptake onto crushed cement even at low concentrations of superplasticiser (0.2%). Therefore, enhanced solubility is likely to play at least some part.

Very different results are obtained when metal uptake experiments are performed on cement with superplasticiser already present as part of the mix rather than free in solution. In this case, uptake of Ni and Eu by both BFS:OPC and PFA:OPC is almost complete (>98%) and is not reversible. The absence of free ‘ligand’ precludes solubility enhancement but, equally, the superplasticiser (0.5% ADVA Cast 551) is obviously not effective at blocking metal binding sites. Presumably, interactions between the superplasticiser and the cement during the early stages of hydration lead to the polymer becoming incorporated into cement hydration phases and, therefore, unavailable for subsequent interactions with the metals. Direct evidence that the first few seconds in the

crystallisation of cement are crucial to its development has recently been obtained using *in situ* synchrotron X-ray diffraction (81).

Monoliths prepared with BFS:OPC and 0.5% ADVA Cast 551 suffered from bleed; little or no bleed was found in samples prepared without superplasticiser or in samples of PFA:OPC. A similar observation was made by Morgan and Constable (53) where much more bleed and segregation was observed in a 9:1 BFS:OPC cement than in a 3:1 PFA:OPC cement, both prepared with 0.3% and 0.8% ADVA Cast 551. They suggested that de-flocculation of the cement particles had occurred due to the presence of the superplasticiser, resulting in greater packing density of the powders on curing.

Whatever the cause, a significant proportion of the original metal inventory was found in the BFS:OPC bleed water after 48 hours, varying from 19% in the case of nickel to 32% for uranium. Autoradiography of the monoliths showed accumulation of uranium and thorium in the region adjacent to, and in contact with, the bleed water. Therefore, the bulk of the metal inventory had not been incorporated into the cement.

The effectiveness of superplasticisers in dispersing colloidal cement phases has been ascribed to early attachment of the polymer to calcium aluminate (C_3A), which hinders attachment of sulphate ions to form ettringite (94). Over time, the superplasticiser is replaced by SO_4^{2-} and the cement gains in strength. Compositional differences between the BFS and PFA must have a bearing on this process, in the case of the former causing bleed and mobilisation of normally insoluble metals. It is possible that the higher sulphur content of slag reduces or retards initial uptake of the superplasticiser by C_3A, leaving it free to bind to the metal. As shown above, when available in solution, ADVA Cast is highly effective at both limiting metal uptake and releasing metals back to solution.

On longer timescales, the only metal to leach in appreciable concentrations from the cement monoliths was nickel. Even here, less than 0.005% of the original inventory was detected in the leachate.

The results of this research confirm the findings of earlier work on superplasticiser-amended cements, specifically their ability to bind and retain metal species. The metals studied encompass a range of oxidation states from Ni (II), through Eu (III) and Th (IV) to U (VI). Uranium, under oxidising conditions and in hexavalent form, is a relatively soluble element, though less so at high pH. Thorium, in contrast, exists only in the tetravalent state and is extremely insoluble across most of the pH range. Its apparent mobility here is of potentially great significance as it may indicate similar behaviour by other tetravalent actinide species, notably Pu(IV) and Np(IV).

Acknowledgements

The authors would like to thank the EPSRC DIAMOND Consortium and the Nuclear Decommissioning Authority for funding this research. Special thanks are given to Dr Sneh Jain, Dr Monica Felipe-Sotelo and Mr John Hinchliff for their technical support, advice and encouragement.

References

ALDRIDGE, S., 2005. *Some Aspects of Near Field Chemistry in a Nuclear Waste Repository*, PhD Thesis, Loughborough University.

AMEMIYA, Y. and MIYAHARA, J., 1988. Imaging Plate Illuminates Many Fields. *Nature,* **336**(6194), pp. 89-90.

CETINER, Z.S., 2007. Initial assessment of hydrous Thorium(IV) solubility and speciation in geological environments: An experimental approach in presence of organic ligands. *Asian Journal of Chemistry,* **19**(4), pp. 3228-3238.

CONNER, J.R., 1990. *Chemical fixation and solidification of hazardous wastes.* USA: Van Nostrand Reinhold.

FELMY, A. and QAFOKU, O., 2004. An aqueous thermodynamic model for the complexation of nickel with EDTA valid to high base concentration. *Journal of Solution Chemistry,* **33**(9), pp. 1161-1180.

GLASSER, F., 2001. Mineralogical aspects of cement in radioactive waste disposal. *Mineralogical Magazine,* **65**(5), pp. 621-633.

GREENFIELD, B., ILETT, D., ITO, M., MCCROHON, R., HEATH, T., TWEED, C., WILLIAMS, S. and YUI, M., 1998. The effect of cement additives on radionuclide solubilities. *Radiochimica Acta,* **82**, pp. 27-32.

HEWLETT, P.C., ed, 1998. *Lea's Chemistry of Cement and Concrete.* 4th edn. New York, USA: John Wiley & Sons Inc.

MCCROHON, R. and WILLIAMS, S.J., 1997. *Effect of Sikament 10 superplasticiser on radionuclide solubility: A report produced for UK Nirex Ltd.* .

MORGAN, S. and CONSTABLE, M., 2008. *Superplasticiser Irradiation Trials: Preparation and evaluation testing of grout samples containing ADVA Cast 551. A report produced for Magnox Electric Ltd (North).* 4510177929 (14-2007/08N additional task). WMT.

PETIT, J., WIRQUIN, E. and DUTHOIT, B., 2005. Influence of temperature on yield value of highly flowable micromortars made with sulfonate-based superplasticizers. *Cement and Concrete Research,* **35**(2), pp. 256-266.

PLANK, J., SCHROEFL, C., GRUBER, M., LESTI, M. and SIEBER, R., 2009. Effectiveness of Polycarboxylate Superplasticizers in Ultra-High Strength Concrete: The Importance of PCE Compatibility with Silica Fume. *Journal of Advanced Concrete Technology,* **7**(1), pp. 5-12.

POYRY ENERGY LTD, 2011. *The 2010 UK Radioactive Waste Inventory; Report produced for the Department of Energy and Climate Change (DECC) and the Nuclear Decommissioning Authority (NDA).* URN 10D/987 NDA/ST/STY(11)006.

RAMACHANDRAN, V.S., ed, 1995. *Concrete Admixtures Handbook.* 2nd edn. New Jersey, USA: Noyes Publications.

SCHLEGEL, M., POINTEAU, I., COREAU, N. and REILLER, P., 2004. Mechanism of europium retention by calcium silicate hydrates: An EXAFS study RID G-4731-2010. *Environmental science & technology,* **38**(16), pp. 4423-4431.

SCHLEGEL, M., SARFRAZ, A., MÜLLER, U., PANNE, U. and EMMERLING, F., 2012. First Seconds in a Building?s Life?In?Situ Synchrotron X-Ray Diffraction Study of Cement Hydration on the Millisecond Timescale. *Angewandte Chemie International Edition,* **51**(20), pp. 4993-4996.

SHANNON, R., 1976. Revised Effective Ionic-Radii and Systematic Studies of Interatomic Distances in Halides and Chalcogenides. *Acta Crystallographica Section a,* **32**, pp. 751-767.

TAKAHASHI, S., SAKAI, E. and SUGIYAMA, T., 2007. Study on Leaching of Hexavalent Chromium from Hardened Concretes Using Tank Leaching Test. *Journal of Advanced Concrete Technology,* **5**(2), pp. 201.

WARWICK, P., EVANS, N. and LEWIS, T., 2008. *Effect of "As Disposed" Complexants on the solubility of Nickel (II), Thorium (IV) and Uranium (VI).* NDA Report:NR3256A.

YAMADA, K., TAKAHASHI, T., HANEHARA, S. and MATSUHISA, M., 2000. Effects of the chemical structure on the properties of polycarboxylate-type superplasticizer. *Cement and Concrete Research,* **30**(2), pp. 197-207.

Table 1 Cement Formulations (prepared without superplasticiser, SP)

Sample	Water (g)	BFS (g)	PFA (g)	OPC (g)	w/s
BFS:OPC	52.92	132.3	0	14.7	0.36
PFA:OPC	52.92	0	110.25	36.75	0.36

Table 2 Cement Formulations (prepared with superplasticiser, SP)

Sample	Water (g)	% SP	ADVA Cast 551 (g)	BFS (g)	PFA (g)	OPC (g)	w/s
BFS:OPC	51.92	0.5	1	132.3	0	14.7	0.36
PFA:OPC	51.92	0.5	1	0	110.25	36.75	0.36

Table 3 Formulations for leaching experiments on cement monoliths

Sample	OPC (g)	BFS (g)	PFA (g)	w/s ratio	$UO_2(NO_3)_2$ (g)	$Th(NO_3)_4$ (g)	$Ni(NO_3)_2$ (g)
BFS:OPC No SP	14.7	132.3	-	0.36	-	-	-
BFS:OPC No SP – U(VI)	14.7	132.3	-	0.36	0.7	-	-
BFS:OPC No SP – Th(IV)	14.7	132.3	-	0.36	-	0.08	-
BFS:OPC No SP – Ni(II)	14.7	132.3	-	0.36	-	-	0.14
BFS:OPC 0.5% SP	14.7	132.3	-	0.36	-	-	-
BFS:OPC 0.5% SP – U(VI)	14.7	132.3	-	0.36	0.7	-	-
BFS:OPC 0.5% SP – Th(IV)	14.7	132.3	-	0.36	-	0.08	-
BFS:OPC 0.5% SP Ni(II)	14.7	132.3	-	0.36	-	-	0.14
PFA:OPC No SP	36.75	-	110.25	0.36	-	-	-
PFA:OPC No SP – U(VI)	36.75	-	110.25	0.36	0.7	-	-
PFA:OPC No SP – Th(IV)	36.75	-	110.25	0.36	-	0.08	-
PFA:OPC No SP – Ni(II)	36.75	-	110.25	0.36	-	-	0.14
PFA:OPC 0.5% SP	36.75	-	110.25	0.36	-	-	-

PFA:OPC 0.5% SP – U(VI)	36.75	-	110.25	0.36	0.7	-	-
PFA:OPC 0.5% SP – Th(IV)	36.75	-	110.25	0.36	-	0.08	-
PFA:OPC 0.5% SP – Ni(II)	36.75	-	110.25	0.36	-	-	0.14

Table 4 Uptake of Ni by crushed grouts prepared with 0.5% ADVA Cast 551

Sample	**[Ni] Bound (mol dm^{-3})**	**[Ni] Solution (mol dm^{-3})**	**% Uptake**
BFS:OPC (0.5% SP)	2.7×10^{-9}	6.8×10^{-11}	98
PFA:OPC (0.5% SP)	2.6×10^{-9}	2.5×10^{-10}	98

Table 5 Uptake of Eu by crushed grouts prepared with 0.5% ADVA Cast 551

Sample	**[Eu] Bound (mol dm^{-3})**	**[Eu] Solution (mol dm^{-3})**	**% Uptake**
BFS:OPC (0.5% SP)	3.84×10^{-10}	<LOD	>99
PFA:OPC (0.5% SP)	3.70×10^{-10}	<LOD	>99

Table 6 Nickel desorption from crushed grouts prepared with 0.5% ADVA Cast 551

Sample	**[Ni] Originally Bound (mol dm^{-3})**	**[Ni] Desorbed (mol dm^{-3})**	**% Desorption**
BFS:OPC (0.5% SP)	2.66×10^{-9}	6.73×10^{-13}	0.03
PFA:OPC (0.5% SP)	2.65×10^{-9}	7.68×10^{-13}	0.03

Table 7 Europium desorption from crushed grouts prepared with 0.5% ADVA Cast 551

Sample	[Eu] Originally Bound (mol dm^{-3})	[Eu] Desorbed (mol dm^{-3})	% Desorption
BFS:OPC (0.5% SP)	3.84 x 10^{-10}	1.14 x 10^{-12}	0.3
PFA:OPC (0.5% SP)	3.70 x 10^{-10}	7.48x 10^{-13}	0.2

Table 8 Leaching of Ni, U and Th from BFS:OPC monoliths

Sample	Metal added (mol dm^{-3})	Metal leached in mix water	Metal actually in block (mol dm^{-3})	% Leached in Mix water	Metal Leached (mol dm^{-3})	% Leach
Ni No SP	1.47E-02	<LOD*	0.015	<0.0001	5.16E-07	0.004
Ni 0.5% SP	1.52E-02	2.85E-03	1.23E-02	19	2.34E-07	0.002
U No SP	3.36E-02	1.21E-06	3.36E-02	0.004	<LOD*	<0.0001
U 0.5% SP	3.49E-02	1.12E-02	2.37E-02	32	<LOD*	<0.0001
Th No SP	3.39E-03	8.07E-08	3.39E-03	0.002	<LOD*	<0.0001
Th 0.5% SP	3.53E-03	9.15E-04	2.62E-03	26	<LOD*	<0.0001

*ICP-MS LODs for U, Th and Ni are 8E-9 mol dm^{-3}, 4E-9 mol dm^{-3} and 6E-8 mol dm^{-3} respectively

Table 9 Leaching of Ni, U and Th from PFA:OPC monoliths

Sample	Metal added (mol dm^{-3})	Metal Leached (mol dm^{-3})	% Leach
Ni No SP	1.47E-02	1.80E-09	0.000012
Ni 0.5% SP	1.48E-02	2.71E-08	0.00018
U No SP	3.43E-02	2.59E-07	0.00076
U 0.5% SP	3.45E-02	6.42E-07	0.0019
Th No SP	3.31E-03	<LOD	<0.0000001
Th 0.5% SP	3.53E-03	<LOD	<0.0000001

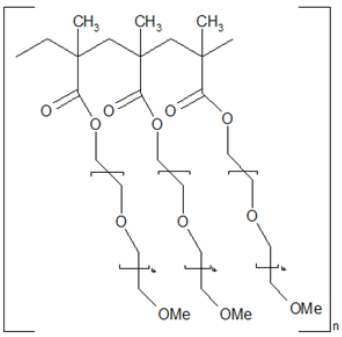

Figure 1 Comb type polycarboxylate superplasticiser, ADVA Cast 551

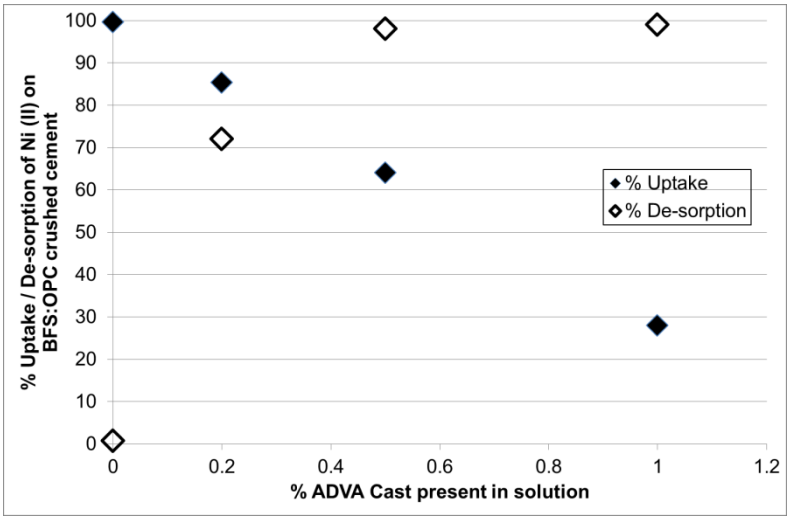

Figure 2 % Uptake and %de-sorption of Ni (II) to crushed BFS:OPC grout in the presence of ADVA Cast 551

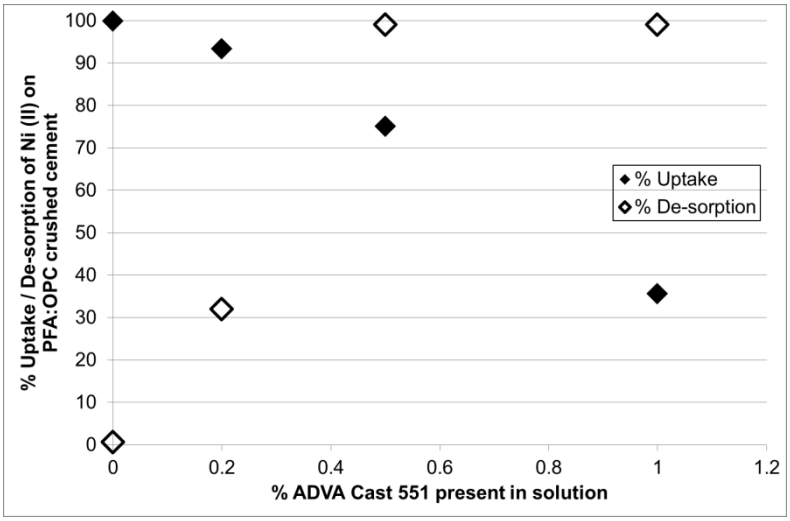

Figure 3 % Uptake and % de-sorption of Ni (II) to crushed PFA:OPC grout in the presence of ADVA Cast 551

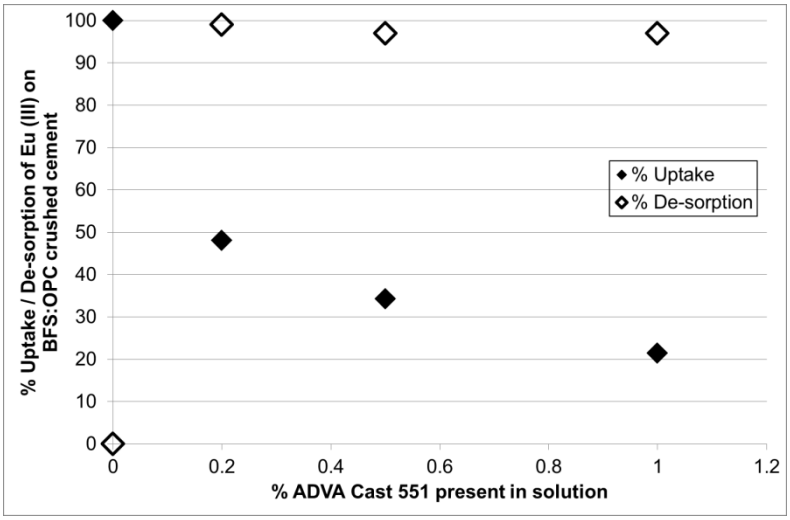

Figure 4 % Uptake and % de-sorption of Eu (III) to crushed BFS:OPC grout in the presence of ADVA Cast 551

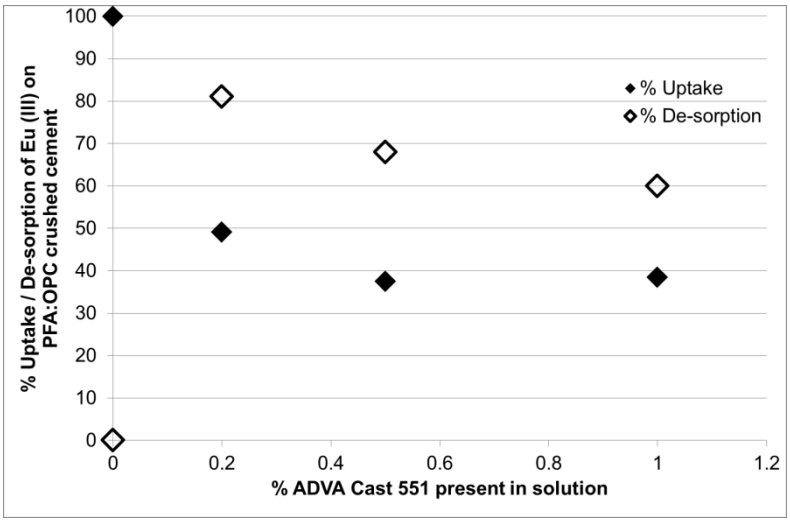

Figure 5 % Uptake and % desorption of Eu (III) to crushed PFA:OPC grout in the presence of ADVA Cast 551

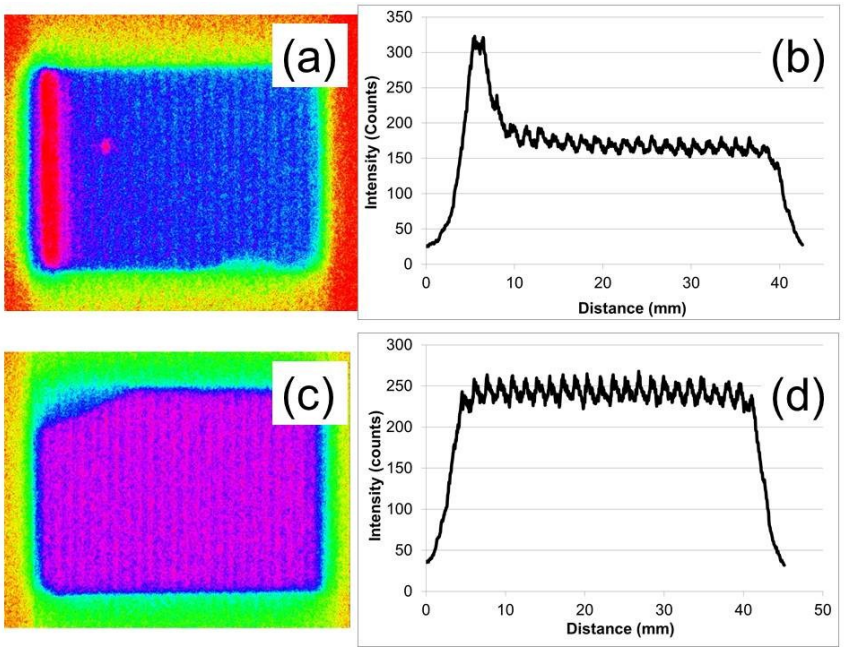

Figure 6 (a) Autoradiography image and (b) Profile Plot of BFA:OPC cement prepared with 0.5% ADVA Cast 551 and containing U (VI) and (c) Autoradiography image and (d) Profile Plot of BFS:OPC cement prepared with no superplasticiser and containing U (VI)

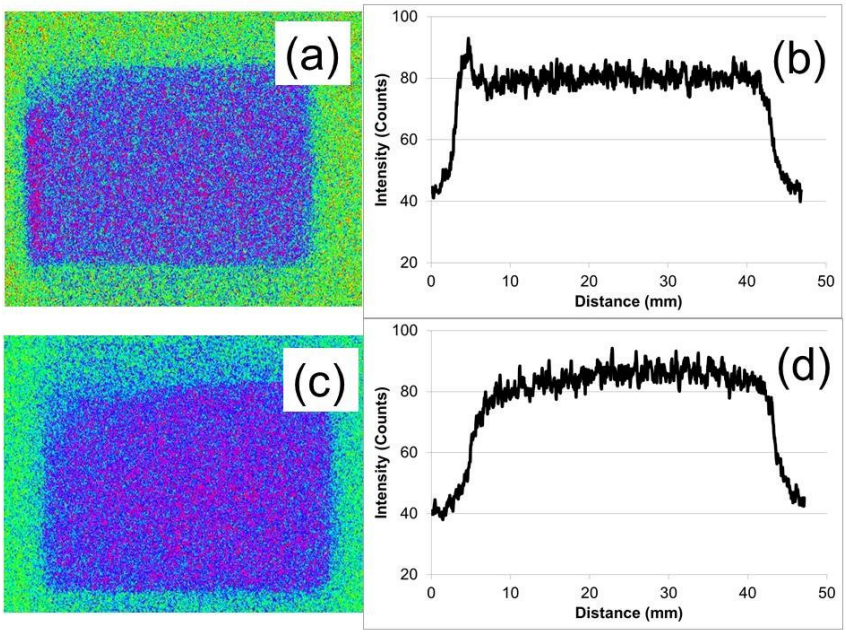

Figure 7 (a) Autoradiography image and (b) Profile Plot of BFS:OPC cement prepared with 0.5% ADVA Cast 551 and containing Th (IV) and (c) Autoradiography image and (d) Profile Plot of BFS:OPC cement prepared with no superplasticiser and containing Th (IV)

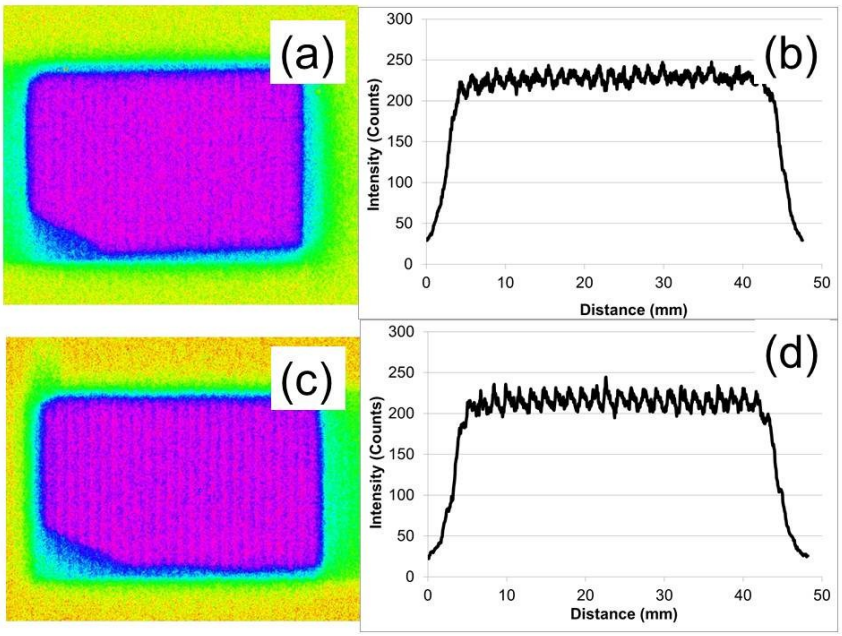

Figure 8 (a) Autoradiography image and (b) Profile Plot of PFA:OPC cement prepared with 0.5% ADVA Cast 551 and containing U (VI) and (c) Autoradiography image and (d) Profile Plot of PFA:OPC cement prepared with no superplasticiser and containing U (VI)

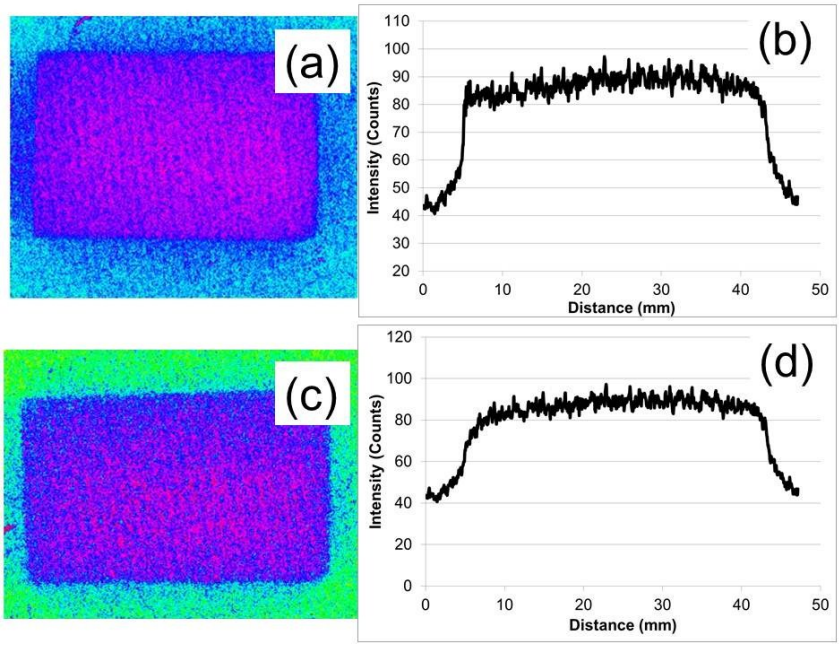

Figure 9 (a) Autoradiography image and (b) Profile Plot of PFA:OPC cement prepared with 0.5% ADVA Cast 551 and containing Th (IV) and (c) Autoradiography image and (d) Profile Plot of PFA:OPC cement prepared with no superplasticiser and containing Th (IV)

6.4 APPENDIX 4 – Record of Conferences Attended

COGER 09' – Presentation: "*Superplasticising Cement Polymers and their potential for use in the disposal of radioactive wastes"*

42nd IUPAC Congress 2009 – Conference Delegate

DIAMOND 09' – Presentation and Poster: *"The Solubility of Ni (II) and U (VI) in High pH Aqueous Solutions in the Presence of Superplasticiser"*

COGER 10' – Presentation: *"Cement Superplasticisers and their Effect on Radionuclide Solubility within the Repository Environment"*

DIAMOND 10' – Presentation and Poster: "*The Effect of Cement Superplasticiser on the Solubility and Sorption of Radionuclides"*

Environmental Radiochemical Analysis 10'– Poster: "*The Effect of Cement Superplasticiser on the Solubility of Radionuclides under Repository Conditions"*

Cement and Concrete Science 11' – Presentation and Poster: "*The Solubility and Sorption Behaviour of Nickel and Europium in the Presence of Cement Superplasticiser"*

DIAMOND 11' – Presentation and Poster: *"Sorption and Leaching Behaviour of Radionuclides in the Presence of ADVA Cast 551"*

NDA 'Geological Disposal' – Poster: *"Analysis and Characterisation of Cement Superplasticiser"*

Loughborough University Research Network Meeting 12' – Presentation: *"The Stability of Cement Superplasticiser and its Effect on Radionuclide Behaviour"*